

**Antigenic site determination on a SAT2 foot-and-mouth disease
virus using a chicken antibody phage display library**

by

Pamela Opperman

Submitted in partial fulfillment of the requirements for the degree
Philosophiae Doctor
in the Faculty of Natural and Agricultural Sciences
University of Pretoria
Pretoria

November 2013

DECLARATION

I declare that the thesis, which I hereby submit for the degree, Philosophiae Doctor (Microbiology) at the University of Pretoria, is my own work and has not previously been submitted by me for a degree at another university.

Signed:

Date:

For Jan and Sarah-Claire

Thank you for all your unconditional love, support and most of all patience.
I could not have done it without the two of you.

ACKNOWLEDGEMENTS

I wish to express my sincere gratitude and appreciation to the following persons and institutions:

To my supervisors **Prof. Jacques Theron, Dr Francois Maree** and **Dr Wilna Vosloo**; thank you for the opportunity to perform this study and for your guidance, encouragement and support throughout the course of the study.

Dr Belinda Blignaut; thank you for supporting me during my studies, and for always being encouraging and allowing me to share ideas with you.

Dr Lia Rotherham; thank you for helping me edit my thesis and for assistance with statistical analyses.

Ms Cordelia Mashau, Mr Wouter van Wyngaardt and the **staff of New Generation Vaccines Programme** at the Agricultural Research Council, Onderstepoort Veterinary Institute; thank you for introducing me to phage display technology and for training received.

Dr Dion du Plessis, from the New Generation Vaccines Programme at the Agricultural Research Council, Onderstepoort Veterinary Institute, for providing the Nkuku[®] phage display library.

Personnel from the Transboundary Animal Diseases Programme at the Agricultural Research Council, Onderstepoort Veterinary Research Institute for support.

Dr Geoffrey Fosgate from the University of Pretoria for assistance with statistical analyses.

Mrs. J. Frischmuth from the Biotechnology Division of the National Bioproducts Unit in Kwa-Zulu Natal, South Africa, for assistance with the purification of the soluble scFvs.

The **South African Department of Science and Technology**, the **Agricultural Research Council** and the **University of Pretoria** for financial support.

The **United States Department of Agriculture**, as well as **MSD Animal Health**, The Netherlands, for financial support.

My **family** and **friends**, especially **Jan**, for all your support and for never giving up on me.

SUMMARY

Antigenic site determination on a SAT2 foot-and-mouth disease virus using a chicken antibody phage display library

by

Pamela Opperman

Supervisor: Prof. J. Theron
Department of Microbiology and Plant Pathology
University of Pretoria

Co-supervisor: Dr F. F. Maree
Transboundary Animal Diseases Programme
Onderstepoort Veterinary Institute, Agricultural Research Council

Co-supervisor: Dr W. Vosloo
Australian Animal Health Laboratory
CSIRO Livestock Industries
Australia

for the degree PhD

Foot-and-mouth disease (FMD) is a highly contagious disease of cloven-hoofed animals. An outbreak of FMD not only severely decreases livestock productivity, but also impacts on both the local and export trade of susceptible animals and their products. This, in turn, negatively impacts the economy of affected countries. Of the seven serotypes that exist for FMD virus (FMDV), the three South African Territories (SAT) types display greater intratypic genomic and antigenic variation than the traditional “Euro-Asian” types. Although antigenic variation represents an important adaptive strategy of FMDV, especially in its maintenance host, it contributes to the decrease of vaccine cross-protection in the field, thus rendering available vaccines less effective. Knowledge of the amino acid residues that comprise the antigenic determinants will allow for the structural design of vaccine seed viruses that may provide improved protection against specific outbreak strains.

The SAT2 type viruses, which are responsible for most of the FMD outbreaks in domestic animals in southern Africa, are the most variable of the SAT serotypes. In order to identify antigenic regions present on a SAT2 FMDV, two approaches were followed. In the first approach, a SAT2 vaccine strain, ZIM/7/83, was panned with a naïve chicken phage-displayed library. Three unique SAT2/ZIM/7/83-specific phage-scFvs were obtained. Of these, phage-scFv2 was able to neutralize the SAT2/ZIM/7/83 virus and following sequencing of neutralization-resistant virus variants, an antigenic site was mapped to include residue 159 of the VP1 capsid protein. In the second approach, genetically modified viruses were generated in which known and predicted epitopes of SAT2/ZIM/7/83 were replaced with those of a disparate virus, SAT2/KNP/19/89, to determine the role of known SAT2 epitopes and to identify new potential antigenic regions. Following characterization of the epitope-replaced mutant viruses and studies with SAT2-specific monoclonal antibodies, two additional antigenic sites were mapped to include residues 71-72 of the VP2 capsid protein.

The information gained from this study will not only increase the knowledge of the antigenic sites of SAT2 viruses and aid in identifying more suitable vaccine strains for SAT2 viruses, but is also the first step towards the production of a SAT2-specific epitope-based vaccine.

TABLE OF CONTENTS

DECLARATION	i
ACKNOWLEDGEMENTS	iii
SUMMARY	iv
LIST OF FIGURES	xii
LIST OF TABLES	xv
LIST OF ABBREVIATIONS	xvi
CHAPTER ONE: LITERATURE REVIEW	1
1.1 GENERAL INTRODUCTION	2
1.2 GLOBAL DISTRIBUTION AND EPIDEMIOLOGY OF FMD	4
1.2.1 Global distribution	4
1.2.2 Epidemiology in Africa	6
1.3 PROPERTIES OF FMDV	7
1.3.1 Classification	7
1.3.2 Viral genome structure and protein functions	7
1.3.2.1 FMDV genome	7
1.3.2.2 FMDV proteins encoded by the ORF	10
1.3.3 Virus structure	14
1.4 INFECTIOUS CYCLE OF FMDV	16
1.4.1 Cellular receptors for FMDV	16
1.4.1.1 Integrin receptors	16
1.4.1.2 Heparan sulfate proteoglycan receptors	18
	vi

1.4.2	Replication cycle	19
1.5	QUASISPECIES NATURE OF FMDV AND VIRUS EVOLUTION	22
1.6	ANTIGENIC NATURE OF FMDV	23
1.6.1	Serotype O	25
1.6.2	Type A	25
1.6.3	Type C	26
1.6.4	Asia-1	26
1.6.5	South African Territories (SAT) types	27
1.7	IMMUNE RESPONSES	28
1.7.1	The innate immune system	28
1.7.2	The adaptive immune system	29
1.7.2.1	Humoral immune responses	29
1.7.2.2	Cellular immune responses	31
1.8	ANTIBODIES	32
1.8.1	Basic structure of antibody molecules	32
1.8.2	Antibody diversity	34
1.9	PHAGE DISPLAY TECHNOLOGY	35
1.9.1	Introduction to phage display	35
1.9.2	Structure and biology of bacteriophages	36
1.9.3	Coat proteins and vectors used for display, and selection of desired clones	38
1.10	ANTIBODY PHAGE DISPLAY LIBRARIES	39
1.10.1	Immune libraries	39
1.10.2	Naïve libraries	41
1.11	AIMS OF THIS STUDY	42

CHAPTER TWO: IDENTIFICATION AND CHARACTERIZATION OF SAT2/ZIM/7/83-SPECIFIC BINDERS FROM THE NKUKU[®] CHICKEN PHAGE DISPLAY LIBRARY **45**

2.1	INTRODUCTION	46
2.2	MATERIALS AND METHODS	48
2.2.1	Cell cultures and virus	48
2.2.2	Virus purification	48
2.2.3	SDS-polyacrylamide gel electrophoresis (SDS-PAGE)	49
2.2.4	Preparation of M13K07 helper phage	49
2.2.4.1	Large scale production of M13K07 helper phage	49
2.2.4.2	Titration of M13K07 helper phage	50
2.2.5	Selection of phage-displayed scFvs against SAT2/ZIM/7/83	50
2.2.6	Polyclonal phage enzyme-linked immunosorbent assay (ELISA)	51
2.2.7	Monoclonal phage ELISA	52
2.2.8	Monoclonal soluble scFv ELISA	52
2.2.9	DNA sequencing of phage-displayed scFvs and sequence analysis	53
2.2.10	Characterization of SAT2/ZIM/7/83-specific binders	53
2.2.10.1	Large scale purification of soluble scFvs	53
2.2.10.2	Binding specificity of phage-displayed and soluble scFvs	53
2.2.10.3	Sensitivity of SAT2/ZIM/7/83-specific binders	54
2.2.10.4	Stability of phage-displayed and soluble scFvs upon long-term storage	54
2.3	RESULTS	55
2.3.1	Selection and identification of phage-displayed scFvs against SAT2/ZIM/7/83	55
2.3.2	Binding specificity of phage-displayed and soluble scFvs against FMDV	55
2.3.3	Sensitivity studies of the SAT2/ZIM/7/83-specific binders	59
2.3.4	Stability of the SAT2/ZIM/7/83-specific binders	62

2.4	DISCUSSION	64
	CHAPTER THREE: MAPPING OF ANTIGENIC DETERMINANTS ON A SAT2 FOOT-AND-MOUTH DISEASE VIRUS USING CHICKEN SINGLE-CHAIN ANTIBODY FRAGMENTS	71
3.1	INTRODUCTION	72
3.2	MATERIALS AND METHODS	74
3.2.1	Cell culture, virus propagation and viruses	74
3.2.2	Characterization of the capsid (P1)-encoding region of SAT2 viruses	74
3.2.2.1	Oligonucleotides	74
3.2.2.2	RNA extraction	77
3.2.2.3	cDNA synthesis	77
3.2.2.4	Polymerase chain reaction (PCR) amplification and analysis	77
3.2.2.5	Nucleotide sequencing and analysis	78
3.2.3	Large scale purification of soluble scFvs	78
3.2.4	Binding specificity of the secreted soluble scFvs	78
3.2.5	Neutralization assays and generation of virus escape mutants	79
3.2.6	Synthetic peptide blocking ELISA	79
3.2.7	Structural modelling	80
3.3	RESULTS	80
3.3.1	Characterization of SAT2/ZIM/7/83-specific scFvs	80
3.3.2	Neutralization studies and the generation of virus escape mutants	81
3.3.3	Binding of soluble scFv2 to SAT2/ZIM/7/83 is reduced by a synthetic peptide	85
3.3.4	Identification of putative antigenic sites	85
3.4	DISCUSSION	91

CHAPTER FOUR: DETERMINING THE EPITOPE DOMINANCE ON THE CAPSID OF A SAT2 FOOT-AND-MOUTH DISEASE VIRUS BY MUTATIONAL ANALYSES **95**

4.1	INTRODUCTION	96
4.2	MATERIALS AND METHODS	98
4.2.1	Cell lines, viruses, plasmids and bacterial strains	98
4.2.2	Monoclonal antibody isolation	98
4.2.3	Epitope prediction	99
4.2.4	Structural modelling	99
4.2.5	Site-directed mutagenesis, sub-cloning and DNA sequencing	99
4.2.6	<i>In vitro</i> RNA synthesis, transfection and virus recovery	103
4.2.7	RNA isolation, cDNA synthesis and PCR amplification	103
4.2.8	Plaque titrations	103
4.2.9	Neutralization of infectivity in cell culture	104
4.2.10	Sandwich ELISA with SAT2-specific MAbs	104
4.2.11	Virus purification	105
4.2.12	Single dilution avidity ELISA (sd A-ELISA)	105
4.2.13	Statistical analyses	106
4.2.14	Ethics statement	106
4.3	RESULTS	106
4.3.1	Prediction of antigenic sites on the SAT2 FMDV capsid	106
4.3.2	Generation of recombinant viruses with altered surface epitopes	108
4.3.3	Effect of the epitope-replaced mutations on plaque morphologies and infectivity titres	110
4.3.4	Antigenicity of recombinant viruses with altered surface epitopes	113
4.3.5	Antigenic profiling of epitope-replaced and parental viruses with SAT2-specific MAbs	113
4.4	DISCUSSION	118

CHAPTER FIVE: CONCLUDING REMARKS	124
REFERENCES	130
APPENDICES	158
PUBLICATIONS AND CONGRESS CONTRIBUTIONS	164

LIST OF FIGURES

Fig. 1.1: Schematic diagram of the FMDV RNA genome.	8
Fig. 1.2: Schematic view of the surface structure of FMDV capsid proteins, the subunits and the viral capsid.	15
Fig. 1.3: Overview of the picornavirus infectious cycle.	20
Fig. 1.4: Mapping of amino acids positions critical for sites involved in neutralization on FMDV structural proteins, and correspondence between antigenic sites described in the different FMDV types.	24
Fig. 1.5: The basic structure of an antibody molecule.	33
Fig. 1.6: Schematic representation of bacteriophage M13.	37
Fig. 1.7: The phage display cycle.	40
Fig. 2.1: SDS-PAGE analysis of sucrose density gradient (SDG)-purified SAT2/ZIM/7/83 virions with a sedimentation value of 146S.	56
Fig. 2.2: Enrichment of phage-displayed scFvs specific for SAT2/ZIM/7/83.	57
Fig. 2.3: Binding of phage-displayed and soluble scFvs to SAT serotype viruses.	60
Fig. 2.4: Binding of affinity-purified soluble scFvs to various concentrations of SAT2/ZIM/7/83.	61
Fig. 2.5: Capturing of SAT2/ZIM/7/83 from a cell culture-infected supernatant by various concentrations of affinity-purified soluble scFvs.	63
Fig. 2.6: Long-term storage stability of the phage-displayed and affinity-purified soluble scFvs.	65
Fig. 2.7: Freeze-thaw stability of the phage-displayed and affinity-purified soluble scFvs.	65
Fig. 3.1: Binding of soluble scFvs to a panel of SAT2 serotype viruses.	82

Fig. 3.2: Virus neutralization assay of soluble scFv2 with SAT2/ZIM/7/83.	83
Fig. 3.3: Amino acid alignment and structural depiction of the amino acid substitutions observed for the SAT2/ZIM/7/83 virus neutralization escape mutants.	84
Fig. 3.4: Binding of soluble scFv2 to immobilized SAT2/ZIM/7/83 in a competitive blocking ELISA in the presence of the EpiR synthetic peptide.	86
Fig. 3.5: Binding of soluble scFv2 to immobilized SAT2/ZIM/7/83 in a competitive blocking ELISA in the presence of 200 μ M of the EpiR peptide and a non-specific positively charged peptide.	86
Fig. 3.6: Binding of soluble scFv1 and scFv3 to SAT2 FMD viruses.	88
Fig. 3.7: Structure of the SAT2/ZIM/7/83 pentamer displaying the hypervariable loops surrounding the 5-fold and 3-fold axis.	89
Fig. 4.1: The location of the surface-exposed amino acid differences between the capsids of FMDV SAT2/KNP/19/89 and SAT2/ZIM/7/83 on a ribbon protein diagram of a modelled pentamer of SAT2/ZIM/7/83.	107
Fig. 4.2: Schematic representation of the epitope replacement strategy used to replace epitopic structures of SAT2/ZIM/7/83 with those of SAT2/KNP/19/89.	109
Fig. 4.3: Surface models of the crystallographic protomers of SAT2/ZIM/7/83 and the epitope-replaced mutant virus v ^{KNP} SAT2, indicating differences in electrostatic potential.	111
Fig. 4.4: Antigenic profiles of the epitope-replaced mutant viruses, as indicated in the figure, and SAT2/KNP/19/89, SAT2/ZIM/7/83 and vSAT2 tested against SAT2 antisera (KNP/19/89 and ZIM/7/83).	114
Fig. 4.5: Avidity index of the parental SAT2/ZIM/7/83 virus and three epitope-replaced mutant viruses.	115
Fig. 4.6: Reactivity of the epitope-replaced mutant viruses and parental viruses with SAT2-specific MAbs.	117

Fig. 4.7: A ribbon protein diagram depicting the proposed binding footprint of the SAT2-specific MAbs onto the capsid protein of a modelled SAT2 pentamer. 119

LIST OF TABLES

Table 2.1: Amino acid sequence alignment of the complementary determining regions (CDR) of the heavy and light chains of the three ZIM/7/83-specific soluble scFvs panned from the Nkuku [®] library	58
Table 3.1: SAT2 viruses used in this study	75
Table 3.2: Oligonucleotides used in this part of the study	76
Table 3.3: Summary of the surface exposed hypervariable regions observed in an amino acid sequence alignment of the P1 polyprotein of the panel of nine SAT2 viruses used in this study	90
Table 4.1: Synthetic oligonucleotides used for introducing SAT2/KNP/19/89 antigenic regions into the genome-length cDNA clone of SAT2/ZIM/7/83	100
Table 4.2: A summary of the surface-exposed amino acid differences between the capsid proteins of FMDV SAT2/KNP/19/89 and SAT2/ZIM/7/83	102
Table 4.3: Parental and recombinant viruses containing the epitope-replaced mutations in the outer capsid proteins VP1 and VP2	112

LIST OF ABBREVIATIONS

α	alpha
A	absorbance
Å	Armstrong
aa	amino acid
AI	avidity index
Ala or A	alanine
AMV	avian myeloblastosis virus
ARC	Agricultural Research Council
Arg or R	arginine
Asn or N	asparagine
Asp or D	aspartic acid
β	beta
BEI	binary ethylenimine
BHK	baby hamster kidney
BME	Eagle's basal medium
bp	base pair
BTV	Bluetongue virus
BTY	bovine thyroid
C	constant
°C	degrees Celsius
<i>ca.</i>	<i>circa</i> (approximately)
CAMR	European Collection of Cell Cultures
CD	cluster of differentiation
cDNA	complementary deoxyribonucleic acid
CDR	complementary determining region
CF	complementation fixation
CFK	crandall feline kidney
CHO	Chinese hamster ovary
cm	centimetre
CPE	cytopathic effect
<i>cre</i>	<i>cis</i> -acting replication element
Cys or C	Cysteine
D	diversity
DAFF	Department of Agriculture, Forestry and Fisheries

DC	dendritic cells
DEFRA	Department for Environment, Food and Rural Affairs
DMSO	dimethyl sulfoxide
DNA	deoxyribonucleic acid
dNTP	deoxynucleoside-5'-triphosphate
<i>e.g.</i>	<i>exempli gratia</i> (for example)
eIF	eukaryotic initiation factor
EDTA	ethylenediaminetetra-acetic acid
ELISA	enzyme-linked immunosorbent assay
EscM	escape mutant
<i>et al.</i>	<i>et alia</i> (and others)
EtBr	ethidium bromide
Fab	antigen binding fragment
FCS	foetal calf serum
Fig.	figure
FMD	foot-and-mouth disease
FMDV	foot-and-mouth disease virus
Fv	antigen variable fragment
<i>g</i>	gravitational force
GC	germinal centers
Gln or Q	Glutamine
Glu or E	Glutamic acid
Gly or G	Glycine
GuSCN	guanidinium thiocyanate
H	heavy
h	hour
HEPES	4-(2-hydroxyethyl)-1-piperazineethanesulfonic acid
His or H	Histidine
HIV	human immunodeficiency virus
H ₂ O ₂	hydrogen peroxide
HRP	horseradish peroxidase
HS	heparan sulfate
H ₂ SO ₄	hydrogen peroxide
HSPG	heparan sulfate proteoglycan
<i>i.e.</i>	<i>id est</i> (that is)
IB-RS-2	Instituto Biologico-Renal Suino-2
ICAM-1	intracellular adhesion molecule-1

IFN	interferon
Ig	immunoglobulin
IL	interleukin
Ile or I	isoleucine
IPTG	isopropyl β -D-1-thiogalactopyranoside
IRES	internal ribosome entry site
J	joining
kb	kilobase pair
kDA	kilodalton
κ	kappa
KNP	Kruger National Park
λ	lambda
L	light
LPBE	liquid-phase blocking enzyme-linked immunosorbent assay
L ^{pro}	leader proteinase
Lys or K	Lysine
M	Molar
mA	milliamperes
MAbs	monoclonal antibodies
MAR	monoclonal antibody-resistant
MDBK	Madin-Darby bovine kidney
MEGA	Molecular Evolutionary Genetics Analysis
MHC	major histocompatibility complex
min	minutes
ml	millilitre
mM	millimolar
MTOC	microtubule organizing centre
NCR	non-coding region
NK	natural killer
nm	nanometre
NMR	nuclear magnetic resonance
OD	optical density
OIE	Office International des Epizooties
ORF	open reading frame
OVI	Onderstepoort Veterinary Institute
<i>p</i>	probability
3C ^{pro}	3C proteinase

PABP	poly (A)-binding protein
PAGE	polyacrylamide gel electrophoresis
PBS	phosphate-buffered saline
PBS/T	1 × PBS containing 0.1% (v/v) Tween-20
PBS-0.05%T	1 × PBS containing 0.05% (v/v) Tween-20
PCBP	poly (C)-binding protein
PCR	polymerase chain reaction
PEG	polyethylene glycol
pfu	plaque forming units
Phe or F	Phenylalanine
PK	pig kidney
PKs	pseudoknots
Poly (A) tract	polyadenylate tract
Poly (C) tract	polycytidylate tract
Pro or P	Proline
PSB	protein solvent buffer
RDRP	RNA-dependent RNA polymerase
RGD	Arg-Gly-Asp
RHA	RNA helicase A
RNA	ribonucleic acid
rpm	revolutions per minute
RPMI	Roswell Park Memorial Institute-1640 medium
RT-PCR	reverse transcriptase-polymerase chain reaction
S	Svedberg unit
SADC	Southern African Development Community
SAT	South African Territories
sc	single chain
scAb	specific antibody molecule
scFv	single chain variable fragment
SD	standard deviation
SDG	sucrose density gradient
SDS	sodium dodecyl sulfate
Ser or S	Serine
TADP	Transboundary Animal Diseases Programme
TAE	Tris-acetate-EDTA
TCID ₅₀	50% tissue culture infective dose
TE	Tris-EDTA

TEMED	tetramethylethylenediamine
TGS	Tris-glycine-SDS
Thr or T	Threonine
TNE	Tris-NaCl-EDTA
TPB	tryptose phosphate broth
Tris	Tris-hydroxymethyl-aminomethane
TY	tryptone-yeast extract-NaCl
TYE	tryptone-yeast extract-NaCl-agar
Tyr or Y	Tyrosine
U	units
µg	microgram
µl	microlitre
µm	micrometre
UK	United Kingdom
USA	United States of America
UTR	untranslated region
V	variable
v/v	volume per volume
Val or V	Valine
VGM	virus growth medium
VN	virus neutralization
VNT	virus neutralization test
VP _g	viral genome-linked protein
w/v	weight per volume

CHAPTER ONE

LITERATURE REVIEW

1.1 GENERAL INTRODUCTION

Foot-and-mouth disease (FMD), of which foot-and-mouth disease virus (FMDV) is the causative agent, is a highly contagious, acute infection of cloven-hoofed animals and is a compulsory notifiable disease (Grubman and Baxt, 2004). Susceptible animals include livestock such as cattle, sheep, goats and pigs, as well as wildlife such as the African buffalo (*Syncerus caffer*), impala, giraffe and all species of deer and antelope (Bengis, 1983). Although the average mortality rate is only *ca.* 1%, and mostly in young animals (Thomson, 1994; Beard and Mason, 2000), the morbidity of infected animals can reach 100% as a consequence of the disease being highly transmissible (Brooksby, 1982; Arzt *et al.*, 2011). FMD has a major economic impact on animal agriculture and can severely affect the livelihood of subsistence farmers in developing countries (Perry and Rich, 2007). Not only does FMD lead to the disruption of trade in animals and animal products (Sutmoller *et al.*, 2003), but it can also affect the condition of food animals and, in turn, the nutrition obtained from the animal products (Gibbs, 1981). The devastating effects of a large outbreak of FMD is evidenced by an outbreak in the United Kingdom during 2001, which was estimated to have cost £8 billion to the agricultural and support industries, as well as the outdoor industry (Samuel and Knowles, 2001b).

FMD spreads rapidly to susceptible animal populations and transmission of the disease may either be direct or indirect. Since FMDV is present in the secretions and excretions of infected animals, the most common route of infection is through direct contact between infected and susceptible animals. Indirect transmission of the disease can occur by mechanical carriage of the virus on vehicles, footwear and clothing, as well as through contact with virus-contaminated animal products such as meat and offal (Hyslop, 1970; Sellers, 1971; Quinn and Markey, 2001). Clinical signs associated with FMD develop after an incubation period of two to five days and include the formation of fluid-filled vesicles on the feet, mouth, nostrils and teats (Thomson, 1994; Charleston and Rodriguez, 2011; Golde *et al.*, 2011). Asymptomatic, persistent infections can be found in ruminants for periods ranging from a few weeks to several years, depending on the animal species, during which time virus can be isolated from the oesophagus and throat fluids (Van Bakkum *et al.*, 1959; Condy *et al.*, 1985). Most cattle carry the virus for six months or less; however, some animals remain persistently infected for up to 3.5 years. African buffalo can be carriers for at least 5 years and the virus can persist within a herd for up to 24 years (Condy *et al.*, 1985). Both naïve and vaccinated

animals are capable of becoming persistently infected following an acute infection. The mechanisms that mediate virus persistence are unclear, but are likely to result from a dynamic equilibrium between the host immune system and the selection of viral antigenic variants at the mucosae of the upper respiratory tract (Gebauer *et al.*, 1988; Salt, 1993).

Countries free of FMD control the disease by restricting the movement of animals and animal products originating from outside the country. If an outbreak occurs, it is controlled by implementing a quarantine area in which infected or in-contact animals are separated from FMD-free animals and, in some cases, euthanasia of affected and in-contact animals is performed. The latter is preferred over vaccination as it ensures that FMD-free status is readily regained following the outbreak (Barteling and Vreeswijk, 1991; Grubman and Baxt, 2004). In countries where FMD is endemic, the disease is controlled by vaccination and zoosanitary measures, *e.g.* monitoring of animal movement and the importation of animals and animal products from affected areas (Leforban, 1999; Kitching *et al.*, 2007a; Rweyemamu *et al.*, 2008; Paton *et al.*, 2009), as well as restrictions on animal movement (Brückner *et al.*, 2002; Thomson *et al.*, 2003).

Vaccination may be used to not only control an FMD outbreak, but also to protect animals from an outbreak. Current FMD vaccines are produced by infecting baby hamster kidney (BHK) cells with virulent FMDV, which is subsequently chemically inactivated with binary ethyleneimine (BEI) and purified by ultrafiltration (Kitching *et al.*, 2007a; Kitching *et al.*, 2007b). Vaccinating against FMD is complicated by the fact that seven antigenically distinct serotypes exist for the disease, each with many intratypic variants. As a result, infection or vaccination against one serotype of FMDV does not provide protection against the other serotypes, or even other subtypes within the same serotype (Brooksby, 1982; Cartwright *et al.*, 1982; Mattion *et al.*, 2004; Paton *et al.*, 2005; Maree *et al.*, 2011). Therefore, there is currently no universal FMD vaccine available and the vaccines currently used in endemic countries normally contain more than one serotype of virus, depending on the epidemiological situation of the country (Parida, 2009).

Rapid and accurate diagnosis of FMD is a prerequisite for effective control of the disease. Consequently, a suspected FMD outbreak needs to be confirmed through prescribed laboratory tests. FMD can be diagnosed by virus isolation on primary bovine thyroid cells or primary pig, calf and lamb kidney cells (Ferris *et al.*, 2006), detection of nucleic acids and

viral antigen, as well as serological tests such as antigen capture enzyme-linked immunosorbant assays (ELISA) (Van Maanen and Terpstra, 1990; De Clercq *et al.*, 2008), complementation fixation (CF) tests, virus neutralization tests (VNT) (Rweyemamu, 1984), reverse transcriptase-polymerase chain reaction (RT-PCR) coupled with automated nucleotide sequencing or real-time RT-PCR (Ferris *et al.*, 2006; Mohapatra *et al.*, 2007; Shaw *et al.*, 2007; Reid *et al.*, 2009).

In this review of the literature, aspects relating to the epidemiology, properties and infectious cycle of FMDV will be discussed. Also included are discussions on the antigenic diversity that exists within FMDV serotypes and immune responses elicited against FMDV following infection or vaccination. This will be followed by a discussion of phage display technology and its application to the construction of antibody phage display libraries to enable rapid selection of antigen-specific recombinant antibodies. This section will be concluded with a brief description of the aims of this investigation.

1.2 GLOBAL DISTRIBUTION AND EPIDEMIOLOGY OF FMD

The first reports pertaining to FMD date back to 1514, when a livestock disease demonstrating signs associated with FMD was described (Bulloch, 1927). During the 17th and 18th centuries, FMD occurred frequently in Germany, France and Italy (Brown, 1986). However, following World War II (1939-1945), the disease has become widely distributed throughout the world. To date, seven distinct FMDV serotypes (Type O, A, C, Asia-1 and the South African Territories [SAT] 1, 2 and 3) have been identified based on the lack of cross-protection following infection or vaccination (Domingo *et al.*, 2002).

1.2.1 Global distribution

FMD is wide-spread in central and east Asia, as well as in the Middle East. Taiwan experienced a FMD epidemic in 1913-1914 and from 1924-1929, after which it was free of the disease until 1997. During 1997, a devastating outbreak of type O spread rapidly through the swine herds in Taiwan. The cause of the outbreak was never determined, but the farm on which the disease first appeared was near a port city renowned for its pig-smuggling industry and illegal slaughterhouses. The outbreak was controlled through extensive vaccination, using combined vaccines for the O₁, A₂₄ and Asia-1 strains. In 2007, Taiwan was considered

to be FMD-free; however, the country still implements vaccination programmes thus restricting meat exports. China experienced its first FMD outbreak of serotype Asia-1 in 2005, which subsequently spread to Beijing (Guo *et al.*, 2006). Since then, reports have been received of FMD outbreaks in 2009 and 2010 (type A), and in 2011 (type O). South Korea suffered an outbreak of a rare type A virus early in January 2010, followed by a type O outbreak shortly after and a severe outbreak of FMD during 2010-2011 (Yoon *et al.*, 2012).

In February of 2001 the United Kingdom experienced its first FMD outbreak since 1967, which caused a crisis in British agriculture and tourism (Scudamore and Harris, 2002). In order to control the widespread outbreak of the serotype O Pan-Asia strain (Knowles *et al.*, 2001), all infected and in-contact susceptible animals were culled. Before the outbreak was brought under control in September of 2001, it had spread to Ireland, the Netherlands and France (Samuel and Knowles, 2001b; Sangare *et al.*, 2001). The United Kingdom regained its FMD-free status without vaccination in January of 2002 (Scudamore and Harris, 2002). However, it suffered another outbreak in 2007 in Surrey. The nearby Pirbright laboratory was working with the same virus strain at the time and was identified as the possible source of infection (DEFRA, 2007). Fortunately, the outbreak was contained quickly and trade restrictions were lifted within three months (FMD Reference Laboratory Network Report, 2007).

Multiple outbreaks of FMD occurred in the United States of America (USA), Argentina, Uruguay, Brazil and Paraguay in the 1870s (Mohler, 1952). Following its introduction into the Americas, the spread of FMD followed very different pathways. In North America the disease had random introductions, mainly from European livestock imports (Mohler, 1952), but was eradicated from the USA and Canada in 1929 and 1953, respectively (Sutmoller *et al.*, 2003). In South America, FMD spread rapidly through the bovine populations reaching endemic-epidemic proportions in practically every region. A severe outbreak of FMD in Mexico (1947-1952), the recurrence of the disease in Canada (1956), spread of the disease to Colombia, Venezuela and Ecuador (1950; 1956), as well as the USA banning the importation of animals and animal products led to the establishment of a campaign called “Plan of Action 1988-2009: Hemispheric Program for the Eradication of Foot-and-mouth Disease” (Naranjo and Cosivi, 2013). Following its implementation, the incidence of disease started to decline in 1993; however, a large outbreak of types O and A occurred in Argentina, Brazil, Paraguay and Uruguay in 2000-2001 (Piccone *et al.*, 2002; Naranjo and Cosivi, 2013). Despite this,

South America as a whole managed to lower the incidence of FMD outbreaks, with 85% of the bovine population being recognized by the OIE as FMD-free with or without vaccination (Naranjo and Cosivi, 2013). However, although much progress was made in controlling the disease within the given period, there are still regions within South America where the infection is circulating endemically.

1.2.2 Epidemiology in Africa

In southern Africa, the epidemiology of FMD is unique in that the South African Territories (SAT) type 1, 2 and 3 predominate. SAT2 is responsible for most of the FMD outbreaks (Condy *et al.*, 1969; Vosloo *et al.*, 2002), followed by SAT1 and then SAT3 (Thomson, 1994; Bastos *et al.*, 2001; Knowles and Samuel, 2003). These viruses are maintained in wildlife, particularly the African buffalo (*Syncerus caffer*), which provide a potential source of infection for domestic livestock (Dawe *et al.*, 1994; Vosloo *et al.*, 2007). As a consequence of the Rinderpest panzootic of 1896-1905, which decimated the cattle population and the maintenance host of FMDV, the disease was absent from the southern African region for several decades. However, in March of 1931, FMD mysteriously re-appeared in south-eastern Zimbabwe. Since its re-emergence, regular outbreaks of FMD have occurred in Zimbabwe, Botswana and South Africa (Thomson, 1994). This prompted the Southern African Development Community (SADC) countries to implement improved disease control measures such as vaccination and fencing.

In the last decade, the numbers of FMD outbreaks in southern Africa have increased significantly. Outbreaks occurred in Mozambique (2001-2002, 2010), Zimbabwe (2000-2003, 2009-2010), Zambia (2004-2010), Botswana (2002 and 2005-2010), Namibia (2007-2010), Malawi (2008-2009) and Angola (2009) (Records of the OIE). South Africa experienced SAT1 outbreaks during 2000, 2002-2003, 2009-2011, SAT2 outbreaks during 2001, 2003-2005, 2009, 2011-2012, and a SAT3 outbreak was reported in 2006 (Blignaut, 2012; FMD Reference Laboratory Network Reports; Records of the OIE and the Agricultural Research Council [ARC]). SAT3 virus was also recovered from buffalo in KwaZulu-Natal, immediately south of the Mozambique border, in 2011 (Records of the OIE and ARC). A serotype O outbreak occurred in 2001 that was thought to have started in East Asia and culminated in the 2001 United Kingdom outbreak (Knowles *et al.*, 2001). This was the first

time that South Africa has experienced an FMD outbreak caused by a serotype other than the SAT serotypes (Sangare *et al.*, 2001).

During 2012, outbreaks of SAT2, which normally occur only in sub-Saharan Africa, were reported in domesticated livestock in North Africa (Libya and Egypt) and the Middle East (Palestinian Autonomous Territories and Bahrain) (Valdazo-Gonzalez *et al.*, 2012). A SAT2 outbreak has not been reported in Egypt for at least 50 years. This recent outbreak was associated with a high mortality rate, especially in young cattle, and affected more than 80 000 animals (Valdazo-Gonzalez *et al.*, 2012).

1.3 PROPERTIES OF FMDV

1.3.1 Classification

FMDV belongs to the family *Picornaviridae* (Semler and Wimmer, 2002), which comprises of nine genera (King *et al.*, 2000), and contains the etiological agents of many diseases of medical and agricultural importance (Martinez-Salas and Saiz, 2008). FMDV and the closely related Equine rhinitis A virus both belong to the genus *Aphthovirus* (Li *et al.*, 1996).

1.3.2 Viral genome structure and protein functions

1.3.2.1 FMDV genome

The FMDV genome is a positive-sense single-stranded RNA molecule of *ca.* 8450 nucleotides in length (Bachrach, 1977), enclosed in a protein capsid (Forss *et al.*, 1984; Belsham, 2005). The viral RNA genome consists of a single open reading frame (ORF) flanked by two untranslated regions (UTRs), both of which display complex secondary structure (Sobrino *et al.*, 2001).

- **5'-UTR**

The 5'-UTR of FMDV is highly variable, *ca.* 1300 bases in length (Forss *et al.*, 1984) and contains the structural and functional elements needed for virus replication (Fig. 1.1) (Rueckert, 1996; Agol *et al.*, 1999; Paul, 2002). Covalently linked to the 5'-UTR of the genome is the virus-encoded protein VP_g (viral genome-linked protein) (Grubman, 1980; Beck *et al.*, 1983), which is encoded by the 3B-coding region located in the P3 region of the

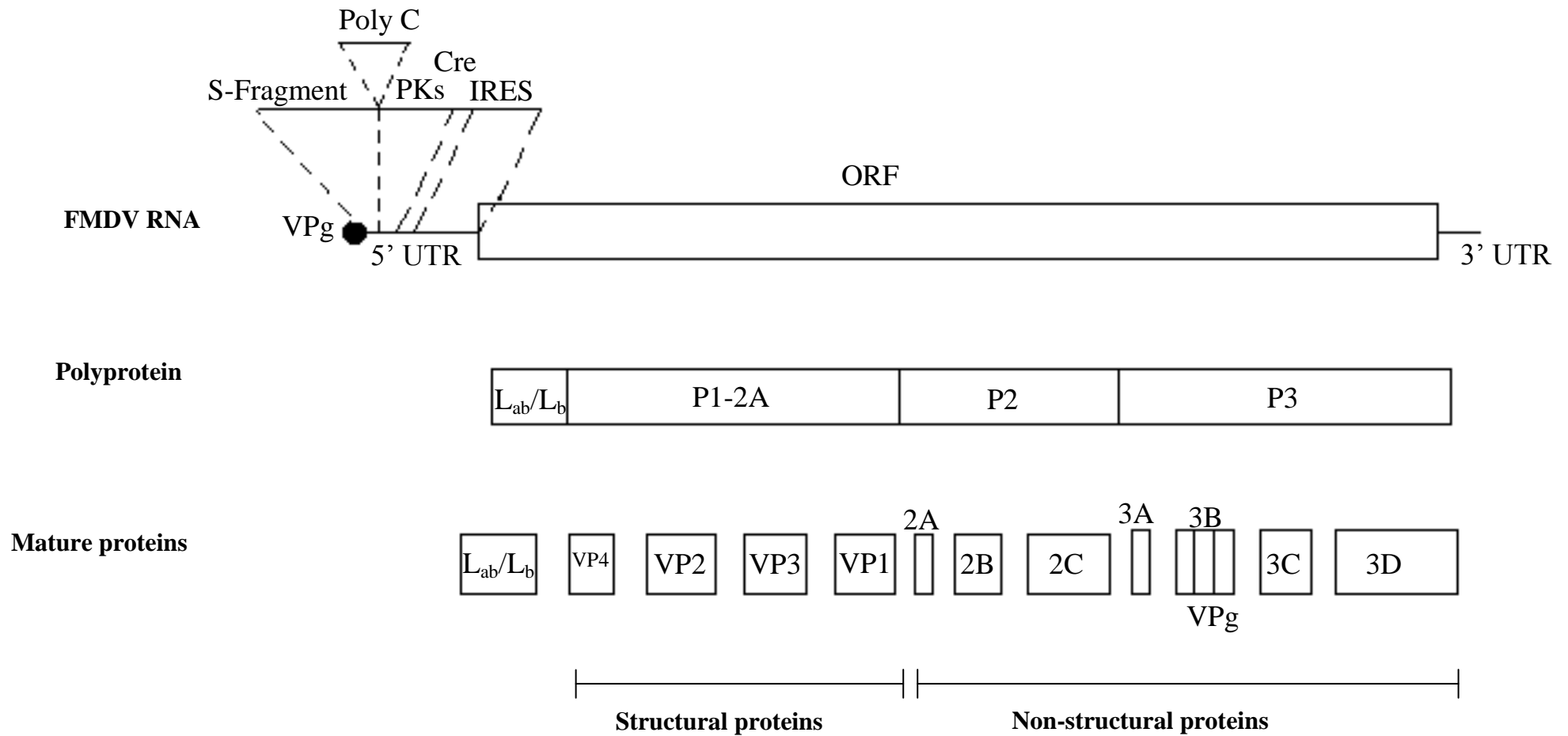


Fig. 1.1: Schematic diagram of the FMDV RNA genome. The 5' and 3' untranslated regions (UTR), the encoded polyproteins and the mature viral proteins are indicated.

ORF. The first region of the 5'-UTR, known as the small (S)-fragment, is *ca.* 370 nucleotides in length and has a sequence that is capable of folding into a long stem-loop structure (Newton *et al.*, 1985). It has been suggested that the S-fragment plays a role during RNA replication.

Following the S-fragment is a 100 to 400 nucleotide long RNase T1-resistant tract composed of *ca.* 90% cytosine (C) residues, known as the poly-cytidylate tract (poly (C) tract). The poly (C) tract is unique to *Aphtho-* and *Cardioviruses* (Brown *et al.*, 1974). Initial reports suggested that the length of the poly (C) tract plays a role in virulence (Harris and Brown, 1977). However, viruses containing a poly (C) tract of only two C residues have been reported to be virulent in mice, but they display higher particle:infectious doses than viruses with a long poly (C) tract (Rieder *et al.*, 1993). A cellular poly (C)-binding protein (PCBP), together with host and viral proteins, is postulated to bring together the 5'- and 3'-ends of the poliovirus genome in a structure that is capable of regulating the switch from translation to replication during the viral infectious cycle (Barton *et al.*, 2001; Herold and Andino, 2001). For FMDV, the PCBP associates with the poly (C) tract, suggesting that the poly (C) tract might play a similar role in genome circularization (Mason *et al.*, 2003). However, the exact biological function of the poly (C) tract is not yet well understood.

The poly (C) tract separates the S-fragment from the large (L)-fragment (Fig. 1.1). The L-fragment contains a number of highly conserved secondary structures, including tandem nucleotide repeats of pseudoknots (PKs), a *cis*-acting replication element (*cre*) and the internal ribosome entry site (IRES) (Clarke *et al.*, 1987; Martinez-Salas, 1999; Mason *et al.*, 2002). Although the function of the pseudoknots is not yet known (Clarke *et al.*, 1987), the *cre*, a short hairpin element containing a highly conserved AAACA pentanucleotide in the loop region, is used as a template for the addition of U residues to the protein primer 3B. It also plays an important role during transcription by allowing circularization of the viral genome to occur (Mason *et al.*, 2002; Tiley *et al.*, 2003). The highly structured IRES is *ca.* 440 nucleotides in length and contains five major domains, named H through L. Cap-independent translation of the viral RNA is directed by the IRES (Martinez-Salas, 1999; Beales *et al.*, 2003), resulting in ribosome recruitment to an internal site within the viral RNA (Pacheco *et al.*, 2010).

- **3'-UTR**

The 3'-end of the genome, which stimulates IRES activity and is needed for viral infectivity, contains a 90-nucleotide untranslated region (3'-UTR) and a poly (A) tract (Fig. 1.1). The 3'-UTR is composed of two stem-loops that are highly conserved, and interact with viral and host proteins during RNA replication (Pilipenko *et al.*, 1992). The poly (A) tract, which varies in length, plays a role in various processes including, genome circularization (Barton *et al.*, 2001; Herold and Andino, 2001) and is also thought to contain *cis*-acting sequences required for initiation of replication (Mason *et al.*, 2003; Grubman and Baxt, 2004).

1.3.2.2 FMDV proteins encoded by the ORF

- **The Leader protease**

The Leader proteinase (L^{pro}) is encoded by the 5'-end of the ORF (Fig. 1.1) (Robertson *et al.*, 1985). Within the L^{pro}-encoding region of all seven FMDV serotypes are two in-frame AUG codons, separated by a highly variable 80 to 84-nucleotide tract (Sangar *et al.*, 1987). The two in-frame AUG codons synthesize two forms of the Leader (L) protein, Lab and Lb, respectively (Beck *et al.*, 1983; Sangar *et al.*, 1987). Although both proteins have been detected *in vitro* and in infected cells (Clarke *et al.*, 1985), it has been suggested that Lb is the major protein synthesized *in vivo* (Cao *et al.*, 1995). Both Lab and Lb catalyze their proteolytic excision from the growing polyprotein at its carboxy (C)-terminus (Strebel and Beck, 1986; Vakharia *et al.*, 1987), and initiate the cleavage of the eukaryotic translation initiation factor eIF-4G (Devaney *et al.*, 1988; Medina *et al.*, 1993). Since eIF-4G is a component of the cap-binding complex required for translation of most cellular mRNAs (Meerovitch and Sonenberg, 1993), cleavage of eIF-4G results in the shutting-off of host cap-dependent mRNA translation (Devaney *et al.*, 1988; Mayer *et al.*, 2008) and is marked by a sharp decline in host protein synthesis *ca.* 30 min after infection (Rueckert, 1996). Subsequently, the virus-induced decrease in cellular protein synthesis is followed by increased cap-independent synthesis of viral proteins. The host innate immune response is suppressed by both proteins through the inhibition of interferon-beta (INF-β) mRNA expression. The L^{pro} is not only essential for pathogenesis and permitting virus transmission in livestock hosts, but it has also been associated with virus virulence (De Los Santos *et al.*, 2006; Piccone *et al.*, 2010).

- **The viral capsid proteins**

The P1 polyprotein, which begins directly downstream of the L protein, is the precursor of the viral capsid proteins VP1, VP2, VP3 and VP4 (Fig. 1.1) (Grubman and Baxt, 1982; Domingo *et al.*, 1990; Belsham, 1993; Sobrino *et al.*, 2001; Domingo *et al.*, 2002). These proteins are also referred to as the structural proteins. The polyprotein is rapidly cleaved into proteins VP0, VP3 and VP1 by the 3C proteinase (3C^{pro}) (Bablanian and Grubman, 1993). Upon encapsidation of the RNA, VP0 is autocatalytically cleaved into proteins VP4 and VP2 (Harber *et al.*, 1991; Lee *et al.*, 1993).

All the capsid proteins, except VP4 which is internally located, play a role in antigenicity and binding to a subset of Arg-Gly-Asp (RGD)-dependent integrins and heparan sulfate proteoglycan receptors located on the surface of cells. There is a high degree of variability amongst these proteins, with the exception of VP4, which is conserved. The VP1 proteins contribute most to the accessible surface of the virus particle, are most variable and are responsible for virus attachment and entry via a highly mobile loop protruding from its surface, known as the β G- β H loop (Acharya *et al.*, 1989; Logan *et al.*, 1993; Fry *et al.*, 1999). This highly disordered, flexible, external loop contains the highly conserved three-amino-acid-sequence RGD at its apex (Fox *et al.*, 1989; Logan *et al.*, 1993; Lea *et al.*, 1994; Mason *et al.*, 1994; Curry *et al.*, 1996).

Proteins VP2 and VP3 alternate around the 2- and 3-fold axes, and it has been suggested that a histidine-rich region at the VP2/VP3 interface is responsible for acid-induced capsid disassembly. Protonation of these residues at a pH below 6.5 may cause electrostatic repulsive forces across the pentamer interface, thereby resulting in the capsid opening up (Acharya *et al.*, 1989; Curry *et al.*, 1995; Ellard *et al.*, 1999). Multiple immunologically important regions present on VP1, VP2 and VP3 have been identified for types A, O and C (Kitson *et al.*, 1990; Crowther *et al.*, 1993a; Mateu *et al.*, 1995). The internally located VP4 protein is modified by a myristate group at its amino (N)-terminus, which has been reported to be essential for capsid assembly and stability (Chow *et al.*, 1987; Acharya *et al.*, 1989).

- **The P2 non-structural proteins**

Non-structural proteins derived from the P2- and P3-coding regions of the genome participate in RNA replication, and in the folding and assembly of structural proteins (Porter, 1993). The

P2 polyprotein precursor is proteolytically processed into the three mature polypeptides 2A, 2B and 2C (Rueckert and Wimmer, 1984). The 18-amino-acid peptide 2A (Robertson *et al.*, 1985; Donnelly *et al.*, 1997) remains associated with the P1 polyprotein precursor following primary cleavage (Vakharia *et al.*, 1987; Donnelly *et al.*, 2001; Mason *et al.*, 2003) and induces P1/2A polypeptide release from the rest of the genome through modification of the cellular translation apparatus. 2A is cleaved from the P1 region by 3C^{pro} in the later stage of processing and its function as an independent protein is not yet known.

The 3C^{pro} cleaves the 2BC precursor to reveal the 2B and 2C proteins (Vakharia *et al.*, 1987). Limited research has been completed on protein 2B of FMDV and the exact function of this protein is not known. This small hydrophobic protein is localized in the endoplasmic reticulum and the Golgi complex. The 2BC protein blocks the transport of proteins between the endoplasmic reticulum and the Golgi complex (Moffat *et al.*, 2005; Moffat *et al.*, 2007), which can result in the major histocompatibility complex (MHC) class I molecules on the surface of the infected cells being poorly expressed and ultimately limiting the cellular immune response (Grubman *et al.*, 2008). Picornaviral proteins 2B and 2C have been implicated in virus-induced cytopathic effects (CPE). Protein 2B has been implicated in enhancing membrane permeability and blocking of protein secretory pathways, as well as virus-induced CPE (Doedens and Kirkegaard, 1995; van Kuppeveld *et al.*, 1997a; van Kuppeveld *et al.*, 1997b; Jecht *et al.*, 1998).

Protein 2C of FMDV contains three nucleotide triphosphate-binding motifs (GXXXXGK, DXXG, NKXD) and helicase motifs (Dever *et al.*, 1987; Dmitrieva *et al.*, 1991). It is a highly conserved peptide with ATPase and RNA-binding activity, which are both required to stimulate stable hexamerization of 2C (Sweeney *et al.*, 2010). Ribonucleoprotein complex formation at the 5'-end of the genome, as a result of the interaction of RNA helicase A (RHA) with 2C, 3A and a cellular poly (A)-binding protein (PABP) (Lawrence and Rieder, 2009), has been shown to play an important role in the replication of FMDV. The 2C protein and its precursor 2BC are associated with cell membranes and induce cell membrane vesicle proliferation (Bienz *et al.*, 1990). In infected cells, 2C is involved in the formation of membrane vesicles where it co-localizes with viral RNA replication complexes. In addition, mutations that confer resistance to guanidine hydrochloride, an inhibitor of viral RNA replication, are located in 2C, thus implying a role for this protein in viral RNA synthesis (Saunders *et al.*, 1985; Klein *et al.*, 2000).

- **The P3 non-structural proteins**

The P3 polypeptide precursor is proteolytically processed to yield the four mature proteins 3A, 3B, 3C^{pro} and 3D^{pol} (Fig. 1.1). The protein 3A of FMDV is longer than that of other picornaviruses; 153 amino acids as compared to the 87 amino acids for poliovirus (Mason *et al.*, 2003), and is proposed to be the membrane anchor for the picornavirus replication complex (Weber *et al.*, 1996; Xiang *et al.*, 1997). It is associated to viral-induced membrane vesicles and contributes to CPE and the inhibition of protein secretion (Doedens and Kirkegaard, 1995; Wessels *et al.*, 2006), as well as pathogenesis of FMDV (Nunez *et al.*, 2001; Mason *et al.*, 2003). A type O FMDV outbreak strain, which had deletions in the C-terminus of 3A, caused devastating disease in pigs but was attenuated in cattle (Beard and Mason, 2000; Pacheco *et al.*, 2003).

The 3B region codes for three tandem, non-identical copies of the VP_g protein and participates in the initiation of RNA replication, as well as playing a role in the encapsidation of viral RNA (Hogle *et al.*, 1985; Xiang *et al.*, 1997; Barclay *et al.*, 1998). Each of the VP_g proteins contains a Tyr-3, which is known to be involved in phosphodiester linkage to the viral RNA (Forss and Schaller, 1982). It is still unclear why FMDV is the only picornavirus to encode three tandem repeats of the VP_g protein. However, limited research has shown that the tandem repeats could be an important component of the viral replication complex by enhancing transcription. Viable viruses can be recovered from infectious RNA carrying a single copy of the 3B gene, but the level of infectivity correlates with the number of 3B gene copies present in the RNA (Falk *et al.*, 1992).

The 3C proteinase (3C^{pro}) is a cysteine protease (Birtley *et al.*, 2005) responsible for catalyzing 10 of the 13 proteolytic cleavage events necessary for polyprotein processing (Vakharia *et al.*, 1987; Clarke and Sangar, 1988). The cleavage of L^{pro} from P1, 2A from P1-2A, and the maturation cleavage of VP0 into VP4 and VP2 (Bablanian and Grubman, 1993) are not processed by 3C^{pro}. Recent studies have indicated that a surface β B loop within the 3C^{pro} adopts a β -ribbon structure, which is similar in conformation to regions on other picornaviral 3C proteases and some serine proteases. The β -ribbon folds over the peptide-binding cleft and contributes to substrate recognition (Sweeney *et al.*, 2007). Residues located on the surface of the 3C^{pro}, opposite from the catalytic sites of the protease, have also been shown to be essential for VP_g uridylylation, which is the first stage in the replication of

picornavirus RNA (Nayak *et al.*, 2006). The 3C^{pro} is also implicated in changes in the cell morphology of FMDV infections. FMDV infection results in a lack of binding of the microtubules to the microtubule organizing centre (MTOC) due to the loss of γ -tubulin from the MTOC, which can thus change the cell morphology (Armer *et al.*, 2008). The proteolytic processing of the histone protein H3, which leads to inhibition of host transcription (Grigera and Tisminetzky, 1984; Falk *et al.*, 1990; Tesar and Marquardt, 1990) in infected cells, and the elongation factors eIF4G and eIF4A, which results in the termination of host cell transcription, are also induced by the 3C^{pro} (Falk *et al.*, 1990; Tesar and Marquardt, 1990). Thus, the cleavage of eIF-4G and histone H3 results in an almost complete breakdown of host cell functions during viral infection.

As in other picornaviruses, protein 3D^{pol} is the RNA-dependent RNA polymerase (RDRP) (Polatnick and Arlinghaus, 1967; Newman *et al.*, 1979) responsible for the replication of the RNA genome via negative strand intermediates. A number of specific amino acid residues have been identified as being important for preserving the functional integrity of the RDRP. The 3D^{pol} is highly conserved both in nucleotide and amino acid sequence among the different FMDV serotypes (Martinez-Salas *et al.*, 1985; George *et al.*, 2001).

1.3.3 Virus structure

The FMD virions are *ca.* 22-25 nm in diameter (Bachrach, 1968; Storey *et al.*, 2007) and consist of 70% protein, 30% RNA and a limited amount of lipid (Bachrach *et al.*, 1964). They are distinguished from other picornaviruses by their lability at pH values below 6.8 (Acharya *et al.*, 1989; Curry *et al.*, 1995; Ellard *et al.*, 1999), the presence of a hydrophobic pore and its smooth surface. The pore, situated at the 5-fold axis, not only leaves part of the VP3 protein exposed, but also allows small molecules such as caesium to enter, thus resulting in FMDV having a higher buoyancy than the other picornaviruses (Acharya *et al.*, 1989; Rueckert, 1996). Unlike other picornaviruses, such as entero- or cardioviruses, which contain receptor-binding canyons or pits, the receptor-binding site of FMDV is located on the protruding, surface-exposed β G- β H loop of VP1 (Acharya *et al.*, 1989;1990; Rueckert, 1996).

The capsid consists of 60 copies of each of the four capsid proteins, namely VP4, VP2, VP3 and VP1. The surface capsid proteins (VP1 to VP3) have an eight-stranded anti-parallel β -barrel structure and are arranged in a sandwich structure of two four-stranded β -sheets, while

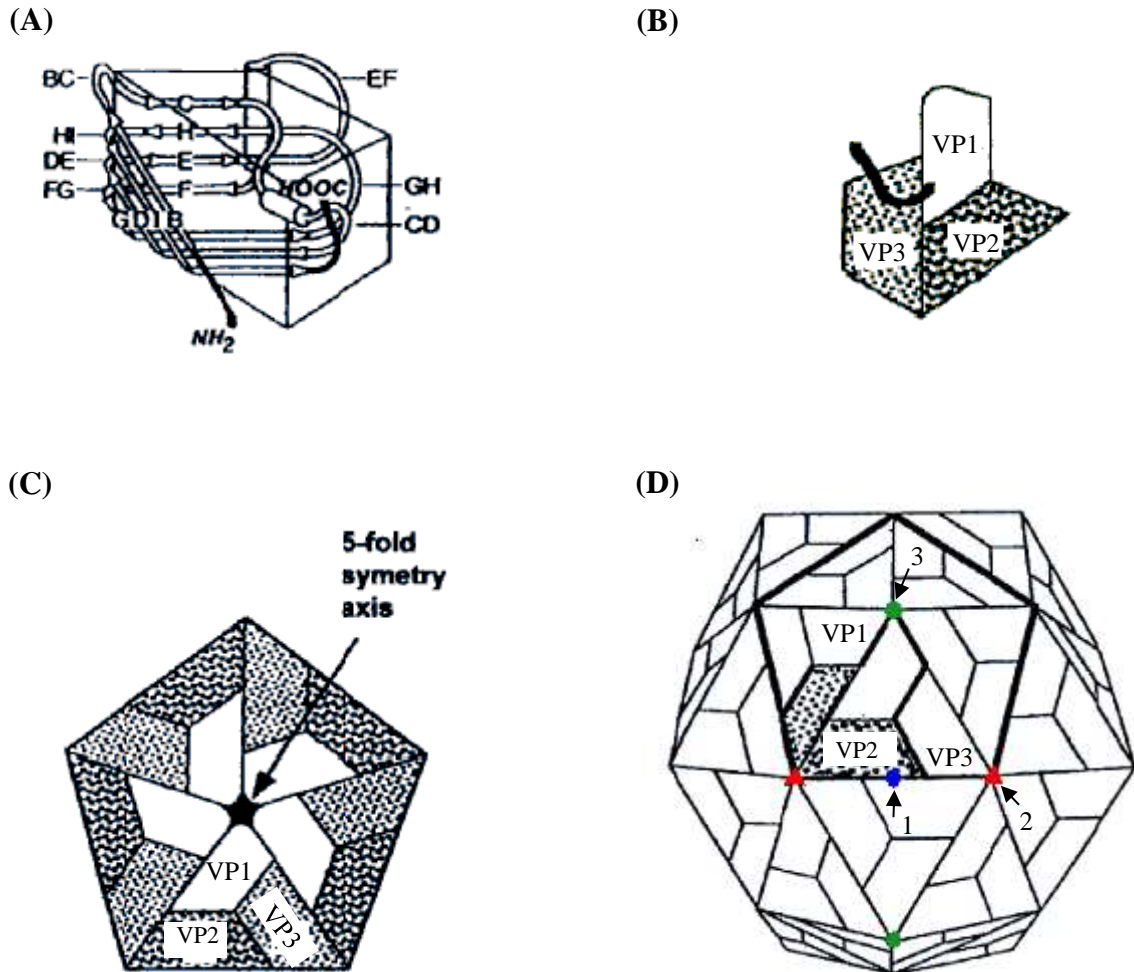


Fig. 1.2: Schematic view of the surface structure of FMDV capsid proteins, the subunits and the viral capsid. (A) Schematic representation indicating the eight-stranded β -sandwich core of proteins VP2, VP3 and VP1. The β -strands are indicated as B, I, D, G, C, H, E and F and are joined through connecting loops. (B) The arrangement of the external capsid proteins (VP2, VP3 and VP1) in a biological protomer. The location of the C- and N-terminal domain of VP1 is indicated by a black ribbon. (C) Arrangement of five protomers into a pentamer. (D) Structure of the virion capsid, consisting of 60 protomers. Each protomer is composed of one copy of VP4, VP2, VP3 and VP1. The 2-fold, 3-fold and 5-fold axes are indicated, in blue by an ellipse (1), in red by a triangle (2) and in green by a circle (3), respectively. A pentamer is outlined in the capsid, and a protomer is indicated inside the pentamer. (Taken from Saiz *et al.*, 2002)

VP4 is buried within the capsid (Acharya *et al.*, 1989). A single copy of each capsid protein assembles to produce a protomer, five protomers form a pentamer and twelve pentamers assemble into a complete icosahedral capsid that encloses the viral genome (Acharya *et al.*, 1989). Five copies of the VP1 protein are located around the icosahedral 5-fold axes, while the VP2 and VP3 proteins alternate around the 2- and 3-fold axes (Fig. 1.2).

1.4 INFECTIOUS CYCLE OF FMDV

1.4.1 Cellular receptors for FMDV

Over the last few years, much progress has been made in identifying cellular receptors for FMDV. This has led to an improved understanding of how FMDV targets epithelial cells, the preferred cell type infected by FMDV, and of the mechanisms underlying disease transmission. Whereas field isolates of FMDV utilize integrin receptors for cell internalization, cell cultured viruses have the ability to use either integrins or heparan sulfate receptors (Baranowski *et al.*, 1998; Neff *et al.*, 1998).

1.4.1.1 Integrin receptors

Integrins are a family of α/β heterodimeric transmembrane glycoproteins that contribute to various different processes, *e.g.* cell-cell and cell-extracellular matrix adhesion, as well as the induction of signal transduction pathways that regulate various processes such as cell proliferation, morphology, migration and apoptosis (Hynes, 1992; Fernandez *et al.*, 1998). Several integrins, including $\alpha_v\beta_1$, $\alpha_v\beta_3$, $\alpha_v\beta_6$, $\alpha_5\beta_1$ and $\alpha_v\beta_8$, bind their ligands via an RGD sequence (Fox *et al.*, 1989; Baxt and Becker, 1990; Hynes, 1992; Mason *et al.*, 1994; Nishimura *et al.*, 1994; Schnapp *et al.*, 1995; Jackson *et al.*, 2003). The β G- β H loop of the capsid protein VP1, containing an RGD sequence at its apex, has been shown to be important for binding FMDV to susceptible cells. Treatment of the virus with trypsin, which removes both the β G- β H loop and the C-terminus of protein VP1, resulted in virus particles that were less infectious than untreated virus. This effect was attributed to the inability of the virus to attach to cells, presumably through the disruption of the attachment site of the virus (Wild and Brown, 1967; Wild *et al.*, 1969; Strohmaier *et al.*, 1982). The residues that follow the RGD sequence, more specifically the first and fourth residues (RGD+1 and RGD+4), have been shown to play an important role in the recognition of RGD-dependent integrins by FMDV

(Rieder *et al.*, 1994; Mateu *et al.*, 1996; Jackson *et al.*, 1997; Kraft *et al.*, 1999; Jackson *et al.*, 2002; Jackson *et al.*, 2004).

Despite the presence of an RGD sequence on capsid protein VP1, FMDV does not use all of these RGD-dependent integrin receptors for binding to host cells. For example, integrins $\alpha_5\beta_1$ and $\alpha_v\beta_5$ are not used by FMDV to initiate infection of cultured cells (Neff *et al.*, 1998; Baranowski *et al.*, 2000; Jackson *et al.*, 2000). FMDV initiates infection, in cell culture, by binding to any of the four members of the α_v subgroup of the integrin family of cellular receptors, *i.e.* $\alpha_v\beta_1$, $\alpha_v\beta_3$, $\alpha_v\beta_6$ and $\alpha_v\beta_8$ (Berinstein *et al.*, 1995; Jackson *et al.*, 1997; Neff *et al.*, 1998; Jackson *et al.*, 2000; Neff *et al.*, 2000; Jackson *et al.*, 2002; Duque and Baxt, 2003; Jackson *et al.*, 2004).

In vitro, $\alpha_v\beta_3$, $\alpha_v\beta_6$ and $\alpha_v\beta_8$ are expressed on Madin-Darby bovine kidney cells (MDBK), primary bovine thyroid cells (BTY) and a pig kidney cell line known as Instituto Biologico Renal Suino-2 (IB-RS-2) (Burman *et al.*, 2006), respectively. The above-mentioned cell lines are generally used in FMDV diagnostics. The integrin expression on BHK cells, a cell line normally used in FMD vaccine production and diagnosis, is not known. The different serotypes of FMDV utilize the integrins with different efficacies *in vitro*. In general, $\alpha_v\beta_6$ acts as a high-affinity receptor for FMDV, while $\alpha_v\beta_3$ interacts with the virus with a much lower affinity (Duque and Baxt, 2003). In cell culture, serotype A viruses utilize both $\alpha_v\beta_3$ and $\alpha_v\beta_6$, whereas type O viruses preferentially utilize the $\alpha_v\beta_6$ integrin (Duque *et al.*, 2004). SAT serotype viruses have demonstrated the same trend, preferentially utilizing $\alpha_v\beta_6$ over $\alpha_v\beta_3$ (Maree *et al.*, 2011; Maree *et al.*, 2013).

Although the role of integrins *in vitro* has been well studied, their role in tissue tropism *in vivo* and in FMD pathogenesis remains unclear. Integrins $\alpha_v\beta_3$ and $\alpha_v\beta_6$ are expressed on epithelial cells at sites where FMDV replication is known to occur during natural infection (Monaghan *et al.*, 2005; Brown *et al.*, 2006). It is thought that $\alpha_v\beta_6$ is a major receptor in cell tropism, as it is expressed on the epithelial cells to a greater extent than $\alpha_v\beta_3$. On the other hand, $\alpha_v\beta_3$ is thought to act as a secondary receptor that assists the virus to spread to secondary sites of infection due to its location on blood vessels (O'Donnell *et al.*, 2009).

1.4.1.2 Heparan sulfate proteoglycan receptors

Propagation of FMDV in cell culture may lead to the rapid selection of mutant viruses, which are characterized by multiple phenotypic alterations, including enhanced replication capacity, enhanced resistance to neutralizing monoclonal antibodies (MAbs), expanded cell tropism and attenuation for cattle (Holland *et al.*, 1991; Martinez *et al.*, 1991; Baranowski *et al.*, 1998; Baranowski *et al.*, 2000). These phenotypic traits have also been found to be associated with a limited number of capsid alterations that confer to FMDV the capacity to use RGD-independent methods of cell binding such as utilization of heparan sulfate proteoglycan (HSPG) as receptors (Mason *et al.*, 1993; Fry *et al.*, 1999; Baranowski *et al.*, 2000). HSPG is widely distributed in animal tissues, occurring on almost all cell types as part of the extracellular matrix (Kjellen and Lindahl, 1991).

The FMDV type O virus O₁BFS was the first FMD virus identified as being able to use HSPG as cellular receptors (Jackson *et al.*, 1996). Subsequently, several viruses of other FMDV serotypes have been identified that also use heparan sulfate (HS) as a cellular receptor (Baranowski *et al.*, 1998; Fry *et al.*, 1999). Binding to heparan sulfate, a highly sulfated polymer of disaccharide repeats carrying a negative charge (Kjellen and Lindahl, 1991; Fry *et al.*, 1999), involves the acquisition of positively charged amino acid residues at the FMDV capsid surface. Sa-Carvalho *et al.* (1997) demonstrated that serial passaging of FMDV strains in BHK and Chinese hamster ovary (CHO) cells led to alterations of specific amino acid residues that resulted in an increase of positively charged residues at the capsid surface. In the case of type O₁BFS, these alterations comprised, amongst other, substitution of His-56 on protein VP3 with an Arg. This alteration coincided with an increased affinity for HS. However, the location of the acquired positively charged residues appears to vary for different FMDV strains or even for the same virus clone with different passage histories in cell culture (Baranowski *et al.*, 1998; Escarmis *et al.*, 1998).

Sulfated heparan is thought to bind to a shallow depression of the FMDV protomer, thus making contact with all three major capsid proteins. The three sides of the depression are formed by the β 1 strand of protein VP3, the C-terminus of protein VP1 and the α B helix of protein VP2 (Fry *et al.*, 1999). The base of the depression is formed by a 3_{10} helix running in the same direction as the sugar. Notably, based on structural data, the RGD integrin recognition motif in the β G- β H loop of protein VP1 is *ca.* 15Å from the closest sugar moiety

(Fry *et al.*, 1999). Thus, the integrin recognition site is unaffected by heparan binding and the two receptor binding sites therefore appear to be independent of each other. This may explain why multiply passaged FMDVs, despite having an enhanced affinity for HS as cell surface receptor, still maintain the ability to also use integrin cell receptors (Baranowski *et al.*, 2000). They therefore exist as a mixture of HSPG- and integrin-using virus particles (Maree *et al.*, 2011).

FMDV has also been shown to enter susceptible cells through integrin- and HS-independent pathways (Mason *et al.*, 1993; Mason *et al.*, 1994; Baxt and Mason, 1995; Baranowski *et al.*, 1998; Baranowski *et al.*, 2000; Zhao *et al.*, 2003). For example, antibody-complexed FMDV has been reported to enter cells that express the immunoglobulin Fc receptor in the presence of virus-specific antibodies (Mason *et al.*, 1993; Baxt and Mason, 1995; Juleff *et al.*, 2009; Summerfield *et al.*, 2009). The virus can also enter cells through genetically engineered receptors containing either portions of a virus-binding antibody (Mason *et al.*, 1994) or by fusing the antigen-binding domain of an FMDV-specific antibody molecule (scAB) to the cell surface intracellular adhesion molecule-1 (ICAM-1) (Rieder *et al.*, 1996). The FMDV can even lack the RGD motif (Martinez *et al.*, 1997) or contain an altered RGD motif, *i.e.* RGG (Baranowski *et al.*, 1998; Baranowski *et al.*, 2000), yet it still retains entry through HS-independent means. These findings suggest that a possible third mechanism for cell recognition by FMDV exists.

1.4.2 Replication cycle

The FMDV infectious cycle is initiated by the attachment of the virus to receptors exposed on the cell surface (Tamkun *et al.*, 1986) via an RGD sequence found within the surface-exposed β G- β H loop of capsid protein VP1 (Fox *et al.*, 1989; Mason *et al.*, 1994). Although the highly conserved RGD tripeptide is characteristic of the ligands of several members of the integrin family (Hynes, 1992), tissue culture-adapted FMDV strains can utilize other receptors such as HSPG in an RGD-independent manner (Jackson *et al.*, 1996; Sa-Carvalho *et al.*, 1997). An overview of the picornavirus infectious cycle is depicted in Fig 1.3; please note that the FMDV infection cycle differs slightly at certain stages such as the effects on apoptosis.

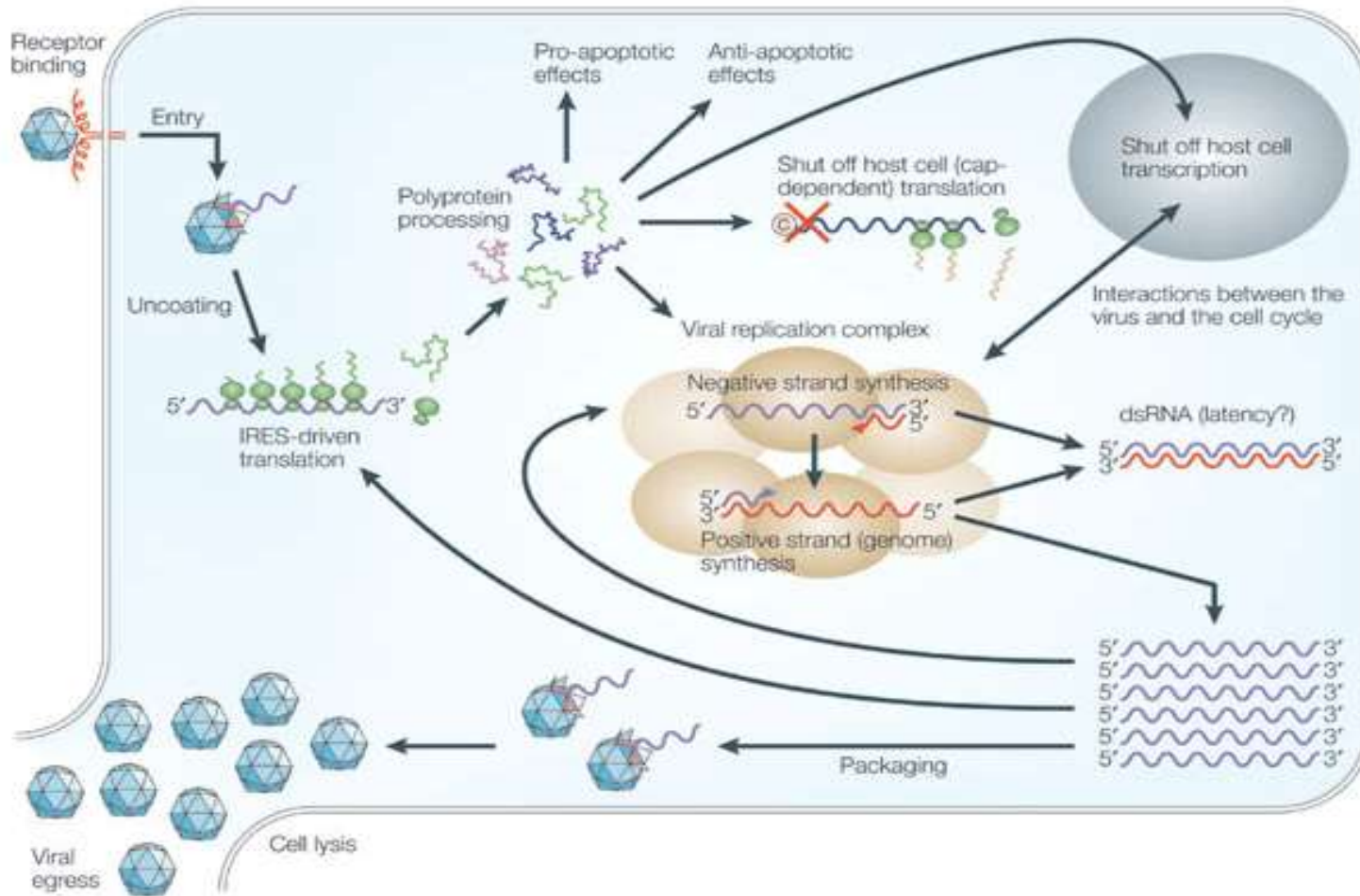


Fig. 1.3: Overview of the picornavirus infectious cycle. (Taken from Whitton *et al.*, 2005)

Following binding of the virion to the cell surface receptor, the virus-receptor complex is invaginated and internalized by endocytosis to form a clathrin-coated vesicle (endosome) (Madshus *et al.*, 1984a;b; Berryman *et al.*, 2005; O'Donnell *et al.*, 2005). Virus uptake via HSPG receptors also occurs by endocytosis, but is caveola-mediated (O'Donnell *et al.*, 2005; O'Donnell *et al.*, 2008). Acidification of the endosome leads to the release of 12 pentameric units and viral RNA (Cavanagh *et al.*, 1978; Grubman and Baxt, 2004), as well as the unfolding of the hydrophobic regions buried inside the viral capsid (Curry *et al.*, 1995). Fusion of the lipid bilayer with the hydrophobic regions of the exposed capsid proteins leads to the formation of a pore through which the viral RNA is transferred across the endosome membrane to the cytosol (Madshus *et al.*, 1984a;b; Rueckert, 1996).

Once in the cytoplasm, induction of viral RNA translation and cessation of cellular RNA translation occurs simultaneously. The VP_g protein is released from the 5'-UTR of the viral RNA (Lee *et al.*, 1977; Ambros *et al.*, 1978). Host translation is down-regulated by the L^{pro} and the IRES forms a secondary structure, which is able to bind ribosomes and deliver them directly to the polyprotein initiation codon in a cap-independent manner (Kuhn *et al.*, 1990; Martinez-Salas *et al.*, 1996), resulting in synthesis of a single polypeptide. Translation is initiated in the L-fragment of the viral genome by the two in-frame AUG codons (Beck *et al.*, 1983; Sangar *et al.*, 1987). The leader proteinase, which is the first protein to be synthesized, cleaves itself from the rest of the growing polyprotein (Strebel and Beck, 1986) before cleaving eIF-4G. The RNA strand directs synthesis of the viral polyprotein, which is cleaved into individual proteins as synthesis progresses (Vakharia *et al.*, 1987; Bablanian and Grubman, 1993; Rueckert, 1996; Belsham, 2005).

The single polyprotein encoded by the viral ORF is processed to produce the three polyprotein precursors P1-2A, P2 and P3 (Domingo *et al.*, 1990; Belsham, 1993). The P1-2A polyprotein is obtained following the autocatalytic cleavage of L^{pro} from P1 (Strebel and Beck, 1986), and the 2A cleavage between P1-2A and 2B (Ryan *et al.*, 1989). The P1-2A precursor is then cleaved by the 3C^{pro} to produce VP0, VP3 and VP1. Besides the cleavage of L^{pro} from P1, the cleavage of 2A and the maturation cleavage of VP0 to VP4 and VP2, all other cleavages are performed by 3C^{pro} and results in several mature structural and non-structural proteins (Vakharia *et al.*, 1987; Clarke and Sangar, 1988; Bablanian and Grubman, 1993).

The RNA-dependent RNA polymerase 3D^{pol}, produced by the cleavage of P3, copies the positive-sense viral RNA to produce complementary negative-sense RNA. Progeny virus positive-sense strands are synthesized repeatedly from these negative-sense templates by a peeling-off mechanism (Joklik, 1980). The progeny positive-sense RNA strands are either translated or packaged into progeny virions (Joklik, 1980; Rueckert, 1996; Nayak *et al.*, 2005). Virus assembly involves the formation of capsid protomers, five of which assemble into pentamers, followed by packaging of the positive-sense VP_g-RNA to form provirions (uncleaved VP0) (Guttman and Baltimore, 1977; Belsham, 1993; Rueckert, 1996) or empty capsids (uncleaved VP0 lacking RNA) with a sedimentation rate of 75S and of unknown significance (Rueckert, 1996; Grubman and Baxt, 2004). The final step in virion maturation involves the autocatalytic cleavage of VP0 into VP4 and VP2, which not only completes the assembly process but is also required for the formation of infectious virus particles (Harber *et al.*, 1991; Lee *et al.*, 1993; Knipe *et al.*, 1997). The mechanism of this maturation cleavage is unknown. The mature virions, with a sedimentation rate of 146S, are then released from the host cells by lysis (Belsham, 1993; Rueckert, 1996).

1.5 QUASISPECIES NATURE OF FMDV AND VIRUS EVOLUTION

Knowledge of the antigenic structure of FMDV can greatly improve understanding of the interactions between the virus and the immune system that results in neutralization of the virus *in vivo*. The identification of FMDV antigenic sites has relied mainly on analysis of monoclonal antibody-resistant (MAR) virus mutants, as well as on the evolution of the antigenicity and immunogenicity of viral peptides (Section 1.6; Minor, 1990; Usherwood and Nash, 1995).

The multiple subtypes that exist for each of the seven FMDV serotypes occur as a result of the continuous circulation of the virus in the field and the quasispecies nature of RNA viruses (Haydon *et al.*, 2001; Domingo *et al.*, 2003). FMDV, like most RNA viruses, has high mutation rates due to the absence of proofreading enzymes during RNA replication (Holland *et al.*, 1982). The high mutation rate results in different FMDV replicated genomes occurring together with the original parental genome, thus resulting in quasispecies (Eigen, 1971; Eigen and Schuster, 1979). The newly replicated variants can differ from the parental strain by 0.1 to 10 base positions (Haydon *et al.*, 2001). The environments in which the virus replicates

and adapts to, *e.g.* cell culture (*in vitro*) or a certain host species (*in vivo*), also influence which mutations may occur. Immunological pressure and physical conditions, *e.g.* pH or temperature, can lead to changes such as thermal and acid lability of the FMDV particles, a change in plaque morphology, as well as variants with altered host range, antigenicity and virulence *in vitro* (Beard and Mason, 2000; Nunez *et al.*, 2001).

Most of the variation occurs within three of the major surface-exposed structural proteins, *i.e.* VP1, VP2 and VP3, which, in turn, results in antigenic variation. Mutations have also been reported to occur in the non-structural protein-coding regions of the genome. However, these mutations are not common, as the proteins encoded by these regions are needed for viral replication and changes in these areas are normally lethal. In addition to variation as a result of mutation, FMDV has also been shown to undergo RNA recombination in tissue culture. Recombination events were originally thought to occur mostly within the non-structural protein-coding regions. More recent studies have, however, indicated that RNA recombination can take place at the outside boundaries of the outer capsid-coding regions, thus contributing to the genetic diversity in FMDV field isolates (Tosh *et al.*, 2002; Heath *et al.*, 2006; Simmonds, 2006; Jackson *et al.*, 2007).

1.6 ANTIGENIC NATURE OF FMDV

The high antigenic diversity that exists within the FMDV serotypes hinders FMD control by vaccination. Consequently, several studies have been performed to identify important neutralizing antigenic sites. It was long believed that FMDV had a single antigenic site situated on the protruding β G- β H loop of VP1 (Laporte *et al.*, 1973; Bachrach *et al.*, 1975; Adam *et al.*, 1978; Meloen *et al.*, 1979; Strohmaier *et al.*, 1982), since immunogenicity and cell attachment of FMDV were abrogated by trypsin cleavage of VP1 (Wild *et al.*, 1969). However, the production of MAbs and the sequencing of MAR mutants have been powerful tools in identifying the amino acid footprint of different antigenic sites. To date, several antigenic sites have been identified for serotypes A, O, C and Asia-1 (Fig. 1.4). These antigenic sites are either continuous (linear/sequential), where they are composed of successive adjacent amino acids (linear sequence), or discontinuous (conformational), where they are composed of residues that are not sequentially connected by peptide bonds. Discontinuous antigenic sites are composed of different sections of a protein molecule that are

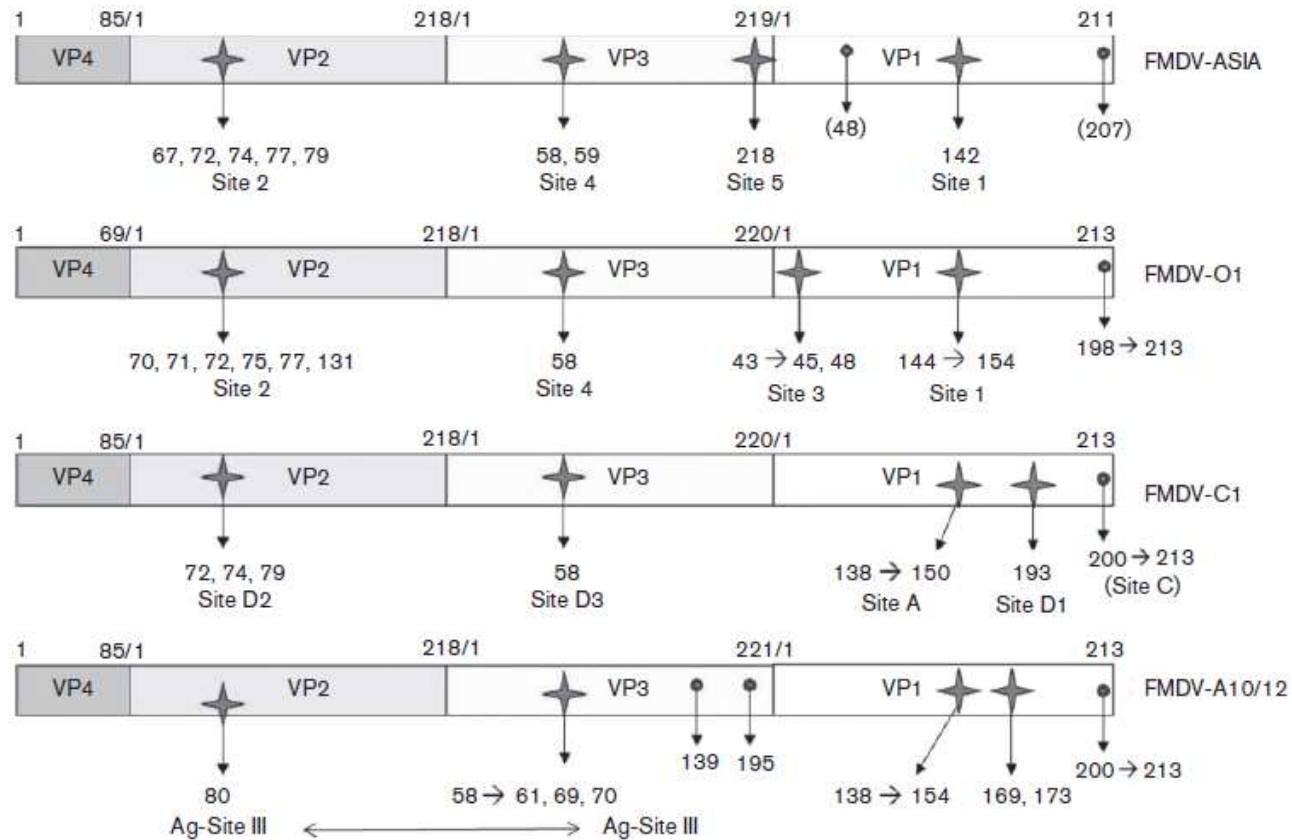


Fig. 1.4: Mapping of amino acids positions critical for sites involved in neutralization on FMDV structural proteins, and correspondence between antigenic sites described in the different FMDV types. (Taken from Grazioli *et al.*, 2013)

brought together in the folded 3D structure of the virion (Atassi, 1984; Benjamin *et al.*, 1984; Barlow *et al.*, 1986; Geysen *et al.*, 1986).

1.6.1 Serotype O

Five independent neutralizing antigenic sites, involving the three capsid proteins of FMDV, have been identified. The structural resolution of O₁BFS (Acharya *et al.*, 1989) has allowed the position of these sites on the surface of the capsid to be determined. Site 1 is a conformationally independent, trypsin-sensitive site that is situated on the β G- β H loop of VP1 encompassing the C-terminus. Residues 144, 148, 154 and 208 have been identified as playing an important role in site 1. The remaining four sites are all conformationally dependent and trypsin-resistant. Site 2, which has been suggested to be the dominant neutralizing antigenic site in serotype O (Mahapatra *et al.*, 2012), is situated in VP2 and involves residues 70-73, 75, 77 and 131. The β B- β C loop of VP1 (residues 43-44 and 48) constitutes site 3, while site 4 involves residues 56 and 58-59 on the β -B “knob” of VP3, and site 5 involves a single amino acid, 149, of VP1 (Haresnape and McCahon, 1983; McCullough *et al.*, 1987a; Xie *et al.*, 1987; Pfaff *et al.*, 1988; McCahon *et al.*, 1989; Kitson *et al.*, 1990; Crowther *et al.*, 1993a; Barnett *et al.*, 1998; Aktas and Samuel, 2000). Site 5 is believed to be formed by a particular orientation of the VP1 β G- β H loop, for instance, when the loop is in a “down” position and is close to other surface residues (Parry *et al.*, 1990; Crowther *et al.*, 1993a).

1.6.2 Type A

For serotype A viruses, five independent neutralizing antibody sites have been identified (Thomas *et al.*, 1988a; Baxt *et al.*, 1989; Bolwell *et al.*, 1989; Mahapatra *et al.*, 2011; Maree *et al.*, 2011) and the locations of these sites on the surface of the capsid have been determined (Fry *et al.*, 2005; Mahapatra *et al.*, 2011). MAR mutants of A₁₀, A₁₂, A₂₂ and A₂₄ revealed at least three sites present in VP1, VP2 and VP3 (Thomas *et al.*, 1988b; Baxt *et al.*, 1989; Bolwell *et al.*, 1989). These sites correspond to site 1, 2 and 4 of O₁BFS, respectively (Kitson *et al.*, 1990).

Site 1 encompasses the β G- β H loop of the VP1 protein involving residues 142-157, which has been identified for A₁₀, A₁₂, A₂₂ and A₂₄ (Thomas *et al.*, 1988b; Baxt *et al.*, 1989; Bolwell *et al.*, 1989; Mahapatra *et al.*, 2011). Site 2 includes residues 200-212 of VP1 as identified for

A₁₀ and A₁₂ (Thomas *et al.*, 1988b; Baxt *et al.*, 1989). Site 3 involves residues 82-88 in the β B- β C loop of VP2, 58-61 in the β B- β C loop of VP3, 136-139 in the β E- β F loop and 195 in the β H- β I loop of VP3 for A₁₀ (Thomas *et al.*, 1988b). The critical residues 169 and 175-179 of the β H- β I loop of VP1 formed part of site 4 of A₁₀ (Thomas *et al.*, 1988b) and was confirmed with A₁₂ (Baxt *et al.*, 1989). Site 5 comprises the β B- β C loop of VP3 (residues 69-70). Recently, an antigenic site analogous to site 5 of serotype O was identified for A₂₄ (Mahapatra *et al.*, 2011) and residue 149 of VP1 was identified as being significant.

1.6.3 Type C

For serotype C, at least three antigenic sites exist. Unlike the antigenic sites in serotype A, O and Asia-1, the antigenic sites in serotype C are labelled alphabetically. Site A is located within the β G- β H loop of VP1 and encompasses residues 138-150, and is equivalent to site 1 of O₁BFS (Mateu *et al.*, 1987; Mateu *et al.*, 1989; Mateu *et al.*, 1990). Site C forms part of the C-terminus of VP1 (residues 192 to 209) (Mateu *et al.*, 1990). Antigenic sites A and C are topologically independent in serotype C (Mateu *et al.*, 1989; Mateu *et al.*, 1990), unlike in serotype O where these two antigenic sites form a single discontinuous antigenic site (Xie *et al.*, 1987; Parry *et al.*, 1989). Site D, a major discontinuous antigenic site, includes several loops of VP1 (subsite D1), VP2 (subsite D2) and VP3 (subsite D3) (Lea *et al.*, 1994). Residue 193 of VP1 (near the C-terminus), residues 72, 74 and 79 (on the β B- β C loop) of VP2 and residue 58 of VP3 have been identified as critical residues in subsites D1, D2 and D3, respectively. These critical residues are adjacent to each other, situated on highly exposed regions and are close to the 3-fold axis of the virion (Lea *et al.*, 1994).

1.6.4 Asia-1

Similar to serotype A and O viruses, antigenic sites have been mapped for serotype Asia-1 viruses using MAR mutants (Sanyal *et al.*, 1997; Marquardt *et al.*, 2000; Sanyal *et al.*, 2003). Recently, knowledge of the antigenic map of Asia-1 capsids was strengthened when Grazioli *et al.* (2013) identified four unique antigenic sites, using 24 FMDV isolates of serotype Asia-1. Three of the identified sites corresponded to sites previously described for serotypes A, O and C, and the fourth site was found to be unique to Asia-1.

Site 1 is situated on the β G- β H loop of VP1 and involves residues 140-142 preceding the RGD motif. This site is analogous to site 1 in serotypes O and A, and site A in serotype C

(Stave *et al.*, 1988; Bolwell *et al.*, 1989; Mateu *et al.*, 1990; Marquardt and Freiberg, 2000; Marquardt *et al.*, 2000; Mahapatra *et al.*, 2011). In contrast to serotype A, O and C viruses, the C-terminus of VP1 of Asia-1 has not been shown to be antigenically important (Grazioli *et al.*, 2013). Asia-1 antigenic site 2 comprises of residues 67 to 79 in the β B- β C loop of VP2 (Grazioli *et al.*, 2013). This site corresponds to site 2 in serotype O (Kitson *et al.*, 1990; Aktas and Samuel, 2000), site 3 for serotype A (Thomas *et al.*, 1988b) and site D2 for serotype C (Lea *et al.*, 1994). The third antigenic site to be identified, named site 4, was located within the β -B “knob” of VP3, involving residue 58 or 59 (Grazioli *et al.*, 2013), and is similar to site 4 in serotype O, site 3 of serotype A and site D3 of serotype C (Thomas *et al.*, 1988b; Kitson *et al.*, 1990; Lea *et al.*, 1994). The fourth antigenic site of Asia-1, site 5, was located in the C-terminus (residue 218) of VP3. This site is unique for Asia-1 and is the first of its kind to be described for FMDV (Grazioli *et al.*, 2013).

1.6.5 South African Territories (SAT) types

Contrary to the vast amount of information available on the antigenic sites of the Euro-Asian FMDV serotypes, there is a dearth of knowledge for the SAT serotypes. Limited studies have been performed on the production of MAbs against SAT1 and SAT2 viruses. To date, five antigenic sites have been identified for SAT1 and are designated as sites I (1a, 1b), VI, VII and VIII. Site I is located on the β G- β H loop of VP1 and critical antibody-contact residues include residues 146 and 148 (site 1b), upstream of the RGD motif, and residues 154, 156 and 157 (site 1a), downstream of the RGD motif. These two sites are analogous to site 1 in serotype O and A, and site A in serotype C. Site VI involves amino acid 135 of VP3, a residue not found in other FMDV antigenic sites. This site was associated with additional changes at position 179 or 181 of VP1 or residues 71 or 76 of VP3 (Grazioli *et al.*, 2006). Site VII involved two amino acids in two different proteins, *i.e.* residues 181 of VP1 and 72 of VP2 (Grazioli *et al.*, 2006). It is interesting to note that residue 181 of VP1 is related to site VI in type SAT1, and residue 72 of VP2 corresponds to site 2 described in various FMDV serotypes (O, A, C and Asia-1). Site VIII was mapped at position 111 of VP1 (Grazioli *et al.*, 2006).

In the case of SAT2 serotype viruses, at least two neutralizing epitopes within the VP1 region have been described. Site 1 is a conformationally dependant antigenic site that is located on the β G- β H loop of VP1 and includes residues 147, 148, 149, 154, 156 or 158 (Crowther *et al.*, 1993b; Davidson *et al.*, 1995; Grazioli *et al.*, 2006). Residue 79 of VP2 might also play a role

in forming this antigenic site, indicating an interaction between site I and other surface-exposed sites (Grazioli *et al.*, 2006). Furthermore, residue 79 within the VP2 β B- β C loop is associated with site 2 in O₁BFS, serotype A and Asia-1 (Thomas *et al.*, 1988b; Kitson *et al.*, 1990; Aktas and Samuel, 2000; Grazioli *et al.*, 2013). The second site is an immune-dominant linear site located in the C-terminus (residue 210) of VP1 (Grazioli *et al.*, 2006).

1.7 IMMUNE RESPONSES

Immune responses are typically categorized into either innate immunity or adaptive immunity. The innate immune system responds rapidly and non-specifically to a pathogen, and its response is dependent on a restricted number of germline-encoded receptors, whereas the adaptive immune system is antigen-specific. Both these immune systems are needed to produce an effective immune response to FMDV (Palm and Medzhitov, 2009).

1.7.1.1 The innate immune system

FMDV interacts with the innate immune system in the early stages of infection. However, very little information is available regarding the contribution of the innate immune response during FMDV infection. The complement system is not only an important part of the innate immune response, but also forms a functional bridge between the innate and adaptive immune response resulting in an integrated host defence to pathogens (Dunkelberger and Song, 2010).

Cytokines, which consist of two families namely, interleukins and interferons, are soluble, cell-to-cell signalling molecules that are involved in cell activation and regulation. Cytokines such as the type 1 family of interferon (IFN), produced at the early stages of an immune response, are responsible for a number of biological functions, *e.g.* the development and regulation of the innate and adaptive immune systems and limiting the spread of infection (Theofilopoulos *et al.*, 2005; Juleff, 2009). Type 1 IFN (IFN- α or IFN- β) has been shown to protect pigs against challenge infection against FMD (Chinsangaram *et al.*, 2001; Chinsangaram *et al.*, 2003; Grubman, 2005), and suppression of IFN- α leads to viral spread and increased pathogenesis during acute FMDV infection in pigs (Nfon *et al.*, 2008). Immunization with FMD vaccines also results in the production of IFN- γ , which has been shown to be related to the antigen payload and is indicative of a lack of subclinical infection (Zhang *et al.*, 2002; Barnett *et al.*, 2004; Parida *et al.*, 2005; Eble *et al.*, 2006). Furthermore,

the spread and replication of FMDV is also affected by IFN- γ production (Moraes *et al.*, 2007; Summerfield *et al.*, 2009). Interleukins stimulate and regulate the immune response. Following vaccination, levels of IL-6, IL-8, IL-10 and IL-12 are elevated (Barnard *et al.*, 2005). Moreover, IL-10 production has been linked to FMDV infection in pigs and may suppress T cell activation during acute infection, while also being associated with T cell-independent antibody responses (Diaz-San Segundo *et al.*, 2010).

Macrophages and neutrophils have also been shown to provide a link between the innate and adaptive immune responses. They not only play an important role in phagocytosis and killing of pathogens, but also in antigen presentation (Sandilands *et al.*, 2005). Dendritic cells (DCs) form part of the antigen presenting cell family and are able to stimulate naïve T cells (Kapsenberg, 2003). However, their role in FMD pathogenesis is unclear. The presence of anti-FMDV antibodies has been linked to a change in affinity and the uptake of antibody-opsinized virus by DC-expressed Fc receptors (Summerfield *et al.*, 2009; Arzt *et al.*, 2011). This, in turn, may result in FMDV being localized to the lymphoid follicles shortly after infection (Juleff *et al.*, 2008). The lymph follicles then develop into germinal centers (GCs) following antigen exposure. It is proposed that important events that activate the early phase of the adaptive immune response occur within the GCs (Arzt *et al.*, 2011).

Natural killer (NK) cells are lymphoid cells that recognize and kill infected cells or tumor cells, without harming healthy cells (Lanier, 2005). Although little is known about the interaction of NK cells with FMDV (Storset *et al.*, 2004), it has been shown that FMDV-infected cells were lysed in a non-MHC restricted manner by cells with the same phenotype as NK cells (Amadori *et al.*, 1992). The viral down-regulation of MHC class I on FMDV-infected epithelium may also be influenced by NK cell activity (Sanz-Parra *et al.*, 1998). However, this may also be attributed to the viral immune system preventing cytolysis by MHC class I-restricted T lymphocytes (Grubman *et al.*, 2008; Summerfield *et al.*, 2009).

1.7.2 The adaptive immune system

1.7.2.1 Humoral immune responses

The immune response elicited against FMDV, following immunization or infection, results in the production of specific neutralizing antibodies to the structural proteins of the virus (Pay & Hingley, 1987; Salt, 1993). Most immunological studies have been directed at the humoral

immune response since the principle method of protection against FMDV is thought to be the induction of high levels of neutralizing antibodies.

Humoral immunity is mediated by antibodies produced by B cells, which are generated in the bone marrow. They recognize antigens through an antigen-specific B cell receptor that is formed by somatic recombination of germline-encoded genes (Murre, 2007). Due to the importance of antibodies in the humoral immune response, the different classes and subclasses of virus neutralizing antibodies present in the serum and probang samples of FMDV-infected cattle have been studied.

The first neutralizing antibodies elicited against FMDV are IgM antibodies and they reach a peak between 5 to 14 days post-infection (Doel, 1996; Golde *et al.*, 2008; Juleff *et al.*, 2009). In cattle, IgG1 and IgG2 antibodies appear from five days and onward, and the IgG immune response peaks at 10 to 14 days post-infection (Collen, 1994; Juleff *et al.*, 2009). In pigs, IgG is detected 4 to 7 days post-infection and the maximum levels are reached between 15 to 20 days (Doel, 1996; Pacheco *et al.*, 2010). Pigs and cattle that are protected against FMD, following vaccination, elicit higher levels of IgG1 compared to IgG2 (Barnett *et al.*, 2002; Juleff *et al.*, 2009; Capozzo *et al.*, 2011). Seven days after challenge, IgA can be detected in serum with titres peaking around 7 to 14 days. The titre then declines slowly, except in carrier animals where a second late response is seen at day 28. IgA can also be detected in probang samples at day 4 and again with a peak titre at day 14 (Salt *et al.*, 1996).

Virus neutralization by antibodies can be mediated by a number of different mechanisms, *e.g.* aggregation of virions, destabilization of the virion structure and inhibition of virion attachment to target cells. However, the mechanism of choice is determined by the properties of both the virion epitope and the antibody to which it reacts (Reading and Dimmock, 2007). The *in vivo* neutralization of a virus by antibodies involves interaction of antibodies with cells and molecules of the innate immune system (Reading and Dimmock, 2007). *In vitro*, FMDV neutralization occurs by inhibiting cell attachment either due to steric hindrance or destabilization of the capsid, thus resulting in loss of infectivity (McCullough *et al.*, 1987b; McCullough *et al.*, 1992). Such steric hindrance can be caused by the binding of antibodies that block the cell attachment site on the virus particle (Wohlfart *et al.*, 1985; Reading and Dimmock, 2007).

Following FMDV infection or vaccination, the humoral response is rapid and provides protection against re-infection with homologous virus strains (Pay and Hingley, 1987; McCullough *et al.*, 1992; Salt, 1993). In ruminants, the immune response following FMDV infection can provide protection for several years and the levels of protection correlate well with serum neutralizing antibody titres (Brocchi *et al.*, 1998). The long-term immune response may be attributed to antigen retention on follicular dendritic cells within the germinal center of mandibular lymph nodes. FMDV binds to the light zone of the germinal center cells that not only produces a virus-specific IgG response (Gatto *et al.*, 2007; Allen and Cyster, 2008; Harwood *et al.*, 2008), but the FMD viral particles or immune complexes are also maintained in a non-replicating state (Juleff *et al.*, 2008). This long-term immunity is in sharp contrast to the protection provided following vaccination with current inactivated FMD vaccines, which provide short-term protection and short-term serum neutralizing antibody titres (Doel, 2005).

1.7.2.2 Cellular immune responses

The cell-mediated immune response relies on T lymphocytes acting as a defence against intracellular pathogens, of which T-helper lymphocytes (Th/CD4⁺) and T-cytotoxic lymphocytes (Tc/CD8⁺) are considered to be the most important. T cell-mediated immune responses are pathogen-specific and are controlled by the MHC class I and class II molecules, which present foreign peptides to the immune system (Townsend *et al.*, 1985; Townsend *et al.*, 1986). However, the role that T cells play in protecting animals from FMDV is still unclear, since specific T cell-mediated anti-viral responses (CD4⁺ and CD8⁺) have been observed both *in vitro* and *in vivo* (Glass *et al.*, 1991; Blanco *et al.*, 2001; Bautista *et al.*, 2003).

Following infection with FMDV, MHC class I molecules are reduced and infected cells are unable to present viral peptides to T lymphocytes. The virus, in turn, escapes the cytotoxic immune response of the host (Sanz-Parra *et al.*, 1998). MHC class I restricted CD8⁺ T cell responses have been found in cattle following infection or vaccination. A CD8⁺ T cell epitope, present within the VP1 structural protein, was shown to induce virus-infected cell killing by $\alpha\beta$ CD8⁺ T cells, but not CD4⁺ T cells (Guzman *et al.*, 2008). CD4⁺ T cell responses also play an important role in protection against FMDV following vaccination and infection (Glass *et al.*, 1991; Gerner *et al.*, 2006; Li *et al.*, 2008; Golde *et al.*, 2011). FMDV

antigens are degraded into peptides within the dendritic cells. The peptides fuse with FMDV-specific MHC class II molecules and results in the production of Th1 (IFN- γ), as well as Th2 (IL-4, IL-5 and IL-13) responses (Golde *et al.*, 2008). The processed antigen is then recognized by the specific Th-lymphocytes, which induce B-lymphocyte proliferation and differentiation into antibody-producing cells, and later memory cell development (Banchereau and Steinman, 1998; Tizard, 2000; McCullough, 2004).

1.8 ANTIBODIES

Antibodies, also referred to as immunoglobulins (Ig), are produced by B cells and are used by the immune system to identify and neutralize foreign molecules, *e.g.* bacteria and viruses (Dasgupta, 1999; Janeway *et al.*, 2001). In addition to being amongst the principal effectors of the adaptive immune system, antibodies have also been harnessed extensively as diagnostic and research reagents. Although polyclonal and monoclonal antibodies (MAbs) have been used in a wide variety of applications, the principal advantages of MAbs are their homogeneity and consistency. The monospecificity provided by MAbs is useful in evaluating changes in molecular conformation, protein-protein interactions and in the identification of single members of protein families (Nelson *et al.*, 2000; Lipman *et al.*, 2005). There are two different methods to obtain MAbs, *i.e.* hybridoma technology and recombinant antibody technology. Despite its contribution to major scientific advances, the hybridoma technology has several limitations, amongst other, its high cost, it requires considerable time and expertise, and the technology relies on the use of laboratory animals (Kohler and Milstein, 1975; Willats, 2002; Pandey, 2010). In addition, many molecules are not immunogenic in mice or are toxic and therefore cannot be used as antigens (Plesica and Braun, 1967; Dintzis *et al.*, 1976). These limitations can be overcome by making use of recombinant antibody technology as a means to select MAbs. Twenty eight years after its development (Smith, 1985), antibody phage display using filamentous bacteriophages has had a major influence in the fields of immunology, cell biology, basic research and diagnostics (Yip and Ward, 2002; Pitaksajakul *et al.*, 2010; Meyer *et al.*, 2011; Schirrmann *et al.*, 2011). Consequently, this topic will be introduced by a brief overview of antibodies and their diversity.

1.8.1 Basic structure of antibody molecules

All antibodies are Y-shaped glycoproteins (Fig. 1.5) that are formed from two identical heavy

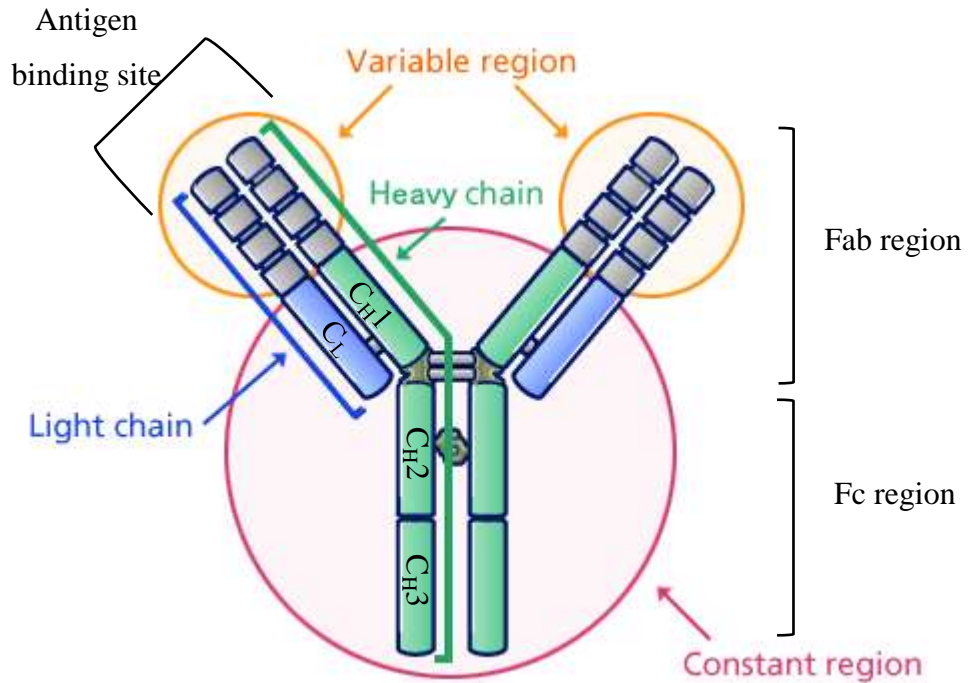


Fig. 1.5: The basic structure of an antibody molecule. Each antibody is composed of four polypeptides; two identical heavy chains and two identical light chains that are joined by disulphide bonds to form a Y-shaped molecule. Each heavy chain contains one variable domain (grey blocks), followed by three constant domains (green block); the first constant domain, C_{H1}, is separated from the second (C_{H2}) and third C_{H3}) constant domains by a hinge region. Each light chain is composed of one variable domain (V_L) and one constant (C_L) domain (blue block). The antigen binding site is composed of the variable region of one light and one heavy chain, which are situated opposite each other in the linked antibody structure. Each arm of the Y-shaped antibody molecule contains a Fab (fragment, antigen binding) region, while the base of the molecule contains an Fc (fragment, crystalline) region. (Figure adapted from www.kyowa-kirin.co.jp)

(H) chains and two identical light (L) chains. Each arm of the Y-shaped antibody molecule contains a single light chain linked to a heavy chain by a disulphide bond (Janeway *et al.*, 2001; Gupta, 2009). In mammals there are two types of light chain, designated as lambda (λ) and kappa (κ), and each light chain has two successive domains, *i.e.* a C-terminal constant domain (C_L) and an N-terminal variable domain (V_L) (Harlow and Lane, 1988; Roitt *et al.*, 1998; Ramakrishnam *et al.*, 2001). However, unlike the light chain, which only contains one constant region, the heavy chain may contain multiple constant regions (Roitt *et al.*, 1998; Burton, 2001; Tropp, 2012).

Each arm of the Y-shaped antibody molecule contains a site that can recognize and bind to a specific antigen, and is known as the Fab (fragment, antigen binding) region (Janeway *et al.*, 2001). The paratope is shaped at the N-terminal end of the antibody by the variable domains from the heavy and light chains. Specifically, six highly variable loops (three each on the light [V_L] and heavy [V_H] chains), called complementary determining regions (CDRs), are responsible for binding to the antigen (Amit *et al.*, 1986; Elgert, 2009). At the base of the Y-shaped antibody is a region called the Fc (fragment, crystalline) region that plays a role in modulating immune cell activity (Janeway *et al.*, 2001).

1.8.2 Antibody diversity

Mammals encounter a multitude of pathogens on a daily basis. The ability of their immune systems to generate antibodies providing protection against such a large variety of pathogens results from a series of tightly controlled recombination events within the antibody gene segments of the heavy and light chain. These recombination events, which take place during lymphocyte development, result in an enormous diversity of antigen receptors (antibody diversity). The generation of such diversity circumvents the need for genomes to be inconceivably large in order to harbour all the information needed to allow the animal to respond to all the pathogens it may encounter (Tonegawa *et al.*, 1974).

The variable (V) and constant (C) gene segments of the light chains are not joined directly, but are separated by the joining (J) gene segment of *ca.* 1500 base pairs (Early *et al.*, 1980). During maturation of lymphoid cells, there is rearrangement of the DNA such that one of the V gene segments is joined to one of five J gene segments, thus resulting in a VJC alignment (Alberts *et al.*, 2002). The variable region of the heavy chain is encoded by a DNA sequence

formed by three gene segments, *i.e.* a V, J and a diversity (D) gene segment (Early *et al.*, 1980; Alberts *et al.*, 2002). The D segment, which is located between the V and the J-constant gene segments, is highly variable in both the number of codons that are present, as well as the sequence of the base pairs (Roitt *et al.*, 1998). Two recombination events take place, the first joining a D gene segment to a J-constant gene segment and any DNA between these two gene segments is deleted. The D-J recombination is followed by the joining of one V gene segment from a region upstream of the newly formed D-J complex, resulting in a rearranged VDJ gene segment (Roitt *et al.*, 1998). Diversity is furthermore created by junctional diversity. In this instance, different codons are created when nucleotides are lost or gained when combinatorial joining occurs, resulting in the coding ends of exons being modified (Max *et al.*, 1979; Sakano *et al.*, 1979). Following the rearrangement of the VJ_L or VDJ_H the gene segments are transcribed continuing through the C region of the gene. The mRNA is then created by joining the V, J or V, D, J and C gene segments through RNA splicing and is translated into either light or heavy chains (Roitt *et al.*, 1998).

Within the variable region of each chain three areas of hypervariability exist, known as CDRs, which constitute the majority of the contact residues for binding of the antibody to the antigen. CDR1 and 2 are located in the variable region, whereas recombination junctions produce sequences that encode amino acids for CDR3. Recombination provides both different assortments of the various CDRs and, due to the fact that recombination is not always precise, diversity occurs in the CDR3. More than half of the heavy or light chain variable regions contain point mutations in the antigen-binding regions, as well as in the CDRs that further increase antibody diversity (Tonegawa, 1983; Levy *et al.*, 1989; Roitt *et al.*, 1998). The exact cause of these point mutations is unknown; however, they appear to fine-tune the binding site that results in a better fit for the antigen-antibody interaction. This process is known as affinity maturation.

1.9 PHAGE DISPLAY TECHNOLOGY

1.9.1 Introduction to phage display

Phage display refers to an *in vitro* selection technique that enables polypeptides with desired properties to be extracted from a large collection of variants. A gene of interest is fused to that of a phage coat protein, resulting in phage particles that display the encoded protein at its

surface and contain the gene, thus providing a direct link between phenotype and genotype (Smith, 1985; Arap, 2005). This allows phage libraries to be subjected to a selection step, and recovered clones to be identified by sequencing. Since the initial description of this approach by Smith (1985), it has become established as a powerful method for identifying polypeptides with novel properties, and altering the properties of existing ones (Clackson and Wells, 1994; Smith and Petrenko, 1997; Sidhu, 2000).

Antibody phage display libraries (McCafferty *et al.*, 1990; Clackson *et al.*, 1991; Hoogenboom *et al.*, 1998; Van Wyngaardt *et al.*, 2004), which enables the selection of recombinant antibodies, are considered to represent the most successful *in vitro* antibody selection technology and has allowed for the selection of recombinant antibodies against a wide variety of different targets (Carmen and Jermutus, 2002; Andreotti *et al.*, 2003). Major advantages of antibody phage display libraries compared with MAbs obtained by hybridoma technology (*i.e.* the production of MAbs by a single B lymphocyte) are that it is much quicker to generate antibodies using phage display than hybridoma technology (few weeks versus several months) and the quantity of target antigen required for phage display is much less than what is needed for hybridoma antibody production (micrograms versus milligrams) (Marks *et al.*, 1991; Wang *et al.*, 1995; Burritt *et al.*, 1996; Carmen and Jermutus, 2002; Willats, 2002). The starting point is usually an antibody library of either naïve or immune origin, as discussed in greater detail in Section 1.10.

1.9.2 Structure and biology of bacteriophages

The bacteriophages that are used in phage display technology, *e.g.* M13, f1, fd and ft, are single-stranded DNA viruses that are capable of infecting Gram-negative bacteria, including *Escherichia coli*. Amongst these filamentous coliphages, bacteriophages M13 and fd are most frequently used in phage display technology. These phage particles have dimensions of 900 nm × 9 nm and contain a single-stranded circular DNA molecule, which is 6407 (M13) or 6408 (fd) nucleotides long, and is encapsulated in a long cylindrical protein coat. The protein coat is composed of *ca.* 2800 copies of the major coat protein (gp8). At both termini of the phage particle there are five copies of each of the two minor coat proteins, gp7 and gp9 at the distal end and gp3 and gp6 at the proximal end (Webster, 2001) (Fig. 1.6).

The phages infect *E. coli* through a process that begins with attachment of the phage gp3

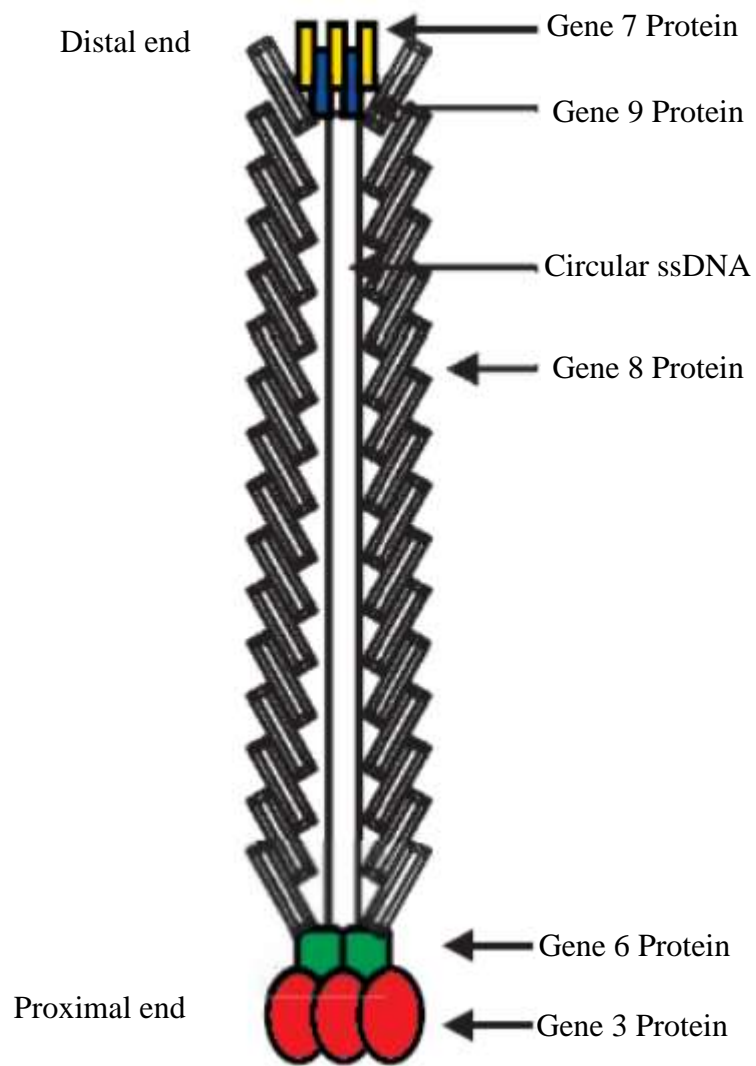


Fig. 1.6: Schematic representation of bacteriophage M13. (Taken from Stopar *et al.*, 2003)

protein to the F pilus of *E. coli*. The circular single-stranded DNA then enters the bacteria and is subsequently converted into a double-stranded replicative form by the host DNA replication machinery (Arap, 2005). By rolling circle replication, the replicative form serves as template for the production of single-stranded DNA. These progeny single strands are released from the cell as filamentous particles following morphogenesis at the cell membrane. A characteristic feature of these coliphages is that replication of the phage DNA does not result in host cell lysis. Rather infected cells continue to grow and divide, albeit at a slower rate than uninfected cells, and extrude virus particles. Up to 1000 phage particles may be released into the medium per cell generation (Russel, 1991).

1.9.3 Coat proteins and vectors used for display, and selection of desired clones

Most of the phage display vectors use the N-terminus of the gp3 or gp8 proteins to display foreign peptides or proteins (Smith and Scott, 1993; Winter *et al.*, 1994; Iannolo *et al.*, 1995; Malik *et al.*, 1996). The 406-amino-acid gp3 protein has two functional domains, *i.e.* an exposed N-terminal domain that binds the F pilus but is not required for phage particle assembly, and a C-terminal domain that is buried in the particle and is an integral part of the capsid structure (Parmley and Smith, 1988). Large peptide inserts of up to 38 amino acids can be introduced into N-terminus terminus of the gp3 protein without the loss of phage infectivity or particle assembly (Arap, 2005). In the phage particle, the 50-amino-acid gp8 protein is largely α -helical with four to five flexible unstructured amino acid residues in the N-terminus. Since the helical lattice positions of the neighbouring N-terminal arms are about 2.7 nm apart, the space between them can be filled with extra amino acids genetically added to the N-terminus of the gp8 coat protein. In this instance, up to 10 amino acids can be added without significantly impairing the viability of the phage (Makowski, 1994; Stopar *et al.*, 2003).

In early examples of phage display, a DNA fragment was inserted into either the gp3 or gp8 gene at the junction between the signal sequence and the native peptide on the phage genome (Smith, 1985; McCafferty *et al.*, 1990; Kang *et al.*, 1991). *E. coli* transfected with the recombinant phages secreted phage particles that displayed on their surface the amino acids encoded by the foreign DNA. As indicated above, a disadvantage of this method of phage display is that polypeptide inserts greater than 10 residues compromise gp8 coat protein function and so cannot be efficiently displayed. This problem has been solved by the use of

phagemid display. In this system, the starting-point is a phagemid plasmid carrying a single copy of the gp3 or gp8 gene. A major advantage of phagemid vectors is their smaller size and ease of cloning, compared to the difficulties of cloning into phage vectors without disrupting the complex structure of overlapping genes, promoters and terminators. This generally translates into much higher library sizes for phagemid vectors (Ponsel *et al.*, 2011). As before, the DNA fragment is inserted into the gp3 or gp8 gene downstream from the signal peptide cleavage site and the construct transformed into *E. coli*. Phage particles displaying the amino acid sequence encoded by the DNA insert are obtained by superinfecting the transformed cells with helper phage. The resulting phage particles are phenotypically mixed and their surfaces are a mosaic of normal coat protein and fusion protein (Barbas and Richard, 1991; Kay and Hoess, 1996; Smith and Petrenko, 1997; Ponsel *et al.*, 2011).

Following the construction of a phage display library or the amplification of an existing library, particular phage-displayed peptides, proteins or antibody fragments can be isolated by a process called panning (Parmley and Smith, 1988). In general, this affinity selection of ligands from the phage display library involves a number of fundamental steps (Fig. 1.7). After preparation of a primary library, the phage particles are exposed to the target for which specific ligands are to be identified. This is followed by removal of non-specific binders by washing and then the target bound phage can be recovered by elution or by direct bacterial infection and amplification of the recovered phage (Parmley and Smith, 1988; Laffly and Sodoyer, 2005). This panning process can be repeated four to six times until a population of best binders is enriched.

1.10 ANTIBODY PHAGE DISPLAY LIBRARIES

The raw material needed for the construction of antibody phage libraries is the V-genes that encode the variable domains of the mammalian antibody. Two different types of antibody phage display libraries exist, an immune library that is derived from animals immunized with a target antigen and a naïve library that is derived from non-immunized animals (Willats, 2002).

1.10.1 Immune libraries

Following immunization with a desired target antigen, IgG sequences are derived from the

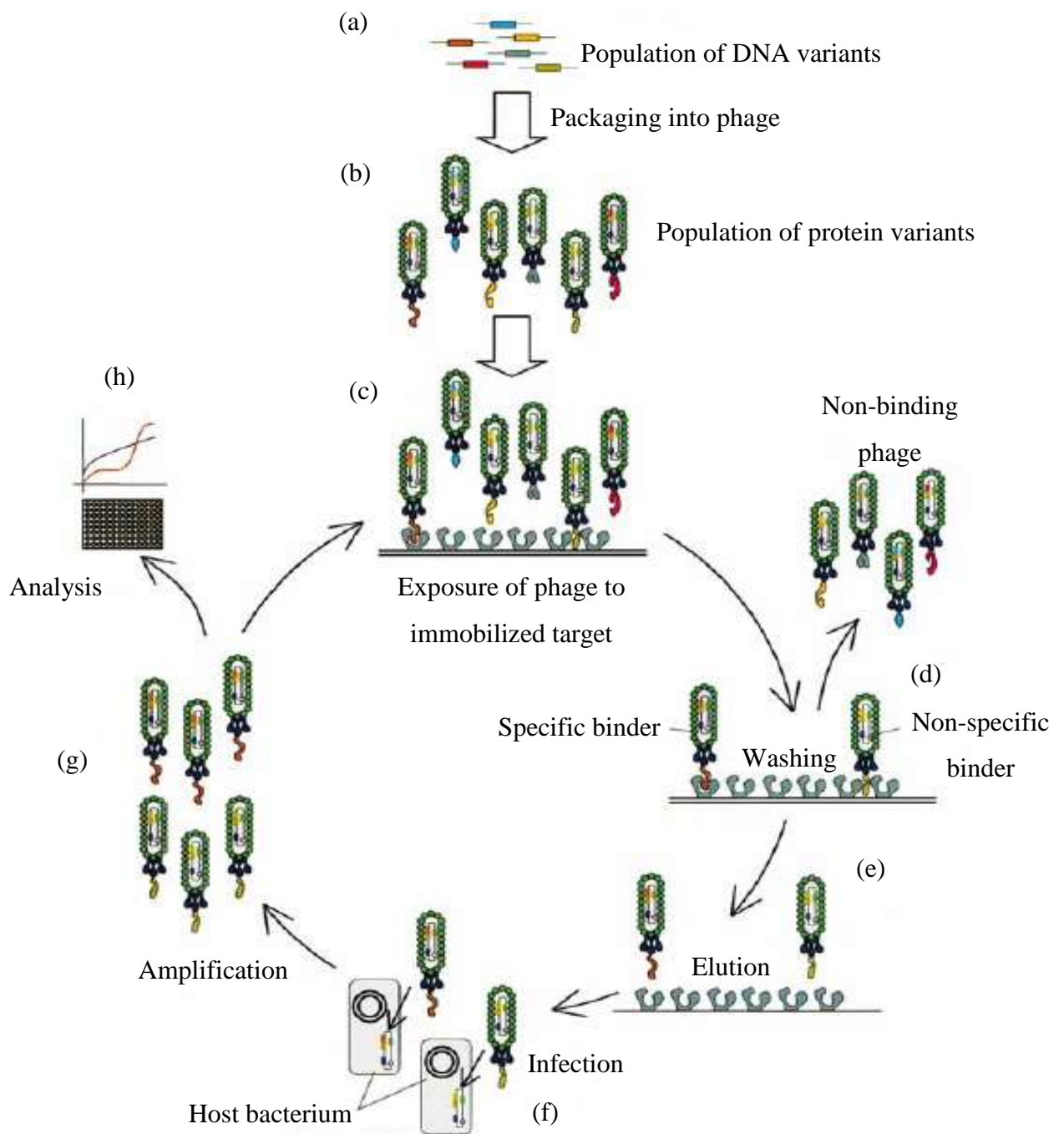


Fig. 1.7: The phage display cycle. A library of variant DNA sequences is created (a) and cloned into phage genomes or phagemid plasmids as fusions to a coat protein gene (b). The phage library displaying variant peptides or proteins is exposed to target molecules and target-specific phages are captured (c). Non-binding phages are washed off (d), whereas bound phages are eluted (e) and used to infect host bacterial cells (f) and thereby amplified. The amplified phage population is greatly enriched for phages displaying peptides or proteins that bind to the target (g). If the panning steps (c) to (f) are repeated the phage population becomes less diverse, but more enriched for target-specific binders. After several rounds of panning, monoclonal phage populations may be selected and analyzed individually (h). (Taken from Willats, 2002)

spleen B cells and the repertoires of isolated V-genes are manipulated and packaged into phage library vectors to create an immune library. The V-genes are specifically chosen, as it is anticipated that selection and affinity maturation of sequences with specificity for the target antigen will have already occurred *in vivo* (Clackson *et al.*, 1991). Therefore, such libraries are pre-biased towards containing antibody fragments with desirable affinities and specificities (Hoogenboom *et al.*, 1998). Although the high affinity of immune libraries towards the desired target antigen is an advantage, it can also be a disadvantage in the sense that if the antigen does not elicit an immune response due to tolerance mechanisms or toxicity no enrichment occurs (Hoogenboom *et al.*, 1998). Furthermore, the diversity is dependent on the immune response of the animal to the antigen and this process may take a long time and will differ from animal to animal (Brichta *et al.*, 2005). Immune libraries may also contain antibodies against antigens that were not used for immunization (Williamson *et al.*, 1997; Bradbury and Marks, 2004). Furthermore, new libraries need to be constructed for every antigen to be tested, a process that can be costly and has a significant ethical impact. Despite these drawbacks, immune libraries have been created successfully using mice (Clackson *et al.*, 1991; Kettleborough *et al.*, 1994), humans (Barbas, 1993; Cai and Garen, 1995), chickens (Davies *et al.*, 1995; Yamanaka *et al.*, 1996), rabbits (Lang *et al.*, 1996) and camels (Arbabi Ghahroudi *et al.*, 1997).

1.10.2 Naïve libraries

The antibody repertoire of non-immunized (naïve) animals is composed mainly of IgMs, which have wide specificity to a variety of different antigens. Therefore, naïve libraries are composed of germline V-gene sequences that are reverse transcribed and amplified from B cell RNA, and the Ig heavy and light chain variable regions are combined randomly to create a naïve library (Winter *et al.*, 1994; Hoogenboom, 1997). Unlike immune libraries that need to be constructed for each target antigen, naïve libraries are not biased to a specific target (Gram *et al.*, 1992; Sheets *et al.*, 1998; De Haard *et al.*, 1999; Van Wyngaardt *et al.*, 2004). Consequently, a single naïve library, which represents the primary repertoire of the donor animal, can be used for the selection of antibodies against a wide variety of antigens (Brichta *et al.*, 2005; Ponsel *et al.*, 2011). Naïve libraries are often referred to as “single-pot” libraries due to their broad specificity (Nissim *et al.*, 1994). Although the construction of naïve libraries can be time-consuming, require expert skills and need to have a large repertoire to be useful, they can produce results rapidly once constructed.

Naïve libraries can be further divided into semi-synthetic and synthetic libraries, and are distinguished on the basis of the origin of the sequences that were used to create the library. Naïve libraries are derived from natural sources, whereas as semi-synthetic and synthetic libraries are “built” *in vitro*. Semi-synthetic libraries are constructed with V-genes that have been rearranged *in vivo* and linked to CDRs of varying length that have either been partially or completely randomized using synthetic oligonucleotide sequences (Griffiths *et al.*, 1994; Nissim *et al.*, 1994; De Kruif *et al.*, 1995; Carmen and Jermutus, 2002; Van Wyngaardt *et al.*, 2004). In the case of synthetic libraries, the CDR sequence of selected frameworks is modified by introducing mutations (Barbas *et al.*, 1992; Hoogenboom and Winter, 1992; Hoogenboom, 1997). The introduction of such variability into a library can greatly increase the library’s antibody repertoire. The CDR3 region is normally randomized and spliced with J regions in the construction of synthetic and semi-synthetic libraries (Hoogenboom and Winter, 1992; Hoogenboom *et al.*, 1998), as the amino acids residues comprising this region are highly variable and contribute to the antigen binding domain in humans and mice (Chothia and Lesk, 1987; Kabat and Wu, 1991; Barbas *et al.*, 1992; Xu and Davis, 2000).

1.11 AIMS OF THIS STUDY

It is well accepted that virus-neutralizing antibodies are the most important factor imparting protection against FMDV (Pay and Hingley, 1987; McCullough *et al.*, 1992; Salt, 1993). To date, several immunodominant neutralizing antigenic sites have been described on structural protrusions located in the three surface-exposed capsid proteins of the virus. However, immunoglobulin-specific protection can be attained in the absence of a response to these immunodominant neutralizing epitopes (Dunn *et al.*, 1998), indicating the existence of other unidentified epitopes. Information regarding the antigenic structure of FMDV may contribute to an increased understanding of the interactions between the virus and the host immune system, and can also assist in the design of improved vaccines.

Consequently, several studies have been performed previously to determine the neutralizing antigenic sites of representative viruses from serotypes A, O, C and Asia-1. Although monoclonal antibodies are frequently used for this purpose, recombinant antibodies obtained from phage display libraries have also been used with success to map epitopes of serotype O

viruses (Harmsen *et al.*, 2007; Yu *et al.*, 2011) and other animal viruses, including African swine fever virus (Wang and Yu, 2009) and Bluetongue virus (Wang *et al.*, 1995; Qin *et al.*, 2013). In this regard, a phage display library, known as the Nkuku[®] library, was constructed by the New Generations Vaccines Programme at the ARC-OVI (Van Wyngaardt *et al.*, 2004). This library comprises the naïve immunoglobulin repertoire of the chicken and is sufficiently diverse to recognize a variety of different haptens, proteins and viruses (Fehrsen *et al.*, 2005; Rakabe, 2008; Sixholo, 2008; Wemmer *et al.*, 2010). These results thus suggest that the Nkuku[®] library is a potentially valuable resource from which recombinant antibodies against FMDV may be readily obtained.

In contrast to the Euro-Asia FMDV serotypes, there is limited information regarding antigenic sites of the SAT serotypes. Amongst SAT viruses, the SAT2 type viruses are responsible for most of the FMD outbreaks in domestic animals in southern Africa, followed by SAT1 and SAT3 (Maree *et al.*, 2011). The control of FMD in southern Africa relies on combinations of SAT1, SAT2 and SAT3 vaccine antigens relevant to a specific geographic area. However, SAT2 vaccine antigens are believed to be weakly immunogenic and induce a narrow immunogenic response. In addition, SAT2 serotype viruses are highly variable, necessitating frequent development of new vaccine strains. Therefore, there is a need to develop novel SAT2 vaccines that induce a broad immunogenic response. To achieve this, the antigenic composition of a SAT2 virus, ZIM/7/83, and the role of these antigenic regions in interacting with antibodies were investigated. SAT2/ZIM/7/83 is a bovine-outbreak virus originating from western Zimbabwe and was selected as a vaccine seed virus in the SAT bivalent and trivalent vaccines used in southern Africa. Furthermore, SAT2/ZIM/7/83 displays most of the recommended characteristics suggested for a FMD vaccine, namely rapid and regular growth in cell systems with high virus yields, high content of immunizing antigen in virus harvests and appropriate serological (subtype) specificity (Rweyemamu *et al.*, 1978; Doel, 2003).

The primary aim of this investigation was thus to map antigenic sites on the capsid of the SAT2/ZIM/7/83 virus, and to shed some light on the epitope dominance within the SAT2 serotype. To this end, the specific objectives were the following:

- 1) To isolate and characterize SAT2-specific phage binders from the Nkuku[®] phage display library.

- 2) To map antigenic sites of the SAT2/ZIM/7/83 virus utilizing the SAT2-specific phage displayed binders.

- 3) To determine the role of known and predicted epitopes in the antigenicity of SAT2 viruses, and to identify additional SAT2/ZIM/7/83 antigenic sites utilizing an epitope-replacement approach.

CHAPTER TWO

IDENTIFICATION AND CHARACTERIZATION OF SAT2/ZIM/7/83-SPECIFIC BINDERS FROM THE NKUKU® CHICKEN PHAGE DISPLAY LIBRARY

2.1 INTRODUCTION

Monoclonal antibodies (MAbs) have various academic, medical and commercial applications, ranging from diagnostic testing (Biotech, 1989) to the mapping of viral epitopes (Bolwell *et al.*, 1989; Dubs *et al.*, 1992; Barnett *et al.*, 1998; Mateu *et al.*, 1998). Classically, MAbs are generated by making use of immunization and murine hybridoma technology. This approach, first reported in 1975, relies on the fusion of mouse myeloma cells with B lymphocytes from immunized mice, thus resulting in antibody-producing somatic cell hybrids (Kohler and Milstein, 1975). However, advances in molecular biology have made it possible to produce recombinant antibodies by using the Gram-negative bacterium *Escherichia coli* (Hoogenboom *et al.*, 1991). Antibody fragments such as the antigen binding fragment (Fab), antigen variable fragment (Fv) and linker-stabilized single chain (sc) Fv have all been expressed in *E. coli* or displayed as fusions to phage coat proteins (Griffiths and Duncan, 1998).

The concept of phage display was first introduced by Smith in 1985. Fragments of the *EcoRI* restriction endonuclease enzyme were displayed as polypeptide fusions to the gene 3 coat protein of the f1 phage particle, allowing the peptides to be displayed on the surface of the mature phage particle. Subsequently, McCafferty *et al.* (1994) demonstrated the display of functional antibody fragments in phages by successfully introducing the V_H and V_L fragments of the anti-lysozyme antibody, with a linker, into the N-terminus of the gene 3 coat protein of a phage vector. A major advantage associated with the use of phage display technology as a means to generate antibodies, as opposed to the traditional hybridoma technology, is that access to naïve libraries can result in the rapid (three weeks) generation of antigen-specific scFv or Fab. In contrast, antibody production using hybridoma technology takes a minimum of five to six months (Smith, 1985; Clackson *et al.*, 1991; Greenwell and Rughooputh, 2001; Carmen and Jermutus, 2002).

Although most of the large combinatorial libraries are based on human immunoglobulin genes, phage antibodies, however, can be derived from a number of alternative donors such as camels (Arbabi Ghahroudi *et al.*, 1997), llamas (Koh *et al.*, 2010), cattle (O'Brien *et al.*, 1999), rabbits (Ridder *et al.*, 1995), sheep (Li *et al.*, 2000) and chickens (Davies *et al.*, 1995). The chicken is a particularly attractive source of immunoglobulin genes, since the chicken antibody repertoire can be accessed relatively easily because of the way in which its diversity is generated. Molecular diversity in the immunoglobulins of mammals occurs through the

somatic recombination of a diverse set of variable (V), diversity (D) and joining (J) gene segments of the heavy (H) and light (L) chains (Tonegawa, 1983). In contrast, only one functional V and J gene segment exists in the single immunoglobulin H and L chain loci of chickens. These regions undergo V(D)J rearrangement; VJ rearrangement occurs in the light chain and VDJ rearrangement in the heavy chain. Diversity occurs by gene conversion, in which sequences are transplanted from upstream pseudogenes in both heavy and light chain V regions and is generated in such a way that all V regions in mature B cells have essentially identical amino acid sequences at both termini (Reynaud *et al.*, 1985; Reynaud *et al.*, 1987; Thompson *et al.*, 1987; Reynaud *et al.*, 1989; Davies *et al.*, 1995). Thus, the amplification of V region genes in chickens is greatly simplified such that the entire naïve antibody repertoire of a chicken can be PCR amplified using one set of oligonucleotides for the H chain and another for the L chain. This is in sharp contrast to mammals where a number of PCR oligonucleotide sets are required to amplify each of the V gene segments. The potential of the chicken as a source of recombinant antibody fragments was demonstrated by Davies *et al.* (1995) who constructed a small naïve library (2.7×10^7 clones) that yielded scFv phage antibodies against three different proteins.

More recently the construction of a large phagemid-based chicken scFv library, known as the Nkuku[®] library, was reported. The Nkuku[®] library comprises the naïve immunoglobulin repertoire of the chicken; however, in order to maximize the number of possible paratopes that can be obtained, synthetically randomized sequences of the H chain in the CDR3 region were incorporated (Van Wyngaardt *et al.*, 2004). The amino acids comprising the CDR3 of the chicken IgY, like that of mammalian IgG, display the most variability and contribute greatly to antigen binding (Chothia and Lesk, 1987; Kabat and Wu, 1991). The *ca.* 2×10^9 clones comprising the Nkuku[®] library have been shown to be sufficiently diverse for recognition of a variety of different haptens, proteins and viruses (Van Wyngaardt *et al.*, 2004; Fehrsen *et al.*, 2005; Rakabe, 2008; Sixholo, 2008; Wemmer *et al.*, 2010).

Based on the above, the primary objectives of this part of the study were to select and characterize recombinant antibody fragments from the Nkuku[®] library directed against the foot-and-mouth disease virus (FMDV), SAT2/ZIM/7/83. This virus has been used for many years with great success as a SAT2 vaccine strain at the Transboundary Animal Diseases Programme of the Agricultural Research Council, Onderstepoort Veterinary Institute (TADP-ARC-OVI). It can be envisaged that the identification of SAT2/ZIM/7/83-specific antibodies

will greatly facilitate the mapping of antigenic sites on the SAT2 virus, which could ultimately be used in the rational design of more effective FMD vaccines for use in southern Africa. Since recombinant antibodies are relatively cheap to produce, they may also enable the development of cheaper diagnostic assays (Bahara *et al.*, 2013). In particular, chicken recombinant antibodies have become popular in diagnostic research due to their robust nature (Narat, 2003; Nilsson *et al.*, 2007) and their lack of cross-reactivity with mammalian antibodies (Larsson *et al.*, 1991; Shimamoto *et al.*, 2005).

2.2 MATERIALS AND METHODS

2.2.1 Cell cultures and virus

Baby hamster kidney (BHK) cells strain 21 clone 13 (ATCC CCL-10) were maintained in Eagle's Basal Medium (BME; Invitrogen) supplemented with 10% (v/v) foetal calf serum (FCS; Delta Bioproducts), 1× antibiotic-antimycotic solution (Invitrogen), 1 mM L-glutamine (Invitrogen) and 10% (v/v) tryptose phosphate broth (TPB; Sigma-Aldrich). The Myc1-9E10 murine hybridoma (ECACC 85102202), which expresses the anti-c-Myc MAb 9E10, was obtained from the European Collection of Cell Cultures (CAMR, UK) and cultured in protein-free hybridoma medium (Invitrogen).

The SAT2 FMDV vaccine strain SAT2/ZIM/7/83 (passage history: B₁BHK₅B₁; B=bovine) is a bovine virus that originated from an outbreak in western Zimbabwe during 1983 (Van Rensburg *et al.*, 2004).

2.2.2 Virus purification

Confluent BHK-21 cell monolayers (12 × 750 cm² plastic roller bottles; Corning) were infected with SAT2/ZIM/7/83 in BME medium containing 1× antibiotic-antimycotic solution and 25 mM HEPES buffer. Following incubation for 12-16 h at 37°C, the cells in each roller bottle were lysed by addition of 600 µl of 10% (v/v) Triton X-100 and 2.4 ml of 0.5 M EDTA (pH > 7.4). The supernatants were pooled and subjected to centrifugation at 9800 × g for 30 min. The 146S virus particles were precipitated from the recovered supernatant with 8% (w/v) polyethylene glycol (PEG)-8000 (Sigma-Aldrich) at 4°C for 3 h, collected by centrifugation and suspended in 10 ml of TNE buffer (50 mM Tris [pH 7.5], 150 mM NaCl, 10 mM EDTA). An additional clarification step was performed by addition of 300 µl of 0.5 M EDTA and centrifugation at 9800 × g for 30 min. The virus particles were purified on a

10-50% (w/v) sucrose density gradient (SDG), prepared in TNE buffer, as described by Knipe *et al.* (1997). The gradients were centrifuged in a Beckman ultracentrifuge at $46\,000 \times g$ for 17 h. Fractions of 1.5 ml were collected from the bottom of the gradient, and the absorbance at wavelengths of 259 nm and 280 nm was determined on a Nanodrop™ ND 1000 spectrophotometer. Peak fractions corresponding to 146S virion particles (extinction coefficient $E_{259\text{nm}}[1\%] = 78.8$) were pooled and the amount of antigen (μg) was calculated as described previously (Doel and Mowat, 1985).

2.2.3 SDS-polyacrylamide gel electrophoresis (SDS-PAGE)

An aliquot (20 μl) of the pooled peak fractions, corresponding to the 146S virion particles, was mixed with an equal volume of $2 \times$ PSB buffer (20% [v/v] glycerol, 10% [v/v] β -mercaptoethanol, 6% [w/v] SDS, 0.125 M Tris, 0.15 mM bromophenol blue) and heated to 95°C for 3 min. The samples were subsequently analyzed by SDS-PAGE as described by Laemmli (1970). A 5% (w/v) acrylamide stacking gel and 12% (w/v) acrylamide separating gel was used, of which the acrylamide:bisacrylamide ratio was 30:0.8. The low-porosity separating gel (0.375 M Tris-HCl [pH 8.8]; 0.1% [w/v] SDS) and high-porosity stacking gel (0.125 M Tris-HCl [pH 6.8]; 0.1% [w/v] SDS) were each polymerized by addition of 0.1% (w/v) ammonium persulfate and 0.001% (v/v) TEMED. The TGS electrophoresis buffer consisted of 25 mM Tris, 2 M glycine and 0.1% [w/v] SDS, and electrophoresis was performed at 120 V and 30 mA for 2-3 h. Following electrophoresis, the gels were stained for 1 h with Gelcode® blue stain reagent (Pierce) and then destained in distilled water.

2.2.4 Preparation of M13K07 helper phage

2.2.4.1 Large scale production of M13K07 helper phage

Escherichia coli TG1 (Stratagene) was cultured in $2 \times$ TY medium (1.6% [w/v] tryptone, 1% [w/v] yeast extract, 0.5% [w/v] NaCl) overnight at 37°C with shaking. The culture was then diluted 100-fold into fresh medium and incubated until an OD_{600} of 0.5 was reached. A serial dilution of M13K07 helper phage, kindly provided by Mr W. Van Wyngaardt, ARC-OVI, was prepared in $2 \times$ TY medium, and infected into the *E. coli* TG1 cells for 10 min at 37°C without shaking. The phage-infected cells were subsequently added to pre-warmed (44°C) molten H-top agar (0.8% [w/v] NaCl, 1% [w/v] bacto-agar, 0.6% [w/v] agar), mixed and poured on the surface of TYE agar plates (1% [w/v] tryptone, 0.5% [w/v] yeast extract, 0.8% [w/v] NaCl, 1.5% [w/v] agar) supplemented with 20% (w/v) glucose and 100 $\mu\text{g/ml}$

ampicillin (Roche Diagnostics). Following incubation overnight at 37°C, a single plaque was picked and inoculated into 4 ml of 2 × TY medium containing 40 µl of an overnight *E. coli* TG1 culture. The culture was incubated for 2 h at 37°C with shaking (240 rpm), diluted into 800 ml of fresh medium and then incubated for 1 h. Subsequently, kanamycin (Roche Diagnostics) was added to a final concentration of 50 µg/ml and the culture was incubated overnight at 37°C. The bacterial cells were harvested by centrifugation at 10 800 × g for 15 min at 4°C. The phages were precipitated from the cell-free culture supernatant by addition of 200 ml of a 20% (w/v) PEG-8000/2.5 M NaCl solution and, after incubation on ice for 30 min, were collected by centrifugation (10 800 × g, 15 min, 4°C). The phage particles were suspended in 12 ml of 1 × PBS, filter-sterilized with a Minisart® 0.22-µm filter (Sartorius) and then titrated.

2.2.4.2 Titration of M13K07 helper phage

Serial dilutions of the newly prepared M13K07 helper phage (10^{-2} to 10^{-10}), prepared in 2 × TY medium, were infected into mid-logarithmic *E. coli* TG1 cells for 10 min at 37°C. Following infection, equal volumes (100 µl) of the M13K07 dilution and an overnight *E. coli* TG1 culture were added to pre-warmed (44°C) molten H-Top agar, poured on the surface of TYE agar plates supplemented with 20% (w/v) glucose and 100 µg/ml ampicillin, and incubated at 37°C overnight. The titre was calculated and the M13K07 helper phage stock was diluted to 2×10^{12} plaque forming units (pfu)/ml by addition of 1 × PBS prior to storage at -80°C in 50% (v/v) glycerol.

2.2.5 Selection of phage-displayed scFvs against SAT2/ZIM/7/83

Selection of SAT2/ZIM/7/83-specific binders from the Nkuku® phage display library (provided by Dr. D.H. du Plessis, ARC-OVI) was performed as described by Van Wyngaardt *et al.* (2004). For this purpose, 2-ml Maxisorp™ immunotubes (Nunc) were coated overnight at 4°C with 30 µg/ml of purified SAT2/ZIM/7/83, diluted in 1 × PBS. The coating solution was discarded and all subsequent steps were performed at room temperature. The immunotubes were blocked for 1 h with 1 × PBS containing 2% (w/v) casein, and then washed twice with 1 × PBS containing 0.1% (v/v) Tween-20 (PBS/T) and twice with 1 × PBS. Library phage particles (10^{12} - 10^{13} transducing particles), diluted in 2% (w/v) casein and PBS/T, were added to each immunotube and incubated for 1.5 h. Unbound phage particles were removed by washing 20 times with PBS/T, followed by a further 20 washes with 1 ×

PBS. Phage-displayed scFvs that bound to SAT2/ZIM/7/83 were eluted by incubation for 10 min with 1 ml of 100 mM triethylamine (pH 12) and then neutralized by addition of 0.5 ml of 1 M Tris (pH 7.4). The neutralized eluate was used to re-infect exponentially growing *E. coli* TG1 cells before plating on TYE agar plates supplemented with 2% (w/v) glucose and 100 µg/ml ampicillin. Following incubation overnight at 30°C the bacteria were collected and the phagemids rescued by addition of M13K07 helper phage (helper phage:bacteria = 20:1). Infected bacterial cells were incubated overnight at 30°C in 2 × TY medium that contained 100 µg/ml ampicillin and 25 µg/ml kanamycin. Phage-displayed scFvs were subsequently precipitated from the cell-free culture supernatant with one-fifth of the original culture volume of a 20% (w/v) PEG-8000/2.5 M NaCl solution and were then suspended in 1 × PBS for use in the next selection round. Five such selection rounds were performed.

Enrichment was monitored by titration of the input and output phages from each selection round, as well as a polyclonal ELISA of the outputs of the consecutive selection rounds. Monoclonal phage-displayed and soluble scFvs from selection rounds four and five were tested for specific binding to SAT2/ZIM/7/83.

2.2.6 Polyclonal phage enzyme-linked immunosorbent assay (ELISA)

The polyclonal phage ELISA (Van Wyngaardt *et al.*, 2004) was performed by coating 96-well Maxisorp™ immunoplates (Nunc) overnight at 4°C with purified SAT2/ZIM/7/83 (30 µg/ml). Casein (2% [w/v]) in 1 × PBS was used as blocking reagent and negative control to verify the SAT2/ZIM/7/83 specificity of the phage-displayed scFvs. Following blocking for 1 h at 37°C, the plates were washed three times with PBS/T. Prior to their addition to the plates, PEG-precipitated phage-displayed scFvs were diluted 100-fold in 1 × PBS and 25 µl was mixed with an equal volume of 1 × PBS containing 4% (w/v) casein and 0.2% (v/v) Tween-20. The phage-displayed scFvs were added to the plates, incubated for 1 h at 37°C and then washed three times with PBS/T. The phage-displayed scFvs were detected with the MAb B62-FE2 (Progen Biotechnik), which is specific for an epitope on the gp8 phage coat protein of filamentous phages, and horseradish peroxidase (HRP)-conjugated polyclonal rabbit anti-mouse IgG (PO260; Dako). These antibodies were each diluted 1000-fold in PBS/T containing 2% (w/v) casein and incubation was for 1 h at 37°C. After a final wash the substrate/chromogen solution, consisting of 4 mM 3,3',5,5'-Tetramethylbenzidine (Sigma-Aldrich) in substrate buffer (0.1 M citric acid monohydrate, 0.1 M tri-potassium citrate; pH 4.5) and 0.015% (v/v) H₂O₂, was added. The colour reaction was stopped after 10 min with 1

M H₂SO₄ and the absorbance values were recorded at 450 nm with a Labsystems Multiscan Plus photometer.

2.2.7 Monoclonal phage ELISA

To screen monoclonal phage antibodies, individual clones were rescued by transferring inocula from bacterial colonies to the wells of a sterile 96-well cell culture plate (Nunc) containing 2 × TY medium supplemented with 100 µg/ml ampicillin and 2% (w/v) glucose. The bacteria were grown overnight at 30°C with shaking. Subsequently, a 96-well inoculation device (Sigma: Cat No R-2508) was used to transfer cells from the master plate to a second plate that contained 150 µl of fresh medium per well. Following incubation for 2.5 h at 37°C, 50 µl of medium that contained 2 × 10⁹ pfu/ml of the M13K07 helper phage was added to each well. The plate was incubated for 30 min at 37°C without shaking. After centrifugation at 600 × g for 10 min, the supernatants were removed and replaced with 150 µl of 2 × TY medium containing 100 µg/ml ampicillin and 25 µg/ml kanamycin. The plate was then incubated overnight at 30°C with shaking. The bacterial cells were pelleted by centrifugation as above. The supernatants, containing the phage-displayed scFvs, were collected and mixed 1:1 with 1 × PBS containing 4% (w/v) casein and 0.2 % (v/v) Tween-20 prior to testing in ELISA. The monoclonal phage ELISA was performed as described above for the polyclonal phage ELISA.

2.2.8 Monoclonal soluble scFv ELISA

The monoclonal soluble scFv ELISA was performed as described previously by Van Wyngaardt *et al.* (2004). Briefly, soluble scFvs were obtained by inoculating 2 µl of overnight cultures of infected bacterial cells into 100 µl of 2 × TY medium containing 100 µg/ml ampicillin and 0.1% (w/v) glucose. Following incubation for 3 h at 37°C, expression of soluble scFvs was induced by addition of 50 µl of 2 × TY medium containing 100 µg/ml ampicillin and 1 mM IPTG. Incubation was continued for a further 16 h at 30°C. The bacterial cells were pelleted by centrifugation at 600 × g for 10 min and the supernatants, containing the expressed soluble scFvs, were tested in ELISA. Antigen coating of the ELISA plates and all other steps performed were as described for the polyclonal phage ELISA (Section 2.2.6), except that the soluble scFvs were mixed with an equal volume (25 µl) of 1 × PBS containing 4% (w/v) of casein and the plates were washed with 1 × PBS containing 0.05% (v/v) Tween-20. The *c-myc* epitope tag, located at the carboxyl-terminal end of the

soluble scFv, was detected with the anti-c-Myc MAb 9E10 (diluted 1:1 in 1 × PBS containing 4% [w/v] casein), and polyclonal rabbit anti-mouse IgG conjugated to HRP (P0260).

2.2.9 DNA sequencing of phage-displayed scFvs and sequence analysis

Phagemid DNA was isolated with a QIAprep[®] Spin Miniprep Kit (Qiagen) from clones picked from selection rounds four and five that were specific for SAT2/ZIM/7/83. The phagemid DNA was submitted to the Molecular Biology Division of OVI and Inqaba Biotechnical Industries for nucleotide sequencing. The cloned inserts were sequenced with 0.16 μM of the OP52 forward primer (5'-CCCTCATAGTTAGCGTAACG-3'; Van Wyngaardt *et al.*, 2004) and the M13 reverse primer (5'-CAGGAAACAGCTATGAC-3'), and the ABI PRISM[™] Big Dye[™] Terminator Cycling Ready Reaction kit v3.0 (Applied Biosystems). The extension products were resolved on an Applied Biosystems Model 3100 automated DNA sequencer, and the nucleotide sequences obtained were assembled and translated using BioEdit v.7.0.9 (Hall, 1999).

2.2.10 Characterization of SAT2/ZIM/7/83-specific binders

2.2.10.1 Large scale purification of soluble scFvs

Large scale purification of soluble scFvs from 1-L cultures was performed by the Biotechnology Division of the National Bioproducts Unit in Kwa-Zulu Natal, South Africa, on an affinity column that contained 75 ml Sepharose coupled to 100 mg of the Myc tag-specific MAb, 9E10.

2.2.10.2 Binding specificity of phage-displayed and soluble scFvs

The specificity of phage-displayed and soluble scFvs was tested on representative SAT1 and SAT3 viruses, propagated and purified as described in Section 2.2.2. ELISA plates were coated in duplicate with 30 μg/ml of purified SAT2/ZIM/7/83, SAT1/KNP/196/91, SAT3/KNP/10/90, as well as with 30% (w/v) sucrose, 2% (w/v) casein and a BHK-21 cell extract as negative controls. The ELISAs were subsequently performed as described for the monoclonal phage ELISA (Section 2.2.7) and monoclonal soluble scFv ELISA (Section 2.2.8).

2.2.10.3 Sensitivity of SAT2/ZIM/7/83-specific binders

Maxisorp™ immunoplates were coated overnight at 4°C with various concentrations of phage-displayed or affinity-purified soluble scFvs. The phage-displayed and soluble scFvs were applied across the plate and diluted two-fold in 1 × PBS down the plate. The starting concentration (in phage particles/ml) of phage-scFv1 and -scFv2 was 6.9×10^9 and 2.15×10^{13} , respectively. Due to the low yield of phage-scFv3, it was excluded from the assay. The starting concentration of affinity column-purified soluble scFv1, 2 and 3 was 163 µg/ml, 171 µg/ml and 181 µg/ml, respectively. Casein (2% [w/v]) in 1 × PBS was used as blocking reagent and as a negative control. After blocking, the plates were washed with PBS/T and a SAT2/ZIM/7/83 cell culture-infected supernatant (diluted 1:20 in 2% [w/v] casein) was applied to the plates. Following incubation for 1 h at 37°C, bound SAT2/ZIM/7/83 virus was detected by incubating for 1 h at 37°C with SAT2-specific guinea pig antiserum (diluted 50-fold in 2% [w/v] casein), followed by incubation for 1 h with an HRP anti-guinea pig conjugate (diluted 80-fold in 0.5% [w/v] casein). After a final wash, the ELISA plates were processed as described above (Section 2.2.6).

In an alternative approach to measuring the sensitivity of SAT2/ZIM/7/83-specific soluble scFvs, Maxisorp™ immunoplates were coated overnight at 4°C with two-fold dilutions (from 30 to 0.234 µg/ml) of purified SAT2/ZIM/7/83, diluted in 1 × PBS. The ELISA plates were blocked with 2% (w/v) casein, washed and affinity-purified soluble scFvs, diluted 1:1 in 1 × PBS containing 4% (w/v) casein (final concentration of *ca.* 80 µg/ml), were added to each well. All steps were performed as described previously for the monoclonal soluble scFv ELISA (Section 2.2.8).

2.2.10.4 Stability of phage-displayed and soluble scFvs upon long-term storage

Samples of the phage-displayed and affinity-purified soluble scFvs were stored for a period of four months at 4°C. Each month, an aliquot was removed and tested in either the monoclonal phage or scFv ELISAs, as described above (Sections 2.2.7 and 2.2.8, respectively), for their ability to bind to immobilized SAT2/ZIM/7/83. Furthermore, the effect of freezing and thawing on samples of the phage-displayed and affinity-purified soluble scFvs that had been stored at -80°C and -20°C, respectively, was likewise assayed.

2.3 RESULTS

2.3.1 Selection and identification of phage-displayed scFvs against SAT2/ZIM/7/83

The Nkuku[®] library, a large semi-synthetic phage display library based on chicken immunoglobulin genes, was panned by exposing the recombinant antibody repertoire to purified virions of the SAT2 virus ZIM/7/83 (Fig. 2.1). Phage-displayed scFvs that bound to SAT2/ZIM/7/83 were eluted with triethylamine, and enrichment of phage-displayed scFvs specific for the purified SAT2/ZIM/7/83 virus was subsequently monitored by a polyclonal phage ELISA. Polyclonal phage outputs from the five consecutive selection rounds were tested and an aliquot of the library prior to panning was included as a non-enriched control (Fig. 2.2). The non-enriched control produced an absorbance at 450 nm of below 0.180, whereas the output from selection round five produced an absorbance of 2.14, thus indicating that phage pools were enriched with SAT2/ZIM/7/83-specific scFvs during consecutive selection rounds.

Single phage clones picked randomly from round four and five titre plates were subsequently tested in an ELISA to identify monoclonal SAT2/ZIM/7/83-specific binders. The scFvs were expressed in phage-displayed and soluble formats. A total of 188 single clones were screened of which 90 clones expressed phage-displayed scFvs specific to SAT2/ZIM/7/83 with ELISA signals two-fold greater than that of the negative casein controls. Of these, 73 clones secreted soluble scFvs that bound to SAT2/ZIM/7/83. Sequencing of the 73 clones revealed the presence of three unique scFvs binders (Table 2.1), designated scFv1 (27 identical clones), scFv2 (43 identical clones) and scFv3 (3 identical clones) that produced signals of 0.239, 1.770 and 1.23, respectively, in the monoclonal scFv ELISA. The corresponding phage-displayed scFvs produced signals of 2.165 (phage-scFv1), 2.482 (phage-scFv2) and 0.996 (phage-scFv3) in the monoclonal phage ELISA. These representative phage-displayed and soluble scFvs were further characterized.

2.3.2 Binding specificity of phage-displayed and soluble scFvs against FMDV

The SAT2/ZIM/7/83-specific binders were characterized on the basis of their ability to bind to complete 146S virions of representative viruses from the SAT1 and 3 serotypes. The binding of the various phage-displayed and soluble scFvs was determined by an indirect ELISA. In this assay, SAT2/ZIM/7/83 was included as a positive control. Furthermore, 30% sucrose, 2% casein and a BHK-21 cell extract were included as negative controls to verify that the

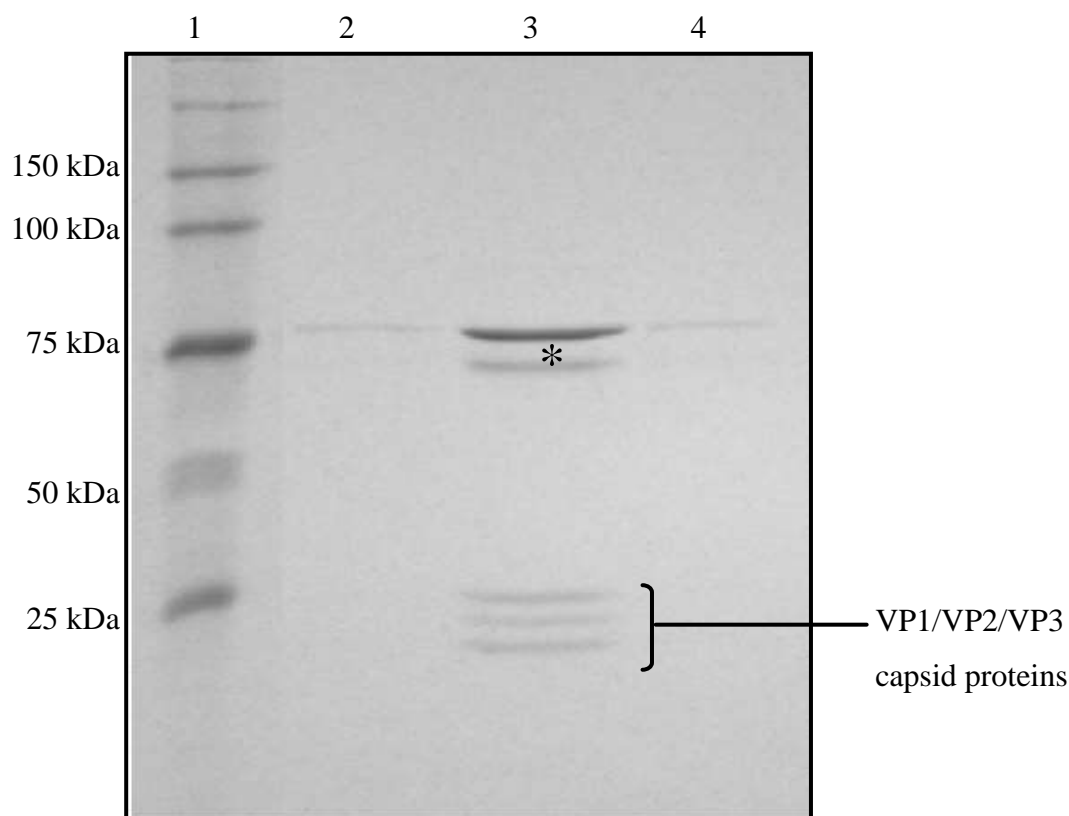


Fig. 2.1: SDS-PAGE analysis of sucrose density gradient (SDG)-purified SAT2/ZIM/7/83 virions with a sedimentation value of 146S. Proteins corresponding with the expected molecular mass of the three FMDV capsid proteins, *i.e.* VP2 (24.3 kDa), VP3 (24.6 kDa) and VP1 (24 kDa), are indicated with a bracket. Due to its small size, the internally located VP4 protein (8.5 kDa) could not be resolved on the 12% SDS-polyacrylamide gel. The 75-kDa protein, indicated by an asterisk, likely represents a tetrameric unit of the four capsid proteins due to incomplete denaturation of the protein sample. Lanes: 1, Broad Range Protein Molecular Weight Marker (Promega); 2, Fraction 7 of the SDSG; 3, Pooled peak fractions (fractions 8, 9 and 10); 4, Fraction 11 of the SDSG.

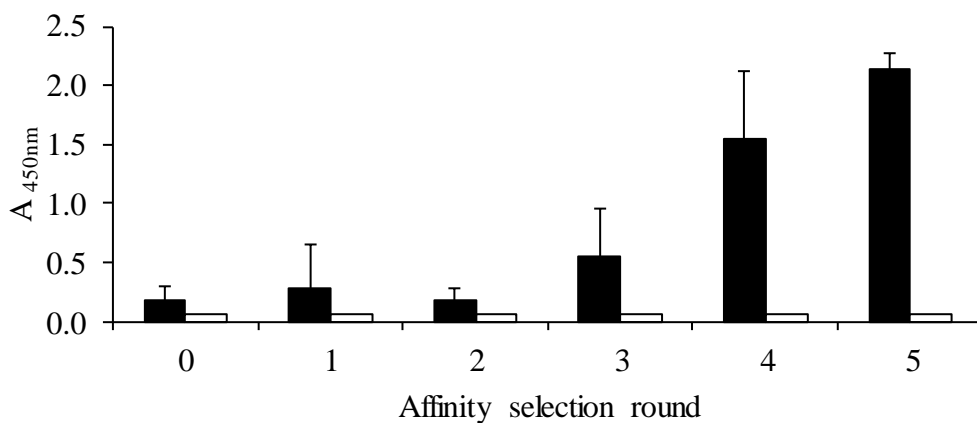


Fig. 2.2: Enrichment of phage-displayed scFvs specific for SAT2/ZIM/7/83. Phage-displayed scFvs were selected by panning on immobilized SAT2/ZIM/7/83 and enrichment of virus-specific phage-displayed scFvs (black bars) was monitored by a polyclonal phage ELISA of the outputs of five consecutive selection rounds (indicated as 1-5 on the x-axis). An aliquot of the Nkuku[®] phage display library prior to panning was included as a non-enriched control (indicated as 0) and 2% (w/v) casein was included as a negative control (white bars). The data are means \pm SD of three experiments.

Table 2.1: Amino acid sequence alignment of the complementary determining regions (CDR) of the heavy and light chains of the three ZIM/7/83-specific soluble scFvs panned from the Nkuku[®] library

	Heavy Chain			Light chain		
	Complementary Determining Region ^a			Complementary Determining Region ^a		
	CDR1	CDR2	CDR3	CDR1	CDR2	CDR3
scFv1	SYEMQ	AGIIDDGSSTYYAPAVKG	SGYDSSYYS-TAADIIDA	SGGGRYTYG	YNDKRPS	GSYGSS-TGI
scFv2	SYDMQ	AGIDDGGS FTGYGA AVKG	TTGSNWG YS---AHLIDA	SG SS-GS YG	YNDKRPS	GGYD SSTYAI
scFv3	SY GMG	AAIQND GSSTYY GA AVKG	DVYDCSSSCGIYGH IDA	SG GS-SS YG	YNDKRPS	GS RDSSN-PI

^a The CDR regions were annotated according to Andris-Widhopf *et al.* (2000) and sequence gaps were introduced to facilitate optimal alignment.

binders did not cross-react with reagents used during virus propagation or purification. The respective phage-displayed and soluble scFvs all bound to SAT2/ZIM/7/83 only. Since none of them bound to the SAT1 virus KNP/196/91 or the SAT3 virus KNP/10/90 (Fig. 2.3), these results suggest that the identified scFvs may therefore be specific to SAT2 viruses.

2.3.3 Sensitivity studies of the SAT2/ZIM/7/83-specific binders

Diagnostic assays investigate the statistical relationship between test results and the presence of disease. For all diagnostic tests there are two critical components that determine its accuracy, *i.e.* sensitivity and specificity. Since the specificity of the binders to SAT2/ZIM/7/83 was already confirmed, the sensitivity of the secreted soluble scFvs was further investigated. As test samples received in the laboratory can be of low concentrations and volumes, the minimal concentration of SAT2/ZIM/7/83 virus to which the soluble scFvs could bind was determined. The SAT2/ZIM/7/83 virus was diluted two-fold, from 30 to 0.234 µg/ml, and coated onto ELISA plates overnight. The following day, affinity-purified soluble scFvs were applied to the pre-coated ELISA plates. The cut-off for positive binding (*ca.* 0.254) was taken as twice that of the negative control, *i.e.* 2% (w/v) casein. Soluble scFv1 and 2 were successfully captured by SAT2/ZIM/7/83 at concentrations varying from 30 to 3.75 µg/ml (Fig. 2.4A-B). At a virus concentration of 1.875 µg/ml, an ELISA signal of 0.205 and 0.238, respectively, was obtained for soluble scFv1 and 2, which was below the cut-off value for positive binding. Soluble scFv3, however, was more sensitive as indicated by its ability to bind to lower concentrations of the SAT2/ZIM/7/83 virus, *i.e.* virus concentrations varying from 30 to 1.875 µg/ml (Fig. 2.4C). Thus, the results indicated that the soluble scFvs were all capable of binding to minimal concentrations of SAT2/ZIM/7/83 and that scFv3 was the most sensitive to SAT2/ZIM/7/83 detection.

As an alternative for the diagnostic assay, ELISA plates can be coated directly with phage-displayed or secreted soluble scFvs. Outbreak viruses received in the laboratory can thus be tested rapidly using pre-coated SAT2/ZIM/7/83-specific phage-displayed or soluble scFv ELISA plates. In order for such a diagnostic ELISA to be feasible, the ability of the phage-displayed and soluble scFvs to retain the correct conformation, as well as antigen-binding activity when immobilized directly onto polystyrene ELISA plates has to be determined. Towards this end, two-fold dilutions of the phage-displayed and affinity-purified soluble scFvs were made and coated directly onto ELISA plates. The concentration of phage-scFv1

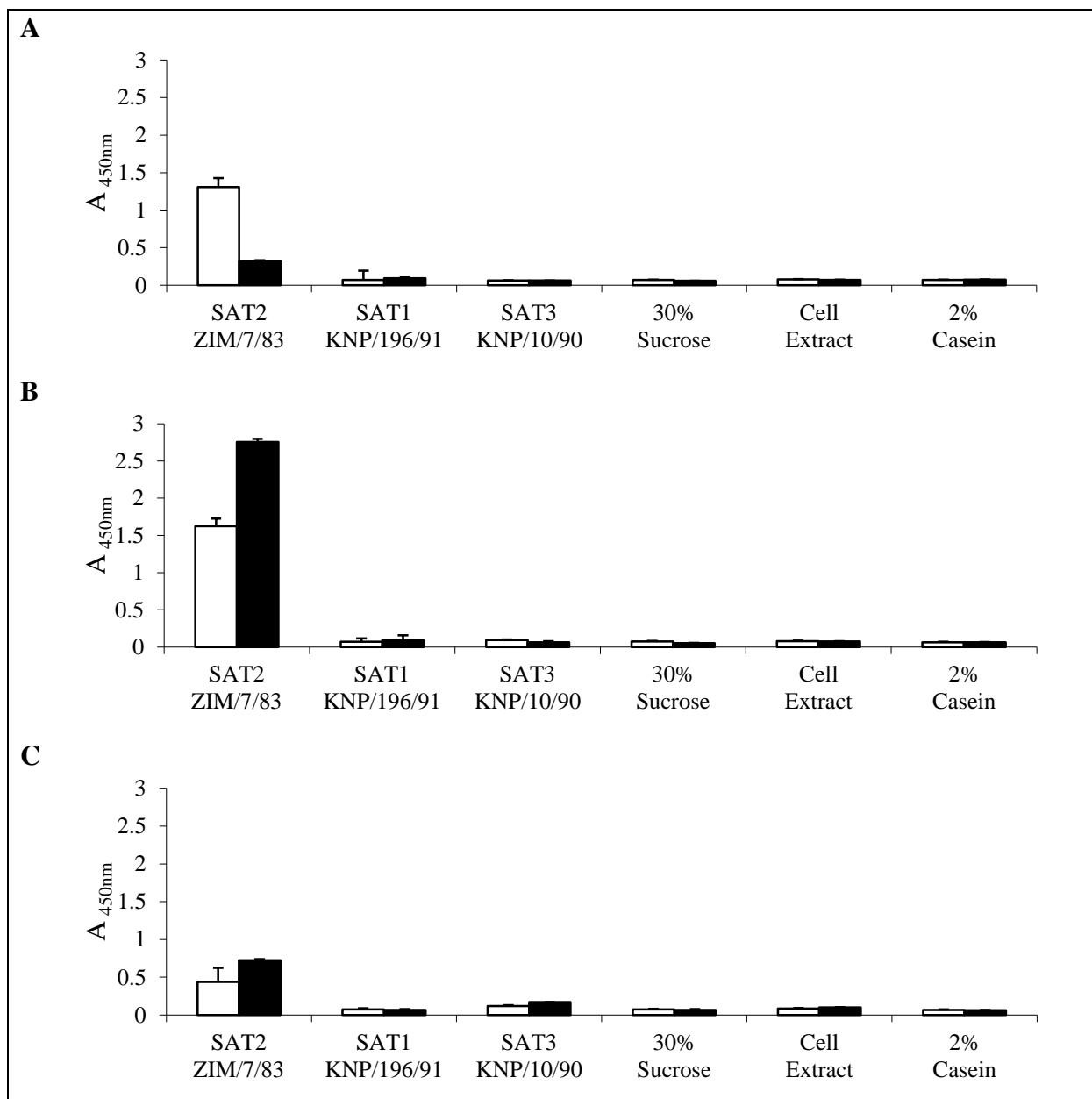


Fig. 2.3: Binding of phage-displayed and soluble scFvs to SAT serotype viruses. An indirect ELISA was performed to determine binding of phage-displayed scFvs (white bars) and soluble scFvs (black bars) to purified 146S virions of SAT2/ZIM/7/83, SAT1/KNP/196/91 and SAT3/KNP10/90. The results are presented for phage-scFv1 and soluble scFv1 (A), phage-scFv2 and soluble scFv2 (B), and phage-scFv3 and soluble scFv3 (C). As negative controls, 30% sucrose, a BHK-21 cell extract and 2% casein were included in the assays. The data are means \pm SD of triplicate repeats.

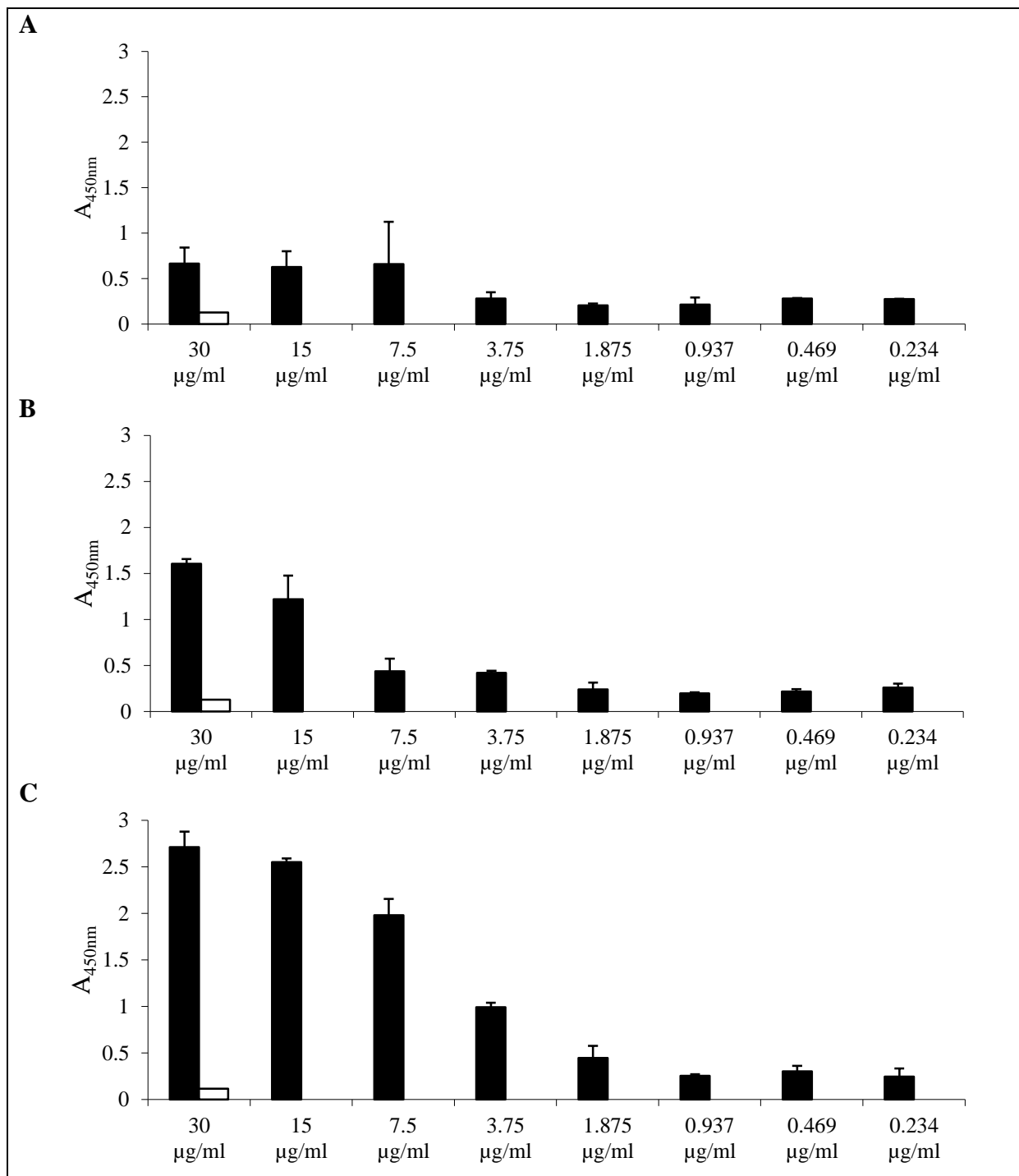


Fig. 2.4: Binding of affinity-purified soluble scFvs to various concentrations of SAT2/ZIM/7/83. An indirect ELISA was performed to determine the binding sensitivity of soluble scFv1 (A), scFv2 (B) and scFv3 (C) to decreasing concentrations of SAT2/ZIM/7/83. The soluble scFvs are indicated as black bars. ELISA plates were coated overnight with two-fold dilutions of SAT2/ZIM/7/83 (30 to 0.234 $\mu\text{g/ml}$). As a negative control, 2% (w/v) casein (white bar) was included in the assay. The data are means \pm SD of duplicate repeats.

ranged from 6.9×10^9 to 5.4×10^7 phage particles/ml and phage-scFv2 ranged from 2.15×10^{13} to 1.68×10^{11} phage particles/ml. The concentration of soluble scFv1 ranged from 163 to 1.27 $\mu\text{g/ml}$, scFv2 ranged from 171 to 1.34 $\mu\text{g/ml}$ and scFv3 from 181 to 1.41 $\mu\text{g/ml}$. Following overnight coating with the various concentrations of phage-displayed and soluble scFvs, SAT2/ZIM/7/83 was captured from a cell culture-infected supernatant.

The ELISA results shown in Fig. 2.5 indicated that soluble scFv1 and 2 were able to retain the correct binding conformation, as well as their antigen-binding activity when immobilized directly onto polystyrene. This was evidenced by their ability to successfully capture virus from infected cell culture supernatants. Soluble scFv1 was able to capture virus at concentrations ranging from 163 to 2.55 $\mu\text{g/ml}$, whereas scFv2 could capture virus at concentrations ranging from 171 to at least 1.34 $\mu\text{g/ml}$. The results also indicated that scFv1 and 2 could capture similar amounts of virus when coated at low concentrations. Soluble scFv3, however, was unable to capture SAT2/ZIM/7/83 antigen as indicated by ELISA signals similar to that of the 2% casein negative control (Fig. 2.5C). Likewise, none of the phage-displayed scFvs were able to capture SAT2/ZIM/7/83 antigen (results not shown). These results indicated that only scFv1 and 2 retained their native conformation when coated onto the polystyrene plates, and were able to successfully capture SAT2/ZIM/7/83 virus.

2.3.4 Stability of the SAT2/ZIM/7/83-specific binders

To determine the long-term storage stability of the phage-displayed and purified soluble scFvs, samples of each were stored at 4°C for four months. Each month an aliquot was removed, and their ability to bind to SAT2/ZIM/7/83 was evaluated in an indirect ELISA. Phage-scFv1 retained its binding ability for one month, as similar ELISA signals were obtained as that at day 0 of storage. There was, however, a steady decline in ELISA signal and after four months the signal was reduced by 70% (Fig. 2.6A). Phage-scFv2 and phage-scFv3 also retained their binding ability for one month at 4°C, with a *ca.* 10% reduction in the ELISA signals. The ELISA signals were reduced by a further *ca.* 33% over the following two months, and a further 33% (phage-scFv2) and 11% (phage-scFv3) after the fourth month (Fig. 2.6A). The stability of the affinity-purified soluble scFvs upon long-term storage at 4°C differed from that of the phage-displayed scFvs. Soluble scFv2 retained its binding ability the best. There was only a 20% reduction in the ELISA signal after storage for three months, whereafter a 80% reduction in the ELISA signal was observed following the fourth month of incubation (Fig. 2.6B). Soluble scFv1 was the most unstable. The ELISA signal was reduced

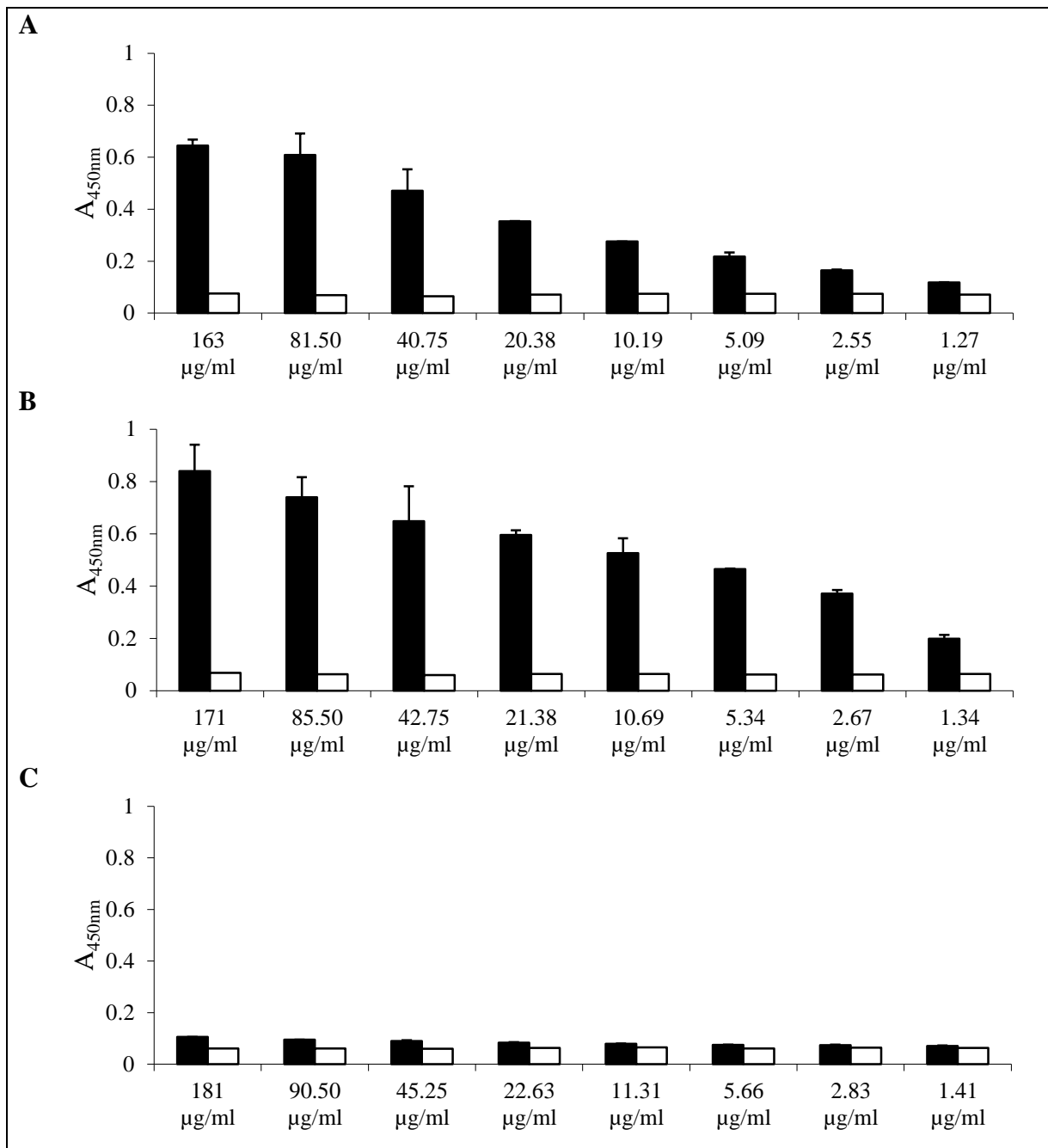


Fig. 2.5: Capturing of SAT2/ZIM/7/83 from a cell culture-infected supernatant by various concentrations of affinity-purified soluble scFvs. An indirect ELISA was performed to determine the sensitivity of decreasing concentrations of soluble scFv1 (A), scFv2 (B) and scFv3 (C) in capturing SAT2/ZIM/7/83 from a cell culture-infected supernatant. The soluble scFvs are indicated as black bars. ELISA plates were coated overnight with two-fold dilutions of the soluble scFvs, as indicated in the figures. As a negative control, 2% (w/v) casein (white bar) was included in the assay. The data are means \pm SD of duplicate repeats.

by 61% following one month's storage and a further 86% reduction in the signal was observed after the next three months of storage (Fig. 2.6B). The storage of soluble scFv3 for one month at 4°C resulted in a 27% reduction in the ELISA signal, followed by an additional 21% reduction within the next two months and a further 64% reduction after the fourth month of storage (Fig. 2.6B). Overall, it would therefore appear that the phage-displayed scFvs are more stable at 4°C than the soluble scFvs, of which phage-scFv3 was most stable and soluble scFv1 the least stable.

The freeze-thaw stability of the phage-displayed and affinity-purified soluble scFvs was also evaluated by performing indirect ELISAs on samples before and after incubation at -80°C (phage-displayed scFvs) and -20°C (soluble scFvs) for at least 30 days. The phage-displayed scFvs remained stable as very similar ELISA signals were obtained following the freeze-thaw cycle (Fig. 2.7A). In the case of soluble scFv2 and 3, there was a slight reduction in the ELISA signal following a freeze-thaw cycle at -20°C (Fig. 2.7B). Therefore, phage-displayed and soluble scFvs are robust enough to withstand freeze-thaw cycles and may be stored at low temperatures.

2.4 DISCUSSION

Control of FMD in southern Africa is essentially through the separation of domestic and wildlife animals using fences, strategic vaccination of susceptible farm animals, restriction of animal movement, and frequent inspections and serological surveillance of animals in the controlled areas (Vosloo *et al.*, 2002). The current FMD vaccines are chemically-inactivated whole-virus preparations. However, the effective administration and optimal induction of protective immunity against clinical disease are hampered by several factors, *e.g.* antigen stability and matching the antigenic profiles of vaccines and field viruses. The serological diagnosis of FMD is performed using the OIE-recommended liquid-phase blocking enzyme-linked immunosorbent assay (LPBE) for the detection of antibodies to FMDV. Albeit that LPBEs for detecting antibodies to SAT1, SAT2 and SAT3 viruses are well established; given the prevalence and genetic diversity of the SAT-type viruses (Van Rensburg and Nel, 1999; Knowles and Samuel, 2003; Maree *et al.*, 2011), there is still a need for the improvement of the sensitivity and specificity of the SAT1, SAT2 and SAT3 LPBEs. In addition, the antigenic variability of contemporary field strains needs to be measured against the vaccine

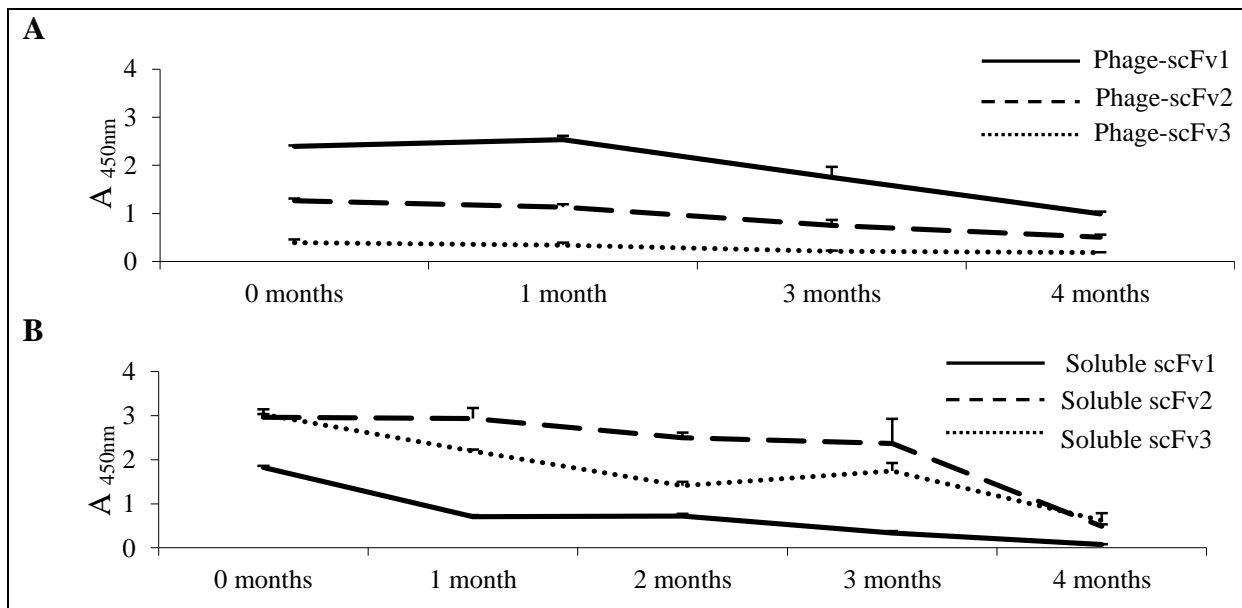


Fig. 2.6: Long-term storage stability of the phage-displayed and affinity-purified soluble scFvs. The phage-displayed (A) and soluble scFvs (B) were stored at 4°C. Aliquots were removed at different time intervals, as indicated in the figures, and their ability to bind to SAT2/ZIM/7/83 was evaluated in an indirect ELISA. The data are means ± SD of at least duplicate repeats.

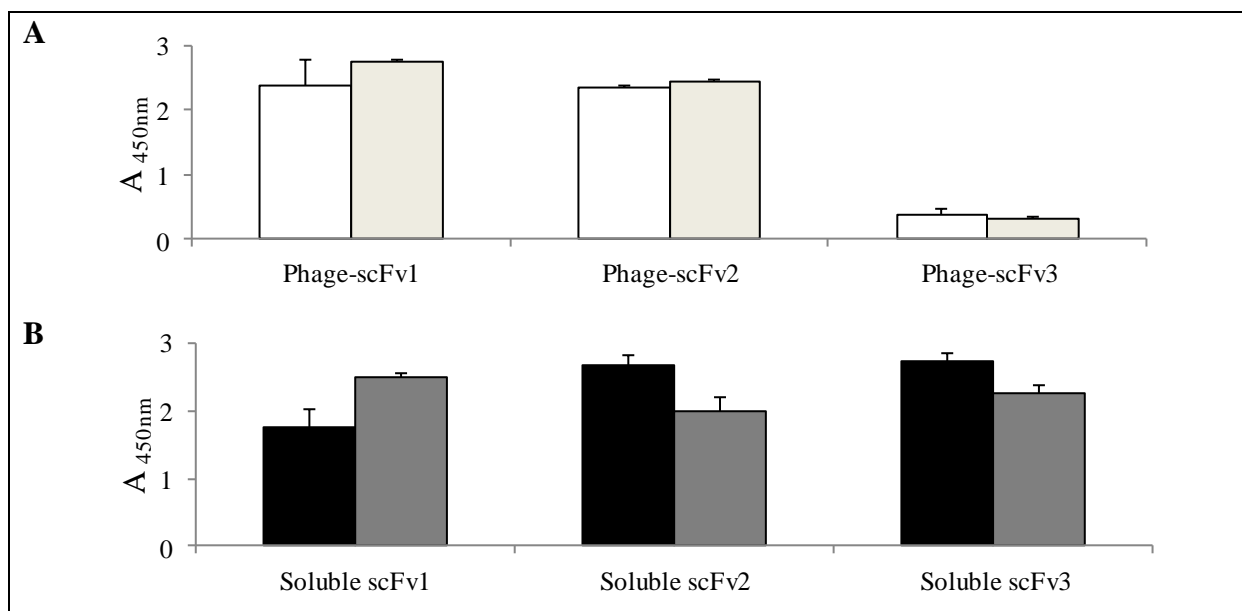


Fig. 2.7: Freeze-thaw stability of the phage-displayed and affinity-purified soluble scFvs. (A) Phage-displayed scFvs were evaluated in an indirect ELISA prior to storage at -80°C (white bars) and after thawing of the stored samples (light grey bars) for their ability to bind to immobilized SAT2/ZIM/7/83. (B) Soluble scFvs were similarly assayed, except that the samples were stored at -20°C (black bars) prior to thawing (dark grey bars). The data are means ± SD of triplicate repeats.

strains in order to determine which vaccine strain will best afford protection. Currently, it is time-consuming utilizing the *in vitro* virus neutralization (VN) assay to determine on an antigenic level whether the current vaccine strains will protect against viruses isolated from the field, which, in turn, impacts negatively on decisions regarding disease control. Therefore, instead of the current laborious VN assay, a suitable panel of MAbs that recognize exposed antigenic epitopes can be used in ELISAs to generate this information within a day. Furthermore, addressing the problem of antigenic variation may lead to the improved design of antigens for vaccines and diagnostic tests that are appropriate for a particular outbreak.

Robust immunoreagents with high affinity and specificity for use in diagnostic and vaccine development can be generated by phage display technology. In this chapter the selection and characterization SAT2-specific binders from the naïve semi-synthetic Nkuku[®] chicken IgY phage display library was described. These virus-specific binders can be used to determine antigenic sites on the SAT2/ZIM/7/83 virus (Chapter 3), which could ultimately be used in the structural design of more effective vaccines for southern Africa. Additionally, the sensitivity and stability of the recombinant antibodies were investigated in order to evaluate their usefulness as capturing or detection reagents in an ELISA assay.

Recombinant antibodies are selected from naïve phage display libraries when pre-existing paratopes bind to exposed and complementary parts of the immobilized antigen. The possibility of obtaining antigen-specific binders therefore depends on the presence and accessibility of appropriate surface-exposed structures of the antigen, in this case the FMD virion. The quality and the size of the naïve library also plays an important role in the success of phage display (Carmen and Jermutus, 2002), as paratopes that are not present within the library cannot be isolated. To date, panning with the naïve semi-synthetic Nkuku[®] library, which contains *ca.* 2×10^9 clones (Van Wyngaardt *et al.*, 2004), has yielded numerous high-affinity antibodies that were directed against a variety of different types of target molecules of both veterinary and medical importance (Van Wyngaardt *et al.*, 2004; Fehrsen *et al.*, 2005; Rakabe, 2008; Sixholo, 2008; Wemmer *et al.*, 2010). Therefore, we investigated whether SAT2-specific binders were present and could be selected from the Nkuku[®] library. Three unique SAT2-specific binders were identified after five rounds of panning with purified SAT2/ZIM/7/83. Similar numbers of unique binders have been obtained following panning of the library with other viruses. Two unique Bluetongue virus (BTV)-specific scFvs, each with their own distinct behaviour, were obtained following panning of the library with BTV

(Fehrsen *et al.*, 2005) and three binders were obtained against the 16-kDa antigen of *M. tuberculosis* (Hsp 16.3) (Sixholo *et al.*, 2011).

All three binders identified in this study specifically recognized and bound to SAT2/ZIM/7/83, and did not cross-react with representative viruses from the SAT1 or SAT3 serotypes or to reagents used during the virus purification and panning processes. In addition to the amino acid differences observed among the three binders, each also displayed unique characteristics. Soluble scFv1 generally provided low ELISA signals, whereas scFv2 and 3 provided higher ELISA signals. Low ELISA signals of the soluble scFvs are not uncommon and may be due to low expression levels or to a low inherent affinity when the fragments are used as a soluble protein, outside the phage display context (Van Wyngaardt *et al.*, 2004). The low scFv signal may also appear exaggerated by the amplified detection of the phage by virtue of the 300 subunits of the phage “tail”. The greater binding avidities afforded by the multivalent display on the phage is likely to be of significance when binding to a large multivalent antigen such as the FMDV particle, and is in sharp contrast to the moderate binding affinities of the monomeric scFv fragments (Marks *et al.*, 1991; Hoogenboom and Winter, 1992; Griffiths *et al.*, 1993; Nissim *et al.*, 1994; O'Connell *et al.*, 2002). However, studies have indicated that the introduction of random mutations in the gene coding for the scFv and the length of the linker within the scFv can increase the bacterial expression of the scFvs, which results in an increased ELISA signal (Turner *et al.*, 1997; Sixholo *et al.*, 2011). The introduction of such mutations can potentially be used to increase the expression and subsequently, the ELISA signal of soluble scFv1.

To use the soluble scFvs in an ELISA test to measure antigenic variability between SAT2 viruses and to determine whether a vaccine strain will afford protection against emerging outbreak isolates the sensitivity of the assay is crucial. Therefore, we investigated the possibility of coating the soluble scFvs, as well as the phage-displayed scFvs directly onto an ELISA plate and determining whether and how much antigen they are capable of capturing. In order for an ELISA to perform effectively, the antibodies need to be efficiently immobilized in a way that they retain both the antibody conformation and the antigen-binding activity (Jung *et al.*, 2008; Nakanishi *et al.*, 2008). Hydrophobicity, surface charge, as well as co-adsorption of, or exchange with surfactants, co-polymers and other proteins are all important factors that determine the stability and specificity of adsorbed antibodies in ELISAs (Qian *et al.*, 2000). For most conventional ELISAs, whole monoclonal or polyclonal

antibodies are immobilized onto the polystyrene surfaces by physical adsorption (Kumada *et al.*, 2009a; Kumada *et al.*, 2009b). However, when small antibody fragments, such as soluble scFvs, are immobilized directly onto solid supports the hydrophobic interaction results in the linked V_H and V_L chain regions being juxtaposed, thus forming a paratope which, in turn, can cause the antigen-binding activity to become impaired due to the conformation change (Torrance *et al.*, 2006; Wemmer *et al.*, 2010).

Stable paratopes do not distort when they are adsorbed onto solid surfaces and are an indication of a good immunocapture reagent. Coating of the SAT2-specific soluble scFvs directly onto ELISA plates resulted in only scFv1 and 2 retaining their native conformation and forming a stable paratope as measured by their ability to capture SAT2/ZIM/7/83 virus successfully. Furthermore, these immobilized scFvs proved to be sensitive as a minimal concentration of *ca.* 3.75 µg/ml of purified SAT2/ZIM/7/83 could be detected, thus indicating that these two soluble scFvs are potentially good immunocapture reagents. Soluble scFv3 did not retain the ability to capture SAT2/ZIM/7/83, suggesting poor paratope stability. Soluble scFvs have been used successfully to coat ELISA plates when expressed as fusions to the light chain constant domain (C_L) (McGregor *et al.*, 1994) or to the leucine zipper domain (Kerschbaumer *et al.*, 1997). The indirect immobilization of scFvs using peptide tags and ligand partners has also been found to be successful. In future, such strategies may be explored if soluble scFv3 is to be used in an ELISA-based assay.

The ability of antibodies to withstand physical and chemical stress can determine whether they would be good candidates to be used in immunoassays, and can also shed light on their shelf-life and storage or shipping requirements. No significant decrease was seen in the antigen-binding activities of both the phage-displayed and soluble scFvs in an ELISA, following a freeze-thaw cycle (Fig. 2.7). Furthermore, soluble scFv2 has been freeze-thawed several times without a significant reduction in antigen-binding activity (results not shown). Similar robustness of soluble scFvs has been observed previously (Wemmer *et al.*, 2010). The robustness of phage-displayed and soluble scFvs may differ somewhat; some may be able to handle elevated temperatures (Wemmer *et al.*, 2010) and some may be able to handle long-term storage at 4°C while still retaining their antigen-binding capacity. Wemmer *et al.* (2010) showed that two soluble scFvs against *M. bovis* and *M. tuberculosis*, respectively, remained functional after storage at 4°C for up to three weeks, whereas Sixholo (2008) showed that certain *M. tuberculosis*-specific soluble scFvs were functional after storage at 4°C for only

two weeks. Of the three SAT2-specific binders identified in this study, scFv2 and 3 were the most stable and retained their antigen-binding ability beyond one month's incubation at 4°C. In contrast, soluble scFv1 lost more than half of its antigen-binding capacity in the same time frame (Fig. 2.6). These results are encouraging as it has been shown previously that soluble scFvs have a tendency to aggregate upon concentration or prolonged storage at 4°C (Kortt *et al.*, 1995; Ewert *et al.*, 2002), thus inhibiting their antigen-binding ability in the ELISA. The results also indicated that the SAT2-specific phage-displayed scFvs were more stable at 4°C than the soluble scFvs (Fig. 2.6). All three phage-displayed scFvs retained their antigen-binding ability following one month's storage at 4°C after which a gradual decline was observed. It is not surprising that the phage-displayed scFvs were more stable as evidence has indicated that PEG-precipitated phage-displayed scFvs are stable at 4°C anywhere from several weeks up to fourth months (Steinberger *et al.*, 2001). These results suggest that assays designed using well-characterized phage-displayed antibodies could be used as reagents in suboptimal conditions. Phage-displayed antibodies have been used with success as immunochemical reagents for western blotting and immunohistochemistry (Nissim *et al.*, 1994; Neri *et al.*, 1998).

The intrinsic stability of scFvs is related to their amino acid sequence. Point mutations at residues 52 and 66 of the V_H domain of a Asn to Ser and Lys to Arg, respectively, as well as having a Pro at position 8 of the V_L chain have all been shown to contribute to the stabilizing of mammalian scFvs (Spada *et al.*, 1998; Worn and Pluckthun, 2001; Brockmann *et al.*, 2005). None of the SAT2-specific binders had the Asn to Ser substitution at residue 52 of the V_H domain; nevertheless, an Arg was present at residue 66 of the V_H domain in all three binders as was the Pro at residue 8 of the V_L chain (results not shown). However, to date, there is insufficient data to confirm whether these residues play a role in the stability of chicken scFvs (Wemmer *et al.*, 2010). Since the stability of the three scFv binders varied, it would appear that these residues do not play a role in the stability of the chicken scFv framework. Due to the way in which diversity is generated in the chicken (see Introduction), all chicken antibodies have very similar frameworks (Reynaud *et al.*, 1985; Davies *et al.*, 1995). Therefore, any variation in their physical properties, *e.g.* stability, will most probably be a result of amino acid sequences within the CDRs which make up *ca.* 28% of the scFv.

In this study the selection and characterization of three SAT2-specific FMDV binders from the naïve Nkuku[®] phage display library was described. In many research contexts, there is a

need to map an epitope to a distinct portion of the natural protein. If the epitope is not conformation-dependent and possibly continuous, phage display libraries, like the one used in this study, can provide a cheap and quick alternative to the traditional hybridoma approach for the generation of virus-specific MAbs. The SAT2-specific binders identified in this study will be used to map epitopes on a SAT2 FMDV. The information generated will shed some light on the dearth of knowledge that exists concerning SAT2 epitopes and may ultimately assist in the selection of a broadly neutralizing SAT2 vaccine strain. The possibility of using these SAT2-specific scFvs as immunoreagents, *e.g.* in an ELISA, especially scFv1 and 2, is promising. These two soluble scFvs retained their natural conformation following adsorption onto polystyrene plates and could capture purified 146S virion particles, as well as virus from infected cell culture supernatants. Furthermore, both of these soluble scFvs withstood a freeze-thaw cycle and were stable for at least one month at 4°C. The SAT2-specificity of these soluble scFvs can also be used in a diagnostic assay for serotyping of FMD, especially between the SAT serotypes. Since the serotype specificity of these binders has been confirmed as SAT2-specific, further investigation regarding the specificity of these binders within the SAT2 serotype (intratypic specificity) is warranted. We would ultimately like to use these scFvs in an ELISA-based assay to quickly determine whether the current FMD vaccine will provide protection for current and circulating virus strains. We are aware, however, that more than the three SAT2-specific scFvs described here will be needed for an effective assay. The SAT2-specific scFv repertoire may in future be expanded by constructing and panning libraries from infected host animals.

CHAPTER THREE

MAPPING OF ANTIGENIC DETERMINANTS ON A SAT2 FOOT-AND-MOUTH DISEASE VIRUS USING CHICKEN SINGLE-CHAIN ANTIBODY FRAGMENTS

3.1 INTRODUCTION

Foot-and-mouth disease (FMD) is a highly contagious disease of even-toed ungulates and ranks as one of the most important infectious animal diseases due to its economic impact. The causative agent, FMD virus (FMDV), is a single-stranded, positive-sense RNA virus and the prototype member of the *Aphthovirus* genus in the family *Picornaviridae* (King *et al.*, 2000). The South African Territories (SAT) types 1, 2 and 3 are confined to Africa where six of the seven FMDV serotypes occur (Brooksby, 1972; Ferris and Donaldson, 1992; Vosloo *et al.*, 2002). The SAT types are maintained within African buffalo (*Syncerus caffer*) populations, which provide a potential source of infection for domestic livestock and other susceptible wildlife (Dawe *et al.*, 1994; Bastos *et al.*, 2000; Vosloo and Thomson, 2004), as well as the opportunity for antigenic and molecular evolution of the virus to occur (Vosloo *et al.*, 1996; Bastos *et al.*, 2001; Bastos *et al.*, 2003a; Bastos *et al.*, 2003b).

The FMDV capsid is composed of 60 copies of each of four structural proteins namely, VP1, VP2 and VP3, which are surface exposed, and the internally located VP4 protein (Morrell *et al.*, 1987; Acharya *et al.*, 1989). The capsid shares many structural features with that of other picornaviruses, including the similar orientation of the β -barrel structures of the three outer capsid proteins. It has been shown that the majority of FMDV-neutralizing antibodies are directed against epitopes located in the three surface-exposed capsid proteins of the virus, of which the flexible β G- β H loop in VP1 is antigenically important (Xie *et al.*, 1987; Thomas *et al.*, 1988b; Acharya *et al.*, 1989; Kitson *et al.*, 1990). Antigenic variation results from changes to the viral capsid as a consequence of the high mutation rate of the virus (Holland *et al.*, 1982; Domingo, 1997), thus contributing to the generation of a spectrum of antigenic subtypes within each serotype. Furthermore, each FMDV isolate is antigenically unique in its fine epitopic composition such that the location of these antigenic sites and their antigenic features vary between the different serotypes. This results in decreased vaccine efficacy and effectiveness of vaccination programs in the field (Feigelstock *et al.*, 1996). Several studies have been carried out to delineate the neutralizing antigenic sites of representative viruses from serotypes A (Thomas *et al.*, 1988b; Baxt *et al.*, 1989; Bolwell *et al.*, 1989), O (Kitson *et al.*, 1990; Crowther *et al.*, 1993a), C (Mateu *et al.*, 1990) and Asia-1 (Sanyal *et al.*, 1997). In these studies, monoclonal antibodies (MAbs) were pivotal in identifying critical amino acid residues of the different neutralizing antigenic sites.

Despite the fact that the SAT2 serotype has been responsible for most of the FMD outbreaks in domestic livestock in southern Africa (Thomson and Bastos, 2004), limited studies aimed at the production of MAbs specific for this serotype have been performed. These MAbs nevertheless allowed the identification of at least two neutralizing epitopes, one within the β G- β H loop of VP1 (Crowther *et al.*, 1993b; Davidson *et al.*, 1995; Grazioli *et al.*, 2006) and one at the C-terminus of VP1 (Grazioli *et al.*, 2006). Evidence from studies using FMDV serotypes C (Feigelstock *et al.*, 1992; Mateu *et al.*, 1995), A (Thomas *et al.*, 1988b) and SAT1 (Grazioli *et al.*, 2006) indicated that antigenic sites on VP2 and VP3 are also important in the generation of an immune response following infection or vaccination. Therefore, all such antigenic determinants have to be considered in the design of vaccines for regional control of FMD.

Direct or structural approaches to identify antigenic sites on large protein structures like viral capsids include the use of X-ray crystallography, nuclear magnetic resonance (NMR) and electron microscopy (Kleymann *et al.*, 1995; Guthridge *et al.*, 2001). However, functional methods like competition assays, virus neutralization escape mutants, protein fragmentation methods and the use of synthetic peptides or peptide libraries are also essential in the mapping of neutralizing epitopes or antigenic sites on viral capsids (Crowther *et al.*, 1993b; Irving *et al.*, 2001; Joseph *et al.*, 2002; Bich *et al.*, 2008). Many recombinant antibodies have been produced and selected through the construction of phage display libraries (Carmen and Jermutus, 2002). Antibody libraries can be constructed from either immunized (immune library) or non-immunized (naïve library) sources. Although immune libraries are more specific (reviewed in Winter *et al.*, 1994) their construction is time-consuming (Brichta *et al.*, 2005), whereas naïve libraries are not confined to any specific target and therefore contain a broad range of specificities (Gram *et al.*, 1992; Van Wyngaardt *et al.*, 2004; Brichta *et al.*, 2005). Furthermore, access to naïve libraries may produce rapid results and could circumvent many of the complexities normally related to the conventional production of antibodies (Smith, 1985; Clackson *et al.*, 1991). This advantageous property of naïve libraries has been exploited to select three SAT2/ZIM/7/83-specific binders from the large naïve and semi-synthetic Nkuku[®] library.

In this part of the study the aim was to identify antigenic sites of a SAT2 virus that could be used in the rational design of more effective vaccines for southern Africa. Of the three recombinant soluble scFvs panned from the Nkuku[®] library, one was used to generate virus

neutralization escape mutants that facilitated the identification of a neutralizing epitope of a SAT2 virus, while the two non-neutralizing soluble scFvs were further analyzed to determine their putative binding sites to the virus. The binding profiles and specificity of these soluble scFvs for representative SAT2 field isolates were also determined for application in the control of new and re-emerging FMDV outbreaks.

3.2 MATERIALS AND METHODS

3.2.1 Cell culture, virus propagation and viruses

Baby hamster kidney cells (BHK) strain 21 clone 13 (ATCC CCL-10), used for virus propagation, were maintained as described previously (Chapter 2, Section 2.2.1). Instituto Biologico Renal Suino-2 (IB-RS-2) cells, used during virus neutralization tests (VNT), were maintained in RPMI medium (Sigma-Aldrich) supplemented with 10% (v/v) foetal calf serum (FCS; Invitrogen) and $1 \times$ antibiotics (Invitrogen). A Mycl-9E10 hybridoma (ECACC 85102202) was cultured in protein-free hybridoma medium (Invitrogen).

The 146S virus particles of the SAT2 viruses were concentrated with 8% (w/v) polyethylene glycol (PEG)-8000 (Sigma-Aldrich) and purified on 10-50% (w/v) sucrose density gradients (SDG), prepared in TNE buffer (50 mM Tris [pH 7.4], 150 mM NaCl, 10 mM EDTA), as described previously (Chapter 2, Section 2.2.2). Peak fractions corresponding to the 146S virus particles were pooled, analyzed by SDS-PAGE and the amount of antigen (μg) calculated (Chapter 2, Section 2.2.2).

The SAT2 viruses included in this study, *i.e.* ZIM/7/83, ZIM/5/83, ZIM/7/89, ZIM/13/01, ZIM/8/94, ZIM/4/97, ZIM/44/97, ZIM/5/02 and ZIM/2/88, form part of the virus bank at the Transboundary Animal Diseases Programme (TADP), Onderstepoort, South Africa. The viruses, together with a description of their passage histories and GenBank accession numbers, are indicated in Table 3.1.

3.2.2 Characterization of the capsid (P1)-encoding region of SAT2 viruses

3.2.2.1 Oligonucleotides

Oligonucleotides used in the cDNA synthesis, PCR amplification and nucleotide sequencing procedures were custom-synthesized by Inqaba Biotechnical Industries or Invitrogen, and are described in Table 3.2.

Table 3.1: SAT2 viruses used in this study

Virus strain	Species of origin	Year of sampling	*Passage history	GenBank accession no.
ZIM/7/83	Bovine	1983	B ₁ BHK ₅ B ₁ BHK ₄	DQ009726
ZIM/5/83	Bovine	1983	BTY ₄ RS ₂ BHK ₅	JQ639289
ZIM/7/89	Buffalo	1989	B ₁ PK ₁ RS ₂ BHK ₅	JQ639296
ZIM/13/01	Bovine	2001	RS ₂ BHK ₅	JQ639292
ZIM/8/94	Buffalo	1994	BTY ₁ RS ₄ BHK ₅	JQ639290
ZIM/4/97	Bovine	1997	B ₁ PK ₁ RS ₂ BHK ₅	JQ639293
ZIM/44/97	Buffalo	1997	BTY ₁ RS ₄ BHK ₅	JQ639291
ZIM/5/02	Bovine	2002	PK ₁ RS ₄ BHK ₇	JQ639295
ZIM/2/88	Buffalo	1988	CFK ₁ RS ₁ BHK ₈	JQ639294

*Abbreviations: BTY, primary bovine thyroid cells; PK, pig kidney cells; CFK, crandall feline kidney cells

Table 3.2: Oligonucleotides used in this part of the study

Oligonucleotide	*Sequence	Purpose
WDA	5'-GAAGGGCCCAGGGTTGGA CT C-3'	cDNA synthesis, PCR amplification, nucleotide sequencing
2B	5'-GACATGTCCTCCTGCATCTG-3'	Antisense, situated in 2B, cDNA
NCR1	5'-TACCAAGCGACACTCGGGATCT-3'	Sense, situated in NCR, cDNA
Sequence 1	5'-CGTCGATGAGCCACTCTT-3'	Sequencing of P1
Sequence 2	5'-CATCAAAGGCACTGAAC-3'	Sequencing of P1
Sequence 3	5'-ACAACACGACACGGTACC-3'	Sequencing of P1
Sequence 4	5'-TTGTGCGAAGCGTGGTTGT-3'	Sequencing of P1
Sequence 5	5'-CACCAGCACGCAGTTCAA-3'	Sequencing of P1
Sequence 7	5'-GGTAGCAGTGGGCYGC-3'	Sequencing of P1
Sequence 10	5'-GACCCBAAGACCGCAGA-3'	Sequencing of P1
Sequence 11	5'-GGGAYACAGGAYTGA ACT-3'	Sequencing of P1
Sequence 30	5'-ACACAGGTCCTACTCAC-3'	Sequencing of P1
Sequence 41	5'-TTATGACCTGTTTTGATGTGGC-3'	Sequencing of P1
Sequence 156	5'-GGCATTACCTACGGGTACGC-3'	Sequencing of P1
Sequence 157	5'-GTTTAACGGCGGGTCACTTC-3'	Sequencing of P1
Sequence 158	5'-CGGTGACCGTGCCGTCTTGGC-3'	Sequencing of P1
Sau 11	5'-GACTGCCACGGACGGTTCTC-3'	Sequencing of P1
P621	5'-GGACATATCTTGTTGCATG-3'	Sequencing of P1
P622	5'-GCACTGACACCACGTCTAC-3'	Sequencing of P1

*In selected oligonucleotides, the abbreviation representing ambiguities is Y = C/T

3.2.2.2 RNA extraction

RNA was extracted from virus-infected cell cultures using a modified guanidinium thiocyanate (GuSCN)/silica method, as described by Boom *et al.* (1990). Briefly, the cells of a 200- μ l cell culture sample were lysed by addition of L6 buffer (8.3 M GuSCN, 80 mM Tris-HCl [pH 6.4], 36 mM EDTA, 33 mM TritonX-100) containing an aliquot of a 4% (w/v) silica suspension. Following incubation for 5 min at room temperature, the silica-bound nucleic acid was collected by centrifugation at $13\,500 \times g$ for 15 s and rinsed with L2 wash buffer (10.2 M GuSCN, 0.1 M Tris-HCl [pH 6.4]), 70% ethanol and acetone, respectively, before being air-dried. The nucleic acids were eluted from the silica matrix at 56°C for 2 min in a final volume of 30 μ l of $1 \times$ TE buffer (10 mM Tris-HCl, 2 mM EDTA; pH 7.4) containing RNasin[®] ribonuclease inhibitor (40 U/ μ l; Promega), and stored at -70°C.

3.2.2.3 cDNA synthesis

The viral RNA was reverse-transcribed using a mixture of random hexanucleotides, together with the antisense oligonucleotide 2B, which anneals at the 2A/2B junction (Table 3.2). The reaction mixture contained *ca.* 1 to 3 μ g of RNA, 0.23 μ M of oligonucleotide 2B, 4.55 μ M of a random hexanucleotide mixture (Roche Diagnostics), $1 \times$ AMV-RT buffer (50 mM KCl, 10 mM MgCl₂, 0.5 mM spermidine, 10 mM DTT), 0.34 mM of each dNTP (Roche Diagnostics), 2% (v/v) DMSO and 20 U of RNasin[®] (40 U/ μ l; Promega). Following denaturation of the RNA by incubating at 70°C for 3 min, 40 U of the AMV-Reverse Transcriptase (10 U/ μ l; Promega) was added and the RNA was reverse transcribed at 42°C for 2 h. After incubation, the enzyme was inactivated by heating to 80°C for 2 min and the reaction mixtures were stored at 4°C.

3.2.2.4 Polymerase chain reaction (PCR) amplification and analysis

The Leader-P1-2A coding region of the SAT2 viruses was amplified using the Expand Long Template PCR system (Roche Diagnostics). Each PCR reaction mixture (50 μ l) contained 3 μ l of the first strand cDNA reaction mixture, 0.3 μ M of each oligonucleotide NCR1 and WDA (Table 3.2), 2.5 U of Expand Long Template DNA polymerase, $1 \times$ Expand buffer, 0.75 mM MgCl₂ and 2 μ M of each dNTP. The tubes were placed in a GeneAmp[®] 9700 thermal cycler (Applied Biosystems) and after initial denaturation at 94°C of 2 min, the reactions were subjected to 33 cycles using the following temperature profile: denaturation at 94°C for 20 s, annealing at 55°C for 20 s and elongation at 68°C for 4 min. After the last

cycle, the reactions were kept at 68°C for 7 min to complete synthesis of all strands. The PCR-amplified products were visualized by electrophoresis on a 1.5% (w/v) agarose gel containing 0.5 µg/ml EtBr, using 1 × TAE (40 mM Tris-acetate, 2 mM EDTA; pH 8) as electrophoresis buffer. The size of the amplified DNA fragments was estimated against a DNA molecular weight marker (100-bp DNA ladder or phage λ DNA digested with *HindIII*; Promega). The amplicons were purified from agarose gels with the Nucleospin[®] Extract kit (Macherey-Nagel) according to the manufacturer's instructions.

3.2.2.5 Nucleotide sequencing and analysis

The nucleotide sequence of the gel-purified amplicons was determined using 0.16 µM of the appropriate oligonucleotide (Table 3.2) and the ABI PRISM[™] Big Dye[™] Terminator Cycling Ready Reaction kit v3.0 (Applied Biosystems). The extension products were resolved on an ABI PRISM[™] 3100 automated sequencer (Applied Biosystems). Direct DNA sequencing of amplicons yielded a consensus sequence representing the most probable nucleotide for each position. Sequences of the *ca.* 2.2-kb P1-coding region were compiled and edited using BioEdit v.7.0.9 software (Hall, 1999), and the amino acid sequences were deduced and aligned with Clustal-X in BioEdit v.7.0.9 software (Hall, 1999). The GenBank accession numbers of the SAT2 viruses are summarized in Table 3.1. Phylogenetic trees were constructed in MEGA 4.0 (Tamura *et al.*, 2007) using neighbour-joining algorithms and node reliability is supported by 1000 bootstrap replications.

3.2.3 Large scale purification of soluble scFvs

The soluble scFvs, described in Chapter 2, were purified on a large scale from 1-L cultures by the Biotechnology Division of the National Bioproducts Unit in Kwa-Zulu Natal, South Africa, on an affinity column that contained 75 ml Sepharose coupled to 100 mg of the Myc tag-specific MAb, 9E10.

3.2.4 Binding specificity of the secreted soluble scFvs

The binding specificity of the soluble scFvs to the SAT2 viruses, indicated in Table 3.1, was determined at various antigen concentrations. Maxisorp[™] ELISA plate wells were coated with two-fold dilutions (from 30 to 0.94 µg/ml) of the antigens, blocked with 2% (w/v) casein and the purified soluble scFvs (Section 3.2.3), diluted two-fold in 1 × PBS containing 4% (w/v) casein (final concentration of *ca.* 80 µg/ml), were added. Binding of the soluble scFvs

to the immobilized SAT2 viruses was detected as described in the monoclonal soluble scFv ELISA (Chapter 2, Section 2.2.8), and the results for the 7.5 µg/ml coating concentration were compared.

3.2.5 Neutralization assays and generation of virus escape mutants

The 50% tissue culture infective dose (TCID₅₀) of SAT2/ZIM/7/83 was determined on IB-RS-2 cells (Esterhuysen *et al.*, 1988) and the resulting virus titre was used to calculate the dilutions subsequently used in the VNT. Triplicate repeats of the appropriate SAT2/ZIM/7/83 dilutions in RPMI medium, containing *ca.* 500, 50 and 5 infectious particles, were applied across a microtitre plate and diluted two-fold down the plate. The soluble scFvs (*ca.* 0.167 mg/ml) and phage-displayed scFvs (*ca.* 2.3×10^{12} - 1.8×10^{13} phage particles/ml) were added to each well and a control plate without soluble and phage-displayed scFvs was also included. Following incubation for 1 h at 37°C in an atmosphere of 5% CO₂, IB-RS-2 cells (0.3×10^6 cells/ml) in RPMI medium supplemented with 1% (v/v) FCS and antibiotics (virus growth medium; VGM), was added. The microtitre plates were incubated for 72 h at 37°C, examined microscopically and the cytopathic effect (CPE) was scored as a measure of neutralization. Based on the results obtained, soluble scFv2 was chosen to generate virus neutralization escape mutants, as described below.

Virus neutralization escape mutants were generated as described by Crowther *et al.* (1993b). For this purpose, *ca.* 25 infectious virus particles of SAT2/ZIM/7/83 were diluted two-fold in RPMI medium containing antibiotics before being mixed with an equal volume of scFv2 (17 µg). The suspension was incubated for 30 min at 37°C and applied to an IB-RS-2 cell monolayer in a 96-well microtitre plate. Following incubation for 1 h at 37°C, the virus-scFv complexes were removed. The monolayer was washed twice with RPMI medium and then VGM, containing a 1:50 dilution of scFv2 (3 µg/ml), was added. The SAT2/ZIM/7/83 virus was passaged three consecutive times under scFv pressure. Virus escape mutants were characterized by nucleotide sequencing of cDNA copies of the P1-encoding region, as described previously (Section 3.2.2).

3.2.6 Synthetic peptide blocking ELISA

Two different synthetic peptides, synthesized by GenScript Corp., were used in a blocking ELISA to confirm the presence of the predicted antigenic site on SAT2/ZIM/7/83. The sequence of the 40-mer peptide (KYTQQSTAIRGDRAVLA AKYANTKRKLPSTFNF

GYVTADK), designated EpiR, was derived from the VP1 β G- β H loop region of SAT2/ZIM/7/83 that contains the predicted epitope (marked in bold and underlined). A 30-mer peptide, which had the sequence AAVESAAVESAAVESAAVESAAVESAAVES, was used as a non-competitive negative control in the assays. Maxisorp™ ELISA plates were coated overnight at 4°C with purified SAT2/ZIM/7/83 (ca. 25 μ g/ml) and blocked with 2% (w/v) casein. Equal volumes of soluble scFv2 (ca. 5.3 μ g/ml) in 4% (w/v) casein and peptides in 1 \times PBS (400-50 μ M) were mixed. As a non-inhibition control the peptides were replaced with 1 \times PBS and mixed with the soluble scFvs. The soluble scFv and peptide solutions were incubated for 1 h at 30°C with shaking (100 rpm) before being added to the pre-blocked ELISA plates. The ELISA plates were incubated for 1 h and binding of soluble scFv2 fragments to immobilized SAT2/ZIM/7/83 was detected as described in the monoclonal soluble scFv ELISA (Chapter 2, Section 2.2.8). To determine the nature of the interaction between EpiR peptide and soluble scFv2, a peptide blocking assay was performed using a third non-specific positively charged 22-mer peptide, designated PosCharge (MGKFTSFLKRAGSATKKALTS). The peptide blocking ELISA was performed as above, except only 200 μ M of the EpiR and the PosCharge peptides were incubated with soluble scFv2.

3.2.7 Structural modelling

A homology model of the SAT2 capsid proteins was built using Modeller 9v3 (Sali and Blundell, 1993) with O₁BFS (Logan *et al.*, 1993) as template. The model was based on the optimal alignment of the SAT2 virus, ZIM/7/83, P1 sequence to the corresponding sequence of O₁BFS. The satisfaction of spatial restraints, as described by empirical databases, was used to calculate homology modelled structure. Structures were visualized and the surface-exposed residues identified with PyMol v1.1rc2pre (DeLano Scientific LLC).

3.3 RESULTS

3.3.1 Characterization of SAT2/ZIM/7/83-specific scFvs

It has previously been established that the SAT2/ZIM/7/83-specific scFvs were unable to bind to SAT1 and SAT3 viruses, suggesting that the identified scFvs may be specific for SAT2 viruses (Chapter 2, Fig. 2.3). This apparent specificity to the SAT2 FMDV serotype was subsequently investigated by making use of a panel of SAT2 viruses. Binding of the three

soluble scFvs to complete 146S virions of these viruses was determined by an indirect ELISA. The results, indicated in Fig. 3.1 (A-C), showed that the three soluble scFvs bound to all eight SAT2 viruses, albeit with apparent different binding profiles. Soluble scFv2 bound to all the SAT2 viruses with similar ELISA absorbance signals, whereas the ELISA signal for soluble scFv1 and 3 was generally reduced with a few exceptions, *i.e.* ZIM/13/01, ZIM/8/94 and ZIM/7/89 for scFv1 (Fig. 3.1A), and ZIM/7/89 for scFv3 (Fig. 3.1C).

3.3.2 Neutralization studies and the generation of virus escape mutants

Towards mapping of the binding sites of the binders to the SAT2 virion, the phage-displayed and soluble scFvs were evaluated for their ability to neutralize SAT2/ZIM/7/83 *in vitro*. None of the phage-displayed scFvs showed virus neutralizing activity (results not shown), whereas only one of the soluble scFvs was capable of neutralizing SAT2/ZIM/7/83. In contrast to soluble scFv1 and 3, soluble scFv2 showed neutralizing activity of SAT2/ZIM/7/83. Considerably less CPE was observed for the soluble scFv2 assay compared to the control assay that lacked soluble scFvs (Fig. 3.2). Subsequently, virus neutralization escape mutants were generated by serial passage of the SAT2/ZIM/7/83 virus in the presence of soluble scFv2, and the P1 nucleotide sequence of two viruses that escaped neutralization was determined. Comparative analysis of the deduced amino acid sequences indicated that both virus neutralization escape mutants harboured two amino acid changes located in the VP1 protein. The first escape mutant (EscM1) contained a threonine (T) to serine (S) change at position 4 (T4→S) and an arginine (R) to histidine (H) change at position 159 (R159→H) of VP1. The second escape mutant (EscM2) also contained the T4→S change, but at position 159 one of two amino acids were present, either an R, as seen in the parental virus, or a H, as seen in EscM1 (Fig. 3.3A). The two amino acid residues observed at this position can be accounted for by the genetic heterogeneity due to the quasispecies nature of the FMDV genome. Each FMD viral population consists of a “mixture” of genomes (Domingo and Holland, 1997), allowing for the selection of variants upon environmental changes, *e.g.* immune pressure.

Mapping of the location of the observed variant amino acids on a model of the ZIM/7/83 protomer indicated that the T4→S change was hidden from the virion surface, and distantly located from any of the sequences known to be involved in antigenicity of the virus. Notably, the R159→H change was located on the surface of the pentamer, at the C-terminal base of the β G- β H loop (Fig. 3.3B).

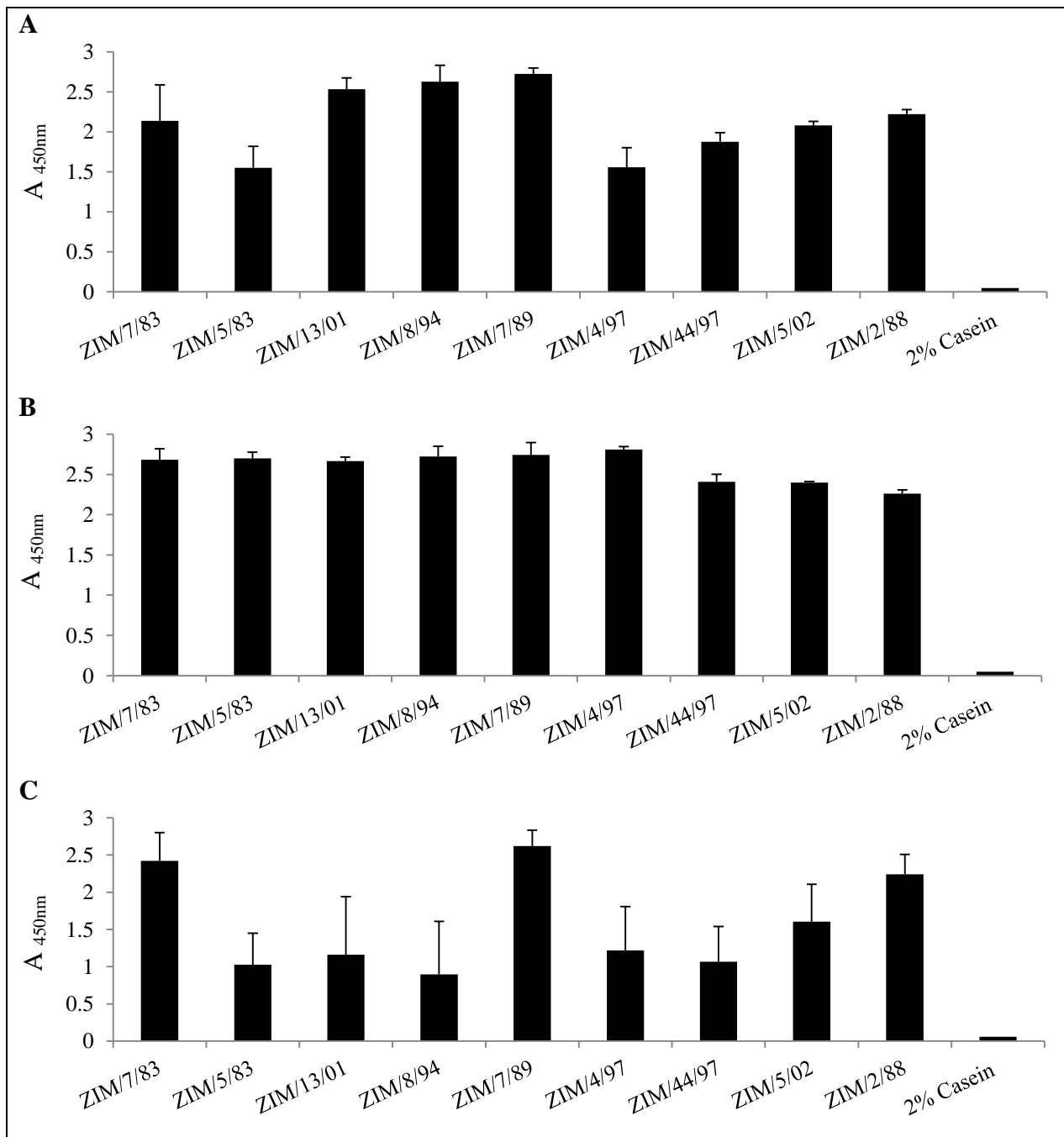


Fig. 3.1: Binding of soluble scFvs to a panel of SAT2 serotype viruses. An indirect ELISA was performed to determine binding of soluble scFv1 (A), scFv2 (B) and scFv3 (C) to purified 146S virions of the SAT2 serotype viruses indicated in the figure. As a negative control, 2% (w/v) casein was included in the assays. The data are means \pm SD of two independent experiments.

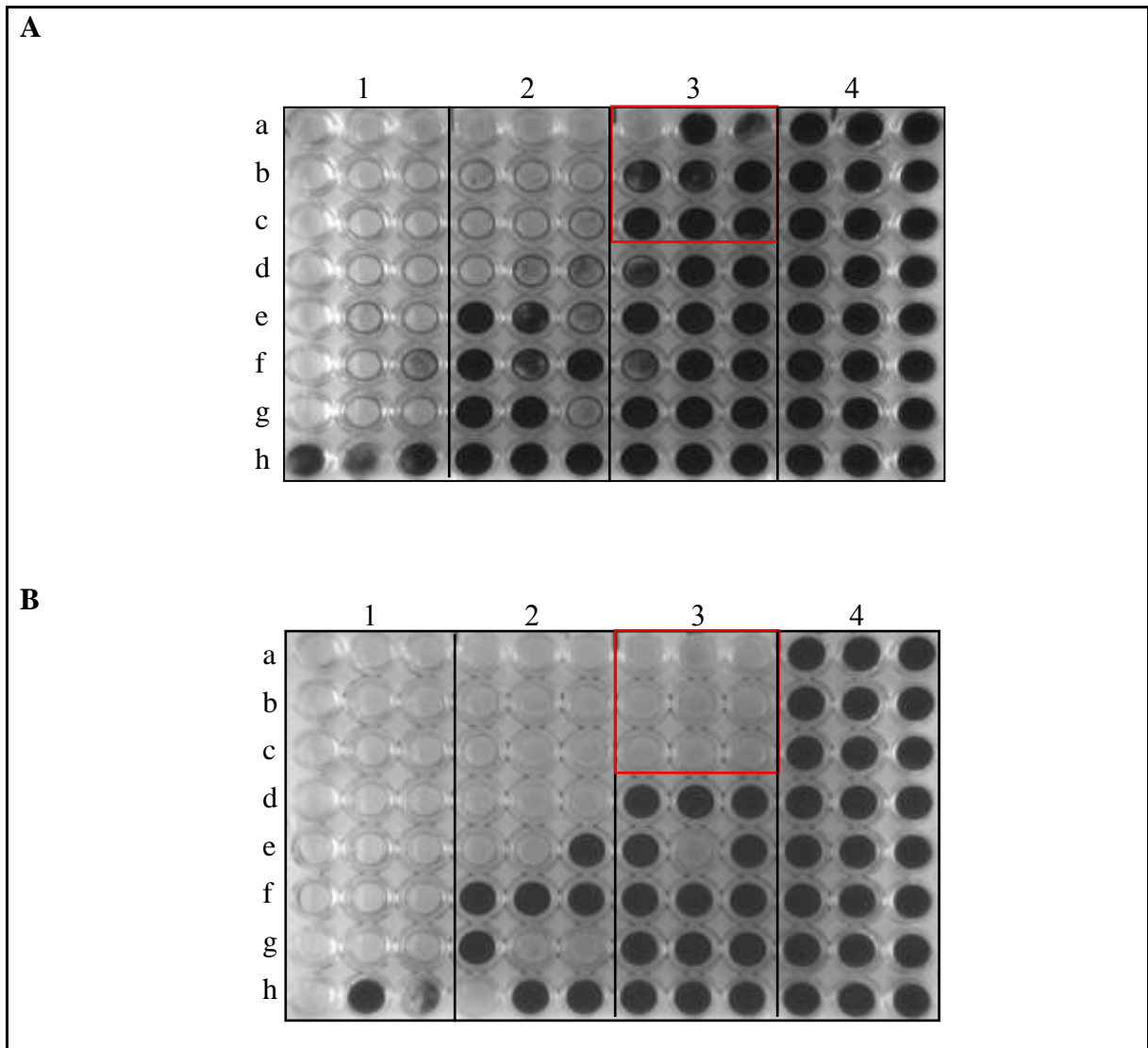


Fig. 3.2: Virus neutralization assay of soluble scFv2 with SAT2/ZIM/7/83. (A) Infectious SAT2/ZIM/7/83 virus particles, *ca.* 500 (1), 50 (2) and 5 (3), were added across the microtitre plate (row a) and diluted two-fold down the microtitre plate (until row h). Soluble scFv2 (*ca.* 0.167 mg/ml) was then added to all the wells in columns 1 to 3 of the microtitre plate. Column 4 represents a negative control in which IB-RS-2 cells were incubated in the presence of soluble scFv2 and SAT2/ZIM/7/83 was omitted. (B) A control plate was included in which soluble scFv2 was omitted. Column 4 represents a negative control in which IB-RS-2 cells were incubated in the absence of SAT2/ZIM/7/83 and soluble scFv2. Clear wells indicate 100% CPE, whereas black-coloured wells indicate 0% CPE. The area blocked in red indicates neutralization of the SAT2/ZIM/7/83 virus by soluble scFv2.

3.3.3 Binding of soluble scFv2 to SAT2/ZIM/7/83 is reduced by a synthetic peptide

To confirm the role of residue 159 of VP1 as part of the binding site of soluble scFv2, a synthetic peptide (EpiR), of which the sequence was derived from the predicted epitope site on SAT2/ZIM/7/83, was used in a blocking ELISA together with soluble scFv2. Binding of soluble scFv2 to SAT2/ZIM/7/83 was not noticeably inhibited at concentrations of 50-200 μM of the EpiR peptide, as compared to binding of soluble scFv2 to SAT2/ZIM/7/83 in the absence of EpiR. However, the ELISA signal was reduced by 24% and 45% (Fig. 3.4) in the presence of higher concentrations of EpiR (300 μM and 400 μM , respectively). A control peptide, which sequence displayed no homology to the putative binding site, did not inhibit binding of soluble scFv2 to SAT2/ZIM/7/83. Taken together, the results indicate that the binding of soluble scFv2 to SAT2/ZIM/7/83 was reduced in a concentration-dependent manner by pre-incubation with EpiR.

Next, a possible mechanism for the interaction of soluble scFv2 with the EpiR peptide was investigated. Analysis of EpiR revealed that the putative binding site contains an array of three positively-charged residues, *i.e.* KRK (Fig. 3.5A). Consequently, the inhibitory effect of a peptide containing two clusters of positively-charged residues in close proximity to each other, *i.e.* KR and KK, was tested. Both the putative binding site of EpiR (KRK) as well as one of the positive clusters of the positively-charged random peptide are preceded by a threonine amino acid. The results of the blocking ELISA indicated that both the EpiR peptide and the non-specific positively-charged peptide inhibited the binding of soluble scFv2 to immobilized SAT2/ZIM/7/83 equally well (Fig. 3.5B). EpiR and the positively-charged random peptide inhibited the binding by 43% and 44%, respectively. These results therefore indicated that the binding of the peptides to soluble scFv2 is most likely through ionic interaction.

3.3.4 Identification of putative antigenic sites

The different binding profiles observed for scFv1 and 3 to the panel of SAT2 viruses (Fig. 3.1) were used to identify their potential binding footprints on the SAT2 capsid. The data presented in Fig. 3.1 relied on there being a saturating concentration of virus antigen (30 $\mu\text{g/ml}$) available for the soluble scFvs to bind to. Therefore, the binding profiles of scFv1 and 3 were further examined using an indirect ELISA and nine SAT2 viruses with decreasing virus antigen concentrations (Appendix A to this thesis). The differences in binding observed

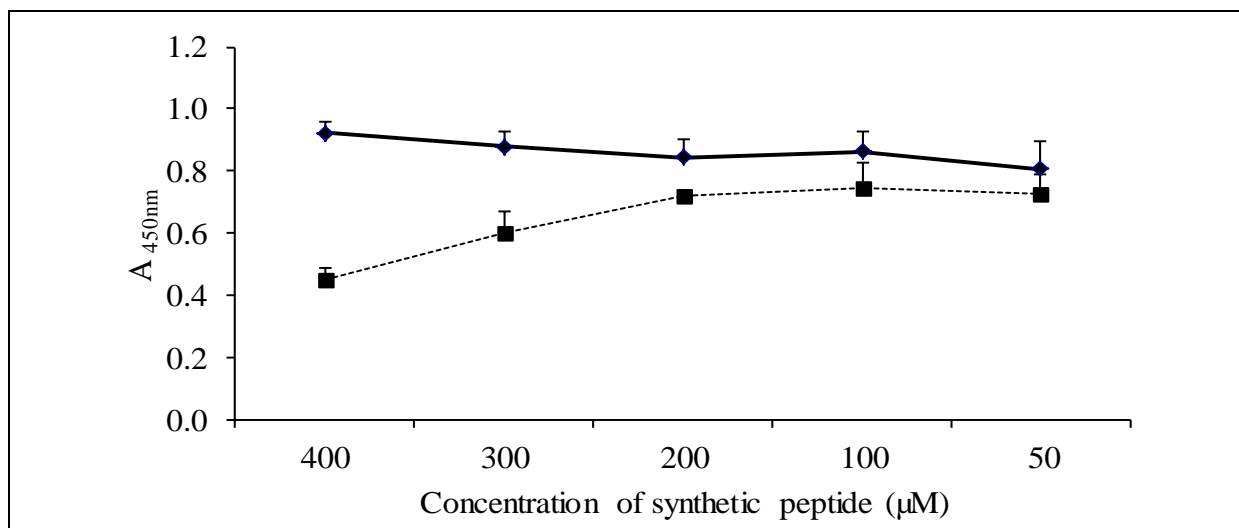


Fig. 3.4: Binding of soluble scFv2 to immobilized SAT2/ZIM/7/83 in a competitive blocking ELISA in the presence of the EpiR synthetic peptide (■). A competitive blocking ELISA was performed to determine whether the synthetic peptide, EpiR, inhibits binding of soluble scFv2 to immobilized SAT2/ZIM/7/83. Various concentrations (400-50 µM) of the synthetic peptide EpiR (■) were tested. A non-inhibition control (◆), in which the peptide was replaced with 1 × PBS and mixed with soluble scFv2, was included. The data are means ± SD of three independent experiments.

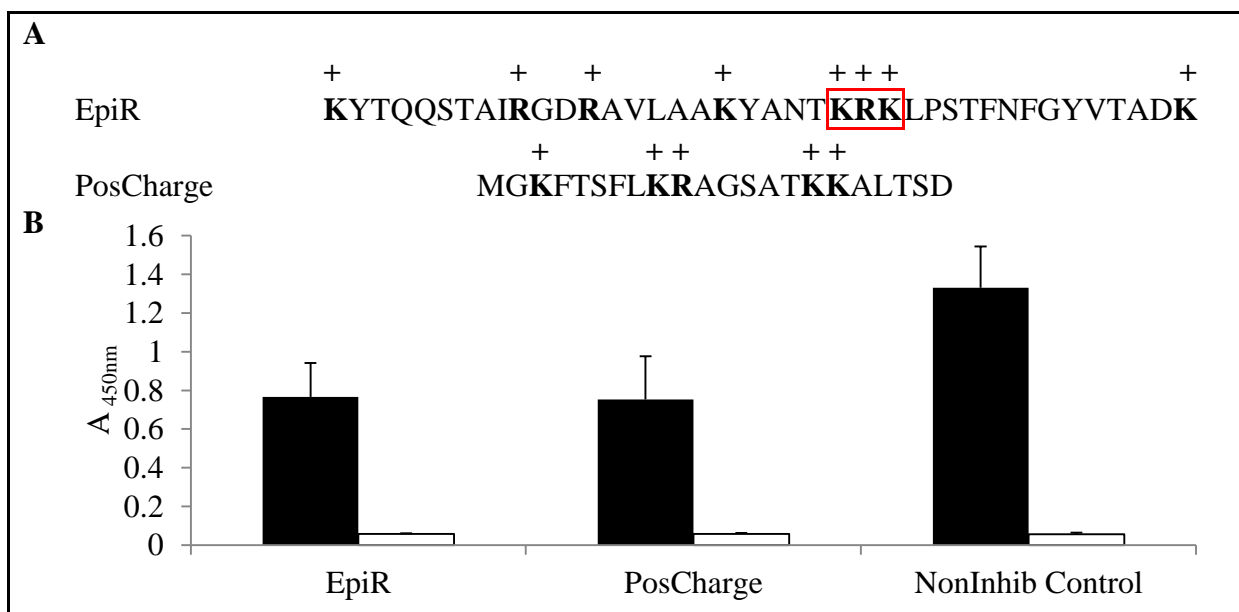


Fig. 3.5: Binding of soluble scFv2 to immobilized SAT2/ZIM/7/83 in a competitive blocking ELISA in the presence of 200 µM of the EpiR peptide and a non-specific positively charged peptide (PosCharge). (A) The amino acid sequence of the EpiR and PosCharge peptides used in the blocking ELISA are indicated. (B) A competitive blocking ELISA was performed to determine whether the non-specific positively charged peptide inhibits binding of soluble scFv2 (black bars) to immobilized SAT2/ZIM/7/83. In this assay, the synthetic peptide EpiR, a non-inhibition control (NonInhib control), in which the peptide was replaced with 1 × PBS, as well as 2% (w/v) casein (white bars) was included. The data are means ± SD of three independent experiments.

for a particular soluble scFv to the panel of SAT2 viruses were then compared to differences observed in the deduced amino acid sequence of the P1 region of the SAT2 viruses in order to predict the potential binding footprint of each soluble scFv. It has previously been shown that surface-exposed amino acid differences can be used to predict a change in antigenicity and may provide information regarding antibody footprints on the virus capsid (Reeve *et al.*, 2010; Maree *et al.*, 2011).

At a concentration of 7.5 µg/ml, soluble scFv1 reacted similarly to SAT2/ZIM/7/83, SAT2/ZIM/44/97, SAT2/ZIM/8/94, SAT2/ZIM/2/88, SAT2/ZIM/13/01 and SAT2/ZIM/5/02. The binding profile of soluble scFv1 to SAT2/ZIM/4/97 and SAT2/ZIM/5/83 was reduced by *ca.* 80% and increased by *ca.* 37% to SAT2/ZIM/7/89 when compared to SAT2/ZIM/7/83 (Fig. 3.6). In contrast, soluble scFv3 reacted similarly to SAT2/ZIM/7/83, SAT2/ZIM/7/89 and SAT2/ZIM/2/88. The binding of scFv3 was reduced by *ca.* 55% to SAT2/ZIM/5/02, *ca.* 75% to SAT2/ZIM/4/97, SAT2/ZIM/44/97, SAT2/ZIM/5/83 and SAT2/ZIM/13/01, and *ca.* 80% to SAT2/ZIM/8/94 (Fig. 3.6).

At least 10% (75 of 740) of the amino acid (aa) residues were variable when comparing the P1 regions of the nine SAT2 viruses (Appendix B to this thesis). A systematic analysis of the capsid proteins revealed the variation was mostly focused in local regions of hypervariability. The hypervariable regions were mapped to a modelled structure of a SAT2 capsid, using O₁BFS (Acharya *et al.*, 1989) as a template. The variability was found to be concentrated in β-β loops surrounding the 5-fold and 3-fold axis of the virion (Fig. 3.7 and Appendix B to this thesis). With the exception of the immunodominant VP1 βG-βH loop (VP1 aa residues 158-160), an additional four surface-exposed hypervariable sites were located within VP1, *i.e.* βB-βC loop (aa residues 43-48), βE-βF loop (aa residues 85/98-99), βF-βG loop (aa residues 108-111) and the C-terminus (aa residues 198/200-201). At least two other variable loops were identified, one located in VP2 [βE-βF loop (aa residues 133-134)] and one in VP3 [βB-βC loop (aa residues 56; 58)] (Table 3.3).

Since soluble scFvs 1 and 3 bind to complete 146S virions of SAT2 viruses but do not cause neutralization of the SAT2/ZIM/7/83 virus *in vitro*, they may recognize the surface-exposed variable β-β structure of VP1, VP2 or VP3 without interfering with the RGD-integrin interaction. In this regard, SAT2/ZIM/5/02, SAT2/ZIM/4/97, SAT2/ZIM/44/97, SAT2/ZIM/13/01 and SAT2/ZIM/8/94 differ from SAT2/ZIM/7/83, SAT2/ZIM/7/89 and

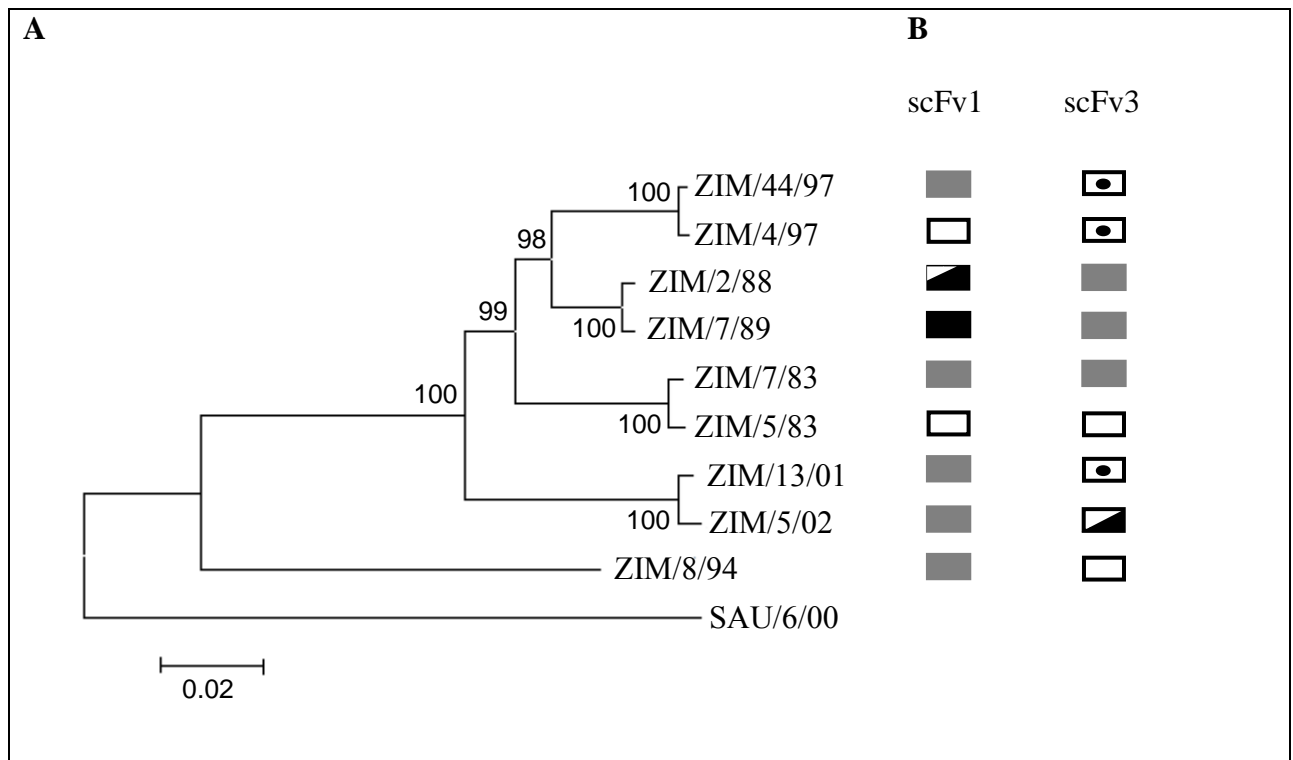


Fig. 3.6: Binding of soluble scFv1 and scFv3 to SAT2 FMD viruses. (A) Phylogenetic tree depicting the gene relationship of the P1 region of the SAT2 viruses included in this study. The tree was constructed using a neighbour-joining algorithm and node reliability is supported by 1000 bootstrap replications. The phylogenetic tree was rooted using the SAT2 isolate SAU/6/00 as an outgroup for the P1 phylogenies. (B) Binding of soluble scFv1 and scFv3 to a panel of SAT2 viruses as compared to SAT2/ZIM/7/83. ◻ <25%, ◻◉ 25-45%, ◼ 45-65%, ◼ 65-85%, ■ 85-100%, ■ > 100% binding.

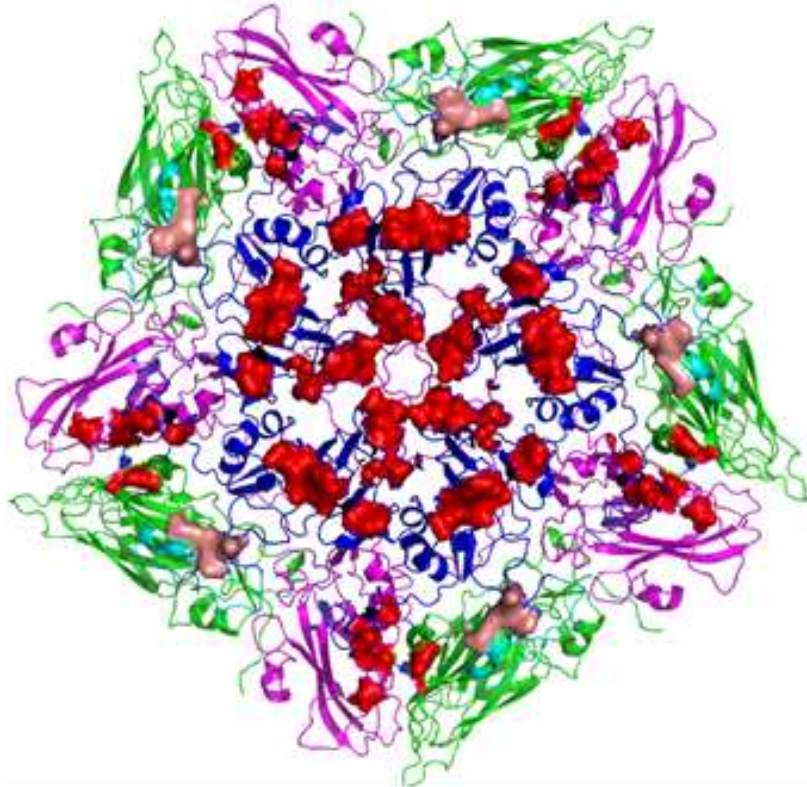


Fig. 3.7: Structure of the SAT2/ZIM/7/83 pentamer displaying the hypervariable loops surrounding the 5-fold and 3-fold axis. Four hypervariable, surface-exposed sites (red) were located within VP1 (blue) and one variable loop in each of VP3 (magenta) and VP2 (green). The β G- β H loop of VP1 is indicated in cyan and the mapped epitope to which soluble scFv2 binds is indicated in pink.

Table 3.3: Summary of the surface exposed hypervariable regions observed in an amino acid sequence alignment of the P1 polyprotein of the panel of nine SAT2 viruses used in this study

Amino acid hypervariable regions*							
Secondary structure elements of capsid							
	VP2	VP3	VP1				
Capsid β-sheets	E-F	B-C	B-C	E-F	F-G	G-H	C _T
Axis	2-fold	3-fold	5-fold	5-fold	5-fold	2-fold	3-fold
SAT2	133-134 [#]	56 [#] ,58 [#]	43-48 [#]	85 [#] , 98-99 [#]	108-110 [#]	158-160 [#]	19 [#] , 200-201 [#]

* Structurally exposed loops were taken into consideration in the identification of the hypervariable regions.

[#] Residues within these regions is surface exposed.

SAT2/ZIM/2/88 at the β B- β C, β E- β F and β F- β G loops surrounding the 5-fold axis of VP1. Amino acid differences here may contribute to the reduced binding of soluble scFv3 to these viruses. Similarly, amino acid differences in the β G- β H loop and the C-terminus of VP1 may explain the reduced binding of soluble scFv1 to SAT2/ZIM/4/97 (Appendix B to this thesis).

3.4 DISCUSSION

In this part of the study, three unique soluble SAT2-specific scFv binders from the Nkuku[®] chicken scFv phage display library were used to map an epitope on the SAT2 virion. Virus neutralization studies performed with the SAT2/ZIM/7/83 virus and the phage-displayed and soluble scFvs indicated that only soluble scFv2 was capable of neutralizing the SAT2/ZIM/7/83 virus and its binding position was successfully mapped to involve residue position 159 of the VP1 protein. The inability of the phage-displayed scFvs to neutralize SAT2/ZIM/7/83 can be attributed to steric hindrance caused as a result of the bulky tubular phage body, which is 930 nm in length (Webster, 2001) and displays the scFvs at its surface. As a result, the phage-displayed scFvs bind and neutralize the virus less efficiently than the small antigen-binding molecule of the soluble scFvs. This theory is in line with the preferential use of scFvs, as opposed to intact antibodies, in diagnostic assays and medical applications due to their smaller size (Ahmad *et al.*, 2012).

Two point mutations occurred in the VP1 protein of the SAT2/ZIM/7/83 virus that escaped neutralization by soluble scFv2. The T4→S change at the N-terminal of VP1 is 4 aa downstream of the VP3/VP1 cleavage site. These residues at the N-terminal of VP1, which have similar polar, hydroxyl-group containing side chains, are located in the internal surface of the capsid in close proximity to the N-terminal of VP2 and VP4. Neutralizing antibodies to the internal epitopes of VP1 and VP4 have been reported in poliovirus and rhinovirus (Roivainen *et al.*, 1993; Li *et al.*, 1994; Katpally *et al.*, 2009). However, neutralizing antibodies to internally located epitopes of FMDV have not been reported. Panning and analysis of binding specificity were performed using intact 146S particles. Therefore, it is unlikely that soluble scFv2 is directed to internally located residues, and T4→S was disregarded as a possible antigenic site. The T4→S residue change could be accounted for either as a result of a compensatory mutational event due to possible structural rearrangements following a distant effect (Grazioli *et al.*, 2006; Mateo and Mateu, 2007) or

due to the quasispecies nature of FMDV. Since the majority of virus escape mutants involve the interaction of a surface-orientated side-chain with a MAb, the surface exposed residue change R159→H in VP1, located at the C-terminal base of the β G- β H loop, was thought to be involved in binding of the soluble scFv2. Additionally, a synthetic peptide with its sequence derived from the VP1 β G- β H loop of SAT2/ZIM/7/83, corresponding to the region of the predicted epitope, reduced binding of soluble scFv2 to SAT2/ZIM/7/83. This led us to believe that the epitope to which soluble scFv2 binds to has been successfully mapped and that residue 159 of VP1 forms part of it. The putative binding site of soluble scFv2, within the EpiR peptide, is composed of three positively charged amino acids (KRK). As both the EpiR peptide and a non-specific positively charged peptide inhibited the binding of soluble scFv2 to immobilized SAT2/ZIM/7/83, it is proposed that the binding of the EpiR peptide to soluble scFv2 is by ionic interaction.

The likelihood that the residue change at position 159 of VP1 forms part of an antigenic site on the SAT2 capsid is supported by the fact that residue 159 of VP1 forms part of the base of the β G- β H loop and the β G- β H loop residues 140-160 have been shown to play an important role in antigenicity in most FMDV serotypes (Pfaff *et al.*, 1988; Thomas *et al.*, 1988b; Barnett *et al.*, 1989; Bolwell *et al.*, 1989; Parry *et al.*, 1989; Crowther *et al.*, 1993a). The antigenic sites Ia and Ib of SAT1 viruses, for example, involve residues on both sides of the RGD motif in the β G- β H loop (Grazioli *et al.*, 2006). In addition, plotting the observed variant amino acid residue on a model of the capsid pentamer of SAT2/ZIM/7/83 indicated that the proposed epitope would be surface exposed and this position coincides with an antigenic region predicted by Reeve *et al.* (2010) and Maree *et al.* (2011) on SAT2/ZIM/7/83. Added to this, the region has previously been identified as an antigenic area in the SAT2 viruses SAT2/RHO/1/48 (Crowther *et al.*, 1993b), as well as in SAT2/ZIM/5/81 (Grazioli *et al.*, 2006). Crowther *et al.* (1993b) identified antigenic sites, the most important of which is a conformation-dependent epitope involving amino acids at position 156 or 158 of VP1. Mice MAbs used to identify this site bound to SAT2/RHO/1/48 only and not to any of the 73 SAT2 field isolates tested, including SAT2/ZIM/7/83, indicating that this site is unique to SAT2/RHO/1/48 (Crowther *et al.*, 1993b). Two neutralizing antigenic sites, both of which are linear, have been identified for SAT2/ZIM/5/81 and one mapped in the C-terminus of VP1 (position 210) and the other within the β G- β H loop region (position 154) (Grazioli *et al.*, 2006). Our results indicated that randomly-linked variable heavy and light chains of IgY amplified from naïve chickens bound to a region on the SAT2 virion that corresponds to that

of MAbs generated from vaccinated mice, and it has the additional advantage that it bound to a panel of SAT2 viruses with a similar profile.

It is proposed that the “mechanism” of virus neutralization by soluble scFv2 is due to steric hindrance caused by soluble scFv2 binding to the C-terminal region of the β G- β H loop. As a result of the binding the presentation of the flexible external loop could be altered in such a way that the highly conserved three-amino-acid-sequence Arg-Gly-Asp (RGD) at its apex, which is involved in binding of FMDV to host cells (Fox *et al.*, 1989; Logan *et al.*, 1993; Lea *et al.*, 1994; Mason *et al.*, 1994; Curry *et al.*, 1996), is blocked from cell surface receptors. This mechanism of neutralization has also been proposed for the site A antigenic site, positioned C-terminal to the β G- β H loop RGD motif for serotype C (Verdaguer *et al.*, 1997; Domingo *et al.*, 1999). The β G- β H loop of VP1 has for many years been regarded as an immunodominant antigenic site of FMDV. However, ongoing research has indicated that other antigenic sites are also important in providing protection against FMDV and eliciting good antibody responses (Fowler *et al.*, 2010). Nevertheless, this study has shown that the soluble scFv2 intratypic conserved “footprint”, which is located in the C-terminal region of the VP1 β G- β H loop where high variation is found in field isolates, may be important as an antigenic site for SAT2 viruses.

Although direct proof of the exact binding sites of soluble scFv1 and 3 to the virion was not provided, the observed variation in the binding profiles of soluble scFv1 and 3 to the panel of SAT2 viruses, the P1 sequences of the SAT2 viruses, as well as structural data was nevertheless used as an indirect way to predict potential footprints of soluble scFv1 and scFv3 on the SAT2 capsid. Comparison of the P1 amino acid sequences of the SAT2 viruses indicated that the variation observed was confined to hypervariable loops of which five were identified in VP1 and one each in VP3 and VP2. The structural orientation of these variable loops on the capsid correlates strongly with previously identified neutralizing epitopes of type A (Thomas *et al.*, 1988b; Baxt *et al.*, 1989) and O (Barnett *et al.*, 1989; Parry *et al.*, 1989; Kitson *et al.*, 1990; Crowther *et al.*, 1993a) viruses. The hypervariable regions may act as topographical regions for binding of soluble scFv1 or scFv3 on the virus capsid and the variation observed in reactivity of these soluble scFvs to the panel of SAT2 virus might be a reflection of the amino acid variation in these regions. For example, soluble scFv1 and scFv3 consistently bind to SAT2/ZIM/7/83 with a high binding profile but to SAT2/ZIM/5/83 with a low binding profile. The P1 regions of these two ancestral SAT2 viruses vary with less

than 1% at an amino acid level. The exact positions of the seven varying residues have been mapped to a modelled structure of the SAT2/ZIM/7/83 capsid. Three of these varying residues are substituted by amino acids similar in character and four of the changes are surface exposed. Thus, it can be suggested that soluble scFv1 or 3 could be binding to a region on the capsid that overlaps with one of the four surface exposed variable residues of SAT2/ZIM/7/83 and SAT2/ZIM/5/83. By including binding profiles and P1 sequences of more viruses the topographical regions for binding of soluble scFv1 or scFv3 on the virus capsid will become more apparent. Direct proof of the role of the above-mentioned regions in binding soluble scFv1 and scFv3 will come from competition assays using appropriately designed overlapping synthetic peptides.

The sensible design of vaccines, in which potent and broadly neutralizing antibodies are elicited, is fast becoming a reliable way to address the vast genetic and antigenic diversity seen in certain pathogens, *e.g.* human immunodeficiency virus (HIV) (Burton *et al.*, 2005; Walker and Burton, 2008). Towards this end, epitope-based vaccine technology has become very appealing in recent years (Sette and Fikes, 2003; Purcell *et al.*, 2007; Shao *et al.*, 2011). Infectious cDNA technology (Rieder *et al.*, 1993; Fowler *et al.*, 2008; Blignaut *et al.*, 2011), used in the development of chimeric FMDV vaccines, may also be used to display identified epitopes for use in epitope-based vaccines. Use of the currently identified epitope, and possibly more epitopes identified in the future, as a first step towards a SAT2-specific epitope-based vaccine is therefore appealing.

In conclusion, it was shown that the antigenic site identified at the C-terminal end of the β G- β H loop of the VP1 protein is not only neutralizing, but it is also specific to the SAT2 FMDV serotype. Furthermore, the finding that the three SAT2-specific FMDV soluble scFvs bind to a panel of SAT2 viruses with different binding profiles indicates that these scFvs have the potential to be used in a scFv-based ELISA for rapid matching of vaccines with outbreak isolates. The availability of such a diagnostic test will greatly aid in vaccine matching procedures. However, more than the three SAT2-specific scFvs described here will be needed for an effective assay.

CHAPTER FOUR

DETERMINING THE EPITOPE DOMINANCE ON THE CAPSID OF A SAT2 FOOT-AND-MOUTH DISEASE VIRUS BY MUTATIONAL ANALYSES

4.1 INTRODUCTION

Genetically modified viruses provide a valuable tool for the manipulation of the biological properties of field and laboratory strains, and represent a promising avenue for the design of safe and effective vaccines. The modification of antigenic regions of human immunodeficiency virus (HIV), by amino acid substitutions in a recombinant virus, has been used to confirm monoclonal antibody (MAb)-binding sites and the antigenic dominance of these epitopes (Kong *et al.*, 2012). In this part of the study, we utilized epitope replacement in a recombinant virus to determine the epitope dominance of an important pathogen in animal health, foot-and-mouth disease virus (FMDV). FMDV, the prototype member of the genus *Aphthovirus* in the family *Picornaviridae*, is a small, non-enveloped, icosahedral virus with a single-stranded, positive-sense RNA genome. The virus capsid is constituted of 60 copies each of four virus-encoded structural proteins, VP1 to VP4; the capsid outer shell is comprised of VP1, VP2 and VP3, while VP4 lines the interior surface (Morrell *et al.*, 1987; Acharya *et al.*, 1989). Although FMDV causes a clinically indistinguishable vesicular disease in cloven-hoofed animals, there are seven distinct serotypes and multiple antigenic types (Samuel and Knowles, 2001a; Bronsvort *et al.*, 2004; Jamal *et al.*, 2011). Control of foot-and-mouth disease (FMD) has been reliant on large-scale vaccination with whole-virus inactivated vaccines (Bachrach, 1968; Garland, 1999). However, the extensive antigenic diversity within the FMDV serotypes impedes the efficacy of vaccines; therefore, the strain composition of FMD vaccines must be selected with caution (Paton *et al.*, 2005; Parida, 2009; Mahapatra *et al.*, 2012).

Due to the strong link that has been reported between the protection of cattle against FMDV and the levels of virus-neutralizing antibodies produced following vaccination (Pay and Hingley, 1987), it has generally been accepted that the most important factor imparting vaccine-induced protection against FMDV is the humoral immune response (McCullough *et al.*, 1992; Salt, 1993). The majority of FMDV-neutralizing antibodies are directed against epitopes located in the three surface-exposed capsid proteins of the virus (Xie *et al.*, 1987; Thomas *et al.*, 1988a; Acharya *et al.*, 1989; Kitson *et al.*, 1990). The mechanism by which antibodies protect against FMDV *in vivo* is poorly understood. However, previous virus studies have indicated that escape from cytotoxic T cells or from neutralizing antibodies may contribute to viral persistence and disease progression (Narayan *et al.*, 1981; Ciurea *et al.*, 2000).

MAbs have been used extensively to identify several antigenic sites on the structural proteins of virions belonging to serotypes A (Thomas *et al.*, 1988a; Baxt *et al.*, 1989; Bolwell *et al.*, 1989), O (Kitson *et al.*, 1990; Crowther *et al.*, 1993a), C (Mateu *et al.*, 1990) and Asia-1 (Sanyal *et al.*, 1997; Grazioli *et al.*, 2004). Not surprisingly, these antigenic sites were located on structural protrusions on the virus surface, formed mainly by the loops connecting β -barrel structures of the three outer capsid proteins. In particular, the β G- β H loop of VP1 has been identified as immunodominant by the use of peptides (Bittle *et al.*, 1982; Pfaff *et al.*, 1982) and is found in all serotypes of FMDV (Xie *et al.*, 1987; Thomas *et al.*, 1988a; Acharya *et al.*, 1989; Kitson *et al.*, 1990; Grazioli *et al.*, 2006). Sequencing of MAb-resistant (MAR) mutants and mapping the topography of the mutations on the X-ray crystallographic structure of O₁BFS (Acharya *et al.*, 1989) resolved five neutralizing antigenic sites on the capsid of serotype O FMDV (Kitson *et al.*, 1990; Crowther *et al.*, 1993a). The β G- β H loop either functions independently [site 5; (Crowther *et al.*, 1993a)] or as a discontinuous epitope that encompasses the highly exposed C-terminus of VP1, particularly residues 200-213. This neutralizing antigenic site has been designated site 1 and has been mapped to critical residues at positions 144, 148, 154 and 208. Site 2 involves several amino acids in the β B- β C and β E- β F loops of VP2, spanning residues 70-73, 75, 77 and 131. Site 3 includes residues 43-45 and 48, inside the β B- β C loop of VP1, while site 4 maps within the β B “knob” of VP3 with crucial residues at positions 56 and 58-59 (Xie *et al.*, 1987; Barnett *et al.*, 1989; McCahon *et al.*, 1989; Parry *et al.*, 1989; Kitson *et al.*, 1990; Mateu *et al.*, 1990).

In the case of SAT2 serotype viruses, studies involving MAR mutants revealed at least two antigenic sites. The antigenic site located in the β G- β H loop of VP1, downstream of the RGD motif, at residues 147, 148, 156, 158 (Crowther *et al.*, 1993b), position 154 (Grazioli *et al.*, 2006) and position 159 (Opperman *et al.*, 2012), is analogous to site 1 of serotype O₁BFS (Kitson *et al.*, 1990). Residue 79 of VP2 might also play a role in forming this antigenic site; however, its role in this site remains unclear (Grazioli *et al.*, 2006). The second identified antigenic site involves residue 210 at the C-terminus of the VP1. In addition, the importance of each of these individual neutralizing antigenic sites in SAT2 viruses is still undefined.

In this part of the study the role of known and predicted epitopes in the antigenicity of SAT2 viruses was investigated. Residues located in ten of the structurally exposed loops of VP1, VP2 and VP3 were selected, mutated and the effect of these mutations on antigenicity was measured with virus neutralization (VN) assays and MAbs. Evidence is presented of epitope

dominance within the SAT2 serotype of FMDV and a new epitope in VP2 for SAT2 viruses was identified. Furthermore, the results revealed the effect of the different surface-exposed mutated residues on the interaction with antibodies in sera from convalescent animals.

4.2 MATERIALS AND METHODS

4.2.1 Cell lines, viruses, plasmids and bacterial strains

Baby hamster kidney-21 cells (BHK-21, ATCC CCL-10) were maintained and propagated as described previously (Chapter 2, Section 2.2.1). The origin of the SAT2 FMDV vaccine strain ZIM/7/83 has been described in Chapter 2 (Section 2.2.1). The SAT2 virus KNP/19/89 (PK₁RS₂BHK₄; PK = pig kidney, RS = Instituto Biologico Renal Suino cells [IB-RS-2; a pig kidney cell line]) is a buffalo virus, originating from the Kruger National Park (KNP) in South Africa during 1989. The plasmid pSAT2, a previously described genome-length infectious cDNA clone of SAT2/ZIM/7/83 (Van Rensburg *et al.*, 2004), was used as the genetic backbone in the construction of recombinant cDNA clones harbouring mutated epitopes. *Escherichia coli* MAX Efficiency DH5 α (genotype: F ϕ 80 Δ lacZ Δ M15 Δ (lacZYA-argF)U169 Δ deoR Δ recA1 Δ endA1 Δ hsdR17 (r_k⁻, m_k⁺) *phoA*supE44 λ ⁻*thi*-1 *gyrA*96 *relA*1), obtained from Life Technologies, was used as the transformation host in cloning experiments.

4.2.2 Monoclonal antibody isolation

Five SAT-specific MAbs were kindly provided by The Pirbright Institute, Pirbright, Woking, UK. The MAbs were prepared by inoculating BALB/c mice with a blend of purified and inactivated 146S particles of SAT1/KEN/11/05 (BTY₁BHK₂; BTY= primary bovine thyroid cells), SAT2/ZIM/5/81 (BHK₂) and SAT3/ZIM/4/81 (RS₂BHK₃). The antigen blend comprised 40 μ g of each antigen. Three doses of the antigen blend in TiterMax[®] Gold Adjuvant (Sigma-Aldrich) were administered subcutaneously three weeks apart, and a final dose of antigen blend in 1 \times PBS was administered intravenously seven days before spleen cells were harvested for fusion with murine myeloma SP2/O cells. Cell fusion and cloning of positive hybridomas was performed according to procedures standardized at The Pirbright Institute (Jones and Howard, 1995). MAbs were screened by ELISA for their reactivity against homologous virus and five SAT2/ZIM/5/81-specific MAbs were selected (mouse IgG1 isotype MAbs 1D5 [14 μ g/ml], DA10 [8 μ g/ml], GE11 [19 μ g/ml], GD12 [15 μ g/ml], and GG1 [22 μ g/ml]).

4.2.3 Epitope prediction

The epitopes mutated in this study were predicted as described in Maree *et al.* (2011). Briefly, potential regions of antigenicity were identified based on the identification of hypervariable regions, defined as more than 60% variable residues within a 10-amino acid region, and positions of high entropy, *i.e.* the uncertainty at each amino acid position (Schneider and Stephens, 1990), within the deduced outer capsid protein sequence of SAT2 viruses. Previous studies indicated that linear amino acid sequences with high variability or residue positions with high entropy, which were structurally exposed when mapped to modelled structures of the capsid proteins, have the potential to be involved in the antigenicity of the virus (Maree *et al.*, 2011). The regions selected for mutation in this study were residues 71-72 and 133-134 of VP2, residues 133-134 of VP3, and residues 48-50, 84-86, 109-111, 137-140, 157-160, 169-171 and 199-201 of VP1.

4.2.4 Structural modelling

A homology model of the SAT2 capsid proteins was built using Modeller 9v3 (Sali and Blundell, 1993) with O₁BFS coordinates (1FOD) as template (Logan *et al.*, 1993). Alignments were performed with Clustal X and modelling scripts were generated with the Structural module of FunGIMS (Maree *et al.*, 2011). Structures were visualized and the surface-exposed residues identified with PyMol v1.1rc2pre (DeLano Scientific LLC).

4.2.5 Site-directed mutagenesis, sub-cloning and DNA sequencing

Site-directed mutagenesis of ten known and putative epitopes located in the VP1, VP2 and VP3 capsid proteins of SAT2/KNP/19/89 (GenBank accession number DQ009735) was used to replace the corresponding epitopes of the genetic disparate virus SAT2/ZIM/7/83 (GenBank accession number DQ009726) using the infectious SAT2 genome-length clone. Overlap-extension PCR mutagenesis was used to introduce the mutations into the pSAT2 plasmid. Briefly, each of the PCR processes involved the use of four oligonucleotides (two inner mutagenic oligonucleotides and two genome-specific oligonucleotides) and three different PCR reactions (Higuchi *et al.*, 1988; Ho *et al.*, 1989). A description of the different oligonucleotides is provided in Table 4.1.

Table 4.1: Synthetic oligonucleotides used for introducing SAT2/KNP/19/89 antigenic regions into the genome-length cDNA clone of SAT2/ZIM/7/83

Mutation ^a	Oligonucleotide sequence (5' to 3')	Orientation	Epitope-replaced DNA clone ^c	Recovered virus ^c
VP2-site2a F	GCTTTTTGATTGGACACCTGAAAAACCATTTGGCACGCTGTATG	Sense	pKNP ^{S2a} SAT2	vKNP ^{S2a} SAT2
VP2-site2a R	CATACAGCGTGCCAAATGGTTTTTCAGGTGTCCATCAAAAAGC	Antisense		
VP2-site2b F	GTGCCGGAGCTGTGCTCGCTTCGGAACAGAGAGGAGTTTCAAC	Sense	pKNP ^{S2b} SAT2	vKNP ^{S2b} SAT2
VP2-site2b R	GTTGAAACTCCTCTCTGTTCCGAAGCGAGCACAGCTCCGGCAC	Antisense		
VP3-site4 F	CACCAGGCATTGAGACTGAAAAGCTGCCCAAGACACCCGAGG	Sense	pKNP ^{S4} SAT2	NR
VP3-site4 R	CCTCGGGTGTCTTGGGCAGCTTTTCAGTCTCAATGCCTGGTG	Antisense		
VP1-site1 F	CAAAGTACGCCAACATCAAACACACGCTCCCCTCTACCTTC	Sense	pKNP ^{S1} SAT2	vKNP ^{S1} SAT2
VP1-site1 R	GAAGGTAGACGGGAGCGTGTGTTTGATGTTGGCTACTTTG	Antisense		
VP1-site3 F	GTTCTGACAAATAGAACCACCTTCAACGTTGACTTGATGGACAA	Sense	pKNP ^{S3} SAT2	vKNP ^{S3} SAT2
VP1-site3 R	GGTGTCCATCAAGTCAACGTTGAAGGTGGTTCATTTGTCAGAAC	Antisense		
VP1-site5 F	CAACGGTGAGTGCAAGTACGAGACGCCCGTCACTGCCATTCGCGGTGAC	Sense	pKNP ^{S5} SAT2	vKNP ^{S5} SAT2
VP1-site5 R	GTCACCGCGAATGGCAGTGACGGGCGTCTCGTACTTGCCTCACCCTTG	Antisense		
VP1-DHR F	TTGCCTGCCTTGGCGACCACCGGCGCGTGTGGTGGCAGCC	Sense	pKNP ^{DHR} SAT2	vKNP ^{DHR} SAT2
VP1-DHR R	GGCTGCCACCACACGCGCCGGTGGTTCGCCAAGGCAGGCAA	Antisense		
VP1-NKG F	CAACCCCATGGTGTTCGAACAAAGGTGTCACGCGTTTTGCTG	Sense	pKNP ^{NKG} SAT2	vKNP ^{NKG} SAT2
VP1-NKG R	CAGCAAAACGGTGACACCTTTGTTTCGAAAACACCATGGGGTTG	Antisense		
VP1-NS F	CCACGTGACCGCCGACAACAGCGTCGACGTTTACTACCGG	Sense	pKNP ^{NS} SAT2	NR
VP1-NS R	CCGGTAGTAAACGTCGACGCTGTTGTCCGGCGTCACTGG	Antisense		
VP1-Cterm F	CTCCTCCCTGGCTACGACTATGCAAGTAGGGACAGGTTTGACA	Sense	pKNP ^{Ct} SAT2	vKNP ^{Ct} SAT2
VP1-Cterm R	CTGTCAAACCTGTCCCTACTTGCATAGTCGTAGCCAGGGAGGAG	Antisense		
Genome-specific outer oligonucleotide sequences		Orientation, Purpose		
2B ^b	GACATGTCCTCCTGCATCTG	Antisense, cDNA		
cDNA-2A ^b	CGCCCCGGGGTTGGACTCAACGTCTCC	Antisense, P1 PCR		
P622 ^b	GCACTGACACCAGTCTAC	Sense, P1 PCR		

^a The structural region that was targeted for mutagenesis.

^b Designated names of the oligonucleotides used for cDNA synthesis and amplification of the capsid-coding region.

^c The mutated genome-length cDNA clone and recombinant virus names are derived from the KNP buffalo isolate, SAT2/KNP/19/89, followed by the structural region that was mutated in superscript, and lastly the SAT2 genetic background of SAT2/ZIM/7/83.

NR: No viable virus was recovered.

Mutations were introduced into distinct PCR products using overlapping inner mutagenic oligonucleotides. Using pSAT2 as template DNA, a “left” PCR was performed by using a common forward outer oligonucleotide (P622) and an antisense inner mutagenic oligonucleotide, whereas the “right” PCR was performed with a sense inner mutagenic oligonucleotide and a common outer reverse oligonucleotide (cDNA-2A). The inner mutagenic oligonucleotides were designed to be between 40 and 49 nucleotides in length and encoded the desired mutation with *ca.* 15 to 20 nucleotides of “correct” sequence, *i.e.* corresponding to that of SAT2/ZIM/7/83, on both sides of the mutation. The two PCRs were performed on a GeneAmp[®] 9700 PCR thermocycler (Applied Biosystems) with the TakaRa ExTaq PCR system, and the following cycling conditions: 95°C for 20 s, 58°C for 20 s, 68°C for 2 min (30 cycles). The two first-round PCR amplicons were gel purified with the Nucleospin[®] Extract kit (Macherey-Nagel) according to the manufacturer’s instructions, mixed in equimolar amounts and extended for 8 cycles of 95°C for 20 s and 74°C for 5 min using the Advantage[®] 2 PCR system (Clontech). The product was then used as template for PCR employing the sense and antisense outer oligonucleotides detailed above. The cycling conditions for this third PCR were 95°C for 20 s and 68°C for 3 min (25 cycles).

The PCR-amplified products were visualized by electrophoresis on a 1.5% (w/v) agarose gel and the size of the amplified DNA fragments was estimated against a DNA molecular weight marker (100-bp DNA ladder or phage λ DNA digested with *HindIII*; Promega). The amplicons were purified from agarose gels with the Nucleospin[®] Extract kit (Macherey-Nagel) according to the manufacturer’s instructions. The gel-purified PCR amplicons of *ca.* 2.2 kb (containing part of the VP2, VP3 and VP1-2A coding region of SAT2/ZIM/7/83 with the newly introduced mutations) were digested with *SspI* (Promega) and *XmaI* (Promega), and then cloned into the unique *SspI* and *XmaI* restriction sites of the pSAT2 plasmid. Replacement of the SAT2/ZIM/7/83 epitopes with those of SAT2/KNP/19/89 was verified by nucleotide sequencing using genome-specific oligonucleotides and the ABI PRISM[™] Big Dye[™] Terminator Cycle Sequencing Ready Reaction kit v3.0 (Applied Biosystems). The extension products were resolved on an ABI PRISM[™] 3100 Genetic Analyzer (Applied Biosystems). No unintended site mutations were found and the epitope-replaced mutant clones are indicated in Table 4.2.

Table 4.2: A summary of the surface-exposed amino acid differences between the capsid proteins of FMDV SAT2/KNP/19/89 and SAT2/ZIM/7/83. The identified surface-exposed loops of SAT2/KNP/19/89 were used to replace the corresponding epitopes of the genetic disparate virus SAT2/ZIM/7/83 using the infectious SAT2 genome-length clone, pSAT2. The amino acid sequences of the epitope-replaced p^{KNP}SAT2 clones, as well as the recovered viruses are also indicated.

	Site 2a	Site 2b	Site 4	Site 3	Site DHR	Site NKG	Site 5	Site 1	Site NS	Site Ct
Capsid protein β-sheet	VP2 βB-βC	VP2 βE-βF	VP3 βE-βF	VP1 βB-βC	VP1 βD-βE	VP1 βF-βG	VP1 βG-βH	VP1 βG-βH	VP1 βH-βI	VP1 C-term
Parental SAT2/ZIM/7/83 ^a	TSDK	LKDR	TDRL	TAFAV	GEHER	SHNNV	YTQQST	NTKHKL	DKPV	DHADR
Parental SAT2/KNP/19/89	TPEK	LRDR	TEKL	TTFNV	GDHRR	SNKGV	YETPVT	NIKHTL	DNSV	DYASR
Epitope-replaced clones	TPEK	LRNR	TEKL	TTFNV	GDHRR	SNKGV	YETPVT	NIKHTL	DNSV	DYASR
Recovered epitope- replaced mutants ^b	TPEK	LRNR	NR	TTFNV	GDHRR	SNKGV	YETPVT	NIKH<u>K</u>L	NR	DYASR

^a The amino acid residues in SAT2/ZIM/7/83 that were mutated to the corresponding region in SAT2/KNP/19/89 are indicated in bold.

^b The mutated amino acid residue in Site 1 that reverted back to the original SAT2/ZIM/7/83 sequence when the epitope-replaced virus was recovered in BHK-21 cells is underlined in bold italics.

NR: No viable virus was recovered from these epitope-replaced mutants.

4.2.6 *In vitro* RNA synthesis, transfection and virus recovery

The constructed epitope-replaced mutant cDNA clones and pSAT2 were linearized at the *Swa*I (Roche Diagnostics) site downstream of the poly-A tract, and used as templates to synthesize RNA *in vitro* with the MEGAScript[®] T7 kit (Ambion) according to the manufacturer's instructions. The RNA transcripts were quantitated by spectrophotometry and *ca.* 3 µg of transcripts was introduced into BHK-21 cells, seeded in 35-mm diameter cell culture plates (Nunc), with Lipofectamine[™] 2000 reagent (Life Technologies) according to the manufacturer's instructions. Transfected monolayers were incubated at 37°C with a 5% CO₂ influx for 48 h in Eagle's basal medium (BME) containing 1% (v/v) foetal calf serum (FCS) and 25 mM HEPES (Invitogen). The virus-containing supernatants were used to infect fresh BHK-21 monolayers (35-mm cell culture plates) and incubated at 37°C for 48 h. Viruses were subsequently harvested from infected cells by a freeze-thaw cycle and passaged four or more times on BHK-21 cells, using 10% of the supernatant of the previous passage. Viruses recovered from transfection included vSAT2, vKNP^{S1}SAT2, vKNP^{S2a}SAT2, vKNP^{S2b}SAT2, vKNP^{S3}SAT2, vKNP^{S5}SAT2, vKNP^{DHR}SAT2, vKNP^{NKG}SAT2 and vKNP^{Ct}SAT2. Following the recovery of viable viruses the external capsid region was obtained by RT-PCR, as described below, and the presence of the mutations was verified with automated sequencing.

4.2.7 RNA isolation, cDNA synthesis and PCR amplification

RNA was extracted from infected tissue culture samples with a guanidinium-based nucleic acid extraction method, as described previously (Bastos, 1998), and used as template for cDNA synthesis. Avian myeloblastosis virus (AMV) reverse transcriptase (Promega) and the genome-specific oligonucleotide 2B (Vangrysperre and De Clercq, 1996) were used for reverse transcription, which was carried out at 42°C for 2 h. The external capsid-coding region of the epitope-replaced mutant viruses was amplified using the Expand High Fidelity PCR system (Roche Diagnostics) and flanking oligonucleotides, P622 and cDNA-2A (Table 4.1).

4.2.8 Plaque titrations

BHK-21 cell monolayers were infected for 1 h with the parental viruses SAT2/ZIM/7/83 and SAT2/KNP/19/89, as well as with vSAT2 and the above-mentioned epitope-replaced mutant viruses, followed by addition of 2 ml of tragacanth overlay (Rieder *et al.*, 1993) and

incubation for 48 h. The cell monolayers were stained with 1% (w/v) methylene blue in 10% ethanol and 10% formaldehyde, prepared with $1 \times$ PBS (pH 7.4). Virus titres were calculated and expressed as the logarithm of the plaque forming units per millilitre (pfu/ml).

4.2.9 Neutralization of infectivity in cell culture

The antigenic diversity of the epitope-replaced mutant viruses in relation to the SAT2/ZIM/7/83 and SAT2/KNP/19/89 viruses was determined with cross-neutralization assays in micro-plates, as described in the OIE Manual of Standards (2009). BHK-21 cells were used as the indicator system in the test. Convalescent bovine reference sera were prepared by intradermolingual inoculation of cattle with 10^4 50% tissue culture infective dose (TCID₅₀) of either SAT2/ZIM/7/83 or SAT2/KNP/19/89. Two cattle were infected with each virus strain and blood was collected at 21 days post-inoculation. Cattle were housed in the biosafety level 3 isolation facility at the Transboundary Animal Diseases Programme (TADP) with the approval of the Onderstepoort Veterinary Institute (OVI) Animal Ethics Committee. The end-point titre of the serum against the homologous and heterologous virus was calculated as the \log_{10} of the reciprocal of the last dilution of serum to neutralize 100 TCID₅₀ virus in 50% of the wells (Rweyemamu *et al.*, 1978; Rweyemamu, 1984). Differences in the average neutralization titre between each of the epitope-replaced mutant viruses and the reference viruses, across four independent experiments, were calculated.

To determine whether the five SAT2-specific MAbs (Section 4.2.2: 1D5, DA10, GE11, GD12 and GG1) were able to neutralize the parental SAT2/ZIM/7/83 and SAT2/KNP/19/89 viruses, as well as the epitope-replaced mutant viruses, cross-neutralization assays were performed using BHK-21 cell cultures as described above. A minor modification to the protocol described above was that the sera were replaced with the SAT2-specific MAbs.

4.2.10 Sandwich ELISA with SAT2-specific MAbs

A sandwich ELISA was used for titration of the five SAT2-specific MAbs (Section 4.2.2) and to characterize the parental and eight epitope-replaced mutant viruses. Maxisorp™ ELISA plates (Nunc) were coated with an optimal dilution of rabbit SAT2 antiserum (SAT2/ZIM/7/83; SAT2/KNP/19/89; SAT2/SAR/16/83) in 50 mM carbonate/bicarbonate buffer (pH 9.6) and stored overnight at 4°C. A serial two-fold dilution (1:5 to 1:40) of the parental or epitope-replaced mutant viruses (supernatant of infected cells) in blocking buffer

(0.05 M Tris, 0.15 M KCl containing 0.5% [w/v] milk powder), was applied to the ELISA plates. Viruses were trapped by incubation at 37°C for 1 h after which the plates were washed with 1 × PBS containing 0.05% (v/v) Tween-20 (PBS-0.05%T). Two-fold dilutions (1:20 to 1:80) of each of the MAbs, prepared in blocking buffer, was added and the plates incubated at 37°C for 1 h. The ELISA plates were washed with PBS-0.05%T and horseradish peroxidase (HRP)-conjugated rabbit anti-mouse IgG (Sigma-Aldrich), diluted 1:20 000 in blocking buffer, was added. Following incubation at 37°C for 1 h and washing of the plates, the ELISA plates were developed as described previously (Chapter 2, Section 2.2.6).

The binding of the MAbs to the epitope-replaced viruses was calculated as follows. The mean absorbance reading at 450 nm (A_{450}) for the binding of each MAb to the epitope-replaced viruses were corrected by subtracting the background value. The adjusted A_{450} values for each MAb to the epitope-replaced viruses were then expressed as a percentage of the mean A_{450} value obtained against vSAT2.

4.2.11 Virus purification

The 146S virus particles of SAT2/ZIM/7/83, vKNP^{SS}SAT2, vKNP^{DHR}SAT2 and vKNP^{NKG}SAT2 were concentrated with 8% (w/v) polyethylene glycol (PEG)-8000 (Sigma-Aldrich) and purified on 10-50% (w/v) sucrose density gradients (SDG), prepared in TNE buffer, as described previously (Chapter 2, Section 2.2.2). Peak fractions corresponding to the 146S virus particles were pooled and the amount of antigen (μ g) calculated.

4.2.12 Single dilution avidity ELISA (sd A-ELISA)

MaxisorpTM ELISA plates were coated, in duplicate, overnight at 4°C with 200 ng of purified virus in 50 mM carbonate/bicarbonate buffer (pH 9.6). The plates were washed with PBS-0.05%T and blocked at 37°C for 1.5 h with blocking buffer containing 1 × PBS, 20% (v/v) FCS, 0.002% (w/v) thimerosal and 0.1% (v/v) phenol red. Following incubation the plates were washed with wash solution (133 mM NaCl, 8.6 mM K₂HPO₄, 1.5 mM KH₂PO₄, 0.05% [v/v] Tween-20 in dH₂O). Serum samples (SAT2/ZIM/7/83 and SAT2/KNP/19/89) were diluted 1:80 in blocking buffer, and added to the plates. A pool of five negative sera was used as a negative control. The plates were incubated at 37°C for 1 h, washed three times with PBS-0.05%T and then 4 M urea in 1 × PBS was added to one plate and 1 × PBS was

added to the remaining plate. Following incubation at room temperature for 15 min, the plates were washed four times with wash solution before the FMDV-specific antibodies were detected with a HRP-labelled anti-bovine conjugate (Sigma-Aldrich), diluted 1:20 000 in blocking buffer. The colorimetric reaction was developed after incubation at 37°C for 1 h and washing of the plates as described previously (Chapter 2, Section 2.2.6). Mean optical density (OD) values of samples and controls were corrected by subtracting mean blank OD values (cOD). The avidity index (AI) was calculated as described previously (Lavoria *et al.*, 2012). Briefly, $AI\% = (cOD \text{ sample with urea} / cOD \text{ sample without urea}) \times 100$.

4.2.13 Statistical analyses

Virus neutralization titres and avidity indexes of epitope-replaced mutant viruses and the SAT2/ZIM/7/83 and SAT2/KNP/19/89 viruses with convalescent bovine reference sera were compared using repeated measures of ANOVA with Bonferroni adjustment of *p* values for post-hoc comparisons. All statistical analyses were performed using GraphPad Prism v5.03 for Windows (GraphPad Software, Inc.).

4.2.14 Ethics statement

All procedures involving animals were approved by the OVI Animal Ethics Committee according to national animal welfare standards and performed with the permission of the Department of Agriculture, Forestry and Fisheries (DAFF).

4.3 RESULTS

4.3.1 Prediction of antigenic sites on the SAT2 FMDV capsid

A combined approach of capsid protein amino acid (aa) sequence alignments and known structural data was used to predict antigenic sites on the surface of SAT2 virions. A complete alignment of the deduced amino acid sequences of the capsid proteins of 23 SAT2 viruses across Africa revealed amino acid regions of high variability (Reeve *et al.*, 2010; Maree *et al.*, 2011) that corresponded or were located in close proximity to previously identified epitopes on types O and A viruses (see Introduction for references). Many of the variable regions were located within flexible structural loops of the viral capsid and have been linked to poor cross-reaction in *in vitro* virus neutralization (VN) assays (Logan *et al.*, 1993; Sanyal *et al.*, 1997).

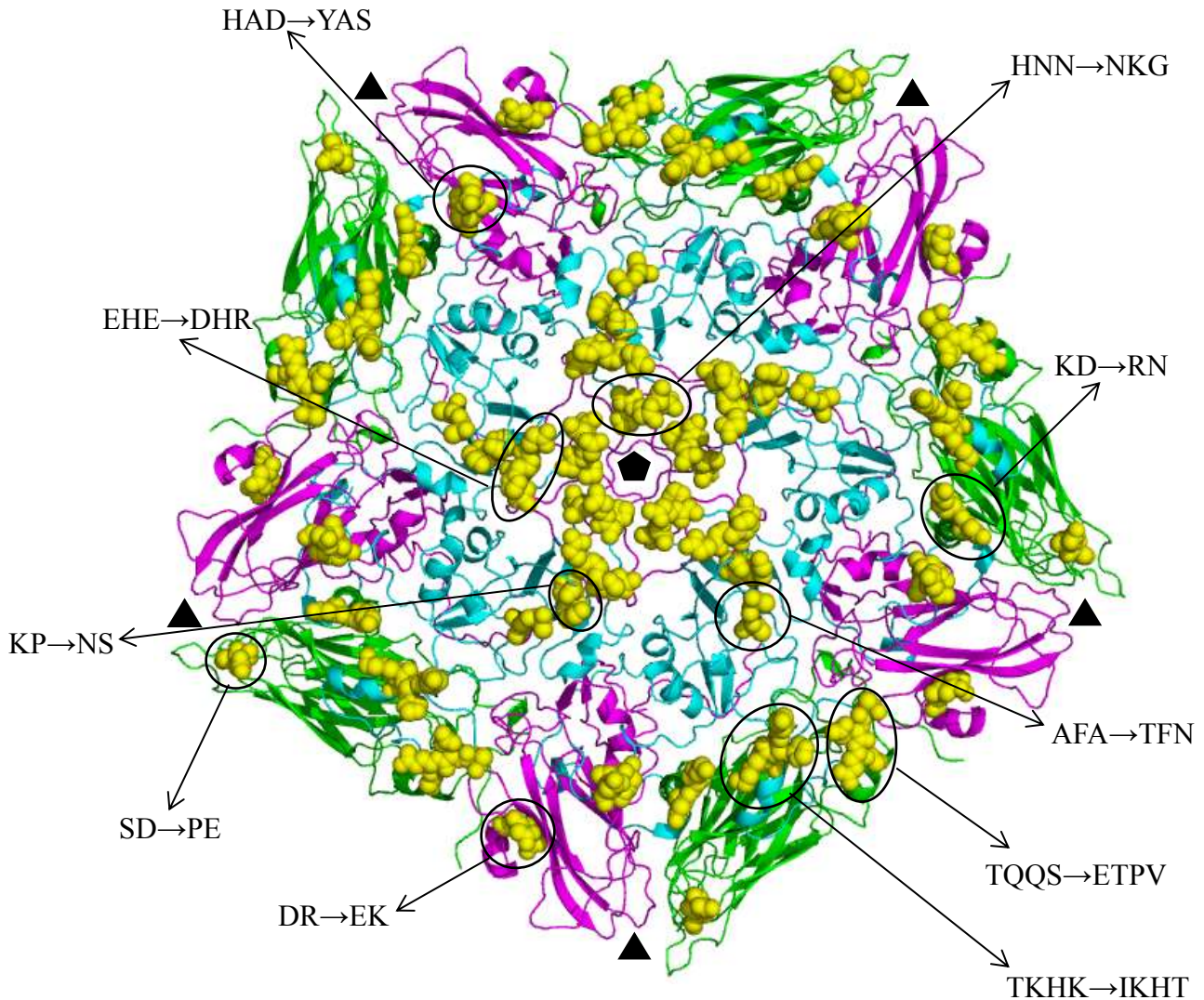


Fig. 4.1: The location of the surface-exposed amino acid differences between the capsids of FMDV SAT2/KNP/19/89 and SAT2/ZIM/7/83 on a ribbon protein diagram of a modelled pentamer of SAT2/ZIM/7/83 (Maree *et al.*, 2011). The protein subunits and structural features are colour coded: VP1 (cyan), VP2 (green) and VP3 (magenta). VP4 has been hidden from the structure. The pore, located at the five-fold axis of the capsid (black pentagon), is shown in the middle of the structure. The three-fold axis is depicted by the black triangles. The positions of amino acid changes, predicted to play a role in antigenicity, are shown as yellow spheres. The amino acid changes are those indicated in Table 4.2 for SAT2/KNP/19/89 and SAT2/ZIM/7/83.

A systematic analysis of the capsid proteins of SAT2/KNP/19/89 (topotype I) and SAT2/ZIM/7/83 (topotype II) revealed that the most variation, 18% (38 of 217 aa), occurred in the VP1 protein, while the VP2 and VP3 proteins varied by *ca.* 4% (9 of 219 aa and 8 of 222 aa, respectively). Comparison of the deduced amino acids and structurally exposed loops revealed that of the four hypervariable regions previously identified in the VP2 region, only two, *i.e.* positions 71-72 (SD→PE; βB-βC) and 133-134 (KD→RN; βE-βF) of VP2 (Table 4.2; Fig. 4.1), had significant surface exposure in the complete virion and were therefore chosen for this study. Only one site of VP3 was variable, *i.e.* residues 133-134 (DR→EK; βE-βF), and seven sites with variable residues were identified in VP1 (Table 4.2; Fig. 4.1). These included residues 48-50 (AFA→TFN; corresponds to site 3 of serotype O), 84-86 (EHE→DHR; βE-βF), 109-111 (HNN→NKG; βF-βG), 137-140 (TQQS→ETPV; βG-βH, corresponds to site 5 of serotype O), 157-160 (TKHK→IKHT; βG-βH, corresponds to site 1 of serotype O), 169-171 (KP→NS; βH-βI), and 199-201 (HAD→YAS; C-terminus of VP1) (Table 4.2; Fig. 4.1). Residues 144-154 and 210 of VP1, both of which fall within previously identified SAT2 antigenic regions (Crowther *et al.*, 1993b; Grazioli *et al.*, 2006; Opperman *et al.*, 2012), were conserved between SAT2/ZIM/7/83 and SAT2/KNP/19/89.

To investigate the consequence of the observed genetic divergence between the SAT2/ZIM/7/83 and SAT2/KNP/19/89 FMDV strains on the antigenicity of the viruses, an epitope replacement strategy was followed in which the exposed putative epitopic structures of SAT2/KNP/19/89 were used to replace those of SAT2/ZIM/7/83.

4.3.2 Generation of recombinant viruses with altered surface epitopes

To study the effects of individual epitope-replaced mutations in a defined genetic background on the antigenic dominance of SAT2 viruses, recombinant virus mutants using the infectious cDNA clone of the SAT2 virus ZIM/7/83, pSAT2 (Fig. 4.2), were constructed. Of the ten putative and known epitopes for SAT2 viruses selected from sequence and structure data, eight represented surface-exposed loops connecting β-β structures in the three outer capsid proteins. However, two mutations, DR→EK (133-134 of VP3) and KP→NS (169-171 of VP1), though they appear to have surface exposure, were somewhat obscured by adjacent structural elements and were selected on the basis of sequence heterogeneity only. The location and the electrostatic effects of these mutations on the virion surface are shown in Fig. 4.3. Introducing or removing charge on the capsid surface may completely abrogate

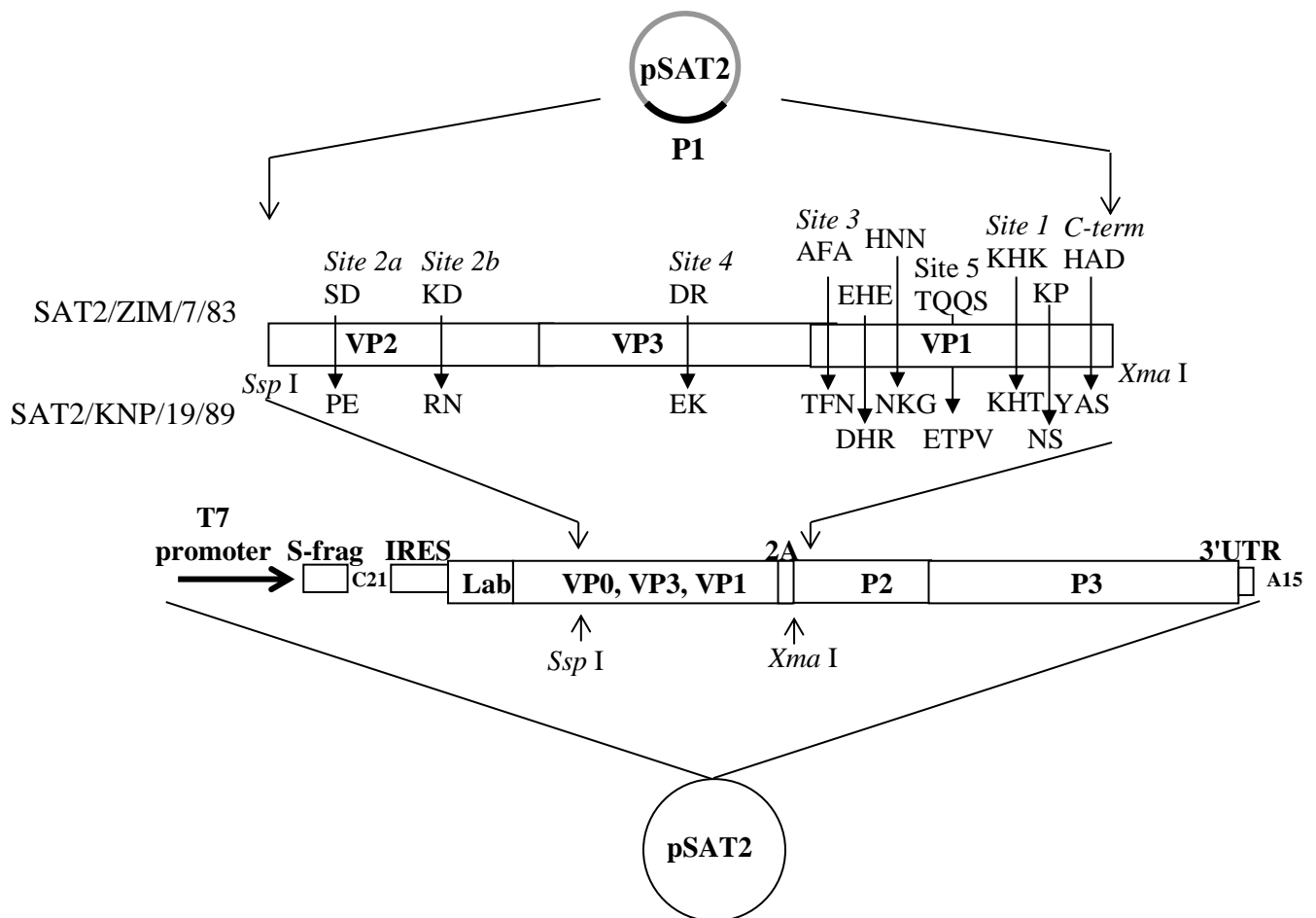


Fig. 4.2: Schematic representation of the epitope replacement strategy used to replace epitopic structures of SAT2/ZIM/7/83 with those of SAT2/KNP/19/89. The ten known and predicted epitopic structures located in the VP1, VP2 and VP3 capsid proteins of SAT2/KNP/19/89, as well as the corresponding epitopes of the genetic disparate virus SAT2/ZIM/7/83 are indicated. Following overlap-extension mutagenesis, as described under Materials and Methods, the epitope mutated P1 regions were cloned into the *Ssp* I and *Xma* I sites of pSAT2, a genome-length cDNA clone of SAT2/ZIM/7/83.

ionic interaction between antibodies and the capsid. Some of the substitutions caused an increase in the net positive charge in the VP1 protein of the derived mutant virus (Fig. 4.3B, C). The EHE→DHR (84-86 of VP1) and HNN→NKG (109-111 of VP1) mutations had a strong effect on the local surface potential of the capsid, creating a distinct patch of surface area that is predominantly positively charged. The TQQS→ETPV (137-140 of VP1) mutation introduced a strong negative charge at the N-terminal base of the βG-βH loop.

The engineered epitope-replaced mutant viruses, designated vKNP^{S2a}SAT2, vKNP^{S2b}SAT2, vKNP^{S3}SAT2, vKNP^{DHR}SAT2, vKNP^{NKG}SAT2, vKNP^{S5}SAT2, vKNP^{S1}SAT2 and vKNP^{Ct}SAT2, were readily obtained from the infectious cDNA clones. High titre stocks were prepared and their genetic identities confirmed by sequencing analysis. Despite numerous attempts to recover viable vKNP^{S1}SAT2, the recovered viable virus either corresponded to the wild-type virus (*i.e.* SAT2/ZIM/7/83) or only the T156→I mutation in VP1 was present (Table 4.2). The K159→T mutation reverted back to SAT2/ZIM/7/83 K159 (Table 4.2). No viruses could be recovered for mutations at positions 133-134 of VP3 (KNP^{S4}SAT2) and 169-171 of VP1 (KNP^{NS}SAT2), despite transfection of a minimum of 20 sequence-correct clones of each mutant.

4.3.3 Effect of the epitope-replaced mutations on plaque morphologies and infectivity titres

Plaque morphologies for the eight viable epitope-replaced mutant viruses, as well as the vSAT2, SAT2/ZIM/7/83 and SAT2/KNP/19/89 viruses were compared on BHK-21 cells (Table 4.3). The two VP2 epitope-replaced mutant viruses, namely vKNP^{S2a}SAT2 and vKNP^{S2b}SAT2, the parental viruses (SAT2/ZIM/7/83 and SAT2/KNP/19/89) and four of the VP1 epitope-replaced mutant viruses (vKNP^{S1}SAT2, vKNP^{S5}SAT2, vKNP^{Ct}SAT2, vKNP^{DHR}SAT2) all formed medium (3-5 mm) and large (6-8 mm) plaques on BHK-21 cells. The virus derived from the genome-length infectious cDNA clone of SAT2/ZIM/7/83, vSAT2, as well as vKNP^{S3}SAT2 and vKNP^{NKG}SAT2 formed small (< 2 mm), medium (3-5 mm) and large (6-8 mm) plaques. Notably, vKNP^{S3}SAT2 mostly formed small and medium plaques with only a few large plaques being observed. vKNP^{S3}SAT2 and vKNP^{S1}SAT2 displayed higher infectivity titres (*ca.* 1.6×10^7 pfu/ml) as opposed to the remaining epitope-replaced mutant viruses and the SAT2/ZIM/7/83 parental virus, which all had similar infectivity titres (ranging from 1.2×10^6 to 7.4×10^6 pfu/ml). The SAT2/KNP/19/89 parental virus had an infectivity titre of 1×10^8 pfu/ml.

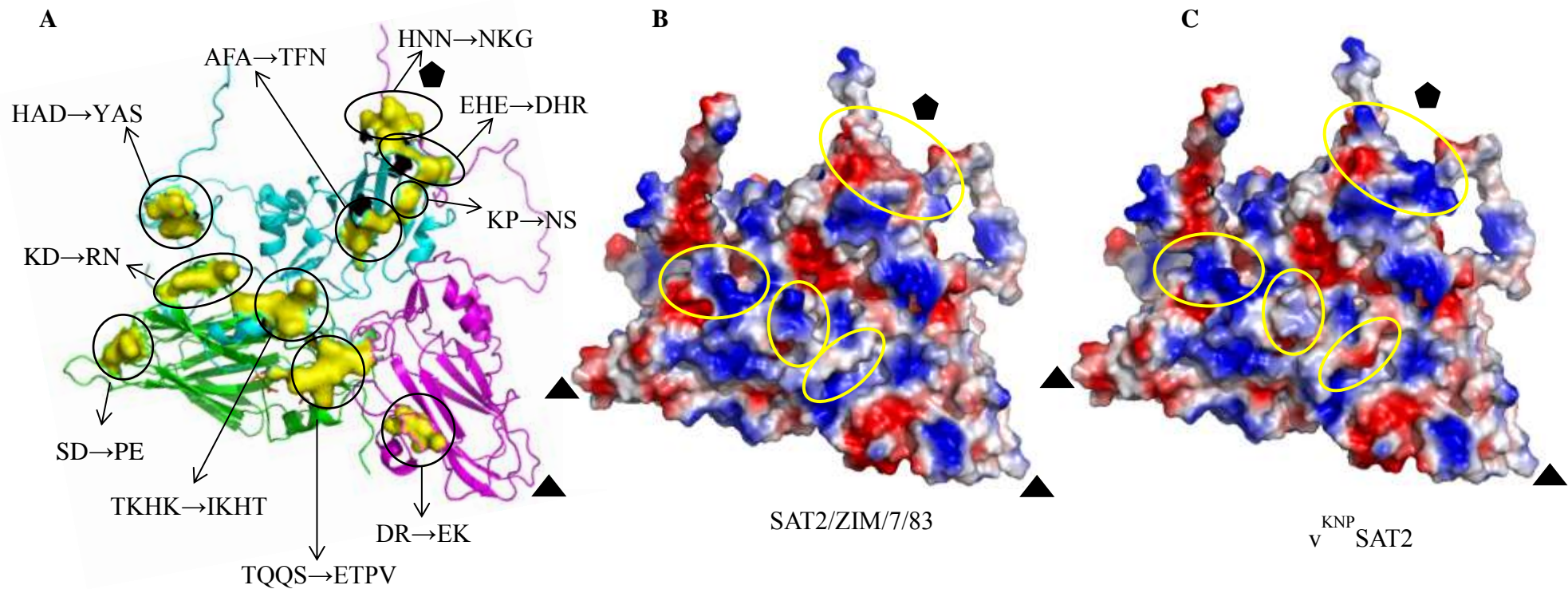


Fig. 4.3: Surface models of the crystallographic protomers of SAT2/ZIM/7/83 and the epitope-replaced mutant virus v^{KNP} SAT2, indicating differences in electrostatic potential. The mutations and their positions on the FMDV protomer are indicated in (A). The electrostatic potential of the SAT2/ZIM/7/83 protomer is shown in (B), whereas the electrostatic potential of the v^{KNP} SAT2 protomer, containing all ten mutations, is indicated in (C). Positively-charged surfaces are shown in blue, and negatively-charged surfaces are in red. The yellow ovals indicate areas of a change in the local electrostatic potential. The black pentagon and triangle shows the five- and three-fold axis of the virion, respectively.

Table 4.3: Parental and recombinant viruses containing the epitope-replaced mutations in the outer capsid proteins VP1 and VP2

Virus	Epitope mutation	Infectivity titre (log pfu/ml)	Passage History	Plaque size on BHK-21 cells
vSAT2 (wild-type)	-	5.4×10^6	BHK ₄	Small (< 2 mm); medium (< 3-5 mm) and large (6-8 mm)
SAT2/ZIM/7/83	-	4.2×10^6	B ₁ BHK ₈	Medium (3-5 mm) and large (6-8 mm)
SAT2/KNP/19/89	-	1.0×10^8	PK ₁ RS ₂ BHK ₄	Medium (3-5 mm) and large (6-8 mm)
vKNP ^{S2a} SAT2	SD→PE	3.2×10^6	BHK ₄	Medium (3-5 mm) and large (6-8 mm)
vKNP ^{S2b} SAT2	KD→RN	3.4×10^6	BHK ₄	Medium (3-5 mm) and large (6-8 mm)
vKNP ^{S3} SAT2	AFA→TFN	1.5×10^7	BHK ₆	Small (< 2 mm) and medium (3-5 mm) and large (6-8 mm)
vKNP ^{S5} SAT2	TQQS→ETPV	1.2×10^6	BHK ₆	Medium (3-5 mm) and large (6-8 mm)
vKNP ^{S1} SAT2	TKHK→IKHK	1.6×10^7	BHK ₄	Medium (3-5 mm) and large (6-8 mm)
vKNP ^{DHR} SAT2	EHE→DHR	4.6×10^6	BHK ₄	Medium (3-5 mm) and large (6-8 mm)
vKNP ^{NKG} SAT2	HNN→NKG	4.4×10^6	BHK ₅	Small (< 2 mm); medium (< 3-5 mm) and large (6-8 mm)
vKNP ^{C1} SAT2	HAD→YAS	7.4×10^6	BHK ₅	Medium (3-5 mm) and large (6-8 mm)

4.3.4 Antigenicity of recombinant viruses with altered surface epitopes

The overall antigenic distance of the epitope-replaced mutant and parental viruses were examined by VN assays using antisera from convalescent cattle raised against the parental viruses SAT2/ZIM/7/83 and SAT2/KNP/19/89. The neutralization titres of the eight epitope-replaced mutant viruses and the parental virus controls are shown in Fig. 4.4. With the exception of one epitope-replaced mutant virus, no significant differences ($p < 0.05$) in the neutralization titres were observed compared to SAT2/ZIM/7/83 for any of the epitope-replaced mutants, when measured against the SAT2/ZIM/7/83 and the SAT2/KNP/19/89 sera. The most dramatic change in the antigenicity of the virus was observed for the TQQS→ETPV mutation in the N-terminal part of the β G- β H loop of VP1, showing a significant increase ($p < 0.05$) of 40% in the neutralization titre with the SAT2/ZIM/7/83 serum (Fig. 4.4).

Next, we determined the avidity index of the convalescent bovine reference sera (SAT2/ZIM/7/83 or SAT2/KNP/19/89) against the parental virus SAT2/ZIM/7/83, the vKNP^{S5}SAT2 mutant virus (TQQS→ETPV) and two other epitope-replaced mutant viruses (vKNP^{DHR}SAT2 and vKNP^{NKG}SAT2). The TQQS→ETPV (site 5) mutation significantly increased ($p < 0.001$) the avidity index of the vKNP^{S5}SAT2 virus to the SAT2/ZIM/7/83 serum (Fig. 4.5A). The avidity index of the vKNP^{DHR}SAT2 and vKNP^{NKG}SAT2 epitope-replaced mutant viruses to the SAT2/ZIM/7/83 serum was not significantly different to that obtained for the parental virus (Fig. 4.5A). Interestingly, the avidity index of the SAT2/KNP/19/89 serum against vKNP^{S5}SAT2 and vKNP^{DHR}SAT2 was significantly higher ($p < 0.001$) than that of the SAT2/ZIM/7/83 (Fig. 4.5B). No significant difference was observed in the avidity index of the SAT2/KNP/19/89 serum for the vKNP^{NKG}SAT2 mutant compared to the SAT2/ZIM/7/83 virus (Fig. 4.5B).

4.3.5 Antigenic profiling of epitope-replaced and parental viruses with SAT2-specific MAbs

The epitope-replaced mutant viruses and the parental SAT2 viruses were characterized on the basis of their reactivity to SAT2-specific MAbs. None of the MAbs were shown to neutralize the viruses *in vitro* using VN assays. The binding profiles of the SAT2-specific MAbs were subsequently examined using a sandwich ELISA (Fig. 4.6). All five of the MAbs reacted to SAT2/ZIM/7/83 and vSAT2. However, two distinct clusters were observed with regards to

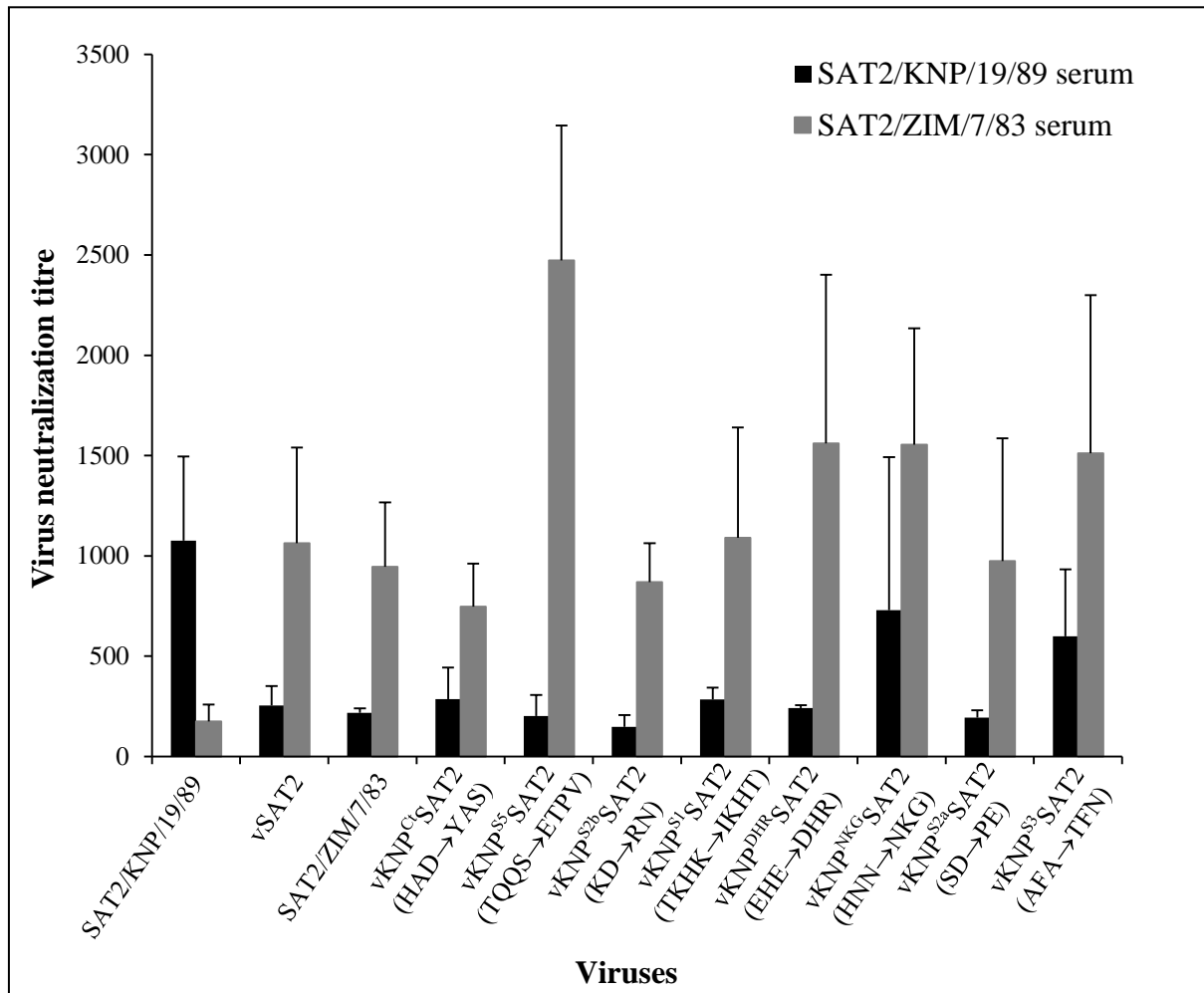


Fig. 4.4: Antigenic profiles of the epitope-replaced mutant viruses, as indicated in the figure, and SAT2/KNP/19/89, SAT2/ZIM/783 and vSAT2 tested against SAT2 antisera (KNP/19/89 and ZIM/7/83). Convalescent cattle antisera were prepared at TADP by intradermolingual inoculation of cattle with 10^4 TCID₅₀ of SAT2/KNP/19/89 or SAT2/ZIM/7/83, and blood was collected at 21 days post-inoculation. The data are means \pm SD of four independent experiments.

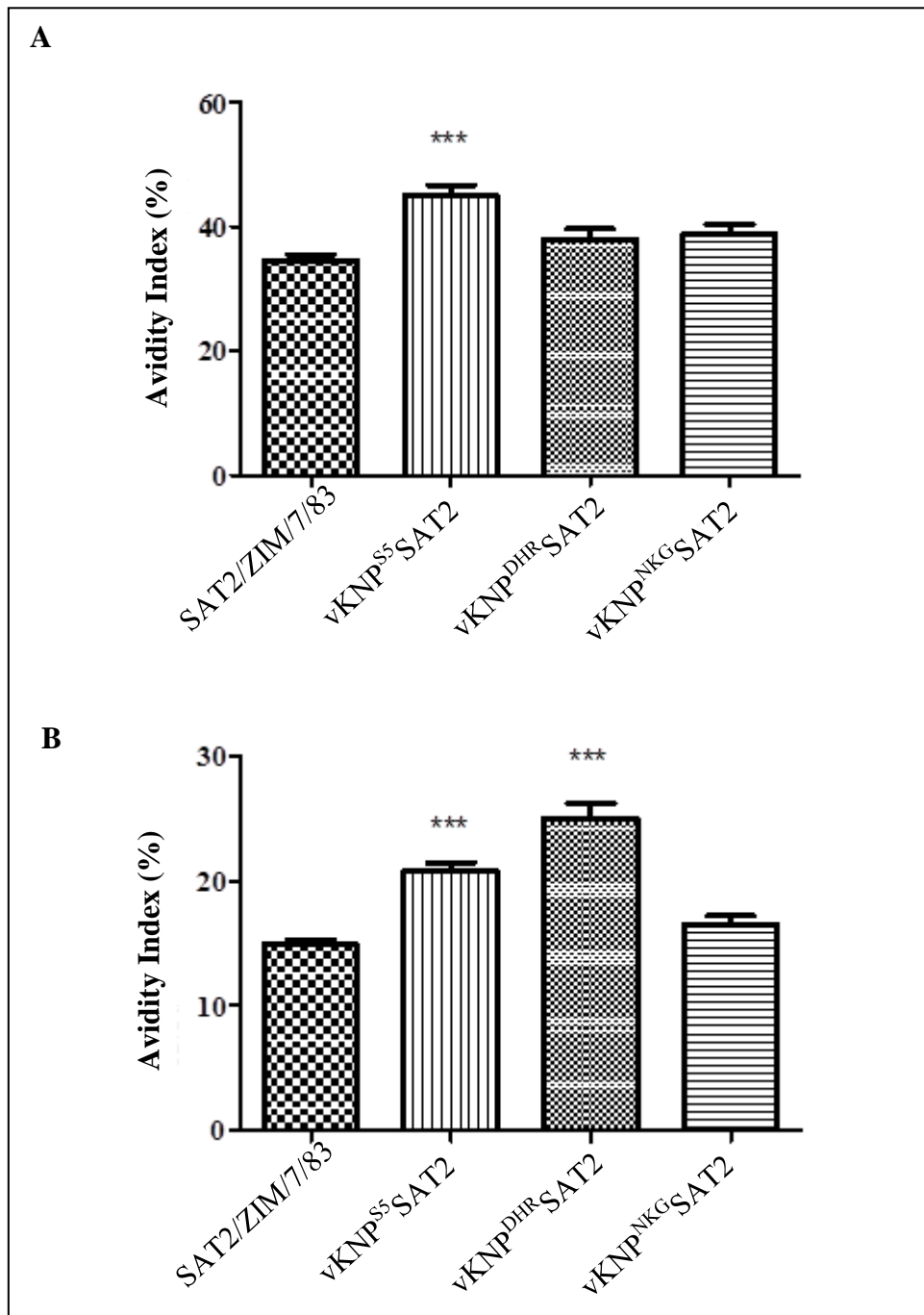


Fig. 4.5: Avidity index of the parental SAT2/ZIM/7/83 virus and three epitope-replaced mutant viruses. The avidity index of the parental virus SAT2/ZIM/7/83, as well as that of the epitope-replaced viruses vKNP^{S5}SAT2, vKNP^{DHR}SAT2 and vKNP^{NKG}SAT2 with the SAT2/ZIM/7/83 serum (A) and the SAT2/KNP/19/89 serum (B) are indicated. The avidity index of the three epitope-replaced mutant viruses was compared to the parental SAT2/ZIM/7/83 virus. Significant differences are indicated by ***. The data are means \pm SD of two independent experiments.

the reactivity of the MAbs to SAT2/KNP/19/89 and the epitope-replaced mutant viruses. MAbs 1D5, GG1, GE11 and DA10 reacted with vSAT2, SAT2/ZIM/7/83, vKNP^{S2b}SAT2, vKNP^{DHR}SAT2, vKNP^{NKG}SAT2, vKNP^{S1}SAT2, vKNP^{S3}SAT2, vKNP^{S5}SAT2 and vKNP^{Ct}SAT2, but not with SAT2/KNP/19/89 and vKNP^{S2a}SAT2. In the second cluster, MAb GD12 reacted with all eight epitope-replaced viruses as well as vSAT2, SAT2/ZIM/7/83 and SAT2/KNP/19/89, albeit with different reactivity. The MAb GD12 showed < 55% reactivity to vKNP^{S2a}SAT2, vKNP^{S2b}SAT2, vKNP^{DHR}SAT2, vKNP^{NKG}SAT2 and SAT2/KNP/19/89 compared to vSAT2 and SAT2/ZIM/7/83 (Fig. 4.6).

The four MAbs that did not react to SAT2/KNP/19/89 and vKNP^{S2a}SAT2 could be divided into two principal binding sub-clusters (Fig. 4.6). The one sub-cluster, consisting of MAbs GG1 and DA10, recognized vSAT2, SAT2/ZIM/7/83 and seven epitope-replaced viruses (vKNP^{S2b}SAT2, vKNP^{DHR}SAT2, vKNP^{NKG}SAT2, vKNP^{S1}SAT2, vKNP^{S3}SAT2, vKNP^{S5}SAT2 and vKNP^{Ct}SAT2) with the same reactivity. The second binding sub-cluster, consisting of MAbs 1D5 and GE11, reacted poorly with vKNP^{S2b}SAT2 and vKNP^{S3}SAT2, *i.e.* less than 55%.

The reasons for the differences in the reactivity patterns to the epitope-replaced and parental viruses may be explained on a structural level. The failure of MAbs 1D5, GG1, GE11 and DA10 to react to SAT2/KNP/19/89 and vKNP^{S2a}SAT2 could be due to the mutation of serine to proline at position 71 of VP2 (Table 4.2; Fig. 4.7). Two of the four MAbs, *i.e.* 1D5 and GE11, also showed poor reactivity to viruses with mutations at residues 133-134 of VP2 (equivalent to site 2B of serotype O) and 48-50 of VP1 (equivalent to site 3 of serotype O). The critical residue substitution in VP2 is the replacement of a negatively charged aspartic residue with asparagine at position 134 and may explain the lower reactivity of the two MAbs to vKNP^{S2b}SAT2 (Table 4.2; Fig. 4.7). The A48→T and A50→N (hydrophilic and bulky) substitutions in VP1 could be contributing to the lower reactivity to vKNP^{S3}SAT2 (Table 4.2; Fig. 4.7). Taken together, the results suggest that residues 71-72 of VP2 are the major contact point for MAbs 1D5 and GE11. It should be noted that the binding footprint of these MAbs have similar reactivity profiles that include residues 133-134 of VP2 and 48-50 of VP1. Structurally, residues 48-50 of VP1 and 133-134 of VP2 are located *ca.* 51 Å and 16 Å from residues 71-72 of VP2, respectively (Fig. 4.7A). The binding footprint of the MAbs GG1 and DA10 on the SAT2 capsid overlaps with that of the above-mentioned MAbs at the critical residues 71-72 of VP2. However, MAbs GG1 and DA10 reacted similarly to the

	1D5	GG1	GE11	GD12	DA10
vKNP ^{Ct} SAT2	■	■	■	■	■
vKNP ^{S1} SAT2	■	■	■	■	■
vKNP ^{S3} SAT2	◻	■	◻	■	■
vKNP ^{S5} SAT2	■	■	■	■	■
vKNP ^{NKG} SAT2	■	■	■	◻	■
vKNP ^{DHR} SAT2	■	■	■	◻	■
vKNP ^{S2a} SAT2	◻	◻	◻	◻	◻
vKNP ^{S2b} SAT2	◻	■	◻	◻	■
SAT2/KNP/19/89	◻	◻	◻	◻	◻
SAT2/ZIM/7/83	■	■	■	■	■
vSAT2	■	■	■	■	■

Fig. 4.6: Reactivity of the epitope-replaced mutant viruses and parental viruses with SAT2-specific MAb. A sandwich ELISA was performed using a 1:10 dilution of the respective viruses and a 1:40 dilution of the MAb. The ELISA was performed in duplicate and the results of one experiment are shown, as the same trend was observed for both ELISAs. The reactivity scale in relation to the interaction of the MAb to the epitope-replaced mutant viruses is as follows: white boxes: 0-15%; half-coloured boxes: 15-55%; and black boxes: 55-100%.

remaining seven epitope-replaced mutant viruses, vSAT2 and SAT2/ZIM/7/83, and thus do not have the same binding footprint of MAbs 1D5 and GE11.

MAB GD12, on the other hand, presents different epitope specificity to SAT2 viruses as elucidated by its ability to react to both vKNPS^{2a}SAT2 and SAT2/KNP/19/89, albeit with lower reactivity. Lower reactivity was also observed for viruses with amino acid substitutions at residues 84-86 and 109-111 of VP1, and residues 133-134 of VP2. Residues 71-72 and 133-134 of VP2 and 84-86 of VP1 are surface exposed in the length of a shallow groove formed by the interaction of VP2, VP3 and VP1, and located *ca.* 16 Å and 33 Å from each other (Fig. 4.7B). However, the role of residues 109-111 of VP1 in the interaction with this MAB is not as evident as it is located in a depression at the five-fold axis of the virion.

4.4 DISCUSSION

Little is known about the neutralizing epitopes for the three SAT serotype viruses. In this part of the study the role of structurally-exposed loops on a SAT2 capsid in the antigenicity of the virus was investigated. Following an epitope replacement strategy, we measured the antigenic diversity of eight epitope-replaced mutant viruses with polyclonal antisera raised against SAT2/ZIM/7/83, used as the genetic background, and SAT2/KNP/19/89, used as the epitope-donor. One of these replacements significantly increased not only the neutralization titre, but also the avidity index to the SAT2/ZIM/7/83 serum as compared to the parental SAT2/ZIM/7/83 virus. Furthermore, antigenic profiling of the epitope-replaced and parental viruses with SAT2-specific MAbs revealed that the major contact point of four of the MAbs is residues 71-72 of VP2 and the binding footprint of two of the MAbs encompasses residues 133-134 of VP2 and 48-50 of VP1.

The FMDV capsid is composed of 60 copies of each of four structural proteins, namely VP1, VP2 and VP3, which are surface exposed, and the internally located VP4 protein (Morrell *et al.*, 1987; Acharya *et al.*, 1989). The conformation and sequence of surface-exposed loops may lead to significant differences in the binding affinity of antibodies and/or receptor interactions (Jin *et al.*, 1992; Mateu *et al.*, 1998). A commonly used method to assess the antigenic matching of FMDV within a serotype is the VNT. However, the role of the surface-exposed loops of the FMDV capsid on antigenicity and their interaction with

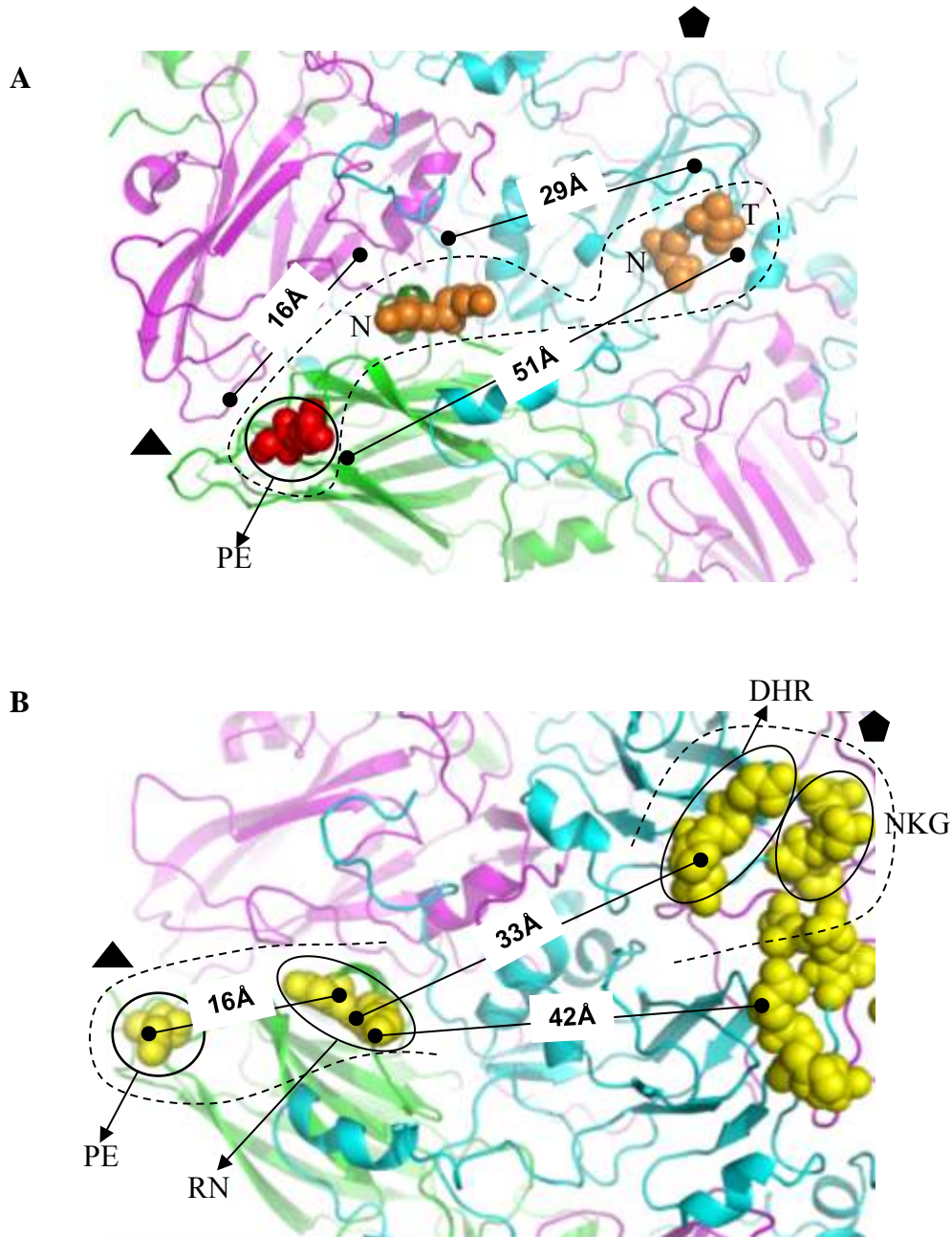


Fig. 4.7: A ribbon protein diagram depicting the proposed binding footprint of the SAT2-specific MAbs onto the capsid protein of a modelled SAT2 pentamer. (A) The critical reactivity residue for MAbs 1D5, GG1, GE11 and DA10, encompassing residues 71-72 (SD→PE) of VP2, is indicated in red spheres. The two other contact points for 1D5 and GE11 are indicated in orange spheres and the putative footprint for the latter two MAbs is shown by the broken line. (B) The putative contact points for the MAb GD12 are shown by the yellow spheres and a putative footprint indicated by the broken line. The estimated distances between the residues that make contact with the MAbs are also indicated. The black pentagon and triangle indicates the five- and three-fold axis of the virion, respectively.

antibodies with different affinities and avidities is still obscure. The results reported from the VNT studies suggest that critical residues located in surface-exposed loops contribute significantly to the stability of antigen-antibody complexes and blocking of virus entry into cells, either by direct contact with the antibody or indirectly by local distortion of side-chains. It has been shown that the affinity of antigen-antibody complexes could be strongly reduced by truncation of specific side-chains within the in-contact epitope (Jin *et al.*, 1992; Cunningham and Wells, 1993; Verdaguer *et al.*, 1998).

The mutant viruses used in this study are all single mutants, in which two to four critical, variable residues located on structurally-exposed loops of the outer capsid proteins, in a comparison between SAT2/ZIM/7/83 and SAT2/KNP/19/89, were mutated. By making use of this strategy, it is expected that the corresponding epitopic regions within SAT2/ZIM/7/83 will be modified, thus abrogating antibody interaction. Studies have indicated both in FMDV (Dunn *et al.*, 1998) and in poliovirus (Rezapkin *et al.*, 2010) that mutations within antigenic sites completely abrogate binding with relevant virus-specific antibodies. Thus, antibodies produced against an intact or naïve epitope will not recognize the mutated epitope. Furthermore, Crowther *et al.* (1993a) reported a 15% drop in neutralization-antibody titre in post-vaccination cattle sera following a single amino acid mutation. Similarly, studies involving synthetic peptides have indicated that adding, removing or changing a single amino acid within the peptide alters the binding or reactivity of the peptide to a MAb (Meloan *et al.*, 1987). Using structural data and sequence alignments as predictors, the mutations introduced in this study have been designed to optimally affect antibody binding in the antibody footprints on the virus capsid. This is expected to change the neutralizing kinetics of the mutant viruses against known antisera. The neutralization profile was then used as a measure of the role of each epitope in the antigenicity of SAT2 viruses.

Of the ten antigenic regions identified in this study, five correspond to epitopes identified in type O₁BFS and one to an epitope identified in SAT2 viruses. Sites 1, 2a, 2b, 3, 4 and 5 all correspond to the same sites identified in type O₁BFS and site 1 (TKHK→TKHT) was also identified in SAT2/RHO/1/48 (Crowther *et al.*, 1993b) and SAT2/ZIM/7/83 (Opperman *et al.*, 2012). For a long time it was believed that the βG-βH loop of VP1 is an immunodominant antigenic site (site 1) on the viral capsid surface of FMDV (Laporte *et al.*, 1973; Bachrach *et al.*, 1975; Adam *et al.*, 1978; Meloan *et al.*, 1979; Strohmaier *et al.*, 1982).

However, substantial evidence has been presented that suggest other antigenic sites may also be important in eliciting protective antibody responses to FMDV (Fowler *et al.*, 2010 and references within). Moreover, Mahapatra *et al.* (2012) indicated that following vaccination, antibodies to all five type O neutralizing antigenic sites were detected in sheep, cattle and pigs with most antibodies directed against antigenic site 2, followed by antigenic site 1.

The neutralization profiles of seven of the epitope-replaced mutant viruses were not significantly different than the neutralization profile of vSAT2 and SAT2/ZIM/7/83 with the SAT2/ZIM/7/83 and the SAT2/KNP/19/89 antisera. No significant difference was observed in the avidity index for the HNN→NKG mutant virus with the SAT2/ZIM/7/83 and the SAT2/KNP/19/89 antisera compared to the SAT2/ZIM/7/83 parental virus. The avidity index of the EHE→DHR mutant did not significantly increase with the SAT2/ZIM/7/83 serum; however, a significant increase was observed with the SAT2/KNP/19/89 serum. The increase in avidity index with the SAT2/KNP/19/89 serum may be due to the presence of non-neutralizing antibodies present in the antiserum that have high avidity to the mutant virus.

Noteworthy, the neutralization profile of the epitope-replaced mutant virus containing the TQQS→ETPV mutation revealed a significantly higher neutralization titre with the SAT2/ZIM/7/83 antisera. The TQQS→ETPV mutation also resulted in a significant increase in the avidity index of the SAT2/ZIM/7/83 serum to this epitope-replaced virus compared to the parental SAT2/ZIM/7/83 virus. High avidity indexes have previously been linked to high neutralization titres (Bachmann *et al.*, 1997; Saika *et al.*, 2008; Leonova and Pavlenko, 2009; Franco Mahecha *et al.*, 2011). The increased neutralization profile seen for the TQQS→ETPV mutation may be due to the increased stability of a neutralizing epitope, as a result of the amino acids changes introduced, thus increasing the binding avidity of the neutralizing antibodies to the epitope.

In an attempt to more precisely dissect the role of each predicted SAT2 epitope in its interaction with antibodies, we measured the reactivity of each mutant virus against five MAbs in a sandwich ELISA as opposed to the traditional generation of virus escape mutants. The ability of the five SAT2-specific MAbs to neutralize the epitope-replaced mutant viruses was also tested. This allowed us to specifically measure the role of each epitope in the antibody-antigen interaction and the identification of at least two novel non-neutralizing, discontinuous epitopes. MAbs 1D5, GG1, GE11 and DA10 had a common interaction site

encompassing residues 71-72 of VP2, confirming, for the first time, the role of this site as an epitope for SAT2 viruses. These residues have recently been suggested to be a possible antigenic region using structure-based B-cell epitope prediction programs (Borley *et al.*, 2013). However, residues 71-72 of VP2 did not function in isolation in the interaction of SAT2 capsids to the MAbs.

In the sub-cluster, consisting of MAbs 1D5 and GE11, there was a significant reduction in reactivity (> 45%) against viruses with mutations at residues 48-50 of VP1 and 133-134 of VP2. This suggests an interaction between the β B- β C and the β E- β F loops of VP2 (site 2) and the β B- β C of VP1 (site 3). Similarly, MAbs GG1 and DA10 have their critical contact site situated at residues 71-72 of VP2; however, it does not show reduction of reactivity to any of the other epitope-replaced mutant viruses. Although we do not have direct structural evidence, it can be hypothesized that these two MAbs may bind to β B- β C of VP2 on opposite sides of the two-fold axis of the virus. Our data provided evidence that the second unique MAb binding footprint, that of GD12, encompasses residues 71-72 and 133-134 of VP2 (site 2), and 84-86 and 109-111 of VP1. None of the SAT2-specific MAbs neutralized any of the epitope-replaced or parental viruses, indicating that these novel epitopes are non-neutralizing. Similarly, a non-neutralizing, conformational epitope at the N-terminus of VP2 has been reported for Asia-1 and other FMDV serotypes (Freiberg *et al.*, 1999; Marquardt and Freiberg, 2000; Rana and Bagchi, 2008). Furthermore, a structural relationship between antigenic sites situated on the exposed loops of different capsid proteins has been noted previously. For Asia-1, a structural relationship exists between antigenic site 2 (residues 67, 72, 74, 77 and 79 of VP2) and antigenic site 4 (residues 58 and 59 of VP3) (Grazioli *et al.*, 2013). Similarly, antigenic site 3 of serotype A encompasses residues 82-88 in the β B- β C loop of VP2, 58-61 in the β B- β C loop of VP3, 136-139 in the β E- β F loop and 195 in the β H- β I loop of VP3 for A10 (Thomas *et al.*, 1988b). Also, the major discontinuous antigenic site of serotype C, site D, includes several loops of VP1 (subsite D1), VP2 (subsite D2) and VP3 (subsite D3) (Lea *et al.*, 1994). This is the first time, however, that the β E- β F and β F- β G loops of VP1 are implicated as having a role in the antigenicity of FMDV.

The results revealed in this study provide hope that directed evolution or rational engineering of antigenic sites through mutation of a few of the antigenically relevant positions may broaden the antigenic spectrum within a serotype of FMDV. However, further structural and functional studies are necessary to better understand the structural basis of antigenic variation

and the interaction of the FMDV epitopes in antibody binding. FMD vaccines based on chemically inactivated virus with engineered epitopes might elicit broad immune responses. This approach also allows for the introduction of improved T-cell epitopes and mutations on the inter-pentamer interfaces to improve stability of the capsid, thereby potentially inducing long-lived immune responses. This, in turn, will have a positive impact on the control of FMD by vaccination in endemic regions.

CHAPTER FIVE

CONCLUDING REMARKS

In many parts of the world, foot-and-mouth disease (FMD) has either been eradicated or controlled by preventative vaccination strategies using chemically inactivated vaccines (Doel, 2003; Rodriguez and Grubman, 2009). However, the extensive variability that exists within the South African Territories (SAT) type viruses hampers the control of FMD in southern Africa, as distinct genetic and antigenic variants exist in different geographical regions (Vosloo *et al.*, 1995; Bastos *et al.*, 2001; Bastos *et al.*, 2003b). Antigenic variation is the result of either single or multiple amino acid changes in surface-exposed loops of the viral capsid (antigenic drift) or conformational changes (antigenic shift). Knowledge of the amino acid residues that comprise the antigenic determinants of SAT type viruses is essential for the rational design of vaccine seed viruses that antigenically match circulating emerging or re-emerging viruses, as well as induce a broad immunological response. To address the lack of information regarding antigenic regions of the SAT serotypes, the aim of this study was to identify antigenic sites on a SAT2 foot-and-mouth disease virus (FMDV) using two different approaches. In this conclusion, the new information that has been discovered during this investigation will be summarized briefly and suggestions regarding future research will be made.

The first approach that was used to identify antigenic sites on a SAT2 FMDV relied on the panning of a SAT2 vaccine strain, ZIM/7/83, with a naïve semi-synthetic chicken IgY phage display library, known as the Nkuku[®] library (Van Wyngaardt *et al.*, 2004). Three unique SAT2/ZIM/7/83-specific single-chain variable fragments (scFvs) were isolated, designated scFv1, scFv2 and scFv3. Characterization of these soluble scFvs revealed that only scFv2 was capable of neutralizing the SAT2/ZIM/7/83 virus and was subsequently used to generate neutralization-resistant virus variants. Sequence analysis of the P1 region of virus escaping neutralization revealed two residue changes. The first of these, a Thr to Ser change at residue 4 of the N-terminal of VP1, was hidden from the virion surface and was consequently not considered as an antigenic region. The second residue change, from His to Arg, occurred at position 159 of the VP1 protein. Residue 159 is not only surface exposed, but is located at the C-terminal base of the β G- β H loop, a known immunogenic region of FMDV. A synthetic peptide, of which the sequence corresponded to the predicted antigenic site of the VP1 β G- β H loop of SAT2/ZIM/7/83, inhibited binding of soluble scFv2 to the virus in a concentration-dependent manner. This newly mapped neutralizing epitope can therefore be

considered in the design of SAT2 vaccine seed viruses for the regional control of FMD in Africa.

In addition to using recombinant scFvs for the localization of antigenic determinants and the identification of protective epitopes, they can also be exploited as immunoreagents for the design of improved diagnostic tests (Chowdhury and Wu, 2005; Schirrmann *et al.*, 2011; Ahmad *et al.*, 2012). In this regard, results obtained during the course of this study indicated that the isolated soluble scFvs cross-reacted with a panel of eight SAT2 viruses, albeit with different binding profiles, but did not cross-react with representative viruses from the SAT1 or SAT3 serotypes. Additionally, the sensitivity and stability of the soluble scFvs were investigated in order to evaluate their usefulness as capturing or detection reagents in an ELISA assay. The results indicated that only soluble scFv1 and 2 retained their native conformation following adsorption onto polystyrene plates and they could capture purified SAT2/ZIM/7/83 virion particles, as well as virus from infected cell culture supernatants. Furthermore, both of these soluble scFvs withstood a freeze-thaw cycle and were stable for at least one month at 4°C. Based on the data obtained, soluble scFv2 may be used in a diagnostic assay to identify SAT2 serotype viruses, whereas soluble scFv1, based on its varying binding profiles to SAT2 viruses, may be used to differentiate viruses within the SAT2 serotype (intra-typic differences). Nevertheless, for such assays to be reliable it would be necessary to expand the current panel of SAT2-specific scFvs. This may be achieved in future through the construction and panning of a SAT2-specific immune phage display library.

As an alternate approach to identify antigenic sites in SAT2/ZIM/7/83, an epitope replacement strategy was followed. Capsid protein amino acid sequence alignments and known structural data were used to predict antigenic sites on the surface of a SAT2 virion. Ten putative antigenic sites were identified on the SAT2/ZIM/7/83 capsid, the majority of which were structurally exposed and situated on highly variable loops. Using reverse genetics, the identified putative epitopic structures of SAT2/ZIM/7/83 were replaced with the corresponding region of the antigenically disparate virus SAT2/KNP/19/89 and eight epitope-replaced viruses were recovered. Despite numerous attempts, it was not possible to recover viable epitope-replaced viruses following replacement of amino acid residues 133-134 of VP3 and 169-171 of VP1. The introduction of these mutations may have resulted in conformational alterations in the capsid structure that abrogated the interaction of amino

acids critical for the stabilization of the capsid structure. The above variable regions were obscured somewhat by adjacent structural elements and may be more important in structural stabilization due to intra-molecular interactions. Therefore, a compensatory mutational event may be essential to recover these viruses (Mateo and Mateu, 2007). The overall antigenic distance of the epitope-replaced mutant and parental viruses were examined by virus neutralization assays using convalescent antisera from cattle raised against the SAT2/ZIM/7/83 and SAT2/KNP/19/89 parental viruses. The results indicated that an epitope-replaced virus, containing a TQQS to ETPV mutation in the N-terminal part of the β G- β H loop of VP1, showed an increase in both the neutralization titre and avidity index when compared to the parental SAT2/ZIM/7/83 virus with anti-SAT2/ZIM/7/83 sera. Our data supports previous observations that a high avidity index is associated with increased neutralization *in vitro* (Bachmann *et al.*, 1997; Saika *et al.*, 2008; Leonova and Pavlenko, 2009; Franco Mahecha *et al.*, 2011). The avidity index is a direct function of high-affinity antibodies in the sera. It is reasonable to expect that higher affinity antibodies will bind and block virus entry in cultured cells more effectively, thus leading to better neutralization *in vitro*. It is also encouraging to know that high neutralization titres and the presence of high-avidity antibodies have been correlated as markers of protection (Trautman and Bennett, 1979; Black *et al.*, 1984; Jin *et al.*, 2007; Franco Mahecha *et al.*, 2011; Lavoria *et al.*, 2012). Therefore, the inclusion of this epitope within a vaccine strain should provide increased protection. However, to date we do not have direct evidence nor have we investigated the protection afforded by this mutant virus in animals.

Antigenic profiling of the epitope-replaced and parental viruses with five non-neutralizing SAT2-specific monoclonal antibodies (MAbs) led to the identification of two non-neutralizing antigenic regions. Both regions were mapped to incorporate residues 71-72 of VP2 as the major contact point of the MAbs. This is the first time this antigenic region has been identified on the capsid of a SAT2 FMDV. The first MAb footprint encompassed residues 71-72 and 133-134 of VP2 and 48-50 of VP1. The binding footprint of the second antigenic region was shown to incorporate residues 71-72 and 133-134 of VP2, as well as residues 84-86 and 109-111 of VP1. Unlike previous studies where the identification of epitopes relied on residue changes that abrogate binding of MAbs, but with no information on how different epitopic units contribute to the interaction with the MAb, we described the complete binding footprint of an antibody within the FMD capsid. The complementary determining regions (CDRs) of the heavy and light chain variable regions of an antibody

interact with an antigen, and the CDR3 is the most diverse (Amit *et al.*, 1986; Elgert, 2009). Interestingly, the bovine Ig heavy chain has a very long CDR3, which can be more than 60 residues in length (Saini *et al.*, 1999; Saini *et al.*, 2003) and may span a spatial distance of up to 45 Å (Dr R Reeve, personal communication). As the CDR3 region is the most heterogeneous, the three-dimensional structure of the antigen-binding site is influenced by its length (Reth, 1994). Therefore, the structural design of engineered vaccines with increased antigenicity will need to incorporate the entire binding footprint identified in this study, *i.e.* all three contact points of the binding antibody.

Although protection is linked to the presence of high levels of neutralizing antibodies in the serum, *in vitro* non-neutralizing monoclonal antibodies have been shown to induce protection in mice (McCullough *et al.*, 1986). It was hypothesized that high levels of specific antibody might interfere directly with virus infection of the cells and the lower concentrations of antibodies, which were non-neutralizing (*in vitro*) but protective, were presumably reflecting antibody-dependent enhancement of phagocytosis of the virus. For FMDV, opsonisation of the virus-antibody complex enhances phagocytosis by monocytes and macrophages *in vitro*. Therefore, if non-neutralizing antigenic sites are included in vaccines the innate immune response can be enhanced against antigenically less related FMDV challenge strains and restrict their ability to replicate. We believe that the results generated during this study are a step closer to understanding the role of epitopes on the virus capsid in the interaction with antibodies generated by the host in order to protect the host against infection.

In conclusion, the three new antigenic sites identified in this study, together with two previously identified sites of the FMDV SAT2 serotype (Crowther *et al.*, 1993b; Grazioli *et al.*, 2006), has greatly increased our knowledge concerning the antigenic composition of SAT2 FMD viruses. This information will not only aid in the selection of antigenically appropriate vaccines, but may also provide a step forward in the production of engineered vaccines in which the antigenic regions of current FMDV vaccines can be altered in order to broaden their antigenic range and increase cross-protection with other FMDV. The availability of a FMDV vaccine with improved antigenic coverage, specifically engineered for the SAT types, will induce a more effective and a broader range of protection, and therefore farmers will need to vaccinate their livestock less frequently. As livestock farming is very important for rural economies in southern Africa, Transboundary Animal Diseases (TAD) such as FMD have a significant effect on the productivity, as well as opportunities for

regional and intercontinental trade in livestock and livestock products and therefore the livelihood of resource-poor farmers. The availability of such a vaccine will lead to increased productivity, alleviation of poverty and hence, strengthen the socioeconomic status of the poor and thus positively impact disease control.

Future research should attempt to identify additional neutralizing epitopes of the SAT2 serotype, possibly by the construction and panning of a SAT2-specific immune library. The known neutralizing epitopes, together with any epitopes that show increased neutralization, should be included in a custom-engineered vaccine with the aim of increased antigenic coverage against multiple SAT2 virus strains. This vaccine can then be validated in an animal trial to determine if, in a field environment, the vaccine does indeed induce a broader antigenic coverage. Once proof-of-concept has been achieved, this approach can be applied to SAT1 and SAT3 vaccine strains as well as to the other FMD serotypes. Ultimately, this approach can be utilized in the development of a custom-engineered vaccine for southern Africa that will provide broad antigenic coverage across all the SAT serotypes.

REFERENCES

- ACHARYA, R., FRY, E., STUART, D., FOX, G., ROWLANDS, D. & BROWN, F. 1989. The three-dimensional structure of foot-and-mouth disease virus at 2.9 Å resolution. *Nature*, 337, 709-16.
- ACHARYA, R., FRY, E., STUART, D., FOX, G., ROWLANDS, D. & BROWN, F. 1990. The structure of foot-and-mouth disease virus: implications for its physical and biological properties. *Vet Microbiol*, 23, 21-34.
- ADAM, K. H., KAADEN, O. R. & STROHMAIER, K. 1978. Isolation of immunizing cyanogen bromide-peptides of foot-and-mouth disease virus. *Biochem Biophys Res Commun*, 84, 677-83.
- AGOL, V. I., PAUL, A. V. & WIMMER, E. 1999. Paradoxes of the replication of picornaviral genomes. *Virus Res*, 62, 129-47.
- AHMAD, Z. A., YEAP, S. K., ALI, A. M., HO, W. Y., ALITHEEN, N. B. & HAMID, M. 2012. scFv antibody: principles and clinical application. *Clin Dev Immunol*, 2012, 980250.
- AKTAS, S. & SAMUEL, A. R. 2000. Identification of antigenic epitopes on the foot-and-mouth disease virus isolate O1/Manisa/Turkey/69 using monoclonal antibodies. *Rev Sci Tech*, 19, 744-53.
- ALBERTS, B., JOHNSON, A., LEWIS, J., RAFF, M., ROBERTS, K. & P., W. 2002. The adaptive immune system: Generation of antibody diversity. *Molecular biology of the cell*. New York: Garland Science.
- ALLEN, C. D. & CYSTER, J. G. 2008. Follicular dendritic cell networks of primary follicles and germinal centers: phenotype and function. *Semin Immunol*, 20, 14-25.
- AMADORI, M., ARCHETTI, I. L., VERARDI, R. & BERNERI, C. 1992. Isolation of mononuclear cytotoxic cells from cattle vaccinated against foot-and-mouth disease. *Arch Virol*, 122, 293-306.
- AMBROS, V., PETTERSSON, R. F. & BALTIMORE, D. 1978. An enzymatic activity in uninfected cells that cleaves the linkage between poliovirion RNA and the 5' terminal protein. *Cell*, 15, 1439-46.
- AMIT, A. G., MARIUZZA, R. A., PHILLIPS, S. E. & POLJAK, R. J. 1986. Three-dimensional structure of an antigen-antibody complex at 2.8 Å resolution. *Science*, 233, 747-53.
- ANDREOTTI, P. E., LUDWIG, G. V., PERUSKI, A. H., TUIE, J. J., MORSE, S. S. & PERUSKI, L. F., JR. 2003. Immunoassay of infectious agents. *Biotechniques*, 35, 850-9.
- ANDRIS-WIDHOPF, J., RADER, C., STEINBERGER, P., FULLER, R. & BARBAS, C. F., 3RD 2000. Methods for the generation of chicken monoclonal antibody fragments by phage display. *J Immunol Methods*, 242, 159-81.
- ARAP, M. A. 2005. Phage display technology - Applications and innovations. *Genetics and Molecular Biology*, 28, 1-9.
- ARBABI GHAHROUDI, M., DESMYTER, A., WYNS, L., HAMERS, R. & MUYLDERMANS, S. 1997. Selection and identification of single domain antibody fragments from camel heavy-chain antibodies. *FEBS Lett*, 414, 521-6.
- ARMER, H., MOFFAT, K., WILEMAN, T., BELSHAM, G. J., JACKSON, T., DUPREX, W. P., RYAN, M. & MONAGHAN, P. 2008. Foot-and-mouth disease virus, but not bovine enterovirus, targets the host cell cytoskeleton via the nonstructural protein 3Cpro. *J Virol*, 82, 10556-66.
- ARZT, J., JULEFF, N., ZHANG, Z. & RODRIGUEZ, L. L. 2011. The pathogenesis of foot-and-mouth disease I: viral pathways in cattle. *Transbound Emerg Dis*, 58, 291-304.
- ATASSI, M. Z. 1984. Antigenic structures of proteins. Their determination has revealed important aspects of immune recognition and generated strategies for synthetic mimicking of protein binding sites. *Eur J Biochem*, 145, 1-20.
- BABLANIAN, G. M. & GRUBMAN, M. J. 1993. Characterization of the foot-and-mouth disease virus 3C protease expressed in *Escherichia coli*. *Virology*, 197, 320-7.
- BACHMANN, M. F., KALINKE, U., ALTHAGE, A., FREER, G., BURKHART, C., ROOST, H., AGUET, M., HENGARTNER, H. & ZINKERNAGEL, R. M. 1997. The role of antibody concentration and avidity in antiviral protection. *Science*, 276, 2024-7.
- BACHRACH, H. L. 1968. Foot-and-mouth disease. *Annu Rev Microbiol*, 22, 201-44.

- BACHRACH, H. L. 1977. Foot-and-mouth disease virus: Properties, molecular biology and immunogenecity. *Beltsville Symp Agric Res*, 1, 3-32.
- BACHRACH, H. L., MOORE, D. M., MCKERCHER, P. D. & POLATNICK, J. 1975. Immune and antibody responses to an isolated capsid protein of foot-and-mouth disease virus. *J Immunol*, 115, 1636-41.
- BACHRACH, H. L., TRAUTMAN, R. & BREESE, S. S., JR. 1964. Chemical physical properties of virtually pure foot-and-mouth disease virus. *Am J Vet Res*, 25, 333-42.
- BAHARA, N. H. H., TYE, G. J., CHOONG, Y. S., ONG, E. B. B., ISMAIL, A. & LIM, T. S. 2013. Phage display antibodies for diagnostic applications. *Biologicals*, 41, 209-216.
- BANCHEREAU, J. & STEINMAN, R. M. 1998. Dendritic cells and the control of immunity. *Nature*, 392, 245-52.
- BARANOWSKI, E., RUIZ-JARABO, C. M., SEVILLA, N., ANDREU, D., BECK, E. & DOMINGO, E. 2000. Cell recognition by foot-and-mouth disease virus that lacks the RGD integrin-binding motif: flexibility in aphthovirus receptor usage. *J Virol*, 74, 1641-7.
- BARANOWSKI, E., SEVILLA, N., VERDAGUER, N., RUIZ-JARABO, C. M., BECK, E. & DOMINGO, E. 1998. Multiple virulence determinants of foot-and-mouth disease virus in cell culture. *J Virol*, 72, 6362-72.
- BARBAS, C. F., 3RD 1993. Recent advances in phage display. *Curr Opin Biotechnol*, 4, 526-30.
- BARBAS, C. F., 3RD, BAIN, J. D., HOEKSTRA, D. M. & LERNER, R. A. 1992. Semisynthetic combinatorial antibody libraries: a chemical solution to the diversity problem. *Proc Natl Acad Sci U S A*, 89, 4457-61.
- BARBAS, C. F. R. & RICHARD, L. A. 1991. Combinatorial immunoglobulin libraries on the surface of phage (Phabs): Rapid selection of antigen-specific fabs. *Methods*, 2, 119-124.
- BARCLAY, W., LI, Q., HUTCHINSON, G., MOON, D., RICHARDSON, A., PERCY, N., ALMOND, J. W. & EVANS, D. J. 1998. Encapsidation studies of poliovirus subgenomic replicons. *J Gen Virol*, 79, 1725-34.
- BARLOW, D. J., EDWARDS, M. S. & THORNTON, J. M. 1986. Continuous and discontinuous protein antigenic determinants. *Nature*, 322, 747-8.
- BARNARD, A. L., ARRIENS, A., COX, S., BARNETT, P., KRISTENSEN, B., SUMMERFIELD, A. & MCCULLOUGH, K. C. 2005. Immune response characteristics following emergency vaccination of pigs against foot-and-mouth disease. *Vaccine*, 23, 1037-47.
- BARNETT, P. V., COX, S. J., AGGARWAL, N., GERBER, H. & MCCULLOUGH, K. C. 2002. Further studies on the early protective responses of pigs following immunisation with high potency foot-and-mouth disease vaccine. *Vaccine*, 20, 3197-208.
- BARNETT, P. V., KEEL, P., REID, S., ARMSTRONG, R. M., STATHAM, R. J., VOYCE, C., AGGARWAL, N. & COX, S. J. 2004. Evidence that high potency foot-and-mouth disease vaccine inhibits local virus replication and prevents the "carrier" state in sheep. *Vaccine*, 22, 1221-32.
- BARNETT, P. V., OULDRIDGE, E. J., ROWLANDS, D. J., BROWN, F. & PARRY, N. R. 1989. Neutralizing epitopes of type O foot-and-mouth disease virus. I. Identification and characterization of three functionally independent, conformational sites. *J Gen Virol*, 70, 1483-91.
- BARNETT, P. V., SAMUEL, A. R., PULLEN, L., ANSELL, D., BUTCHER, R. N. & PARKHOUSE, R. M. 1998. Monoclonal antibodies, against O1 serotype foot-and-mouth disease virus, from a natural bovine host, recognize similar antigenic features to those defined by the mouse. *J Gen Virol*, 79, 1687-97.
- BARTELING, S. J. & VREESWIJK, J. 1991. Developments in foot-and-mouth disease vaccines. *Vaccine*, 9, 75-88.
- BARTON, D. J., O'DONNELL, B. J. & FLANEGAN, J. B. 2001. 5' cloverleaf in poliovirus RNA is a *cis*-acting replication element required for negative-strand synthesis. *EMBO J*, 20, 1439-48.
- BASTOS, A. D. 1998. Detection and characterization of foot-and-mouth disease virus in sub-Saharan Africa. *Onderstepoort J Vet Res*, 65, 37-47.
- BASTOS, A. D., ANDERSON, E. C., BENGIS, R. G., KEET, D. F., WINTERBACH, H. K. & THOMSON, G. R. 2003a. Molecular epidemiology of SAT3-type foot-and-mouth disease. *Virus Genes*, 27, 283-90.

- BASTOS, A. D., BOSHOFF, C. I., KEET, D. F., BENGIS, R. G. & THOMSON, G. R. 2000. Natural transmission of foot-and-mouth disease virus between African buffalo (*Syncerus caffer*) and impala (*Aepyceros melampus*) in the Kruger National Park, South Africa. *Epidemiol Infect*, 124, 591-8.
- BASTOS, A. D., HAYDON, D. T., FORSBERG, R., KNOWLES, N. J., ANDERSON, E. C., BENGIS, R. G., NEL, L. H. & THOMSON, G. R. 2001. Genetic heterogeneity of SAT-1 type foot-and-mouth disease viruses in southern Africa. *Arch Virol*, 146, 1537-51.
- BASTOS, A. D., HAYDON, D. T., SANGARE, O., BOSHOFF, C. I., EDRICH, J. L. & THOMSON, G. R. 2003b. The implications of virus diversity within the SAT 2 serotype for control of foot-and-mouth disease in sub-Saharan Africa. *J Gen Virol*, 84, 1595-606.
- BAUTISTA, E. M., FERMAN, G. S. & GOLDE, W. T. 2003. Induction of lymphopenia and inhibition of T cell function during acute infection of swine with foot-and-mouth disease virus (FMDV). *Vet Immunol Immunopathol*, 92, 61-73.
- BAXT, B. & BECKER, Y. 1990. The effect of peptides containing the arginine-glycine-aspartic acid sequence on the adsorption of foot-and-mouth disease virus to tissue culture cells. *Virus Genes*, 4, 73-83.
- BAXT, B. & MASON, P. W. 1995. Foot-and-mouth disease virus undergoes restricted replication in macrophage cell cultures following Fc receptor-mediated adsorption. *Virology*, 207, 503-9.
- BAXT, B., VAKHARIA, V., MOORE, D. M., FRANKE, A. J. & MORGAN, D. O. 1989. Analysis of neutralizing antigenic sites on the surface of type A12 foot-and-mouth disease virus. *J Virol*, 63, 2143-51.
- BEALES, L. P., HOLZENBURG, A. & ROWLANDS, D. J. 2003. Viral internal ribosome entry site structures segregate into two distinct morphologies. *J Virol*, 77, 6574-9.
- BEARD, C. W. & MASON, P. W. 2000. Genetic determinants of altered virulence of Taiwanese foot-and-mouth disease virus. *J Virol*, 74, 987-91.
- BECK, E., FORSS, S., STREBEL, K., CATTANEO, R. & FEIL, G. 1983. Structure of the FMDV translation initiation site and of the structural proteins. *Nucleic Acids Res*, 11, 7873-85.
- BELSHAM, G. J. 1993. Distinctive features of foot-and-mouth disease virus, a member of the picornavirus family; aspects of virus protein synthesis, protein processing and structure. *Prog Biophys Mol Biol*, 60, 241-60.
- BELSHAM, G. J. 2005. Translation and replication of FMDV RNA. *Curr Top Microbiol Immunol*, 288, 43-70.
- BENGIS, R. G. 1983. Annual Report 1981-82: State Veterinarian, Skukuza (Kruger National Park). Pretoria, South Africa: Directorate of Veterinary Services, National Department of Agriculture.
- BENJAMIN, D. C., BERZOFSKY, J. A., EAST, I. J., GURD, F. R. N., HANNUM, C., LEACH, S. J., MARGOLIASH, E., MICHAEL, J. G., MILLER, A., PRAGER, E. M., REICHLIN, M., SERCARZ, E. E., SMITH-GILL, S. J. & TODD, P. E. 1984. The antigenic structure of proteins: a reappraisal. *Annu Rev Immunol*, 2, 67-101.
- BERINSTEIN, A., ROIVAINEN, M., HOVI, T., MASON, P. W. & BAXT, B. 1995. Antibodies to the vitronectin receptor (integrin $\alpha_v\beta_3$) inhibit binding and infection of foot-and-mouth disease virus to cultured cells. *J Virol*, 69, 2664-6.
- BERRYMAN, S., CLARK, S., MONAGHAN, P. & JACKSON, T. 2005. Early events in integrin $\alpha_v\beta_6$ -mediated cell entry of foot-and-mouth disease virus. *J Virol*, 79, 8519-34.
- BICH, C., SCOTT, M., PANAGIOTIDIS, A., WENZEL, R. J., NAZABAL, A. & ZENOBI, R. 2008. Characterization of antibody-antigen interactions: comparison between surface plasmon resonance measurements and high-mass matrix-assisted laser desorption/ionization mass spectrometry. *Anal Biochem*, 375, 35-45.
- BIENZ, K., EGGER, D., TROXLER, M. & PASAMONTES, L. 1990. Structural organization of poliovirus RNA replication is mediated by viral proteins of the P2 genomic region. *J Virol*, 64, 1156-63.
- BIOTECH. 1989. *Monoclonal antibody technology - the basics* [Online]. Available: <http://www.gene.com/ae/AB/ie/MonoclonalAntibody.html> [Accessed 12 August 2013].

- BIRTLEY, J. R., KNOX, S. R., JAULENT, A. M., BRICK, P., LEATHERBARROW, R. J. & CURRY, S. 2005. Crystal structure of foot-and-mouth disease virus 3C protease. New insights into catalytic mechanism and cleavage specificity. *J Biol Chem*, 280, 11520-7.
- BITTLE, J. L., HOUGHTEN, R. A., ALEXANDER, H., SHINNICK, T. M., SUTCLIFFE, J. G., LERNER, R. A., ROWLANDS, D. J. & BROWN, F. 1982. Protection against foot-and-mouth disease by immunization with a chemically synthesized peptide predicted from the viral nucleotide sequence. *Nature*, 298, 30-3.
- BLACK, L., FRANCIS, M. J., RWEYEMAMU, M. M., UMEBARA, O. & BOGE, A. 1984. The relationship between serum antibody titres and protection from foot and mouth disease in pigs after oil emulsion vaccination. *J Biol Stand*, 12, 379-89.
- BLANCO, E., GARCIA-BRIONES, M., SANZ-PARRA, A., GOMES, P., DE OLIVEIRA, E., VALERO, M. L., ANDREU, D., LEY, V. & SOBRINO, F. 2001. Identification of T-cell epitopes in nonstructural proteins of foot-and-mouth disease virus. *J Virol*, 75, 3164-74.
- BLIGNAUT, B. 2012. *Improved vaccines for foot-and-mouth disease control: Evaluation of a chimeric-derived FMD vaccine in relation to a current SAT type vaccine*. Philosophiae Doctor Dissertation, University of Pretoria, .
- BLIGNAUT, B., VISSER, N., THERON, J., RIEDER, E. & MAREE, F. F. 2011. Custom-engineered chimeric foot-and-mouth disease vaccine elicits protective immune responses in pigs. *J Gen Virol*, 92, 849-59.
- BOLWELL, C., CLARKE, B. E., PARRY, N. R., OULDRIDGE, E. J., BROWN, F. & ROWLANDS, D. J. 1989. Epitope mapping of foot-and-mouth disease virus with neutralizing monoclonal antibodies. *J Gen Virol*, 70, 59-68.
- BOOM, R., SOL, C. J., SALIMANS, M. M., JANSEN, C. L., WERTHEIM-VAN DILLEN, P. M. & VAN DER NOORDAA, J. 1990. Rapid and simple method for purification of nucleic acids. *J Clin Microbiol*, 28, 495-503.
- BORLEY, D. W., MAHAPATRA, M., PATON, D. J., ESNOUF, R. M., STUART, D. I. & FRY, E. E. 2013. Evaluation and use of in-silico structure-based epitope prediction with foot-and-mouth disease virus. *PLoS One*, 8, e61122.
- BRADBURY, A. R. & MARKS, J. D. 2004. Antibodies from phage antibody libraries. *J Immunol Methods*, 290, 29-49.
- BRICHTA, J., HNILOVA, M. & VISKOVIC 2005. Generation of hapten-specific recombinant antibodies: antibody phage display technology: a review. *Vet Med*, 50, 231-252.
- BROCCHI, E., DE DIEGO, M. I., BERLINZANI, A., GAMBA, D. & DE SIMONE, F. 1998. Diagnostic potential of Mab-based ELISAs for antibodies to non-structural proteins of foot-and-mouth disease virus to differentiate infection from vaccination. *Vet Q*, 20 S20-24.
- BROCKMANN, E. C., COOPER, M., STROMSTEN, N., VEHNIAINEN, M. & SAVIRANTA, P. 2005. Selecting for antibody scFv fragments with improved stability using phage display with denaturation under reducing conditions. *J Immunol Methods*, 296, 159-70.
- BRONSVOORT, B. M., RADFORD, A. D., TANYA, V. N., NFON, C., KITCHING, R. P. & MORGAN, K. L. 2004. Molecular epidemiology of foot-and-mouth disease viruses in the Adamawa province of Cameroon. *J Clin Microbiol*, 42, 2186-96.
- BROOKSBY, J. B. 1972. Epizootiology of foot-and-mouth disease virus in developing countries. *World Anim Rev*, 3, 10-13.
- BROOKSBY, J. B. 1982. Portraits of viruses: foot-and-mouth disease virus. *Intervirology*, 18, 1-23.
- BROWN, F. 1986. Foot-and-mouth disease--one of the remaining great plagues. *Proc R Soc Lond B Biol Sci*, 229, 215-26.
- BROWN, F., NEWMAN, J., STOTT, J., PORTER, A., FRISBY, D., NEWTON, C., CAREY, N. & FELLNER, P. 1974. Poly(C) in animal viral RNAs. *Nature*, 251, 342-4.
- BROWN, J. K., MCALEESE, S. M., THORNTON, E. M., PATE, J. A., SCHOCK, A., MACRAE, A. I., SCOTT, P. R., MILLER, H. R. & COLLIE, D. D. 2006. Integrin- $\alpha_v\beta_6$, a receptor for foot-and-mouth disease virus, is constitutively expressed in ruminant airways. *J Histochem Cytochem*, 54, 807-16.

- BRÜCKNER, G. K., VOSLOO, W., DU PLESSIS, B. J., KLOECK, P. E., CONNOWAY, L., EKRON, M. D., WEAVER, D. B., DICKASON, C. J., SCHREUDER, F. J., MARAIS, T. & MOGAJANE, M. E. 2002. Foot-and-mouth disease: the experience of South Africa. *Rev Sci Tech*, 21, 751-64.
- BULLOCH, W. 1927. Lister as a pathologist and bacteriologist. *Br Med J*, 1, 654-6.
- BURMAN, A., CLARK, S., ABRESCIA, N. G., FRY, E. E., STUART, D. I. & JACKSON, T. 2006. Specificity of the VP1 GH loop of foot-and-mouth disease virus for α_v integrins. *J Virol*, 80, 9798-810.
- BURRITT, J. B., BOND, C. W., DOSS, K. W. & JESAITIS, A. J. 1996. Filamentous phage display of oligopeptide libraries. *Anal Biochem*, 238, 1-13.
- BURTON, D. R. 2001. Antibody libraries. In: BARBA III, C. F., BURTON, D. R., SCOTT, J. K. & SILVERMAN, G. (eds.) *Phage Display: A laboratory manual*. Cold Spring Harbor, New York: Cold Spring Harbor Laboratory Press.
- BURTON, D. R., STANFIELD, R. L. & WILSON, I. A. 2005. Antibody vs. HIV in a clash of evolutionary titans. *Proc Natl Acad Sci U S A*, 102, 14943-8.
- CAI, X. & GAREN, A. 1995. Anti-melanoma antibodies from melanoma patients immunized with genetically modified autologous tumor cells: selection of specific antibodies from single-chain Fv fusion phage libraries. *Proc Natl Acad Sci U S A*, 92, 6537-41.
- CAO, X., BERGMANN, I. E., FULLKRUG, R. & BECK, E. 1995. Functional analysis of the two alternative translation initiation sites of foot-and-mouth disease virus. *J Virol*, 69, 560-3.
- CAPOZZO, A. V., WILDA, M., BUCAFUSCO, D., DE LOS ANGELES LAVORIA, M., FRANCO-MAHECHA, O. L., MANSILLA, F. C., PEREZ-FILGUEIRA, D. M. & GRIGERA, P. R. 2011. Vesicular stomatitis virus glycoprotein G carrying a tandem dimer of foot-and-mouth disease virus antigenic site A can be used as DNA and peptide vaccine for cattle. *Antiviral Res*, 92, 219-27.
- CARMEN, S. & JERMUTUS, L. 2002. Concepts in antibody phage display. *Brief Funct Genomic Proteomic*, 1, 189-203.
- CARTWRIGHT, B., CHAPMAN, W. G. & SHARPE, R. T. 1982. Stimulation by heterotypic antigens of foot-and-mouth disease virus antibodies in vaccinated cattle. *Res Vet Sci*, 32, 338-42.
- CAVANAGH, D., ROWLANDS, D. J. & BROWN, F. 1978. Early events in the interaction between foot-and-mouth disease virus and primary pig kidney cells. *J Gen Virol*, 41, 255-64.
- CHARLESTON, B. & RODRIGUEZ, L. L. 2011. Understanding foot-and-mouth disease virus early pathogenesis and immune responses. *Transbound Emerg Dis*, 58, 281-2.
- CHINSANGARAM, J., KOSTER, M. & GRUBMAN, M. J. 2001. Inhibition of L-deleted foot-and-mouth disease virus replication by alpha/beta interferon involves double-stranded RNA-dependent protein kinase. *J Virol*, 75, 5498-503.
- CHINSANGARAM, J., MORAES, M. P., KOSTER, M. & GRUBMAN, M. J. 2003. Novel viral disease control strategy: adenovirus expressing alpha interferon rapidly protects swine from foot-and-mouth disease. *J Virol*, 77, 1621-5.
- CHOTHIA, C. & LESK, A. M. 1987. Canonical structures for the hypervariable regions of immunoglobulins. *J Mol Biol*, 196, 901-17.
- CHOW, M., NEWMAN, J. F., FILMAN, D., HOGLE, J. M., ROWLANDS, D. J. & BROWN, F. 1987. Myristylation of picornavirus capsid protein VP4 and its structural significance. *Nature*, 327, 482-6.
- CHOWDHURY, P. S. & WU, H. 2005. Tailor-made antibody therapeutics. *Methods*, 36, 11-24.
- CIUREA, A., KLENERMAN, P., HUNZIKER, L., HORVATH, E., SENN, B. M., OCHSENBEIN, A. F., HENGARTNER, H. & ZINKERNAGEL, R. M. 2000. Viral persistence *in vivo* through selection of neutralizing antibody-escape variants. *Proc Natl Acad Sci U S A*, 97, 2749-54.
- CLACKSON, T., HOOGENBOOM, H. R., GRIFFITHS, A. D. & WINTER, G. 1991. Making antibody fragments using phage display libraries. *Nature*, 352, 624-8.
- CLACKSON, T. & WELLS, J. A. 1994. *In vitro* selection from protein and peptide libraries. *Trends Biotechnol*, 12, 173-84.

- CLARKE, B. E., BROWN, A. L., CURREY, K. M., NEWTON, S. E., ROWLANDS, D. J. & CARROLL, A. R. 1987. Potential secondary and tertiary structure in the genomic RNA of foot-and-mouth disease virus. *Nucleic Acids Res*, 15, 7067-79.
- CLARKE, B. E. & SANGAR, D. V. 1988. Processing and assembly of foot-and-mouth disease virus proteins using subgenomic RNA. *J Gen Virol*, 69, 2313-25.
- CLARKE, B. E., SANGAR, D. V., BURROUGHS, J. N., NEWTON, S. E., CARROLL, A. R. & ROWLANDS, D. J. 1985. Two initiation sites for foot-and-mouth disease virus polyprotein *in vivo*. *J Gen Virol*, 66, 2615-26.
- COLLEN, T. 1994. Foot-and-mouth disease (*Aphthovirus*): viral T cell epitopes. In: GODDEVIS, B. M. L. & MORRISON, I. (eds.) *Cell mediated immunity in ruminants*. Boca Raton, Florida: CRC Press Inc.
- CONDY, J. B., HEDGER, R. S., HAMBLIN, C. & BARNETT, I. T. 1985. The duration of the foot-and-mouth disease virus carrier state in African buffalo (i) in the individual animal and (ii) in a free-living herd. *Comp Immunol Microbiol Infect Dis*, 8, 259-65.
- CONDY, J. B., HERNIMAN, K. A. & HEDGER, R. S. 1969. Foot-and-mouth disease in wildlife in Rhodesia and other African territories. A serological survey. *J Comp Pathol*, 79, 27-31.
- CROWTHER, J. R., FARIAS, S., CARPENTER, W. C. & SAMUEL, A. R. 1993a. Identification of a fifth neutralizable site on type O foot-and-mouth disease virus following characterization of single and quintuple monoclonal antibody escape mutants. *J Gen Virol*, 74, 1547-53.
- CROWTHER, J. R., ROWE, C. A. & BUTCHER, R. 1993b. Characterization of monoclonal antibodies against a type SAT 2 foot-and-mouth disease virus. *Epidemiol Infect*, 111, 391-406.
- CUNNINGHAM, B. C. & WELLS, J. A. 1993. Comparison of a structural and a functional epitope. *J Mol Biol*, 234, 554-63.
- CURRY, S., ABRAMS, C. C., FRY, E., CROWTHER, J. C., BELSHAM, G. J., STUART, D. I. & KING, A. M. 1995. Viral RNA modulates the acid sensitivity of foot-and-mouth disease virus capsids. *J Virol*, 69, 430-8.
- CURRY, S., FRY, E., BLAKEMORE, W., ABU-GHAZALEH, R., JACKSON, T., KING, A., LEA, S., NEWMAN, J., ROWLANDS, D. & STUART, D. 1996. Perturbations in the surface structure of A22 Iraq foot-and-mouth disease virus accompanying coupled changes in host cell specificity and antigenicity. *Structure*, 4, 135-45.
- DASGUPTA, D. 1999. An overview of artificial immune systems and their applications. *Artificial immune systems and their applications*. Berlin Heidelberg, New York: Springer-Verlag.
- DAVIDSON, F. L., CROWTHER, J. R., NQINDI, J., KNOWLES, N. J., THEVASAGAYAM, S. J. & VAN VUUREN, C. J. 1995. Antigenic analysis of SAT 2 serotype foot-and-mouth disease virus isolates from Zimbabwe using monoclonal antibodies. *Epidemiol Infect*, 115, 193-205.
- DAVIES, E. L., SMITH, J. S., BIRKETT, C. R., MANSER, J. M., ANDERSON-DEAR, D. V. & YOUNG, J. R. 1995. Selection of specific phage-display antibodies using libraries derived from chicken immunoglobulin genes. *J Immunol Methods*, 186, 125-35.
- DAWE, P. S., FLANAGAN, F. O., MADEKUROZWA, R. L., SORENSEN, K. J., ANDERSON, E. C., FOGGIN, C. M., FERRIS, N. P. & KNOWLES, N. J. 1994. Natural transmission of foot-and-mouth disease virus from African buffalo (*Syncerus caffer*) to cattle in a wildlife area of Zimbabwe. *Vet Rec*, 134, 230-2.
- DE CLERCQ, K., GORIS, N., BARNETT, P. V. & MACKAY, D. K. 2008. The importance of quality assurance/quality control of diagnostics to increase the confidence in global foot-and-mouth disease control. *Transbound Emerg Dis*, 55, 35-45.
- DE HAARD, H. J., VAN NEER, N., REURS, A., HUFTON, S. E., ROOVERS, R. C., HENDERIKX, P., DE BRUINE, A. P., ARENDS, J. W. & HOOGENBOOM, H. R. 1999. A large non-immunized human Fab fragment phage library that permits rapid isolation and kinetic analysis of high affinity antibodies. *J Biol Chem*, 274, 18218-30.
- DE KRUIF, J., BOEL, E. & LOGTENBERG, T. 1995. Selection and application of human single chain Fv antibody fragments from a semi-synthetic phage antibody display library with designed CDR3 regions. *J Mol Biol*, 248, 97-105.

- DE LOS SANTOS, T., DE AVILA BOTTON, S., WEIBLEN, R. & GRUBMAN, M. J. 2006. The leader proteinase of foot-and-mouth disease virus inhibits the induction of beta interferon mRNA and blocks the host innate immune response. *J Virol*, 80, 1906-14.
- DEFRA 2007. FMD 2007. Summary Epidemiology Report. Department for Environment, Food and Rural Affairs.
- DEVANEY, M. A., VAKHARIA, V. N., LLOYD, R. E., EHRENFELD, E. & GRUBMAN, M. J. 1988. Leader protein of foot-and-mouth disease virus is required for cleavage of the p220 component of the cap-binding protein complex. *J Virol*, 62, 4407-9.
- DEVER, T. E., GLYNIAS, M. J. & MERRICK, W. C. 1987. GTP-binding domain: three consensus sequence elements with distinct spacing. *Proc Natl Acad Sci U S A*, 84, 1814-8.
- DIAZ-SAN SEGUNDO, F., MORAES, M. P., DE LOS SANTOS, T., DIAS, C. C. & GRUBMAN, M. J. 2010. Interferon-induced protection against foot-and-mouth disease virus infection correlates with enhanced tissue-specific innate immune cell infiltration and interferon-stimulated gene expression. *J Virol*, 84, 2063-77.
- DINTZIS, H. M., DINTZIS, R. Z. & VOGELSTEIN, B. 1976. Molecular determinants of immunogenicity: the immunon model of immune response. *Proc Natl Acad Sci U S A*, 73, 3671-5.
- DMITRIEVA, T. M., NORKINA, K. B. & AGOL, V. I. 1991. Encephalomyocarditis virus RNA polymerase preparations, with and without RNA helicase activity. *J Virol*, 65, 2714-7.
- DOEDENS, J. R. & KIRKEGAARD, K. 1995. Inhibition of cellular protein secretion by poliovirus proteins 2B and 3A. *EMBO J*, 14, 894-907.
- DOEL, T. R. 1996. Natural and vaccine-induced immunity to foot-and-mouth disease: the prospects for improved vaccines. *Rev Sci Tech*, 15, 883-911.
- DOEL, T. R. 2003. FMD vaccines. *Virus Res*, 91, 81-99.
- DOEL, T. R. 2005. Natural and vaccine induced immunity to FMD. *Cur Top Microbiol Immunol*, 288, 103-131.
- DOEL, T. R. & MOWAT, G. N. 1985. An international collaborative study on foot-and-mouth disease virus assay methods. 2. Quantification of 146S particles. *J Biol Stand*, 13, 335-44.
- DOMINGO, E. 1997. Rapid evolution of viral RNA genomes. *J Nutr*, 127, 958S-961S.
- DOMINGO, E., BARANOWSKI, E., ESCARMIS, C. & SOBRINO, F. 2002. Foot-and-mouth disease virus. *Comp Immunol Microbiol Infect Dis*, 25, 297-308.
- DOMINGO, E., ESCARMIS, C., BARANOWSKI, E., RUIZ-JARABO, C. M., CARRILLO, E., NUNEZ, J. I. & SOBRINO, F. 2003. Evolution of foot-and-mouth disease virus. *Virus Res*, 91, 47-63.
- DOMINGO, E. & HOLLAND, J. J. 1997. RNA virus mutations and fitness for survival. *Annu Rev Microbiol*, 51, 151-78.
- DOMINGO, E., MATEU, M. G., MARTINEZ, M. A., DOPAZ, J., MOYA, A. & SPOBRINO, F. 1990. Genetic variability and antigenic diversity of foot-and-mouth disease virus. In: KRUSTAK, E., MARUSYK, R., MURPHY, S. & VAN REGNMORTAL, M. (eds.) *Applied Virology Research*. New York, USA: Plenum Publishing Corp.
- DOMINGO, E., VERDAGUER, N., OCHOA, W. F., RUIZ-JARABO, C. M., SEVILLA, N., BARANOWSKI, E., MATEU, M. G. & FITA, I. 1999. Biochemical and structural studies with neutralizing antibodies raised against foot-and-mouth disease virus. *Virus Res*, 62, 169-75.
- DONNELLY, M. L., GANI, D., FLINT, M., MONAGHAN, S. & RYAN, M. D. 1997. The cleavage activities of aphthovirus and cardiovirus 2A proteins. *J Gen Virol*, 78, 13-21.
- DONNELLY, M. L., LUKE, G., MEHROTRA, A., LI, X., HUGHES, L. E., GANI, D. & RYAN, M. D. 2001. Analysis of the aphthovirus 2A/2B polyprotein 'cleavage' mechanism indicates not a proteolytic reaction, but a novel translational effect: a putative ribosomal 'skip'. *J Gen Virol*, 82, 1013-25.
- DUBS, M. C., ALTSCHUH, D. & VAN REGENMORTEL, M. H. 1992. Mapping of viral epitopes with conformationally specific monoclonal antibodies using biosensor technology. *J Chromatogr*, 597, 391-6.
- DUNKELBERGER, J. R. & SONG, W. C. 2010. Complement and its role in innate and adaptive immune responses. *Cell Res*, 20, 34-50.

- DUNN, C. S., SAMUEL, A. R., PULLEN, L. A. & ANDERSON, J. 1998. The biological relevance of virus neutralisation sites for virulence and vaccine protection in the guinea pig model of foot-and-mouth disease. *Virology*, 247, 51-61.
- DUQUE, H. & BAXT, B. 2003. Foot-and-mouth disease virus receptors: comparison of bovine α_V integrin utilization by type A and O viruses. *J Virol*, 77, 2500-11.
- DUQUE, H., LAROCCO, M., GOLDE, W. T. & BAXT, B. 2004. Interactions of foot-and-mouth disease virus with soluble bovine $\alpha_V\beta_3$ and $\alpha_V\beta_6$ integrins. *J Virol*, 78, 9773-81.
- EARLY, P., HUANG, H., DAVIS, M., CALAME, K. & HOOD, L. 1980. An immunoglobulin heavy chain variable region gene is generated from three segments of DNA: V_H , D and J_H . *Cell*, 19, 981-92.
- EBLE, P. L., DE BRUIN, M. G., BOUMA, A., VAN HEMERT-KLUITENBERG, F. & DEKKER, A. 2006. Comparison of immune responses after intra-typic heterologous and homologous vaccination against foot-and-mouth disease virus infection in pigs. *Vaccine*, 24, 1274-81.
- EIGEN, E. & SCHUSTER, P. 1979. *The hypercycle. A principle of natural self-organization.*, Berlin, Springer.
- EIGEN, M. 1971. Selforganization of matter and the evolution of biological macromolecules. *Naturwissenschaften*, 58, 465-523.
- ELGERT, K. D. 2009. Antigenes and Antibodies. *Immunology: Understanding the immune system*. Hoboken, New Jersey: John Wiley and Sons, Inc.
- ELLARD, F. M., DREW, J., BLAKEMORE, W. E., STUART, D. I. & KING, A. M. 1999. Evidence for the role of His-142 of protein 1C in the acid-induced disassembly of foot-and-mouth disease virus capsids. *J Gen Virol*, 80, 1911-8.
- ESCARMIS, C., CARRILLO, E. C., FERRER, M., ARRIAZA, J. F., LOPEZ, N., TAMI, C., VERDAGUER, N., DOMINGO, E. & FRANZE-FERNANDEZ, M. T. 1998. Rapid selection in modified BHK-21 cells of a foot-and-mouth disease virus variant showing alterations in cell tropism. *J Virol*, 72, 10171-9.
- ESTERHUYSEN, J. J., THOMSON, G. R., ASHFORD, W. A., LENTZ, D. W., GAINARU, M. D., SAYER, A. J., MEREDITH, C. D., JANSE VAN RENSBURG, D. & PINI, A. 1988. The suitability of a rolled BHK-21 monolayer system for the production of vaccines against the SAT types of foot-and-mouth disease virus. I. Adaptation of virus isolates to the system, immunogen yields achieved and assessment of subtype cross reactivity. *Onderstepoort J Vet Res*, 55, 77-84.
- EWERT, S., CABBILLAU, C., CONRATH, K. & PLUCKTHUN, A. 2002. Biophysical properties of camelid V_{HH} domains compared to those of human V_{H3} domains. *Biochemistry*, 41, 3628-36.
- FALK, M. M., GRIGERA, P. R., BERGMANN, I. E., ZIBERT, A., MULTHAUP, G. & BECK, E. 1990. Foot-and-mouth disease virus protease 3C induces specific proteolytic cleavage of host cell histone H3. *J Virol*, 64, 748-56.
- FALK, M. M., SOBRINO, F. & BECK, E. 1992. VPg gene amplification correlates with infective particle formation in foot-and-mouth disease virus. *J Virol*, 66, 2251-60.
- FEHRSEN, J., VAN WYNGAARDT, W., MASHAU, C., POTGIETER, A. C., CHAUDHARY, V. K., GUPTA, A., JORDAAN, F. A. & DU PLESSIS, D. H. 2005. Serogroup-reactive and type-specific detection of bluetongue virus antibodies using chicken scFvs in inhibition ELISAs. *J Virol Methods*, 129, 31-9.
- FEIGELSTOCK, D., MATEU, M. G., PICCONE, M. E., DE SIMONE, F., BROCCHI, E., DOMINGO, E. & PALMA, E. L. 1992. Extensive antigenic diversification of foot-and-mouth disease virus by amino acid substitutions outside the major antigenic site. *J Gen Virol*, 73, 3307-11.
- FEIGELSTOCK, D. A., MATEU, M. G., VALERO, M. L., ANDREU, D., DOMINGO, E. & PALMA, E. L. 1996. Emerging foot-and-mouth disease virus variants with antigenically critical amino acid substitutions predicted by model studies using reference viruses. *Vaccine*, 14, 97-102.
- FERNANDEZ, C., CLARK, K., BURROWS, L., SCHOFIELD, N. R. & HUMPHRIES, M. J. 1998. Regulation of the extracellular ligand binding activity of integrins. *Front Biosci*, 3, d684-700.

- FERRIS, N. P. & DONALDSON, A. I. 1992. The World Reference Laboratory for Foot-and-Mouth Disease: a review of thirty-three years of activity (1958-1991). *Rev Sci Tech*, 11, 657-84.
- FERRIS, N. P., KING, D. P., REID, S. M., HUTCHINGS, G. H., SHAW, A. E., PATON, D. J., GORIS, N., HAAS, B., HOFFMANN, B., BROCCHI, E., BUGNETTI, M., DEKKER, A. & DE CLERCQ, K. 2006. Foot-and-mouth disease virus: a first inter-laboratory comparison trial to evaluate virus isolation and RT-PCR detection methods. *Vet Microbiol*, 117, 130-40.
- FMD Reference Laboratory Network. FMD-RLN OIE/FAO Reference Laboratory Network Reports (2005-2011). www.wrlfmd.org/ref_labs/fmd_ref_lab_reports.htm
- FORSS, S. & SCHALLER, H. 1982. A tandem repeat gene in a picornavirus. *Nucleic Acids Res*, 10, 6441-50.
- FORSS, S., STREBEL, K., BECK, E. & SCHALLER, H. 1984. Nucleotide sequence and genome organization of foot-and-mouth disease virus. *Nucleic Acids Res*, 12, 6587-601.
- FOWLER, V. L., KNOWLES, N. J., PATON, D. J. & BARNETT, P. V. 2010. Marker vaccine potential of a foot-and-mouth disease virus with a partial VP1 G-H loop deletion. *Vaccine*, 28, 3428-34.
- FOWLER, V. L., PATON, D. J., RIEDER, E. & BARNETT, P. V. 2008. Chimeric foot-and-mouth disease viruses: evaluation of their efficacy as potential marker vaccines in cattle. *Vaccine*, 26, 1982-9.
- FOX, G., PARRY, N. R., BARNETT, P. V., MCGINN, B., ROWLANDS, D. J. & BROWN, F. 1989. The cell attachment site on foot-and-mouth disease virus includes the amino acid sequence RGD (arginine-glycine-aspartic acid). *J Gen Virol*, 70, 625-37.
- FRANCO MAHECHA, O. L., OGAS CASTELLS, M. L., COMBESSIES, G., LAVORIA, M. A., WILDA, M., MANSILLA, F. C., SEKI, C., GRIGERA, P. R. & CAPOZZO, A. V. 2011. Single dilution Avidity-Blocking ELISA as an alternative to the Bovine Viral Diarrhea Virus neutralization test. *J Virol Methods*, 175, 228-35.
- FREIBERG, B., RAHMAN, M. M. & MARQUARDT, O. 1999. Genetical and immunological analysis of recent Asian type A and O foot-and-mouth disease virus isolates. *Virus Genes*, 19, 167-82.
- FRY, E. E., LEA, S. M., JACKSON, T., NEWMAN, J. W., ELLARD, F. M., BLAKEMORE, W. E., ABU-GHAZALEH, R., SAMUEL, A., KING, A. M. & STUART, D. I. 1999. The structure and function of a foot-and-mouth disease virus-oligosaccharide receptor complex. *EMBO J*, 18, 543-54.
- FRY, E. E., NEWMAN, J. W., CURRY, S., NAJJAM, S., JACKSON, T., BLAKEMORE, W., LEA, S. M., MILLER, L., BURMAN, A., KING, A. M. & STUART, D. I. 2005. Structure of foot-and-mouth disease virus serotype A10₆₁ alone and complexed with oligosaccharide receptor: receptor conservation in the face of antigenic variation. *J Gen Virol*, 86, 1909-20.
- GARLAND, A. J. 1999. Vital elements for the successful control of foot-and-mouth disease by vaccination. *Vaccine*, 17, 1760-6.
- GATTO, D., MARTIN, S. W., BESSA, J., PELLICIOLI, E., SAUDAN, P., HINTON, H. J. & BACHMANN, M. F. 2007. Regulation of memory antibody levels: the role of persisting antigen versus plasma cell life span. *J Immunol*, 178, 67-76.
- GEBAUER, F., DE LA TORRE, J. C., GOMES, I., MATEU, M. G., BARAHONA, H., TIRABOSCHI, B., BERGMANN, I., DE MELLO, P. A. & DOMINGO, E. 1988. Rapid selection of genetic and antigenic variants of foot-and-mouth disease virus during persistence in cattle. *J Virol*, 62, 2041-9.
- GEORGE, M., VENKATARAMANAN, R., PATTNAIK, B., SANYAL, A., GURUMURTHY, C. B., HEMADRI, D. & TOSH, C. 2001. Sequence analysis of the RNA polymerase gene of foot-and-mouth disease virus serotype Asia1. *Virus Genes*, 22, 21-6.
- GERNER, W., DENYER, M. S., TAKAMATSU, H. H., WILEMAN, T. E., WIESMULLER, K. H., PFAFF, E. & SAALMULLER, A. 2006. Identification of novel foot-and-mouth disease virus specific T-cell epitopes in c/c and d/d haplotype miniature swine. *Virus Res*, 121, 223-8.
- GEYSEN, H. M., RODDA, S. J. & MASON, T. J. 1986. A priori delineation of a peptide which mimics a discontinuous antigenic determinant. *Mol Immunol*, 23, 709-15.
- GIBBS, E. P. J. 1981. *Virus diseases of food animals - a world of geography of epidemiology and control*, New York, Academic Press.

- GLASS, E. J., OLIVER, R. A., COLLEN, T., DOEL, T. R., DIMARCHI, R. & SPOONER, R. L. 1991. MHC class II restricted recognition of FMDV peptides by bovine T cells. *Immunology*, 74, 594-9.
- GOLDE, W. T., DE LOS SANTOS, T., ROBINSON, L., GRUBMAN, M. J., SEVILLA, N., SUMMERFIELD, A. & CHARLESTON, B. 2011. Evidence of activation and suppression during the early immune response to foot-and-mouth disease virus. *Transbound Emerg Dis*, 58, 283-90.
- GOLDE, W. T., NFON, C. K. & TOKA, F. N. 2008. Immune evasion during foot-and-mouth disease virus infection of swine. *Immunol Rev*, 225, 85-95.
- GRAM, H., MARCONI, L. A., BARBAS, C. F., 3RD, COLLET, T. A., LERNER, R. A. & KANG, A. S. 1992. *In vitro* selection and affinity maturation of antibodies from a naïve combinatorial immunoglobulin library. *Proc Natl Acad Sci USA*, 89, 3576-80.
- GRAZIOLI, S., FALLACARA, F. & BROCCHI, E. 2004. Mapping of neutralising sites on FMD virus type Asia 1 and relationships with sites described in other serotypes. *Report of the Session of the Research Foot-and-Mouth disease, Group of the Standing Committee of the European commission of Foot and Mouth disease*. Greece.
- GRAZIOLI, S., FALLACARA, F. & BROCCHI, E. 2013. Mapping of antigenic sites of foot-and-mouth disease virus serotype Asia 1 and relationships with sites described in other serotypes. *J Gen Virol*, 94, 559-69.
- GRAZIOLI, S., MORETTI, M., BARBIERI, I., CROSATTI, M. & BROCCHI, E. 2006. Use of monoclonal antibodies to identify and map new antigenic determinants involved in neutralization of FMD viruses type SAT 1 and SAT 2 *European Commission for the control of Foot-and-Mouth Disease: International control of Foot-and-Mouth disease: Tools, Trends and perspectives*. Paphos, Cyprus.
- GREENWELL, P. & RUGHOOPUTH, S. 2001. Beyond hybridoma technology: production of monoclonal antibodies by phage display. *The Biomedical Scientist*, 45, 574-575.
- GRIFFITHS, A. D. & DUNCAN, A. R. 1998. Strategies for selection of antibodies by phage display. *Curr Opin Biotechnol*, 9, 102-8.
- GRIFFITHS, A. D., MALMQVIST, M., MARKS, J. D., BYE, J. M., EMBLETON, M. J., MCCAFFERTY, J., BAIER, M., HOLLIGER, K. P., GORICK, B. D., HUGHES-JONES, N. C. & ET AL. 1993. Human anti-self antibodies with high specificity from phage display libraries. *EMBO J*, 12, 725-34.
- GRIFFITHS, A. D., WILLIAMS, S. C., HARTLEY, O., TOMLINSON, I. M., WATERHOUSE, P., CROSBY, W. L., KONTERMANN, R. E., JONES, P. T., LOW, N. M., ALLISON, T. J. & ET AL. 1994. Isolation of high affinity human antibodies directly from large synthetic repertoires. *EMBO J*, 13, 3245-60.
- GRIGERA, P. R. & TISMINETZKY, S. G. 1984. Histone H3 modification in BHK cells infected with foot-and-mouth disease virus. *Virology*, 136, 10-9.
- GRUBMAN, M. J. 1980. The 5' end of foot-and-mouth disease virion RNA contains a protein covalently linked to the nucleotide pUp. *Arch Virol*, 63, 311-5.
- GRUBMAN, M. J. 2005. Development of novel strategies to control foot-and-mouth disease: marker vaccines and antivirals. *Biologicals*, 33, 227-34.
- GRUBMAN, M. J. & BAXT, B. 1982. Translation of foot-and-mouth disease virion RNA and processing of the primary cleavage products in a rabbit reticulocyte lysate. *Virology*, 116, 19-30.
- GRUBMAN, M. J. & BAXT, B. 2004. Foot-and-mouth disease. *Clin Microbiol Rev*, 17, 465-93.
- GRUBMAN, M. J., MORAES, M. P., DIAZ-SAN SEGUNDO, F., PENA, L. & DE LOS SANTOS, T. 2008. Evading the host immune response: how foot-and-mouth disease virus has become an effective pathogen. *FEMS Immunol Med Microbiol*, 53, 8-17.
- GUO, H., LIU, X., LIU, Z., YIN, H., MA, J., WANG, Y., SHANG, Y., ZHANG, Q., LI, D., GUO, J., LU, Z. & XIE, Q. 2006. Recent outbreaks of foot-and-mouth disease type Asia 1 in China. *J Vet Med B Infect Dis Vet Public Health*, 53, 29-33.
- GUPTA, P. K. 2009. Immune system and vaccines. *Cell and molecular biology*. New Delhi, India: Rastogi Publications.

- GUTHRIDGE, J. M., YOUNG, K., GIPSON, M. G., SARRIAS, M. R., SZAKONYI, G., CHEN, X. S., MALASPINA, A., DONOGHUE, E., JAMES, J. A., LAMBRIS, J. D., MOIR, S. A., PERKINS, S. J. & HOLERS, V. M. 2001. Epitope mapping using the X-ray crystallographic structure of complement receptor type 2 (CR2)/CD21: identification of a highly inhibitory monoclonal antibody that directly recognizes the CR2-C3d interface. *J Immunol*, 167, 5758-66.
- GUTTMAN, N. & BALTIMORE, D. 1977. Morphogenesis of poliovirus. IV. existence of particles sedimenting at 150S and having the properties of provirion. *J Virol*, 23, 363-7.
- GUZMAN, E., TAYLOR, G., CHARLESTON, B., SKINNER, M. A. & ELLIS, S. A. 2008. An MHC-restricted CD8⁺ T-cell response is induced in cattle by foot-and-mouth disease virus (FMDV) infection and also following vaccination with inactivated FMDV. *J Gen Virol*, 89, 667-75.
- HALL, T. A. 1999. BioEdit: a user-friendly biological sequence alignment editor and analysis programme for windows 95/98NT. *Nucleic Acids Symp Ser*, 41, 95-98.
- HARBER, J. J., BRADLEY, J., ANDERSON, C. W. & WIMMER, E. 1991. Catalysis of poliovirus VP0 maturation cleavage is not mediated by serine 10 of VP2. *J Virol*, 65, 326-34.
- HARENAPE, J. M. & MCCAHOON, D. 1983. Four independent antigenic determinants on the capsid polypeptides of aphthovirus. *J Gen Virol*, 64, 2345-55.
- HARLOW, E. & LANE, D. 1988. Antibodies. *Antibodies: A laboratory manual*. Cold Spring Harbor, New York: Cold Spring Harbor Laboratory Press.
- HARMSSEN, M. M., VAN SOLT, C. B., FIJTEN, H. P., VAN KEULEN, L., ROSALIA, R. A., WEERDMEEESTER, K., CORNELISSEN, A. H., DE BRUIN, M. G., EBLE, P. L. & DEKKER, A. 2007. Passive immunization of guinea pigs with llama single-domain antibody fragments against foot-and-mouth disease. *Vet Microbiol*, 120, 193-206.
- HARRIS, T. J. & BROWN, F. 1977. Biochemical analysis of a virulent and an avirulent strain of foot-and-mouth disease virus. *J Gen Virol*, 34, 87-105.
- HARWOOD, L. J., GERBER, H., SOBRINO, F., SUMMERFIELD, A. & MCCULLOUGH, K. C. 2008. Dendritic cell internalization of foot-and-mouth disease virus: influence of heparan sulfate binding on virus uptake and induction of the immune response. *J Virol*, 82, 6379-94.
- HAYDON, D. T., SAMUEL, A. R. & KNOWLES, N. J. 2001. The generation and persistence of genetic variation in foot-and-mouth disease virus. *Prev Vet Med*, 51, 111-24.
- HEATH, L., VAN DER WALT, E., VARSANI, A. & MARTIN, D. P. 2006. Recombination patterns in aphthoviruses mirror those found in other picornaviruses. *J Virol*, 80, 11827-32.
- HEROLD, J. & ANDINO, R. 2001. Poliovirus RNA replication requires genome circularization through a protein-protein bridge. *Mol Cell*, 7, 581-91.
- HIGUCHI, R., KRUMMEL, B. & SAIKI, R. K. 1988. A general method of *in vitro* preparation and specific mutagenesis of DNA fragments: study of protein and DNA interactions. *Nucleic Acids Res*, 16, 7351-67.
- HO, S. N., HUNT, H. D., HORTON, R. M., PULLEN, J. K. & PEASE, L. R. 1989. Site-directed mutagenesis by overlap extension using the polymerase chain reaction. *Gene*, 77, 51-9.
- HOGLE, J. M., CHOW, M. & FILMAN, D. J. 1985. Three-dimensional structure of poliovirus at 2.9 Å resolution. *Science*, 229, 1358-65.
- HOLLAND, J., SPINDLER, K., HORODYSKI, F., GRABAU, E., NICHOL, S. & VANDEPOL, S. 1982. Rapid evolution of RNA genomes. *Science*, 215, 1577-85.
- HOLLAND, J. J., DE LA TORRE, J. C., CLARKE, D. K. & DUARTE, E. 1991. Quantitation of relative fitness and great adaptability of clonal populations of RNA viruses. *J Virol*, 65, 2960-7.
- HOOGENBOOM, H. R. 1997. Designing and optimizing library selection strategies for generating high-affinity antibodies. *Trends Biotechnol*, 15, 62-70.
- HOOGENBOOM, H. R., DE BRUINE, A. P., HUFTON, S. E., HOET, R. M., ARENDS, J. W. & ROOVERS, R. C. 1998. Antibody phage display technology and its applications. *Immunotechnology*, 4, 1-20.

- HOOGENBOOM, H. R., GRIFFITHS, A. D., JOHNSON, K. S., CHISWELL, D. J., HUDSON, P. & WINTER, G. 1991. Multi-subunit proteins on the surface of filamentous phage: methodologies for displaying antibody (Fab) heavy and light chains. *Nucleic Acids Res*, 19, 4133-7.
- HOOGENBOOM, H. R. & WINTER, G. 1992. By-passing immunisation. Human antibodies from synthetic repertoires of germline V_H gene segments rearranged in vitro. *J Mol Biol*, 227, 381-8.
- HYNES, R. O. 1992. Integrins: versatility, modulation, and signaling in cell adhesion. *Cell*, 69, 11-25.
- HYSLOP, N. S. 1970. The epizootiology and epidemiology of foot-and-mouth disease. *Adv Vet Sci Comp Med*, 14, 261-307.
- IANNOLO, G., MINENKOVA, O., PETRUZZELLI, R. & CESARENI, G. 1995. Modifying filamentous phage capsid: limits in the size of the major capsid protein. *J Mol Biol*, 248, 835-44.
- IRVING, M. B., PAN, O. & SCOTT, J. K. 2001. Random-peptide libraries and antigen-fragment libraries for epitope mapping and the development of vaccines and diagnostics. *Curr Opin Chem Biol*, 5, 314-24.
- JACKSON, A. L., O'NEILL, H., MAREE, F., BLIGNAUT, B., CARRILLO, C., RODRIGUEZ, L. & HAYDON, D. T. 2007. Mosaic structure of foot-and-mouth disease virus genomes. *J Gen Virol*, 88, 487-92.
- JACKSON, T., CLARK, S., BERRYMAN, S., BURMAN, A., CAMBIER, S., MU, D., NISHIMURA, S. & KING, A. M. 2004. Integrin $\alpha_V\beta_8$ functions as a receptor for foot-and-mouth disease virus: role of the β -chain cytodomain in integrin-mediated infection. *J Virol*, 78, 4533-40.
- JACKSON, T., ELLARD, F. M., GHAZALEH, R. A., BROOKES, S. M., BLAKEMORE, W. E., CORTEYN, A. H., STUART, D. I., NEWMAN, J. W. & KING, A. M. 1996. Efficient infection of cells in culture by type O foot-and-mouth disease virus requires binding to cell surface heparan sulfate. *J Virol*, 70, 5282-7.
- JACKSON, T., KING, A. M., STUART, D. I. & FRY, E. 2003. Structure and receptor binding. *Virus Res*, 91, 33-46.
- JACKSON, T., MOULD, A. P., SHEPPARD, D. & KING, A. M. 2002. Integrin $\alpha_V\beta_1$ is a receptor for foot-and-mouth disease virus. *J Virol*, 76, 935-41.
- JACKSON, T., SHARMA, A., GHAZALEH, R. A., BLAKEMORE, W. E., ELLARD, F. M., SIMMONS, D. L., NEWMAN, J. W., STUART, D. I. & KING, A. M. 1997. Arginine-glycine-aspartic acid-specific binding by foot-and-mouth disease viruses to the purified integrin $\alpha_V\beta_3$ *in vitro*. *J Virol*, 71, 8357-61.
- JACKSON, T., SHEPPARD, D., DENYER, M., BLAKEMORE, W. & KING, A. M. 2000. The epithelial integrin $\alpha_V\beta_6$ is a receptor for foot-and-mouth disease virus. *J Virol*, 74, 4949-56.
- JAMAL, S. M., FERRARI, G., AHMED, S., NORMANN, P. & BELSHAM, G. J. 2011. Genetic diversity of foot-and-mouth disease virus serotype O in Pakistan and Afghanistan, 1997-2009. *Infect Genet Evol*, 11, 1229-38.
- JANEWAY, C. A. J., TRAVERS, P. & WALPORT, M. 2001. Antigen recognition by B-cell and T-cell receptors. *Immunobiology: The immune system in health and diseases*. New York, USA: Garland Science Publishing.
- JECHT, M., PROBST, C. & GAUSS-MULLER, V. 1998. Membrane permeability induced by hepatitis A virus proteins 2B and 2BC and proteolytic processing of HAV 2BC. *Virology*, 252, 218-27.
- JIN, H., XIAO, W., XIAO, C., YU, Y., KANG, Y., DU, X., WEI, X. & WANG, B. 2007. Protective immune responses against foot-and-mouth disease virus by vaccination with a DNA vaccine expressing virus-like particles. *Viral Immunol*, 20, 429-40.
- JIN, L., FENDLY, B. M. & WELLS, J. A. 1992. High resolution functional analysis of antibody-antigen interactions. *J Mol Biol*, 226, 851-65.
- JOKLIK, W. K. 1980. *Microbiology*, New York, USA, Appleton-Century-Crofts.
- JONES, B. V. & HOWARD, C. J. 1995. Production of stable bovine-murine interspecies hybrids. *Methods Mol Biol*, 45, 41-7.

- JOSEPH, T., LYAKU, J., FREDRICKSON, R. A., CEPICA, A. & KIBENGE, F. S. 2002. Use of epitope mapping to identify a PCR template for protein amplification and detection by enzyme-linked immunosorbent assay of bovine herpesvirus type 1 glycoprotein D. *J Clin Microbiol*, 40, 4045-50.
- JULEFF, N., WINDSOR, M., LEFEVRE, E. A., GUBBINS, S., HAMBLIN, P., REID, E., MCLAUGHLIN, K., BEVERLEY, P. C., MORRISON, I. W. & CHARLESTON, B. 2009. Foot-and-mouth disease virus can induce a specific and rapid CD4⁺ T-cell-independent neutralizing and isotype class-switched antibody response in naïve cattle. *J Virol*, 83, 3626-36.
- JULEFF, N., WINDSOR, M., REID, E., SEAGO, J., ZHANG, Z., MONAGHAN, P., MORRISON, I. W. & CHARLESTON, B. 2008. Foot-and-mouth disease virus persists in the light zone of germinal centres. *PLoS One*, 3, e3434.
- JULEFF, N. D. 2009. *Interactions of foot-and-mouth disease virus with cells in organised lymphoid tissue influence innate and adaptive immune responses*. Doctor of philosophy Dissertation, University of Edinburgh.
- JUNG, Y., JEONG, J. Y. & CHUNG, B. H. 2008. Recent advances in immobilization methods of antibodies on solid supports. *Analyst*, 133, 697-701.
- KABAT, E. A. & WU, T. T. 1991. Identical V region amino acid sequences and segments of sequences in antibodies of different specificities. Relative contributions of VH and VL genes, minigenes, and complementarity-determining regions to binding of antibody-combining sites. *J Immunol*, 147, 1709-19.
- KANG, A. S., BARBAS, C. F., JANDA, K. D., BENKOVIC, S. J. & LERNER, R. A. 1991. Linkage of recognition and replication functions by assembling combinatorial antibody Fab libraries along phage surfaces. *Proc Natl Acad Sci U S A*, 88, 4363-6.
- KAPSENBERG, M. L. 2003. Dendritic-cell control of pathogen-driven T-cell polarization. *Nat Rev Immunol*, 3, 984-93.
- KATPALLY, U., FU, T. M., FREED, D. C., CASIMIRO, D. R. & SMITH, T. J. 2009. Antibodies to the buried N terminus of rhinovirus VP4 exhibit cross-serotypic neutralization. *J Virol*, 83, 7040-8.
- KAY, B. K. & HOESS, R. H. 1996. Principles and applications of phage display. In: KAY, B. K., WINTER, J. & MCCAFFERTY, J. (eds.) *Phage display of peptides and proteins, a laboratory manual*. California: Academic Press.
- KERSCHBAUMER, R. J., HIRSCHL, S., KAUFMANN, A., IBL, M., KOENIG, R. & HIMMLER, G. 1997. Single-chain Fv fusion proteins suitable as coating and detecting reagents in a double antibody sandwich enzyme-linked immunosorbent assay. *Anal Biochem*, 249, 219-27.
- KETTLEBOROUGH, C. A., ANSELL, K. H., ALLEN, R. W., ROSELL-VIVES, E., GUSSOW, D. H. & BENDIG, M. M. 1994. Isolation of tumor cell-specific single-chain Fv from immunized mice using phage-antibody libraries and the re-construction of whole antibodies from these antibody fragments. *Eur J Immunol*, 24, 952-8.
- KING, A. M. Q., BROWN, F., CHRISTIAN, P., HOVI, T., HYYPIA, T., KNOWLES, N. J., LEMON, S. M., MINOR, P. D., PALMENBERG, A. C., SKERN, T. & STANWAY, G. 2000. Picornaviridae. In: VAN REGENMORTEL, M. H. V., FAUQUET, C. M., BISHOP, D. H. L., CALISHER, C. H., CARSTEN, E. B., ESTES, M. K., LEMON, S. M., MANILOFF, J., MAYO, M. A., MCGEOCH, D. J., PRINGLE, C. R. & WICKNER, R. B. (eds.) *Virus Taxonomy: Seventh report of the international committee for the taxonomy of viruses*. New York, San Diego, California,: Academic Press.
- KITCHING, P., HAMMOND, J., JEGGO, M., CHARLESTON, B., PATON, D., RODRIGUEZ, L. & HECKERT, R. 2007a. Global FMD control - is it an option? *Vaccine*, 25, 5660-4.
- KITCHING, R. P., TAYLOR, N. M. & THRUSFIELD, M. V. 2007b. Veterinary epidemiology: vaccination strategies for foot-and-mouth disease. *Nature*, 445, E12.
- KITSON, J. D., MCCAHLON, D. & BELSHAM, G. J. 1990. Sequence analysis of monoclonal antibody resistant mutants of type O foot-and-mouth disease virus: evidence for the involvement of the three surface exposed capsid proteins in four antigenic sites. *Virology*, 179, 26-34.

- KJELLEN, L. & LINDAHL, U. 1991. Proteoglycans: structures and interactions. *Annu Rev Biochem*, 60, 443-75.
- KLEIN, M., HADASCHIK, D., ZIMMERMANN, H., EGGERS, H. J. & NELSEN-SALZ, B. 2000. The picornavirus replication inhibitors HBB and guanidine in the echovirus-9 system: the significance of viral protein 2C. *J Gen Virol*, 81, 895-901.
- KLEYMANN, G., IWATA, S., WIESMULLER, K. H., LUDWIG, B., HAASE, W. & MICHEL, H. 1995. Immunoelectron microscopy and epitope mapping with monoclonal antibodies suggest the existence of an additional N-terminal transmembrane helix in the cytochrome *b* subunit of bacterial ubiquinol:cytochrome-c oxidoreductases. *Eur J Biochem*, 230, 359-63.
- KNIPE, T., RIEDER, E., BAXT, B., WARD, G. & MASON, P. W. 1997. Characterization of synthetic foot-and-mouth disease virus provirions separates acid-mediated disassembly from infectivity. *J Virol*, 71, 2851-6.
- KNOWLES, N. J. & SAMUEL, A. R. 2003. Molecular epidemiology of foot-and-mouth disease virus. *Virus Res*, 91, 65-80.
- KNOWLES, N. J., SAMUEL, A. R., DAVIES, P. R., KITCHING, R. P. & DONALDSON, A. I. 2001. Outbreak of foot-and-mouth disease virus serotype O in the UK caused by a pandemic strain. *Vet Rec*, 148, 258-9.
- KOH, W. W., STEFFENSEN, S., GONZALEZ-PAJUELO, M., HOORELBEKE, B., GORLANI, A., SZYNOL, A., FORSMAN, A., AASA-CHAPMAN, M. M., DE HAARD, H., VERRIPS, T. & WEISS, R. A. 2010. Generation of a family-specific phage library of llama single chain antibody fragments that neutralize HIV-1. *J Biol Chem*, 285, 19116-24.
- KOHLER, G. & MILSTEIN, C. 1975. Continuous cultures of fused cells secreting antibody of predefined specificity. *Nature*, 256, 495-7.
- KONG, R., LI, H., GEORGIEV, I., CHANGELA, A., BIBOLLET-RUCHE, F., DECKER, J. M., ROWLAND-JONES, S. L., JAYE, A., GUAN, Y., LEWIS, G. K., LANGEDIJK, J. P., HAHN, B. H., KWONG, P. D., ROBINSON, J. E. & SHAW, G. M. 2012. Epitope mapping of broadly neutralizing HIV-2 human monoclonal antibodies. *J Virol*, 86, 12115-28.
- KORTT, A. A., GUTHRIE, R. E., HINDS, M. G., POWER, B. E., IVANCIC, N., CALDWELL, J. B., GRUEN, L. C., NORTON, R. S. & HUDSON, P. J. 1995. Solution properties of *Escherichia coli*-expressed V_H domain of anti-neuraminidase antibody NC41. *J Protein Chem*, 14, 167-78.
- KRAFT, S., DIEFENBACH, B., MEHTA, R., JONCZYK, A., LUCKENBACH, G. A. & GOODMAN, S. L. 1999. Definition of an unexpected ligand recognition motif for $\alpha_v\beta_6$ integrin. *J Biol Chem*, 274, 1979-85.
- KUHN, R., LUZ, N. & BECK, E. 1990. Functional analysis of the internal translation initiation site of foot-and-mouth disease virus. *J Virol*, 64, 4625-31.
- KUMADA, Y., HAMASAKI, K., SHIRITANI, Y., NAKAGAWA, A., KUROKI, D., OHSE, T., CHOI, D. H., KATAKURA, Y. & KISHIMOTO, M. 2009a. Direct immobilization of functional single-chain variable fragment antibodies (scFvs) onto a polystyrene plate by genetic fusion of a polystyrene-binding peptide (PS-tag). *Anal Bioanal Chem*, 395, 759-65.
- KUMADA, Y., HAMASAKI, K., SHIRITANI, Y., OHSE, T. & KISHIMOTO, M. 2009b. Efficient immobilization of a ligand antibody with high antigen-binding activity by use of a polystyrene-binding peptide and an intelligent microtiter plate. *J Biotechnol*, 142, 135-41.
- LAEMMLI, U. K. 1970. Cleavage of structural proteins during the assembly of the head of bacteriophage T4. *Nature*, 227, 680-5.
- LAFFLY, E. & SODOYER, R. 2005. Monoclonal and recombinant antibodies, 30 years after. *Hum Antibodies*, 14, 33-55.
- LANG, I. M., BARBAS, C. F., 3RD & SCHLEEF, R. R. 1996. Recombinant rabbit Fab with binding activity to type-1 plasminogen activator inhibitor derived from a phage-display library against human α -granules. *Gene*, 172, 295-8.
- LANIER, L. L. 2005. NK cell recognition. *Annu Rev Immunol*, 23, 225-74.
- LAPORTE, J., GROSCLAUDE, J., WANTYGHM, J., BERNARD, S. & ROUZE, P. 1973. Neutralization of the infective power of the foot-and-mouth disease virus in cell culture by using serums from pigs immunized with a purified viral protein. *C R Acad Sci Hebd Seances Acad Sci D*, 276, 3399-401.

- LARSSON, A., KARLSSON-PARRA, A. & SJOQUIST, J. 1991. Use of chicken antibodies in enzyme immunoassays to avoid interference by rheumatoid factors. *Clin Chem*, 37, 411-4.
- LAVORIA, M. A., DI-GIACOMO, S., BUCAFUSCO, D., FRANCO-MAHECHA, O. L., PEREZ-FILGUEIRA, D. M. & CAPOZZO, A. V. 2012. Avidity and subtyping of specific antibodies applied to the indirect assessment of heterologous protection against foot-and-mouth disease virus in cattle. *Vaccine*, 30, 6845-50.
- LAWRENCE, P. & RIEDER, E. 2009. Identification of RNA helicase A as a new host factor in the replication cycle of foot-and-mouth disease virus. *J Virol*, 83, 11356-66.
- LEA, S., HERNANDEZ, J., BLAKEMORE, W., BROCCHI, E., CURRY, S., DOMINGO, E., FRY, E., ABU-GHAZALEH, R., KING, A., NEWMAN, J. & ET AL. 1994. The structure and antigenicity of a type C foot-and-mouth disease virus. *Structure*, 2, 123-39.
- LEE, W. M., MONROE, S. S. & RUECKERT, R. R. 1993. Role of maturation cleavage in infectivity of picornaviruses: activation of an infectious particle. *J Virol*, 67, 2110-22.
- LEE, Y. F., NOMOTO, A., DETJEN, B. M. & WIMMER, E. 1977. A protein covalently linked to poliovirus genome RNA. *Proc Natl Acad Sci U S A*, 74, 59-63.
- LEFORBAN, Y. 1999. Prevention measures against foot-and-mouth disease in Europe in recent years. *Vaccine*, 17, 1755-9.
- LEONOVA, G. N. & PAVLENKO, E. V. 2009. Characterization of neutralizing antibodies to Far Eastern of tick-borne encephalitis virus subtype and the antibody avidity for four tick-borne encephalitis vaccines in human. *Vaccine*, 27, 2899-904.
- LEVY, N. S., MALIPIERO, U. V., LEBECQUE, S. G. & GEARHART, P. J. 1989. Early onset of somatic mutation in immunoglobulin V_H genes during the primary immune response. *J Exp Med*, 169, 2007-19.
- LI, F., BROWNING, G. F., STUDDERT, M. J. & CRABB, B. S. 1996. Equine rhinovirus 1 is more closely related to foot-and-mouth disease virus than to other picornaviruses. *Proc Natl Acad Sci USA*, 93, 990-5.
- LI, Q., YAFAL, A. G., LEE, Y. M., HOGLE, J. & CHOW, M. 1994. Poliovirus neutralization by antibodies to internal epitopes of VP4 and VP1 results from reversible exposure of these sequences at physiological temperature. *J Virol*, 68, 3965-70.
- LI, X., LIU, R., TANG, H., JIN, M., CHEN, H. & QIAN, P. 2008. Induction of protective immunity in swine by immunization with live attenuated recombinant pseudorabies virus expressing the capsid precursor encoding regions of foot-and-mouth disease virus. *Vaccine*, 26, 2714-22.
- LI, Y., KILPATRICK, J. & WHITELAM, G. C. 2000. Sheep monoclonal antibody fragments generated using a phage display system. *J Immunol Methods*, 236, 133-46.
- LIPMAN, N. S., JACKSON, L. R., TRUDEL, L. J. & WEIS-GARCIA, F. 2005. Monoclonal versus polyclonal antibodies: distinguishing characteristics, applications, and information resources. *ILAR J*, 46, 258-68.
- LOGAN, D., ABU-GHAZALEH, R., BLAKEMORE, W., CURRY, S., JACKSON, T., KING, A., LEA, S., LEWIS, R., NEWMAN, J., PARRY, N. & ET AL. 1993. Structure of a major immunogenic site on foot-and-mouth disease virus. *Nature*, 362, 566-8.
- MADSHUS, I. H., OLSNES, S. & SANDVIG, K. 1984a. Mechanism of entry into the cytosol of poliovirus type 1: requirement for low pH. *J Cell Biol*, 98, 1194-200.
- MADSHUS, I. H., OLSNES, S. & SANDVIG, K. 1984b. Requirements for entry of poliovirus RNA into cells at low pH. *EMBO J*, 3, 1945-50.
- MAHAPATRA, M., HAMBLIN, P. & PATON, D. J. 2012. Foot-and-mouth disease virus epitope dominance in the antibody response of vaccinated animals. *J Gen Virol*, 93, 488-93.
- MAHAPATRA, M., SEKI, C., UPADHYAYA, S., BARNETT, P. V., LA TORRE, J. & PATON, D. J. 2011. Characterisation and epitope mapping of neutralising monoclonal antibodies to A24 Cruzeiro strain of FMDV. *Vet Microbiol*, 149, 242-7.
- MAKOWSKI, L. 1994. Phage display: Structure, assembly and engineering of filamentous bacteriophage M13. *Cur Opin Struct Biol*, 4, 225-230.
- MALIK, P., TERRY, T. D., GOWDA, L. R., LANGARA, A., PETUKHOV, S. A., SYMMONS, M. F., WELSH, L. C., MARVIN, D. A. & PERHAM, R. N. 1996. Role of capsid structure and membrane protein processing in determining the size and copy number of peptides displayed on the major coat protein of filamentous bacteriophage. *J Mol Biol*, 260, 9-21.

- MAREE, F. F., BLIGNAUT, B., DE BEER, T. A. & RIEDER, E. 2013. Analysis of SAT type foot-and-mouth disease virus capsid proteins and the identification of putative amino acid residues affecting virus stability. *PLoS One*, 8, e61612.
- MAREE, F. F., BLIGNAUT, B., ESTERHUYSEN, J. J., DE BEER, T. A., THERON, J., O'NEILL, H. G. & RIEDER, E. 2011. Predicting antigenic sites on the foot-and-mouth disease virus capsid of the South African Territories types using virus neutralization data. *J Gen Virol*, 92, 2297-309.
- MARKS, J. D., HOOGENBOOM, H. R., BONNERT, T. P., MCCAFFERTY, J., GRIFFITHS, A. D. & WINTER, G. 1991. By-passing immunization. Human antibodies from V-gene libraries displayed on phage. *J Mol Biol*, 222, 581-97.
- MARQUARDT, O. & FREIBERG, B. 2000. Antigenic variation among foot-and-mouth disease virus type A field isolates of 1997-1999 from Iran. *Vet Microbiol*, 74, 377-86.
- MARQUARDT, O., RAHMAN, M. M. & FREIBERG, B. 2000. Genetic and antigenic variance of foot-and-mouth disease virus type Asia1. *Arch Virol*, 145, 149-57.
- MARTINEZ-SALAS, E. 1999. Internal ribosome entry site biology and its use in expression vectors. *Curr Opin Biotechnol*, 10, 458-64.
- MARTINEZ-SALAS, E., ORTIN, J. & DOMINGO, E. 1985. Sequence of the viral replicase gene from foot-and-mouth disease virus C1-Santa Pau (C-S8). *Gene*, 35, 55-61.
- MARTINEZ-SALAS, E., REGALADO, M. P. & DOMINGO, E. 1996. Identification of an essential region for internal initiation of translation in the aphthovirus internal ribosome entry site and implications for viral evolution. *J Virol*, 70, 992-8.
- MARTINEZ-SALAS, E. & SAIZ, M. 2008. Foot-and-mouth disease virus. In: METTENLEITER, T. C. & SOBRINO, F. (eds.) *Animal Viruses Molecular Biology*. Norfolk, United Kingdom: Caister Academic Press.
- MARTINEZ, M. A., CARRILLO, C., GONZALEZ-CANDELAS, F., MOYA, A., DOMINGO, E. & SOBRINO, F. 1991. Fitness alteration of foot-and-mouth disease virus mutants: measurement of adaptability of viral quasispecies. *J Virol*, 65, 3954-7.
- MASON, P. W., BAXT, B., BROWN, F., HARBER, J., MURDIN, A. & WIMMER, E. 1993. Antibody-complexed foot-and-mouth disease virus, but not poliovirus, can infect normally insusceptible cells via the Fc receptor. *Virology*, 192, 568-77.
- MASON, P. W., BEZBORODOVA, S. V. & HENRY, T. M. 2002. Identification and characterization of a *cis*-acting replication element (*cre*) adjacent to the internal ribosome entry site of foot-and-mouth disease virus. *J Virol*, 76, 9686-94.
- MASON, P. W., GRUBMAN, M. J. & BAXT, B. 2003. Molecular basis of pathogenesis of FMDV. *Virus Res*, 91, 9-32.
- MASON, P. W., RIEDER, E. & BAXT, B. 1994. RGD sequence of foot-and-mouth disease virus is essential for infecting cells via the natural receptor but can be bypassed by an antibody-dependent enhancement pathway. *Proc Natl Acad Sci U S A*, 91, 1932-6.
- MATEO, R. & MATEU, M. G. 2007. Deterministic, compensatory mutational events in the capsid of foot-and-mouth disease virus in response to the introduction of mutations found in viruses from persistent infections. *J Virol*, 81, 1879-87.
- MATEU, M. G., CAMARERO, J. A., GIRALT, E., ANDREU, D. & DOMINGO, E. 1995. Direct evaluation of the immunodominance of a major antigenic site of foot-and-mouth disease virus in a natural host. *Virology*, 206, 298-306.
- MATEU, M. G., ESCARMIS, C. & DOMINGO, E. 1998. Mutational analysis of discontinuous epitopes of foot-and-mouth disease virus using an unprocessed capsid protomer precursor. *Virus Res*, 53, 27-37.
- MATEU, M. G., MARTINEZ, M. A., CAPUCCI, L., ANDREU, D., GIRALT, E., SOBRINO, F., BROCCHI, E. & DOMINGO, E. 1990. A single amino acid substitution affects multiple overlapping epitopes in the major antigenic site of foot-and-mouth disease virus of serotype C. *J Gen Virol*, 71, 629-37.
- MATEU, M. G., MARTINEZ, M. A., ROCHA, E., ANDREU, D., PAREJO, J., GIRALT, E., SOBRINO, F. & DOMINGO, E. 1989. Implications of a quasispecies genome structure: effect of frequent, naturally occurring amino acid substitutions on the antigenicity of foot-and-mouth disease virus. *Proc Natl Acad Sci U S A*, 86, 5883-7.

- MATEU, M. G., ROCHA, E., VICENTE, O., VAYREDA, F., NAVALPOTRO, C., ANDREU, D., PEDROSO, E., GIRALT, E., ENJUANES, L. & DOMINGO, E. 1987. Reactivity with monoclonal antibodies of viruses from an episode of foot-and-mouth disease. *Virus Res*, 8, 261-74.
- MATEU, M. G., VALERO, M. L., ANDREU, D. & DOMINGO, E. 1996. Systematic replacement of amino acid residues within an Arg-Gly-Asp-containing loop of foot-and-mouth disease virus and effect on cell recognition. *J Biol Chem*, 271, 12814-9.
- MATTION, N., KONIG, G., SEKI, C., SMITSAART, E., MARADEI, E., ROBIOLO, B., DUFFY, S., LEON, E., PICCONE, M., SADIR, A., BOTTINI, R., COSENTINO, B., FALCZUK, A., MARESCA, R., PERIOLO, O., BELLINZONI, R., ESPINOZA, A., TORRE, J. L. & PALMA, E. L. 2004. Reintroduction of foot-and-mouth disease in Argentina: characterisation of the isolates and development of tools for the control and eradication of the disease. *Vaccine*, 22, 4149-62.
- MAX, E. E., SEIDMAN, J. G. & LEDER, P. 1979. Sequences of five potential recombination sites encoded close to an immunoglobulin κ constant region gene. *Proc Natl Acad Sci U S A*, 76, 3450-4.
- MAYER, C., NEUBAUER, D., NCHINDA, A. T., CENCIC, R., TROMPF, K. & SKERN, T. 2008. Residue L143 of the foot-and-mouth disease virus leader proteinase is a determinant of cleavage specificity. *J Virol*, 82, 4656-9.
- MCCAFFERTY, J., FITZGERALD, K. J., EARNSHAW, J., CHISWELL, D. J., LINK, J., SMITH, R. & KENTEN, J. 1994. Selection and rapid purification of murine antibody fragments that bind a transition-state analog by phage display. *Appl Biochem Biotechnol*, 47, 157-71; discussion 171-3.
- MCCAFFERTY, J., GRIFFITHS, A. D., WINTER, G. & CHISWELL, D. J. 1990. Phage antibodies: filamentous phage displaying antibody variable domains. *Nature*, 348, 552-4.
- MCCAHON, D., CROWTHER, J. R., BELSHAM, G. J., KITSON, J. D., DUCHESNE, M., HAVE, P., MELOEN, R. H., MORGAN, D. O. & DE SIMONE, F. 1989. Evidence for at least four antigenic sites on type O foot-and-mouth disease virus involved in neutralization; identification by single and multiple site monoclonal antibody-resistant mutants. *J Gen Virol*, 70, 639-45.
- MCCULLOUGH, K. C. 2004. Immunology of foot-and-mouth disease. In: SOBRINO, F. & DOMINGO, E. (eds.) *Foot and Mouth disease: current perspectives*. UK: Horizon Bioscience.
- MCCULLOUGH, K. C., CROWTHER, J. R., BUTCHER, R. N., CARPENTER, W. C., BROCCHI, E., CAPUCCI, L. & DE SIMONE, F. 1986. Immune protection against foot-and-mouth disease virus studied using virus-neutralizing and non-neutralizing concentrations of monoclonal antibodies. *Immunology*, 58, 421-8.
- MCCULLOUGH, K. C., CROWTHER, J. R., CARPENTER, W. C., BROCCHI, E., CAPUCCI, L., DE SIMONE, F., XIE, Q. & MCCAHON, D. 1987a. Epitopes on foot-and-mouth disease virus particles. I. Topology. *Virology*, 157, 516-25.
- MCCULLOUGH, K. C., DE SIMONE, F., BROCCHI, E., CAPUCCI, L., CROWTHER, J. R. & KIHM, U. 1992. Protective immune response against foot-and-mouth disease. *J Virol*, 66, 1835-40.
- MCCULLOUGH, K. C., SMALE, C. J., CARPENTER, W. C., CROWTHER, J. R., BROCCHI, E. & DE SIMONE, F. 1987b. Conformational alteration in foot-and-mouth disease virus virion capsid structure after complexing with monospecific antibody. *Immunology*, 60, 75-82.
- MCGREGOR, D. P., MOLLOY, P. E., CUNNINGHAM, C. & HARRIS, W. J. 1994. Spontaneous assembly of bivalent single chain antibody fragments in *Escherichia coli*. *Mol Immunol*, 31, 219-26.
- MEDINA, M., DOMINGO, E., BRANGWYN, J. K. & BELSHAM, G. J. 1993. The two species of the foot-and-mouth disease virus leader protein, expressed individually, exhibit the same activities. *Virology*, 194, 355-9.
- MEEROVITCH, J. L. & SONENBERG, N. 1993. Internal initiation of picornavirus RNA translation. *Semin Virol*, 4, 217-227.

- MELOEN, R. H., PUYK, W. C., MEIJER, D. J., LANKHOF, H., POSTHUMUS, W. P. & SCHAAPER, W. M. 1987. Antigenicity and immunogenicity of synthetic peptides of foot-and-mouth disease virus. *J Gen Virol*, 68, 305-14.
- MELOEN, R. H., ROWLANDS, D. J. & BROWN, F. 1979. Comparison of the antibodies elicited by the individual structural polypeptides of foot-and-mouth disease and polio viruses. *J Gen Virol*, 45, 761-3.
- MEYER, T., STRATMANN-SELKE, J., MEENS, J., SCHIRRMANN, T., GERLACH, G. F., FRANK, R., DUBEL, S., STRUTZBERG-MINDER, K. & HUST, M. 2011. Isolation of scFv fragments specific to OmpD of *Salmonella Typhimurium*. *Vet Microbiol*, 147, 162-9.
- MINOR, P. D. 1990. Antigenic structure of picornaviruses. *Curr Top Microbiol Immunol*, 161, 121-54.
- MOFFAT, K., HOWELL, G., KNOX, C., BELSHAM, G. J., MONAGHAN, P., RYAN, M. D. & WILEMAN, T. 2005. Effects of foot-and-mouth disease virus nonstructural proteins on the structure and function of the early secretory pathway: 2BC but not 3A blocks endoplasmic reticulum-to-Golgi transport. *J Virol*, 79, 4382-95.
- MOFFAT, K., KNOX, C., HOWELL, G., CLARK, S. J., YANG, H., BELSHAM, G. J., RYAN, M. & WILEMAN, T. 2007. Inhibition of the secretory pathway by foot-and-mouth disease virus 2BC protein is reproduced by coexpression of 2B with 2C, and the site of inhibition is determined by the subcellular location of 2C. *J Virol*, 81, 1129-39.
- MOHAPATRA, J. K., SUBRAMANIAM, S., TOSH, C., HEMADRI, D., SANYAL, A., PERIYASAMY, T. R. & RASOOL, T. J. 2007. Genotype differentiating RT-PCR and sandwich ELISA: handy tools in epidemiological investigation of foot-and-mouth disease. *J Virol Methods*, 143, 117-21.
- MOHLER, J. R. 1952. Foot-and-mouth disease. *Farmers' Bulletin no. 666*. Washington DC: U.S Government Printing Office.
- MONAGHAN, P., GOLD, S., SIMPSON, J., ZHANG, Z., WEINREB, P. H., VIOLETTE, S. M., ALEXANDERSEN, S. & JACKSON, T. 2005. The $\alpha_v\beta_6$ integrin receptor for foot-and-mouth disease virus is expressed constitutively on the epithelial cells targeted in cattle. *J Gen Virol*, 86, 2769-80.
- MORAES, M. P., DE LOS SANTOS, T., KOSTER, M., TURECEK, T., WANG, H., ANDREYEV, V. G. & GRUBMAN, M. J. 2007. Enhanced antiviral activity against foot-and-mouth disease virus by a combination of type I and II porcine interferons. *J Virol*, 81, 7124-35.
- MORRELL, D. J., MELLOR, E. J., ROWLANDS, D. J. & BROWN, F. 1987. Surface structure and RNA-protein interactions of foot-and-mouth disease virus. *J Gen Virol*, 68, 1649-58.
- MURRE, C. 2007. Epigenetics of antigen-receptor gene assembly. *Curr Opin Genet Dev*, 17, 415-21.
- NAKANISHI, K., SAKIYAMA, T., KUMADA, Y., IMAMURA, K. & IMANAKA, H. 2008. Recent advances in controlled immobilization of proteins onto the surface of the solid substrate and its possible application to proteomics. *Cur Proteomics*, 5, 161-175.
- NARANJO, J. & COSIVI, O. 2013. Elimination of foot-and-mouth disease in South America: lessons and challenges. *Philos Trans R Soc Lond B Biol Sci*, 368, 20120381.
- NARAT, M. 2003. Production of antibodies in chickens. *Food Technol Biotech*, 42, 259-267.
- NARAYAN, O., CLEMENTS, J. E., GRIFFIN, D. E. & WOLINSKY, J. S. 1981. Neutralizing antibody spectrum determines the antigenic profiles of emerging mutants of visna virus. *Infect Immun*, 32, 1045-50.
- NAYAK, A., GOODFELLOW, I. G. & BELSHAM, G. J. 2005. Factors required for the Uridylylation of the foot-and-mouth disease virus 3B1, 3B2, and 3B3 peptides by the RNA-dependent RNA polymerase (3Dpol) in vitro. *J Virol*, 79, 7698-706.
- NAYAK, A., GOODFELLOW, I. G., WOOLAWAY, K. E., BIRTLEY, J., CURRY, S. & BELSHAM, G. J. 2006. Role of RNA structure and RNA binding activity of foot-and-mouth disease virus 3C protein in VPg uridylylation and virus replication. *J Virol*, 80, 9865-75.
- NEFF, S., MASON, P. W. & BAXT, B. 2000. High-efficiency utilization of the bovine integrin $\alpha_v\beta_3$ as a receptor for foot-and-mouth disease virus is dependent on the bovine β_3 subunit. *J Virol*, 74, 7298-306.

- NEFF, S., SA-CARVALHO, D., RIEDER, E., MASON, P. W., BLYSTONE, S. D., BROWN, E. J. & BAXT, B. 1998. Foot-and-mouth disease virus virulent for cattle utilizes the integrin $\alpha_v\beta_3$ as its receptor. *J Virol*, 72, 3587-94.
- NELSON, P. N., REYNOLDS, G. M., WALDRON, E. E., WARD, E., GIANNOPOULOS, K. & MURRAY, P. G. 2000. Monoclonal antibodies. *Mol Pathol*, 53, 111-7.
- NERI, D., PINI, A. & NISSIM, A. 1998. Antibodies from phage display libraries as immunochemical reagents. *Methods Mol Biol*, 80, 475-500.
- NEWMAN, J. F., CARTWRIGHT, B., DOEL, T. R. & BROWN, F. 1979. Purification and identification of the RNA-dependent RNA polymerase of foot-and-mouth disease virus. *J Gen Virol*, 45, 497-507.
- NEWTON, S. E., CARROLL, A. R., CAMPBELL, R. O., CLARKE, B. E. & ROWLANDS, D. J. 1985. The sequence of foot-and-mouth disease virus RNA to the 5' side of the poly(C) tract. *Gene*, 40, 331-6.
- NFON, C. K., FERMAN, G. S., TOKA, F. N., GREGG, D. A. & GOLDE, W. T. 2008. Interferon-alpha production by swine dendritic cells is inhibited during acute infection with foot-and-mouth disease virus. *Viral Immunol*, 21, 68-77.
- NILSSON, E., AMINI, A., WRETLIND, B. & LARSSON, A. 2007. *Pseudomonas aeruginosa* infections are prevented in cystic fibrosis patients by avian antibodies binding *Pseudomonas aeruginosa* flagellin. *J Chromatogr B Analyt Technol Biomed Life Sci*, 856, 75-80.
- NISHIMURA, S. L., SHEPPARD, D. & PYTELA, R. 1994. Integrin $\alpha_v\beta_8$. Interaction with vitronectin and functional divergence of the β_8 cytoplasmic domain. *J Biol Chem*, 269, 28708-15.
- NISSIM, A., HOOGENBOOM, H. R., TOMLINSON, I. M., FLYNN, G., MIDGLEY, C., LANE, D. & WINTER, G. 1994. Antibody fragments from a 'single pot' phage display library as immunochemical reagents. *EMBO J*, 13, 692-8.
- NUNEZ, J. I., BARANOWSKI, E., MOLINA, N., RUIZ-JARABO, C. M., SANCHEZ, C., DOMINGO, E. & SOBRINO, F. 2001. A single amino acid substitution in nonstructural protein 3A can mediate adaptation of foot-and-mouth disease virus to the guinea pig. *J Virol*, 75, 3977-83.
- O'BRIEN, P. M., AITKEN, R., O'NEIL, B. W. & CAMPO, M. S. 1999. Generation of native bovine mAbs by phage display. *Proc Natl Acad Sci U S A*, 96, 640-5.
- O'CONNELL, D., BECERRIL, B., ROY-BURMAN, A., DAWS, M. & MARKS, J. D. 2002. Phage versus phagemid libraries for generation of human monoclonal antibodies. *J Mol Biol*, 321, 49-56.
- O'DONNELL, V., LAROCCO, M. & BAXT, B. 2008. Heparan sulfate-binding foot-and-mouth disease virus enters cells via caveola-mediated endocytosis. *J Virol*, 82, 9075-85.
- O'DONNELL, V., LAROCCO, M., DUQUE, H. & BAXT, B. 2005. Analysis of foot-and-mouth disease virus internalization events in cultured cells. *J Virol*, 79, 8506-18.
- O'DONNELL, V., PACHECO, J. M., GREGG, D. & BAXT, B. 2009. Analysis of foot-and-mouth disease virus integrin receptor expression in tissues from naïve and infected cattle. *J Comp Pathol*, 141, 98-112.
- OIE 2009. *Manual of Diagnostic Tests and Vaccines for Terrestrial Animals*, Paris, Office International des Epizooties.
- OPPERMAN, P. A., MAREE, F. F., VAN WYNGAARDT, W., VOSLOO, W. & THERON, J. 2012. Mapping of antigenic determinants on a SAT2 foot-and-mouth disease virus using chicken single-chain antibody fragments. *Virus Res*, 167, 370-9.
- PACHECO, J. M., ARZT, J. & RODRIGUEZ, L. L. 2010. Early events in the pathogenesis of foot-and-mouth disease in cattle after controlled aerosol exposure. *Vet J*, 183, 46-53.
- PACHECO, J. M., HENRY, T. M., O'DONNELL, V. K., GREGORY, J. B. & MASON, P. W. 2003. Role of nonstructural proteins 3A and 3B in host range and pathogenicity of foot-and-mouth disease virus. *J Virol*, 77, 13017-27.
- PALM, N. W. & MEDZHITOV, R. 2009. Pattern recognition receptors and control of adaptive immunity. *Immunol Rev*, 227, 221-33.
- PANDEY, S. 2010. Hybridoma technology for production of monoclonal antibodies. *Int J Pharm Sci Rev Res*, 1, 88-94.

- PARIDA, S. 2009. Vaccination against foot-and-mouth disease virus: strategies and effectiveness. *Expert Rev Vaccines*, 8, 347-65.
- PARIDA, S., COX, S. J., REID, S. M., HAMBLIN, P., BARNETT, P. V., INOUE, T., ANDERSON, J. & PATON, D. J. 2005. The application of new techniques to the improved detection of persistently infected cattle after vaccination and contact exposure to foot-and-mouth disease. *Vaccine*, 23, 5186-95.
- PARMLEY, S. F. & SMITH, G. P. 1988. Antibody-selectable filamentous *fd* phage vectors: affinity purification of target genes. *Gene*, 73, 305-18.
- PARRY, N., FOX, G., ROWLANDS, D., BROWN, F., FRY, E., ACHARYA, R., LOGAN, D. & STUART, D. 1990. Structural and serological evidence for a novel mechanism of antigenic variation in foot-and-mouth disease virus. *Nature*, 347, 569-72.
- PARRY, N. R., BARNETT, P. V., OULDRIDGE, E. J., ROWLANDS, D. J. & BROWN, F. 1989. Neutralizing epitopes of type O foot-and-mouth disease virus. II. Mapping three conformational sites with synthetic peptide reagents. *J Gen Virol*, 70, 1493-503.
- PATON, D. J., SUMPTION, K. J. & CHARLESTON, B. 2009. Options for control of foot-and-mouth disease: knowledge, capability and policy. *Philos Trans R Soc Lond B Biol Sci*, 364, 2657-67.
- PATON, D. J., VALARCHER, J. F., BERGMANN, I., MATLHO, O. G., ZAKHAROV, V. M., PALMA, E. L. & THOMSON, G. R. 2005. Selection of foot-and-mouth disease vaccine strains-a review. *Rev Sci Tech*, 24, 981-93.
- PAUL, A. V. 2002. Possible unifying mechanism of picornavirus genome replication. In: SEMLER, B. L. & WIMMER, E. (eds.) *Molecular biology of picornaviruses*. Washington, D.C: ASM Press.
- PAY, T. W. & HINGLEY, P. J. 1987. Correlation of 140S antigen dose with the serum neutralizing antibody response and the level of protection induced in cattle by foot-and-mouth disease vaccines. *Vaccine*, 5, 60-4.
- PERRY, B. D. & RICH, K. M. 2007. Poverty impacts of foot-and-mouth disease and the poverty reduction implications of its control. *Vet Rec*, 160, 238-41.
- PFAFF, E., MUSSGAY, M., BOHM, H. O., SCHULZ, G. E. & SCHALLER, H. 1982. Antibodies against a preselected peptide recognize and neutralize foot-and-mouth disease virus. *EMBO J*, 1, 869-74.
- PFAFF, E., THIEL, H. J., BECK, E., STROHMAIER, K. & SCHALLER, H. 1988. Analysis of neutralizing epitopes on foot-and-mouth disease virus. *J Virol*, 62, 2033-40.
- PICCONE, M. E., KONIG, G., SEKI, C., MAZZUCA, G., ROBILOLO, B., MARADEI, E., PERIOLO, O., SADIR, A., FALCZUK, A., LA TORRE, J. & PALMA, E. L. Year. Genetic analysis of type A foot-and-mouth disease isolated in Argentina during the 2000-2001 outbreak. In: EUROPICTamerica, 13-19/05/2002 2002 Sea Crest, USA.
- PICCONE, M. E., PACHECO, J. M., PAUSZEK, S. J., KRAMER, E., RIEDER, E., BORCA, M. V. & RODRIGUEZ, L. L. 2010. The region between the two polyprotein initiation codons of foot-and-mouth disease virus is critical for virulence in cattle. *Virology*, 396, 152-9.
- PILIPENKO, E. V., MASLOVA, S. V., SINYAKOV, A. N. & AGOL, V. I. 1992. Towards identification of *cis*-acting elements involved in the replication of enterovirus and rhinovirus RNAs: a proposal for the existence of tRNA-like terminal structures. *Nucleic Acids Res*, 20, 1739-45.
- PITAKSAJAKUL, P., LEKCHAROENSUK, P., UPGRAGARIN, N., BARBAS, C. F., 3RD, IBRAHIM, M. S., IKUTA, K. & RAMASOOTTA, P. 2010. Fab MAbs specific to HA of influenza virus with H5N1 neutralizing activity selected from immunized chicken phage library. *Biochem Biophys Res Commun*, 395, 496-501.
- PLESICA, O. & BRAUN, W. 1967. Nucleic acids as antigens. In: DIXON, F. J. J. & HUMPHREY, J. H. (eds.) *Advances in Immunology*. New York: Academic Press Inc.
- POLATNICK, J. & ARLINGHAUS, R. B. 1967. Effect of actinomycin D on virus-induced ribonucleic acid polymerase formation in foot-and-mouth disease virus-infected baby hamster kidney cells. *J Virol*, 1, 1130-4.
- PONSEL, D., NEUGEBAUER, J., LADETZKI-BAEHS, K. & TISSOT, K. 2011. High affinity, developability and functional size: the holy grail of combinatorial antibody library generation. *Molecules*, 16, 3675-700.

- PORTER, A. G. 1993. Picornavirus nonstructural proteins: emerging roles in virus replication and inhibition of host cell functions. *J Virol*, 67, 6917-21.
- PURCELL, A. W., MCCLUSKEY, J. & ROSSJOHN, J. 2007. More than one reason to rethink the use of peptides in vaccine design. *Nat Rev Drug Discov*, 6, 404-14.
- QIAN, W., YAO, D., YU, F., XU, B., ZHOU, R., BAO, X. & LU, Z. 2000. Immobilization of antibodies on ultraflat polystyrene surfaces. *Clin Chem*, 46, 1456-63.
- QIN, Y. L., SUN, E. C., LIU, N. H., YANG, T., XU, Q. Y., ZHAO, J., WANG, W. S., WEI, P., FENG, Y. F., LI, J. P. & WU, D. L. 2013. Identification of a linear B-cell epitope within the Bluetongue virus serotype 8 NS2 protein using a phage-displayed random peptide library. *Vet Immunol Immunopathol*, 154, 93-101.
- QUINN, P. & MARKEY, B. 2001. A review of foot-and-mouth disease. *Irish Veterinary journal*, 54, 183-190.
- RAKABE, M. 2008. *Selection of chicken single-chain antibody fragments directed against recombinant VP7 of bluetongue virus*. Master of Science (Veterinary Science) Dissertation, University of Pretoria.
- RAMAKRISHAM, S., PRASANNA, K. G. & RJAN, R. 2001. Chemistry of the blood. *Text book of Medical Biochemistry*. Hyderabad, India: Orient Longman Private Ltd.
- RANA, S. K. & BAGCHI, T. 2008. Development and characterization of monoclonal antibodies against FMD virus type Asia-1 and determination of antigenic variations in the field strains. *Vet Immunol Immunopathol*, 122, 241-9.
- READING, S. A. & DIMMOCK, N. J. 2007. Neutralization of animal virus infectivity by antibody. *Arch Virol*, 152, 1047-59.
- REEVE, R., BLIGNAUT, B., ESTERHUYSEN, J. J., OPPERMAN, P., MATTHEWS, L., FRY, E. E., DE BEER, T. A., THERON, J., RIEDER, E., VOSLOO, W., O'NEILL, H. G., HAYDON, D. T. & MAREE, F. F. 2010. Sequence-based prediction for vaccine strain selection and identification of antigenic variability in foot-and-mouth disease virus. *PLoS Comput Biol*, 6, e1001027.
- REID, S. M., EBERT, K., BACHANEK-BANKOWSKA, K., BATTEN, C., SANDERS, A., WRIGHT, C., SHAW, A. E., RYAN, E. D., HUTCHINGS, G. H., FERRIS, N. P., PATON, D. J. & KING, D. P. 2009. Performance of real-time reverse transcription polymerase chain reaction for the detection of foot-and-mouth disease virus during field outbreaks in the United Kingdom in 2007. *J Vet Diagn Invest*, 21, 321-30.
- RETH, M. 1994. B cell antigen receptors. *Curr Opin Immunol*, 6, 3-8.
- REYNAUD, C. A., ANQUEZ, V., DAHAN, A. & WEILL, J. C. 1985. A single rearrangement event generates most of the chicken immunoglobulin light chain diversity. *Cell*, 40, 283-91.
- REYNAUD, C. A., ANQUEZ, V., GRIMAL, H. & WEILL, J. C. 1987. A hyperconversion mechanism generates the chicken light chain preimmune repertoire. *Cell*, 48, 379-88.
- REYNAUD, C. A., DAHAN, A., ANQUEZ, V. & WEILL, J. C. 1989. Somatic hyperconversion diversifies the single V_H gene of the chicken with a high incidence in the D region. *Cell*, 59, 171-83.
- REZAPKIN, G., NEVEROV, A., CHERKASOVA, E., VIDOR, E., SARAFANOV, A., KOUIAVSKAIA, D., DRAGUNSKY, E. & CHUMAKOV, K. 2010. Repertoire of antibodies against type 1 poliovirus in human sera. *J Virol Methods*, 169, 322-31.
- RIDDER, R., SCHMITZ, R., LEGAY, F. & GRAM, H. 1995. Generation of rabbit monoclonal antibody fragments from a combinatorial phage display library and their production in the yeast *Pichia pastoris*. *Biotechnology*, 13, 255-60.
- RIEDER, E., BAXT, B. & MASON, P. W. 1994. Animal-derived antigenic variants of foot-and-mouth disease virus type A12 have low affinity for cells in culture. *J Virol*, 68, 5296-9.
- RIEDER, E., BERINSTEIN, A., BAXT, B., KANG, A. & MASON, P. W. 1996. Propagation of an attenuated virus by design: engineering a novel receptor for a noninfectious foot-and-mouth disease virus. *Proc Natl Acad Sci U S A*, 93, 10428-33.
- RIEDER, E., BUNCH, T., BROWN, F. & MASON, P. W. 1993. Genetically engineered foot-and-mouth disease viruses with poly(C) tracts of two nucleotides are virulent in mice. *J Virol*, 67, 5139-45.

- ROBERTSON, B. H., GRUBMAN, M. J., WEDDELL, G. N., MOORE, D. M., WELSH, J. D., FISCHER, T., DOWBENKO, D. J., YANSURA, D. G., SMALL, B. & KLEID, D. G. 1985. Nucleotide and amino acid sequence coding for polypeptides of foot-and-mouth disease virus type A12. *J Virol*, 54, 651-60.
- RODRIGUEZ, L. L. & GRUBMAN, M. J. 2009. Foot-and-mouth disease virus vaccines. *Vaccine*, 27 Suppl 4, D90-4.
- ROITT, I., BROSTOFF, J. & MALE, D. 1998. Antibodies and their receptors. *Immunology*. London, UK: Mosby International Ltd.
- ROIVAINEN, M., PIIRAINEN, L. & HOVI, T. 1993. Persistence and class-specificity of neutralizing antibody response induced by trypsin-cleaved type 3 poliovirus in mice. *Vaccine*, 11, 713-7.
- RUECKERT, R. R. 1996. Picornaviridae: The virus and their replication. In: FIELDS, B. N., KNIPE, D. M. & HOWLEY, P. M. (eds.) *Fields Virology*. Philadelphia, USA: Lippincott-Raven Publishers.
- RUECKERT, R. R. & WIMMER, E. 1984. Systematic nomenclature of picornavirus proteins. *J Virol*, 50, 957-9.
- RUSSEL, M. 1991. Filamentous phage assembly. *Mol Microbiol*, 5, 1607-13.
- RWEYEMAMU, M., ROEDER, P., MACKAY, D., SUMPTION, K., BROWNLIE, J., LEFORBAN, Y., VALARCHER, J. F., KNOWLES, N. J. & SARAIVA, V. 2008. Epidemiological patterns of foot-and-mouth disease worldwide. *Transbound Emerg Dis*, 55, 57-72.
- RWEYEMAMU, M. M. 1984. Antigenic variation in foot-and-mouth disease: studies based on the virus neutralization reaction. *J Biol Stand*, 12, 323-37.
- RWEYEMAMU, M. M., BOOTH, J. C., HEAD, M. & PAY, T. W. 1978. Microneutralization tests for serological typing and subtyping of foot-and-mouth disease virus strains. *J Hyg (Lond)*, 81, 107-23.
- RYAN, M. D., BELSHAM, G. J. & KING, A. M. 1989. Specificity of enzyme-substrate interactions in foot-and-mouth disease virus polyprotein processing. *Virology*, 173, 35-45.
- SA-CARVALHO, D., RIEDER, E., BAXT, B., RODARTE, R., TANURI, A. & MASON, P. W. 1997. Tissue culture adaptation of foot-and-mouth disease virus selects viruses that bind to heparin and are attenuated in cattle. *J Virol*, 71, 5115-23.
- SAIKA, S., MATSUNAGA, T., OGAWA, T. & ICHINOHE, S. 2008. Gelatin particle agglutination (PA) antibody: comparison to neutralizing antibody (NT) and hemagglutination inhibition (HI) antibody and relationship to IgG avidity. *Kansenshogaku Zasshi*, 82, 310-6.
- SAINI, S. S., ALLORE, B., JACOBS, R. M. & KAUSHIK, A. 1999. Exceptionally long CDR3H region with multiple cysteine residues in functional bovine IgM antibodies. *Eur J Immunol*, 29, 2420-6.
- SAINI, S. S., FARRUGIA, W., RAMSLAND, P. A. & KAUSHIK, A. K. 2003. Bovine IgM antibodies with exceptionally long complementarity-determining region 3 of the heavy chain share unique structural properties conferring restricted VH + Vlambda pairings. *Int Immunol*, 15, 845-53.
- SAIZ, M., NUNEZ, J. I., JIMENEZ-CLAVERO, M. A., BARANOWSKI, E. & SOBRINO, F. 2002. Foot-and-mouth disease virus: biology and prospects for disease control. *Microbes Infect*, 4, 1183-92.
- SAKANO, H., HUPPI, K., HEINRICH, G. & TONEGAWA, S. 1979. Sequences at the somatic recombination sites of immunoglobulin light-chain genes. *Nature*, 280, 288-94.
- SALI, A. & BLUNDELL, T. L. 1993. Comparative protein modelling by satisfaction of spatial restraints. *J Mol Biol*, 234, 779-815.
- SALT, J. S. 1993. The carrier state in foot-and-mouth disease - an immunological review. *Br Vet J*, 149, 207-23.
- SALT, J. S., MULCAHY, G. & KITCHING, R. P. 1996. Isotype-specific antibody responses to foot-and-mouth disease virus in sera and secretions of 'carrier' and 'non-carrier' cattle. *Epidemiol Infect*, 117, 349-60.
- SAMUEL, A. R. & KNOWLES, N. J. 2001a. Foot-and-mouth disease type O viruses exhibit genetically and geographically distinct evolutionary lineages (topotypes). *J Gen Virol*, 82, 609-21.

- SAMUEL, A. R. & KNOWLES, N. J. 2001b. Foot-and-mouth disease virus: cause of the recent crisis for the UK livestock industry. *Trends Genet*, 17, 421-4.
- SANDILANDS, G. P., AHMED, Z., PERRY, N., DAVISON, M., LUPTON, A. & YOUNG, B. 2005. Cross-linking of neutrophil CD11b results in rapid cell surface expression of molecules required for antigen presentation and T-cell activation. *Immunology*, 114, 354-68.
- SANGAR, D. V., NEWTON, S. E., ROWLANDS, D. J. & CLARKE, B. E. 1987. All foot-and-mouth disease virus serotypes initiate protein synthesis at two separate AUGs. *Nucleic Acids Res*, 15, 3305-15.
- SANGARE, O., BASTOS, A. D., MARQUARDT, O., VENTER, E. H., VOSLOO, W. & THOMSON, G. R. 2001. Molecular epidemiology of serotype O foot-and-mouth disease virus with emphasis on West and South Africa. *Virus Genes*, 22, 345-51.
- SANYAL, A., GURUMURTHY, C. B., VENKATARAMANAN, R., HEMADRI, D. & TOSH, C. 2003. Antigenic characterization of foot-and-mouth disease virus serotype Asia1 field isolates using polyclonal and monoclonal antibodies. *Vet Microbiol*, 93, 1-11.
- SANYAL, A., VENKATARAMANAN, R. & PATTNAIK, B. 1997. Antigenic features of foot-and-mouth disease virus serotype Asia1 as revealed by monoclonal antibodies and neutralization-escape mutants. *Virus Res*, 50, 107-17.
- SANZ-PARRA, A., SOBRINO, F. & LEY, V. 1998. Infection with foot-and-mouth disease virus results in a rapid reduction of MHC class I surface expression. *J Gen Virol*, 79, 433-6.
- SAUNDERS, K., KING, A. M., MCCAHOON, D., NEWMAN, J. W., SLADE, W. R. & FORSS, S. 1985. Recombination and oligonucleotide analysis of guanidine-resistant foot-and-mouth disease virus mutants. *J Virol*, 56, 921-9.
- SCHIRRMANN, T., MEYER, T., SCHUTTE, M., FRENZEL, A. & HUST, M. 2011. Phage display for the generation of antibodies for proteome research, diagnostics and therapy. *Molecules*, 16, 412-26.
- SCHNAPP, L. M., HATCH, N., RAMOS, D. M., KLIMANSKAYA, I. V., SHEPPARD, D. & PYTELA, R. 1995. The human integrin $\alpha_8\beta_1$ functions as a receptor for tenascin, fibronectin, and vitronectin. *J Biol Chem*, 270, 23196-202.
- SCHNEIDER, T. D. & STEPHENS, R. M. 1990. Sequence logos: a new way to display consensus sequences. *Nucleic Acids Res*, 18, 6097-100.
- SCUDAMORE, J. M. & HARRIS, D. M. 2002. Control of foot and mouth disease: lessons from the experience of the outbreak in Great Britain in 2001. *Rev Sci Tech*, 21, 699-710.
- SELLERS, R. F. 1971. Quantitative aspects of the spread of foot-and-mouth disease. *Veterinary bulletin*, 41, 431-39.
- SEMLER, B. & WIMMER, E. 2002. *Molecular Biology of Picornaviruses*, Washington DC, USA., ASM Press.
- SETTE, A. & FIKES, J. 2003. Epitope-based vaccines: an update on epitope identification, vaccine design and delivery. *Curr Opin Immunol*, 15, 461-70.
- SHAO, J. J., WONG, C. K., LIN, T., LEE, S. K., CONG, G. Z., SIN, F. W., DU, J. Z., GAO, S. D., LIU, X. T., CAI, X. P., XIE, Y., CHANG, H. Y. & LIU, J. X. 2011. Promising multiple-epitope recombinant vaccine against foot-and-mouth disease virus type O in swine. *Clin Vaccine Immunol*, 18, 143-9.
- SHAW, A. E., REID, S. M., EBERT, K., HUTCHINGS, G. H., FERRIS, N. P. & KING, D. P. 2007. Implementation of a one-step real-time RT-PCR protocol for diagnosis of foot-and-mouth disease. *J Virol Methods*, 143, 81-5.
- SHEETS, M. D., AMERSDORFER, P., FINNERN, R., SARGENT, P., LINDQUIST, E., SCHIER, R., HEMINGSEN, G., WONG, C., GERHART, J. C. & MARKS, J. D. 1998. Efficient construction of a large nonimmune phage antibody library: the production of high-affinity human single-chain antibodies to protein antigens. *Proc Natl Acad Sci U S A*, 95, 6157-62.
- SHIMAMOTO, T., NISHIBORI, N., AOSASA, M., HORIUCHI, H., FURUSAWA, S. & MATSUDA, H. 2005. Stable production of recombinant chicken antibody in CHO-K1 cell line. *Biologicals*, 33, 169-74.
- SIDHU, S. S. 2000. Phage display in pharmaceutical biotechnology. *Curr Opin Biotechnol*, 11, 610-6.
- SIMMONDS, P. 2006. Recombination and selection in the evolution of picornaviruses and other mammalian positive-stranded RNA viruses. *J Virol*, 80, 11124-40.

- SIXHOLO. 2008. *Engineering recombinant chicken antibodies for improved characteristics*. Master of Science (Veterinary Science) Dissertation, University of Pretoria.
- SIXHOLO, J., VAN WYNGAARDT, W., MASHAU, C., FRISCHMUTH, J., DU PLESSIS, D. H. & FEHRSEN, J. 2011. Improving the characteristics of a mycobacterial 16 kDa-specific chicken scFv. *Biologicals*, 39, 110-6.
- SMITH, G. P. 1985. Filamentous fusion phage: novel expression vectors that display cloned antigens on the virion surface. *Science*, 228, 1315-7.
- SMITH, G. P. & PETRENKO, V. A. 1997. Phage display. *Chem Rev*, 97, 391-410.
- SMITH, G. P. & SCOTT, J. K. 1993. Libraries of peptides and proteins displayed on filamentous phage. *Methods Enzymol*, 217, 228-57.
- SOBRINO, F., SAIZ, M., JIMENEZ-CLAVERO, M. A., NUNEZ, J. I., ROSAS, M. F., BARANOWSKI, E. & LEY, V. 2001. Foot-and-mouth disease virus: a long known virus, but a current threat. *Vet Res*, 32, 1-30.
- SPADA, S., HONEGGER, A. & PLUCKTHUN, A. 1998. Reproducing the natural evolution of protein structural features with the selectively infective phage (SIP) technology. The kink in the first strand of antibody κ domains. *J Mol Biol*, 283, 395-407.
- STAVE, J. W., CARD, J. L., MORGAN, D. O. & VAKHARIA, V. N. 1988. Neutralization sites of type O1 foot-and-mouth disease virus defined by monoclonal antibodies and neutralization-escape virus variants. *Virology*, 162, 21-9.
- STEINBERGER, P., RADER, C. & BARBA III, C. F. 2001. Analysis of selected antibodies. In: BARBAS III, C. F., BURTON, D. R., SCOTT, J. K. & SILVERMAN, G. (eds.) *Phage Display: A laboratory manual*. New York: Cold Spring Harbor Laboratory Press.
- STOPAR, D., SPRUIJT, R. B., WOLFS, C. J. & HEMMINGA, M. A. 2003. Protein-lipid interactions of bacteriophage M13 major coat protein. *Biochim Biophys Acta*, 1611, 5-15.
- STOREY, P., THERON, J., MAREE, F. F. & O'NEILL, H. G. 2007. A second RGD motif in the 1D capsid protein of a SAT1 type foot-and-mouth disease virus field isolate is not essential for attachment to target cells. *Virus Res*, 124, 184-92.
- STORSET, A. K., KULBERG, S., BERG, I., BOYSEN, P., HOPE, J. C. & DISSEN, E. 2004. NKp46 defines a subset of bovine leukocytes with natural killer cell characteristics. *Eur J Immunol*, 34, 669-76.
- STREBEL, K. & BECK, E. 1986. A second protease of foot-and-mouth disease virus. *J Virol*, 58, 893-9.
- STROHMAIER, K., FRANZE, R. & ADAM, K. H. 1982. Location and characterization of the antigenic portion of the FMDV immunizing protein. *J Gen Virol*, 59, 295-306.
- SUMMERFIELD, A., GUZYLACK-PIRIOU, L., HARWOOD, L. & MCCULLOUGH, K. C. 2009. Innate immune responses against foot-and-mouth disease virus: current understanding and future directions. *Vet Immunol Immunopathol*, 128, 205-10.
- SUTMOLLER, P., BARTELING, S. S., OLASCOAGA, R. C. & SUMPTION, K. J. 2003. Control and eradication of foot-and-mouth disease. *Virus Res*, 91, 101-44.
- SWEENEY, T. R., CISNETTO, V., BOSE, D., BAILEY, M., WILSON, J. R., ZHANG, X., BELSHAM, G. J. & CURRY, S. 2010. Foot-and-mouth disease virus 2C is a hexameric AAA+ protein with a coordinated ATP hydrolysis mechanism. *J Biol Chem*, 285, 24347-59.
- SWEENEY, T. R., ROQUE-ROSELL, N., BIRTLEY, J. R., LEATHERBARROW, R. J. & CURRY, S. 2007. Structural and mutagenic analysis of foot-and-mouth disease virus 3C protease reveals the role of the β -ribbon in proteolysis. *J Virol*, 81, 115-24.
- TAMKUN, J. W., DESIMONE, D. W., FONDA, D., PATEL, R. S., BUCK, C., HORWITZ, A. F. & HYNES, R. O. 1986. Structure of integrin, a glycoprotein involved in the transmembrane linkage between fibronectin and actin. *Cell*, 46, 271-82.
- TAMURA, K., DUDLEY, J., NEI, M. & KUMAR, S. 2007. MEGA4: Molecular Evolutionary Genetics Analysis (MEGA) software version 4.0. *Mol Biol Evol*, 24, 1596-9.
- TESAR, M. & MARQUARDT, O. 1990. Foot-and-mouth disease virus protease 3C inhibits cellular transcription and mediates cleavage of histone H3. *Virology*, 174, 364-74.
- THEOFILOPOULOS, A. N., BACCALA, R., BEUTLER, B. & KONO, D. H. 2005. Type I interferons α/β in immunity and autoimmunity. *Annu Rev Immunol*, 23, 307-36.

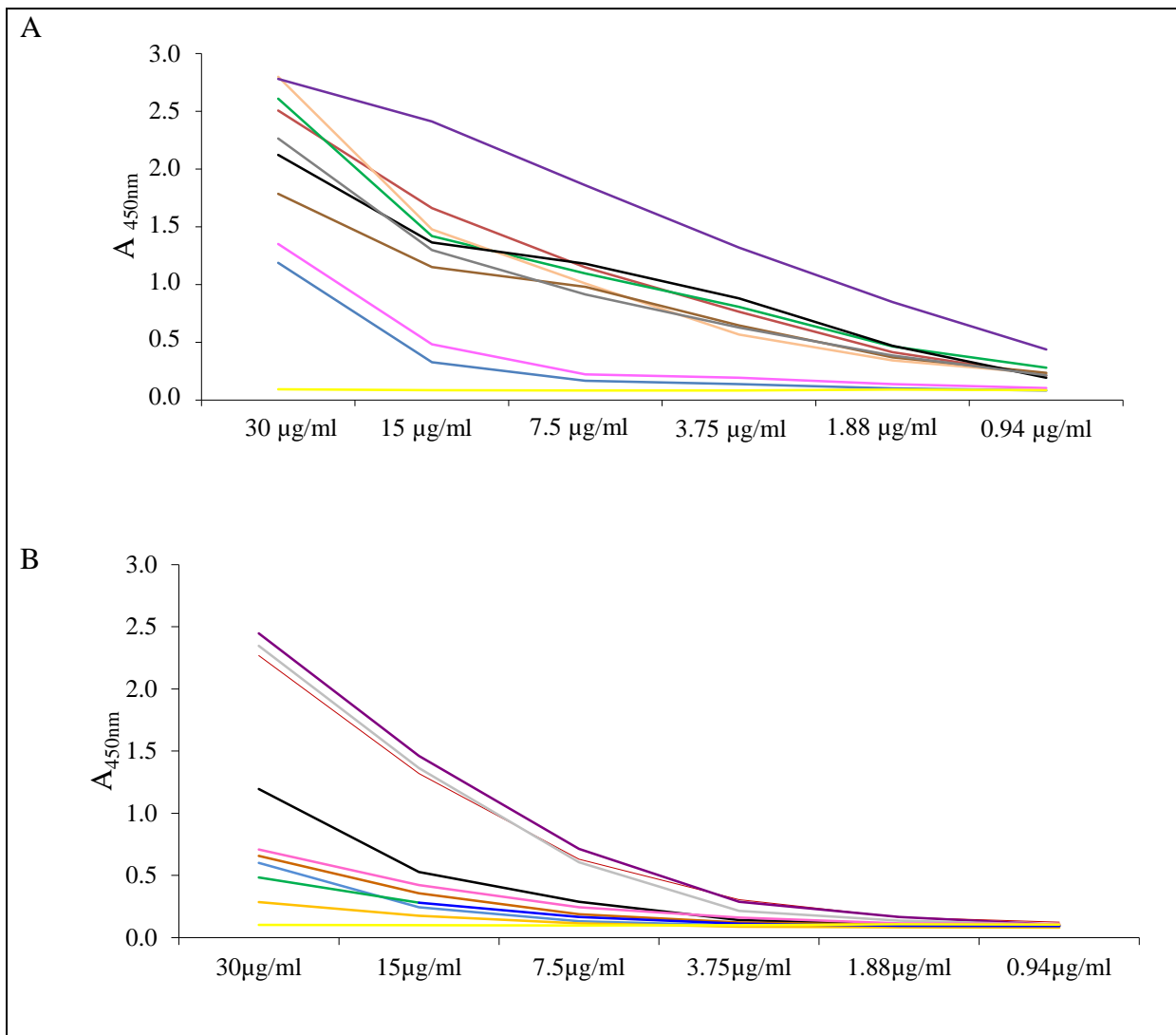
- THOMAS, A. A., WOORTMEIJER, R. J., BARTELING, S. J. & MELOEN, R. H. 1988a. Evidence for more than one important, neutralizing site on foot-and-mouth disease virus. Brief report. *Arch Virol*, 99, 237-42.
- THOMAS, A. A., WOORTMEIJER, R. J., PUIJK, W. & BARTELING, S. J. 1988b. Antigenic sites on foot-and-mouth disease virus type A10. *J Virol*, 62, 2782-9.
- THOMPSON, M. A., HAWKINS, J. W. & PIATIGORSKY, J. 1987. Complete nucleotide sequence of the chicken α A-crystallin gene and its 5' flanking region. *Gene*, 56, 173-84.
- THOMSON, G. R. 1994. Foot-and-mouth disease. In: COETZER, J. A. W., THOMSON, G. R. & TUSTIN, R. C. (eds.) *Infectious Diseases of Livestock with Special Reference to Southern Africa*. Cape Town, South Africa: Oxford University Press.
- THOMSON, G. R. & BASTOS, A. D. S. 2004. Foot-and-mouth disease. In: COETZER, J. A. W. & TUSTIN, R. C. (eds.) *Infectious Diseases of Livestock*. Cape Town, South Africa: Oxford University Press.
- THOMSON, G. R., VOSLOO, W. & BASTOS, A. D. 2003. Foot-and-mouth disease in wildlife. *Virus Res*, 91, 145-61.
- TILEY, L., KING, A. M. & BELSHAM, G. J. 2003. The foot-and-mouth disease virus *cis*-acting replication element (*cre*) can be complemented in trans within infected cells. *J Virol*, 77, 2243-6.
- TIZARD, I. R. 2000. Dendritic cells and antigen processing. *Veterinary Immunology: An Introduction*. Pennsylvania: W.B. Saunders Company.
- TONEGAWA, S. 1983. Somatic generation of antibody diversity. *Nature*, 302, 575-81.
- TONEGAWA, S., STEINBERG, C., DUBE, S. & BERNARDINI, A. 1974. Evidence for somatic generation of antibody diversity. *Proc Natl Acad Sci U S A*, 71, 4027-31.
- TORRANCE, L., ZIEGLER, A., PITTMAN, H., PATERSON, M., TOTH, R. & EGGLESTON, I. 2006. Oriented immobilisation of engineered single-chain antibodies to develop biosensors for virus detection. *J Virol Methods*, 134, 164-70.
- TOSH, C., HEMADRI, D. & SANYAL, A. 2002. Evidence of recombination in the capsid-coding region of type A foot-and-mouth disease virus. *J Gen Virol*, 83, 2455-60.
- TOWNSEND, A. R., GOTCH, F. M. & DAVEY, J. 1985. Cytotoxic T cells recognize fragments of the influenza nucleoprotein. *Cell*, 42, 457-67.
- TOWNSEND, A. R., ROTHBARD, J., GOTCH, F. M., BAHADUR, G., WRAITH, D. & MCMICHAEL, A. J. 1986. The epitopes of influenza nucleoprotein recognized by cytotoxic T lymphocytes can be defined with short synthetic peptides. *Cell*, 44, 959-68.
- TRAUTMAN, R. & BENNETT, C. E. 1979. Relationship between virus neutralization and serum protection bioassays for IgG and IgM antibodies to foot-and-mouth disease virus. *J Gen Virol*, 42, 457-66.
- TROPP, B. E. 2012. Protein structure and function. *Principles of molecular biology: Genes to Proteins*. Burlington, Massachusetts: Jones and Barlett learning.
- TURNER, D. J., RITTER, M. A. & GEORGE, A. J. 1997. Importance of the linker in expression of single-chain Fv antibody fragments: optimisation of peptide sequence using phage display technology. *J Immunol Methods*, 205, 43-54.
- USHERWOOD, E. J. & NASH, A. A. 1995. Lymphocyte recognition of picornaviruses. *J Gen Virol*, 76, 499-508.
- VAKHARIA, V. N., DEVANEY, M. A., MOORE, D. M., DUNN, J. J. & GRUBMAN, M. J. 1987. Proteolytic processing of foot-and-mouth disease virus polyproteins expressed in a cell-free system from clone-derived transcripts. *J Virol*, 61, 3199-207.
- VALDAZO-GONZALEZ, B., KNOWLES, N. J., HAMMOND, J. & KING, D. P. 2012. Genome sequences of SAT 2 foot-and-mouth disease viruses from Egypt and Palestinian Autonomous Territories (Gaza Strip). *J Virol*, 86, 8901-2.
- VAN BEKKUM, J. G., FRENKEL, H. S., FREDERIKS, H. H. J. & FRENKEL, S. 1959. Observations on the carrier state of cattle exposed to foot-and-mouth disease virus. *tijdschr diergeneeskde*, 84, 1159-1164.

- VAN KUPPEVELD, F. J., HOENDEROP, J. G., SMEETS, R. L., WILLEMS, P. H., DIJKMAN, H. B., GALAMA, J. M. & MELCHERS, W. J. 1997a. Coxsackievirus protein 2B modifies endoplasmic reticulum membrane and plasma membrane permeability and facilitates virus release. *EMBO J*, 16, 3519-32.
- VAN KUPPEVELD, F. J., VAN DEN HURK, P. J., VAN DER VLIET, W., GALAMA, J. M. & MELCHERS, W. J. 1997b. Chimeric coxsackie B3 virus genomes that express hybrid coxsackievirus-poliovirus 2B proteins: functional dissection of structural domains involved in RNA replication. *J Gen Virol*, 78, 1833-40.
- VAN MAANEN, C. & TERPSTRA, C. 1990. Quantification of intact 146S foot-and-mouth disease antigen for vaccine production by a double antibody sandwich ELISA using monoclonal antibodies. *Biologicals*, 18, 315-9.
- VAN RENSBURG, H. G., HENRY, T. M. & MASON, P. W. 2004. Studies of genetically defined chimeras of a European type A virus and a South African Territories type 2 virus reveal growth determinants for foot-and-mouth disease virus. *J Gen Virol*, 85, 61-8.
- VAN RENSBURG, H. G. & NEL, L. H. 1999. Characterization of the structural-protein-coding region of SAT 2 type foot-and-mouth disease virus. *Virus Genes*, 19, 229-33.
- VAN WYNGAARDT, W., MALATJI, T., MASHAU, C., FEHRSEN, J., JORDAAN, F., MILTIADOU, D. & DU PLESSIS, D. H. 2004. A large semi-synthetic single-chain Fv phage display library based on chicken immunoglobulin genes. *BMC Biotechnol*, 4, 6.
- VANGRYSPPERRE, W. & DE CLERCQ, K. 1996. Rapid and sensitive polymerase chain reaction based detection and typing of foot-and-mouth disease virus in clinical samples and cell culture isolates, combined with a simultaneous differentiation with other genomically and/or symptomatically related viruses. *Arch Virol*, 141, 331-44.
- VERDAGUER, N., FITA, I., DOMINGO, E. & MATEU, M. G. 1997. Efficient neutralization of foot-and-mouth disease virus by monovalent antibody binding. *J Virol*, 71, 9813-6.
- VERDAGUER, N., SEVILLA, N., VALERO, M. L., STUART, D., BROCCHI, E., ANDREU, D., GIRALT, E., DOMINGO, E., MATEU, M. G. & FITA, I. 1998. A similar pattern of interaction for different antibodies with a major antigenic site of foot-and-mouth disease virus: implications for intratypic antigenic variation. *J Virol*, 72, 739-48.
- VOSLOO, W., BASTOS, A. D., KIRKBRIDE, E., ESTERHUYSEN, J. J., VAN RENSBURG, D. J., BENGIS, R. G., KEET, D. W. & THOMSON, G. R. 1996. Persistent infection of African buffalo (*Syncerus caffer*) with SAT-type foot-and-mouth disease viruses: rate of fixation of mutations, antigenic change and interspecies transmission. *J Gen Virol*, 77, 1457-67.
- VOSLOO, W., BASTOS, A. D., SANGARE, O., HARGREAVES, S. K. & THOMSON, G. R. 2002. Review of the status and control of foot-and-mouth disease in sub-Saharan Africa. *Rev Sci Tech*, 21, 437-49.
- VOSLOO, W., DE KLERK, L. M., BOSHOFF, C. I., BOTHA, B., DWARKA, R. M., KEET, D. & HAYDON, D. T. 2007. Characterisation of a SAT-1 outbreak of foot-and-mouth disease in captive African buffalo (*Syncerus caffer*): clinical symptoms, genetic characterisation and phylogenetic comparison of outbreak isolates. *Vet Microbiol*, 120, 226-40.
- VOSLOO, W., KIRKBRIDE, E., BENGIS, R. G., KEET, D. F. & THOMSON, G. R. 1995. Genome variation in the SAT types of foot-and-mouth disease viruses prevalent in buffalo (*Syncerus caffer*) in the Kruger National Park and other regions of southern Africa, 1986-93. *Epidemiol Infect*, 114, 203-18.
- VOSLOO, W. & THOMSON, G. R. 2004. Natural habitats in which foot-and-mouth disease viruses are maintained. In: DOMINGO, E. & SOBRINO, F. (eds.) *Foot-and-Mouth Disease: Current Perspectives*. Norfolk, United Kingdom: Horizon Bioscience.
- WALKER, B. D. & BURTON, D. R. 2008. Toward an AIDS vaccine. *Science*, 320, 760-4.
- WANG, L. F., DU PLESSIS, D. H., WHITE, J. R., HYATT, A. D. & EATON, B. T. 1995. Use of a gene-targeted phage display random epitope library to map an antigenic determinant on the bluetongue virus outer capsid protein VP5. *J Immunol Methods*, 178, 1-12.
- WANG, L. F. & YU, M. 2009. Epitope mapping using phage-display random fragment libraries. *Methods Mol Biol*, 524, 315-32.

- WEBER, S., GRANZOW, H., WEILAND, F. & MARQUARDT, O. 1996. Intracellular membrane proliferation in *E. coli* induced by foot-and-mouth disease virus 3A gene products. *Virus Genes*, 12, 5-14.
- WEBSTER, R. 2001. Filamentous Phage Biology. In: BARBA III, C. F., BURT, D. S., SCOTT, A. C. & SILVERMAN, G. J. (eds.) *Phage Display: A Laboratory Manual*. Cold Spring Harbor, New York: Cold Spring Harbor Laboratory Press.
- WEMMER, S., MASHAU, C., FEHRSEN, J., VAN WYNGAARDT, W. & DU PLESSIS, D. H. 2010. Chicken scFvs and bivalent scFv-C_H fusions directed against HSP65 of *Mycobacterium bovis*. *Biologicals*, 38, 407-14.
- WESSELS, E., DUIJSINGS, D., LANKE, K. H., VAN DOOREN, S. H., JACKSON, C. L., MELCHERS, W. J. & VAN KUPPEVELD, F. J. 2006. Effects of picornavirus 3A Proteins on Protein Transport and GBF1-dependent COP-I recruitment. *J Virol*, 80, 11852-60.
- WHITTON, J. L., CORNELL, C. T. & FEUER, R. 2005. Host and virus determinants of picornavirus pathogenesis and tropism. *Nat Rev Microbiol*, 3, 765-76.
- WILD, T. F. & BROWN, F. 1967. Nature of the inactivating action of trypsin on foot-and-mouth disease virus. *J Gen Virol*, 1, 247-50.
- WILD, T. F., BURROUGHS, J. N. & BROWN, F. 1969. Surface structure of foot-and-mouth disease virus. *J Gen Virol*, 4, 313-20.
- WILLATS, W. G. 2002. Phage display: practicalities and prospects. *Plant Mol Biol*, 50, 837-54.
- WILLIAMSON, R. A., LAZZAROTTO, T., SANNA, P. P., BASTIDAS, R. B., DALLA CASA, B., CAMPISI, G., BURIONI, R., LANDINI, M. P. & BURTON, D. R. 1997. Use of recombinant human antibody fragments for detection of cytomegalovirus antigenemia. *J Clin Microbiol*, 35, 2047-50.
- WINTER, G., GRIFFITHS, A. D., HAWKINS, R. E. & HOOGENBOOM, H. R. 1994. Making antibodies by phage display technology. *Annu Rev Immunol*, 12, 433-55.
- WOHLFART, C. E., SVENSSON, U. K. & EVERITT, E. 1985. Interaction between HeLa cells and adenovirus type 2 virions neutralized by different antisera. *J Virol*, 56, 896-903.
- WORN, A. & PLUCKTHUN, A. 2001. Stability engineering of antibody single-chain Fv fragments. *J Mol Biol*, 305, 989-1010.
- XIANG, W., ANDINO, A. V. & WIMMER, E. 1997. RNA signals in entro- and rhinovirus genome replication. *Sem Virol*, 8, 256-273.
- XIE, Q. C., MCCAHERN, D., CROWTHER, J. R., BELSHAM, G. J. & MCCULLOUGH, K. C. 1987. Neutralization of foot-and-mouth disease virus can be mediated through any of at least three separate antigenic sites. *J Gen Virol*, 68, 1637-47.
- XU, J. L. & DAVIS, M. M. 2000. Diversity in the CDR3 region of V_H is sufficient for most antibody specificities. *Immunity*, 13, 37-45.
- YAMANAKA, H. I., INOUE, T. & IKEDA-TANAKA, O. 1996. Chicken monoclonal antibody isolated by a phage display system. *J Immunol*, 157, 1156-62.
- YIP, Y. L. & WARD, R. L. 2002. Application of phage display technology to cancer research. *Curr Pharm Biotechnol*, 3, 29-43.
- YOON, H., YOON, S. S., WEE, S. H., KIM, Y. J. & KIM, B. 2012. Clinical manifestations of foot-and-mouth disease during the 2010/2011 epidemic in the Republic of Korea. *Transbound Emerg Dis*, 59, 517-25.
- YU, Y., WANG, H., ZHAO, L., ZHANG, C., JIANG, Z. & YU, L. 2011. Fine mapping of a foot-and-mouth disease virus epitope recognized by serotype-independent monoclonal antibody 4B2. *J Microbiol*, 49, 94-101.
- ZHANG, Z. D., HUTCHING, G., KITCHING, P. & ALEXANDERSEN, S. 2002. The effects of gamma interferon on replication of foot-and-mouth disease virus in persistently infected bovine cells. *Arch Virol*, 147, 2157-67.
- ZHAO, Q., PACHECO, J. M. & MASON, P. W. 2003. Evaluation of genetically engineered derivatives of a Chinese strain of foot-and-mouth disease virus reveals a novel cell-binding site which functions in cell culture and in animals. *J Virol*, 77, 3269-80.

APPENDICES

Appendix A



A1: Indirect ELISA indicating the binding profile of soluble scFv1 (A) and scFv3 (B) to various concentrations of SAT2 viruses. Virus concentrations (30 $\mu\text{g/ml}$ to 0.94 $\mu\text{g/ml}$) are indicated on the x axis and the SAT2 viruses included in the study are indicated as follows: ZIM/7/83 (red), ZIM/5/83 (blue), ZIM/13/01 (green), ZIM/8/94 (orange), ZIM/7/89 (purple), ZIM/4/97 (pink), ZIM/44/97 (brown), ZIM/5/02 (black), ZIM/2/88 (grey). A negative control of 2% (w/v) casein (yellow) was included in the assays.

Appendix B

An alignment of the SAT2 deduced capsid protein sequences used in this study to determine hypervariable regions on the capsid of the SAT2 types. The start of each capsid protein is indicated above the alignment.

Legend:

- HHH** Alpha Helices
- EEE** Beta sheet structures
- VP1** Capsid protein VP1
- VP2** Capsid protein VP2
- VP3** Capsid protein VP3
- VP4** Capsid protein VP4

SAT2 SecStr	VP4				VP2				β A1	
	-----E	EEE-----H-	-----	-----	-----HHHH	HHHHHHHHHH	HHHH-----	-----HHHH--EE		
ZIM/7/83	GAGHSSPVTG	SQNQSGNTGS	IINNYMQQY	QNSMDTQLGD	NAISGGSNEG	STDTTSTHTN	NTQNNDWFSK	LAQSAISGLF	GALLADKKTE	ETTLLEDTRIV
ZIM/5/83A..
ZIM/13/01	...Q...A..
ZIM/4/97	...Q...A..
ZIM/2/88	...Q...A..
ZIM/5/02	...Q...A..
ZIM/7/89	...Q...A..
ZIM/44/97	...Q...A..
ZIM/8/94	...Q...A..

SAT2 SecStr	β A2		α Z		β B		β C		α A		β D	
	EE-----	-EEEEEEEE-	-----	-----EHH	HHHHHHHHH-	-----	-----	---EEEHH---	-----E--E-	-----	HHHHHH----	-EEEE---EE
ZIM/7/83	TTRHGTTTST	TQSSVGITYG	YADADSFPRG	PNTSGLETRV	EQAERFFKEK	LFDWTSKPKF	GTLYVLELPK	DHKGIIYGLT	DAYTYMRNGW	DVQVSATSTQ		
ZIM/5/83	M.....
ZIM/13/01	S.....	I.....	A.....
ZIM/4/97
ZIM/2/88	A.....
ZIM/5/02	S.....	I.....	A.....
ZIM/7/89	A.....
ZIM/44/97
ZIM/8/94	A.....

SAT2 SecStr	β E		α B		β F		β G1		β G2		β H		β I	
	E----EEEH-	-----	---HH-	-----	-----	-----	---EE-	-----	-----	-----	---HHEHEEE-	-----	---EEEE-	---EEEH---
ZIM/7/83	FNGGSLLVAM	VPCLCSLKDR	EEFQLSLYPH	QFINPRTNTT	AHIQVPYLGV	NRHDQGKRHQ	AWSLVVMVLT	PLTTEAQMOS	GTVEVYANIA	PTNVFVAGEK				
ZIM/5/83
ZIM/13/01	S.....
ZIM/4/97
ZIM/2/88
ZIM/5/02	S.....
ZIM/7/89	N.....
ZIM/44/97
ZIM/8/94	RK.....	R.....	I.....	N.....

VP3

SAT2 SecStr	-----EEEE-----E EEE----- αZ βA βB βC αA											
ZIM/7/83	PAKQGIIPVA	CFDGYGGFQN	TDPKTADPIY	GYVYNPSRND	CHGRYSNLLD	VAEACPTFLN	FDGKPYVVTK	NNGDKVMTCF	DVAFTHKVHK	NTFLAGLADY		
ZIM/5/83							F					
ZIM/13/01		.NA.					D	N	I	A		
ZIM/4/97		S										
ZIM/2/88		S						Q				
ZIM/5/02		.NA.					D	N	I	A		
ZIM/7/89		S										
ZIM/44/97		S										
ZIM/8/94		A	S				D					

SAT2 SecStr	EEH---E-E EEE-----HEEE----- βD βE αA βF $\beta G1$ $\beta G2$ βH											
ZIM/7/83	YAQYQGSLNY	HFMYTGPTHH	KAKFMVAYIP	PGIETDRLPK	TPEDAAHCYH	SEWDTGLNSQ	FTFAVPYVSA	SDFSYHTHTDT	PAMATTNGWV	AVFQVTDTHS		
ZIM/5/83							P					
ZIM/13/01	.T			K							Y	
ZIM/4/97	.T			K							Y	
ZIM/2/88	.T			K							Y	
ZIM/5/02	.T			K							Y	
ZIM/7/89	.T			K							Y	
ZIM/44/97	.T			K							Y	
ZIM/8/94	.T			K	S						Y	

VP1

SAT2 SecStr	--HEEEEE-- βI βB βC αA βD											
ZIM/7/83	AEAAVVSVS	AGPDLEFRFP	VDPVRQTTSS	GEGADVTTD	PSTHGGAVTE	KKRVHTDVAF	VMDRFTHVLT	NRTAFVDLDM	DTNEKTLVGG	LLRAATYYFC		
ZIM/5/83						M			A			
ZIM/13/01			I	A		R	M	HA	DK	V		
ZIM/4/97						R	M		K		A	
ZIM/2/88						R	M		K		A	
ZIM/5/02			I	A		R	M	HA	DK	V		
ZIM/7/89						R	M		K		A	
ZIM/44/97						R	M		K		A	
ZIM/8/94			I	TA		R	M	L	H	K	T	S

SAT2 SecStr	α B ---EE---	β E ---E---	β F -----	β G1 -EE-EE-EE-	β G2 HE-----	-----EE--	HHHHHHH-	-----	β H -----	
ZIM/7/83	DLEIACLGEH	ERVWWQPNGA	PRTTTLRDNP	MVFSHNNVTR	FAVPYTAPHR	LLSTRYNGEC	KYTQQSTAIR	GDRAVLAAKY	ANTKHKLPST	FNFGHVTADK
ZIM/5/83E.....
ZIM/13/01	G.....	...N.....	...RD.....A.E.....	...Y.....
ZIM/4/97	K.....A.....V.....	...R.E.....	...Y.....
ZIM/2/88	T.....R.E.....	...Y.....
ZIM/5/02	G.....	...N.....	...RD.....	S.A.E.....	...Y.....
ZIM/7/89	T.....R.E.....	...Y.....
ZIM/44/97	K.....	...A.....	...A.....R.E.....	...Y.....
ZIM/8/94V.T.	K..F.....	...Q.G...	...G.....V.....	...ERV.....Q.T.....E

SAT2 SecStr	β I --HHHHHH--	-----	-----	-----
ZIM/7/83	PVDVYYRMKR	AELYCPRPLL	PGYDHADRDR	FDSPIGVEKQ
ZIM/5/83
ZIM/13/01	T.....	.V...S...
ZIM/4/97E.....
ZIM/2/88N.....
ZIM/5/02	T.....	.V...S...
ZIM/7/89A.....
ZIM/44/97A.....
ZIM/8/94	A.....A...TG...	..A.....

B1: Amino acid sequence alignment of the P1 region of the SAT2 viruses included in this study.

PUBLICATIONS AND CONGRESS CONTRIBUTIONS

Published Papers

REEVE, R., BLIGNAUT, B., ESTERHUYSEN, J.J., **OPPERMAN, P.**, MATTHEWS, L., FRY, E.E., DE BEER, T.A., THERON, J., RIEDER, E., VOSLOO, W., O'NEILL, H.G., HAYDON, D.T. & MAREE, F.F. 2010. Sequence-based prediction for vaccine strain selection and identification of antigenic variability in foot-and-mouth disease virus. *PLoS Comp Biol*, 6, e1001027.

OPPERMAN, P.A., MAREE, F.F., VAN WYNGAARDT, W., VOSLOO, W. & THERON, J. 2012. Mapping of antigenic determinants on a SAT2 foot-and-mouth disease virus using chicken single-chain antibody fragments. *Virus Res*, 167, 370-9.

Papers in Preparation

OPPERMAN, P.A., ROTHERHAM, L.S., ESTERHUYSEN, J., CHARLESTON, B., JULEFF, N., CAPOZZO, A.V., THERON, J. & MAREE, F.F. Determining the epitope dominance on the capsid of a SAT2 foot-and-mouth disease virus by mutational analyses. *In preparation*

National Conference Contributions

MAREE, F.F., VAN RENSBURG, H.G., BÖHMER, B., **STOREY, P.**, THERON, J., RIEDER, E., BAXT, B. & VOSLOO, W. Genome length cDNA clones of the SAT types of foot-and-mouth disease virus provide powerful tools for investigating various properties of the virus. **Plenary paper** presented at the Virology Africa 2005 Conference, November 2005. UCT Graduate School of Business, Cape Town, South Africa.

VOSLOO, W., MAREE, F.F., BÖHMER, B., **STOREY, P.**, LEKOANA, T., ESTERHUYSEN, J.J., VAN RENSBURG, H.G., DWARKA, R.M., SAHLE, M., THERON, J., BAXT, B. & RIEDER, E. Reverse genetics provides tools for investigating receptor usage of different topotypes of the SAT types for foot-and-mouth disease virus. **Sub-plenary paper** presented at the 14th Biennial Congress of South African Society for Microbiology. April 2006, CSIR, Pretoria, South Africa.

OPPERMAN, P., MAREE, F.F., THERON, J. & VOSLOO, W. Mapping of antigenic sites on a SAT2 foot-and-mouth disease virus using a chicken antibody phage display library. **Poster** presented at Faculty day, Faculty of Veterinary Sciences, University of Pretoria, South Africa. September 2007, Pretoria, South Africa.

OPPERMAN, P., MAREE, F.F., THERON, J. & VOSLOO, W. Mapping of antigenic sites on a SAT2 foot-and-mouth disease virus using a chicken antibody phage display library. **Poster** presented at BIO-08, a combined conference supported by the South African Society for Microbiology, Biotech SA and the South African Society for Biochemistry and Molecular Biology. January 2008, Grahamstown, South Africa.

OPPERMAN, P., BLIGNAUT, B., THERON, J., VOSLOO, W. & MAREE, F.F. Determining antigenic sites on a SAT2 foot-and-mouth disease virus to improve vaccine strain selection. **Paper** presented at the Biennial Congress of the South African Society for Microbiology. September 2009, Durban, South Africa.

International Conference Contributions and Invited talks

MAREE, F.F., BLIGNAUT, B., DE BEER, T., **OPPERMAN, P.**, THERON, J. & RIEDER, E. A reverse genetic platform provides a powerful tool for the design of an alternative inactivated vaccine for foot-mouth-disease virus. **Poster** presented at the European Study Group on the Molecular Biology of Picornaviruses. May 2008, Sitges, Barcelona, Spain.

OPPERMAN, P., BLIGNAUT, B., THERON, J., VOSLOO, W., RIEDER, E. & MAREE, F.F. Mapping of antigenic sites on a SAT2 foot-and-mouth disease virus vaccine strain. **Poster** presented at the European Study Group on the Molecular Biology of Picornaviruses. May 2008, Sitges, Barcelona, Spain.

OPPERMAN, P., THERON, J., VOSLOO, W. & MAREE, F.F. Antigenic site determination to improve SAT2 foot-and-mouth disease virus vaccine strain selection. **Paper** presented at the FMD 2010 International Symposium and Workshop. April 2010, Melbourne, Australia.

MAREE, F.F., BLIGNAUT, B., DE BEER, T., **OPPERMAN, P.** & RIEDER, E. Structurally designed foot-and-mouth disease vaccines: Improved vaccines for regional control. **Paper** presented at FMD 2010 International Symposium and Workshop. April 2010, Melbourne, Australia.

MAREE, F.F., BLIGNAUT, B., **OPPERMAN, P.** & RIEDER, E. Vaccines by structural design: Improved recombinant vaccines for FMD control. **Paper** presented at the Global FMD Research Alliance. April 2010, Melbourne, Australia.

MAREE, F.F., BLIGNAUT, B., **OPPERMAN, P.A.**, DE BEER, T., VISSER, N. & RIEDER, E. Engineered vaccines for regional control of foot-and-mouth disease. **Invited oral presentation** at Oxford University, United Kingdom, 2010.

BLIGNAUT, B., THERON, J., **OPPERMAN, P.**, VAN SCHALKWYK, A., MAREE, J.J. Population diversity of chimera and host-adapted foot-and-mouth disease viruses and implications for reverse genetics. **Poster** presented at the European Study Group on the Molecular Biology of Picornaviruses. June 2012, Saint Raphaël, France.

OPPERMAN, P.A., THERON, J. & MAREE, F.F. Determining the epitope dominance on the capsid of a SAT2 foot-and-mouth disease virus by mutational analysis. **Paper** presented at The European Commission for the Control of Foot-and-Mouth Disease (EuFMD). October 2012, Jerez, Spain.

MAREE, F.F., CHITRAY, M., **OPPERMAN, P.** & SCOTT, K. Rational design for an effective vaccine against FMD. **Invited oral presentation** at honoring Marvin J Grubman's scientific career, 2013. Old Saybrook, USA.

MAREE, F.F., CHITRAY, M., **OPPERMAN, P.** & SCOTT, K. Engineered cell culture adaptive mutations in SAT viruses. **Paper** presented at the Wellcome Trust meeting, 2013. Old Saybrook, USA.

OPPERMAN, P., CHITRAY, M., MAREE, F.F. & RIEDER, E. Mapping of antigenic sites of FMDV using a chicken antibody phage display. **Poster** presented at Positive Strand RNA Viruses. May 2013, Boston, USA.